SrcFK is a key mediator of oxidant signalling pathways in Pulmonary Vascular Smooth Muscle

MacKay, Charles Edward

Awarding institution:
King's College London

SrcFK is a key mediator of oxidant signalling pathways in Pulmonary Vascular Smooth Muscle

A thesis submitted by

Charles Edward Mackay

For the degree of Doctor of Philosophy to
King's College London

2016

Department of Asthma, Allergy and Lung Biology
King's College London School of Medicine

Table of contents

Abstract

Oxidative stress is associated with a number of cardiovascular diseases such as atherosclerosis and pulmonary hypertension. Previously, our group has shown that prostaglandin–$F_{2\alpha}$ and hypoxia enhance total tyrosine phosphorylation, activate Src and cause SrcFK-dependent constriction. Combining these observations with the ROS-sensitivity of Src, lead me to investigate whether interaction between SrcFK and ROS makes a central contribution to vascular smooth muscle function.

Intra-pulmonary Arteries (IPA) were dissected from rat lungs, protein was extracted and phosphorylation of known targets of Rho-kinase (MYPT-1) and MLCK (MLC_{20}) as well as Src auto-phosphorylation (Tyr416) was measured. Protein-protein interactions were examined by immune-precipitation/co-immuno-precipitation. Contraction was measured in IPA mounted on a wire myograph. Primary smooth muscle cell lines, generated from IPAs were used to measure ROS production using the luminescent dye L-012 or were transfected with GFP-tagged RhoA or ARHGEF1 to visualise protein translocation in live cells.

In this study, I demonstrate that U46619 and LY83583 induce ROS production in PASMCs. I also demonstrate that U46619 and LY83583 contractile responses in IPA are sensitive to both antioxidants and SrcFK inhibition. U46619, hypoxia and LY83583 also enhance SrcFK autophosphorylation, ROCK activity and MLC_{20} phosphorylation which are blocked by SrcFK inhibition, antioxidants (U46619 and LY83583) and mitochondrial inhibitors (hypoxia). Finally, U46619 and LY83583 promote reversible translocation of eGFP-RhoA or eGFP-ARHGEF1 in a SrcFK dependent and ROS dependent manner. U46619 also enhanced co-immunoprecipitation of ARHGEF1 with SrcFK. Taken together these results suggest SrcFK's play a key role as ROS sensitive intermediates which enhance contractile responses via interactions with ARHGEF1 and enhanced ROCK activity.

Statement

I declare that all of the work in this thesis was performed by myself, Charles E Mackay, except for the following:

- Pulmonary artery smooth muscle phenotype confirmation was performed by Drs Yasin Shaifta and Vladimir Snetkov.

- GFP-Tagged RhoA/ARHGEF1 construct generation was performed by Dr Yasin Shaifta.

- Phospho-tyrosine work with LY83583 and PP2 was performed by Dr Gregory Knock

Acknowledgement

I would first like to thank Dr Gregory A Knock, for his unwavering knowledge, support, guidance, patience and encouragement as my primary supervisor. I am extremely fortunate and grateful to have had you as my supervisor. Your 'hands on' support have really helped me progress through my PhD. Thank you for supporting my abstract submission and presentations both nationally and internationally and for encouraging me to share my research with a wider audience.

I would also like to thank Professor Jeremy ward for his support, knowledge and ideas throughout the three years. You have helped me immensely throughout this process.

To the rest of the Ward lab: Drs Vladimir Snetkov, Jesus Prieto-Lloret and Yasin Shaifta. Thank you for all your help within the laboratory, from finding reagents to teaching me valuable research skills. I appreciate all your patience, help and company throughout my studies. It has been a pleasure to have been able to work in such a well-established and successful laboratory.

Finally, I would like to thank my family for their support, encouragement. Thank you for being considerate and understanding and making this whole process as comfortable as possible.

Abbreviations

α- actin	Alpha actin
ANOVA	Analysis of variance
AngII	Angiotensin II
ASM	Airway smooth muscle
ATP	Adenosine tri-phosphate
ATPγS	Adenosine 5′-O-(3-thiotriphosphate)
ADP	Adenosine di-phosphate
BCA	Bicinchoninic Acid
BMPR-II	Bone morphogenic protein receptor II
CAM	Ca^{2+}/calmodulin complex
CML	Chronic myeloid leukaemia
CO-IP	Co-immunoprecipitation
COPD	Chronic obstructive pulmonary disease
cAMP	Cyclic adenosine mono-phosphate
CPI-17	C-Kinase-activated protein phosphatase 1
DAG	Diacylglycerol
DMEM	Dulbecco's modified eagle's medium
DMSO	Dimethyl sulfoxide
Ebselen	2-Phenyl-1, 2-benzisoselenazol-3(*2*H)-one
ECL	Enhanced chemiluminescence
ECM	Extracellular Matrix
EDHF	Endothelial derived hyperpolarising factor
EGF	Epidermal growth factor
EGFR	Epidermal growth factor receptor
eGFP	Emerald green fluorescent protein
EGTA	Ethylene glycol tetraacetic acid
ETC	Electron transport chain
ET-1	endothelin 1
F-Actin	Filamentous actin
FAK	Focal adhesion kinase

FBS	Fetal Bovine Serum
G-Actin	Globular Actin
GAPDH	Glyceraldehyde-3-3phosphate dehydrogenase
GPCR	G-protein coupled receptor
G-protein	Guanine nucleotide binding proteins
GTP	Guanine tri-phosphate
GTPγS	Guanosine 5′-O-(3-thiotriphosphate)
GDP	Guanine di-phosphate
GPX	Glutathione peroxidase
GSH	Glutathione
HBSS	Hank's balanced salt solution
hPAH	Hereditable Pulmonary hypertension
hPASMCs	Human pulmonary arterial smooth muscle cells
HPV	Hypoxic pulmonary vasoconstriction
HRP	Horse radish peroxidase
H_2O_2	Hydrogen peroxide
Ig	Immunoglobulin
ILK	Integrin-linked kinase
IMS	Intermembrane Space
IP	Immunoprecipitation
IP_3	Inositol triphosphate
IPA	Intrapulmonary artery
iPAH	Idiopathic pulmonary hypertension
JAK	Janus Kinase
LPA	Lysophosphatidic Acid
L-NAME	L-N^G-Nitroarginine methyl ester
LY83583	6-anilino-5,8-quinoline quinone
MAPK	Mitogen-activated protein kinase
MLC	Myosin light chain
MLCK	Myosin light chain kinase
MLCP	Myosin light chain phosphatase
mPAP	Mean arterial pressure

MYPT-1	Myosin phosphatase targeting subunit 1
NCX	Sodium exchanger
NRTK	Non-receptor tyrosine kinase
NO	Nitric oxide
NOX	Nicotinamide adenine dinucleotide phosphate-oxidase
NP-40	Nonyl phenoxypolyethoxylethanol
$O_2^{\bullet-}$	Superoxide
$OONO^-$	Peroxynitrite
OH•	Hydroxyl Radical
PAGE	Polyacrylamide gel electrophoresis
PASMC	Pulmonary arterial smooth muscle cells
PBS	Phosphate buffered saline
PDBU	Phorbol 12, 13-dibutyrate
PDGFR	Platelet-derived growth factor receptor
PE	Phenylephrine
PG	Prostaglandin
Ph	Pleckstrin homology
PAH	Pulmonary arterial hypertension
PH	Pulmonary hypertension
PIP_2	Phosphatidylinositol 4, 5-bisphosphate
PKA	Protein kinase A
PKC	Protein kinase C
PKG	Protein kinase G
PLC	Phospholipase C
PMCA	Plasma membrane Ca^{2+} pump
PSS	Physiological saline solution
PTP	Protein tyrosine phosphatase
PYK2	Protein tyrosine kinase 2
RBD	Rho binding domain
RGS	Regulator of G-protein signalling
RhoA	Ras homolog gene family member A
RhoGAP	Rho GTPase activating protein

RhoGDI	Rho guanine dissociation factor
RhoGEF	Rho guanine nucleotide exchange factor
RISP	Rieske iron-sulphur protein
ROCK	Rho-associated protein kinase
ROS	Reactive oxygen species
RTK	Receptor tyrosine kinase
R_yR	Ryanodine receptor
SDS	Sodium dodecyl sulphate
SEM	Standard error of the mean
SERCA	Sarcoplasmic/endoplasmic reticulum Ca^{2+} pump
SOD	Superoxide dismutase
SPC	Sphingosinephosphoryclcholine
SR	Sarcoplasmic reticulum
Src-FK	Src family kinase
TBS	Tris buffered saline
TBST	Tris buffered saline with tween
Tempol	4-hydroxy-2,2,6,6-tetramethylpiperidine-N-oxyl
TKI	Tyrosine kinase inhibitor
TRP	Transient receptor potential
TXA_2	Thromboxane A-2
VOCC	Voltage operated calcium channels
VSM	Vascular smooth muscle
VSMC's	Vascular smooth muscle cells
ZIPK	Zipper-interacting protein kinase
$[Ca^{2+}]_i$	Intracellular calcium ion concentration

Glossary of Terms

U46619 (U46) – T-type prostanoid receptor agonist.

LY83583 (LY) – A cell permeable quinolinedione and substrate for the oxidoreductase enzyme diaphorase. Therefore an intracellular superoxide generator

Tempol – Antioxidant.

Ebselen – Antioxidant.

PP2 – A selective SrcFK inhibitor.

L-NAME - An analogue of arginine that inhibits the production of nitric oxide (NO).

Rotenone – Inhibits electron transfer from complex 1 of the electron transport chain.

Myxothiazol – Inhibits electron transfer from complex 3 of the electron transport chain.

List of Tables

List of Figures

1. Introduction

1.1 Pulmonary Vasculature

The pulmonary circulation begins when blood is pumped by the heart (right ventricle) into the main pulmonary artery, which immediately divides into the right and left pulmonary arteries supplying each lung. The blood is reoxygenated while passing through the pulmonary capillaries before re-entering the heart and being pumped around the body through the systemic vasculature.

The pulmonary circulation receives the entire cardiac output of the right ventricle. It contains a high-density capillary network, thereby maximising gaseous exchange (CO_2 to O_2 and vice versa). Resistance of the pulmonary circulation is 10-15% of the systemic circulation. This is due to the vessels of the pulmonary microcirculation being short and relatively wide, with low levels of resting tone. The pulmonary circulation network is also numerous, so the total cross-section is comparable to that of the systemic circulation. The sympathetic nervous system, myogenic or metabolic regulation have very little effect in regulating pulmonary resistance. The most important mechanism regulating pulmonary vascular tone is hypoxic pulmonary vasoconstriction (HPV), a process whereby pulmonary arteries constrict in response to hypoxia (systemic vessels typically dilate) thereby maximising the matching of perfusion to ventilation in the lungs.

Understanding the pulmonary circulation is of vital importance as dysregulation within this system can lead to disease states such as pulmonary hypertension and eventually right heart failure. With this in mind, it is also important to investigate the basic signalling pathways in the pulmonary circulation so that they can subsequently be studied in more depth in disease states such as pulmonary hypertension.

1.1.1 Pulmonary Hypertension

Pulmonary hypertension (PH) is a term used to describe a wide spectrum of rare but lethal pulmonary hypertensive conditions that have different aetiologies but similar clinical presentation. The normal resting adult pulmonary pressure is ~16mmHg. However, PH patients have a mean pulmonary arterial pressure (mPAP) of >25 mmHg at rest or >30 mmHg during exercise.

PH was classified initially as primary, if the cause was unknown and secondary if the cause can be identified. More complex classifications have been designed to enable the classification of various manifestations of PH based on pathological, functional and clinical characteristics, currently there are 5 groups [1,2]. Group 1 PH, also known as pulmonary arterial hypertension (PAH), includes heritable and idiopathic PAH (hPAH, iPAH), which are associated with mutations in the bone morphogenetic receptor type II (BMPR-II). Groups 2-5 are forms of secondary PH. Group 2 is associated with left heart disease resulting in increased left atrial pressure that is transmitted to the pulmonary artery. Group 3 PH is due to lung diseases such as chronic obstructive pulmonary disease (COPD) which leads to chronic hypoxia [3]. Pulmonary arteries (PA) constrict in response to alveoli hypoxia, termed hypoxic pulmonary vasoconstriction (HPV). This was initially described by von Euler-Lijestand in 1946[4] and aims to optimise ventilation perfusion by diverting blood away from poorly ventilated areas of the lung. HPV is considered vital in normal pulmonary vasculature, so long as it is short lived and highly localised. Chronic hypoxia triggers pulmonary vascular remodelling leading to pulmonary arterial hypertension followed by right ventricle hypertrophy [5-9]. Group 4 PH includes chronic thromboembolic PH, and is mainly caused by pulmonary embolism. Group 5 PH is associated with a heterogeneous set of conditions such as chronic myeloid leukaemia (CML) and thyroid disease. Secondary PH is managed by treated the cause of the underlying disease.

Pathophysiology

PH is characterised by pulmonary vascular remodelling due to increased pulmonary artery smooth muscle migration, proliferation and neomuscularisation [10,11]. Subsequently, leading to increased pulmonary resistance. The causes of remodelling remain controversial however the RhoA/Rho-Kinase has been implicated in numerous aspects.

The discovery that contraction of vascular smooth muscle, in addition to being regulated by intracellular Ca^{2+} concentration ($[Ca^{2+}]_i$), is also regulated via the monomeric G-protein RhoA and its downstream effector Rho-Kinase[12,13]. Furthermore, chronic hypoxia, which acts as a contributing factor to the development of pulmonary hypertension [14], is linked to enhanced RhoA/Rho-Kinase activity in PH [15]. This has led to enormous interest in the effects of this pathway on vascular function. The RhoA/Rho-Kinase pathway, in addition to regulating the contractile responses of the vasculature via activation of G protein coupled receptor activation (GPCR), also exerts important effects on smooth muscle differentiation, proliferation and migration as well as on endothelium-dependent vasodilatation [16].

As these processes are believed to contribute to PAH and non-PAH PH, regulation of Rho-Kinase and inhibitors of RhoA/Rho-Kinase signalling within vascular smooth muscle have emerged as possible treatments for these conditions.

1.2 Vascular Smooth Muscle

Section Overview

This section will give a brief overview of the structure and function of vascular smooth muscle particularly in relation to contraction. I will also describe a number of mechanism that regulate VSM contraction and the evidence for non-receptor tyrosine kinases in vascular function.

Introduction

Vascular smooth muscle cells (VSMC's) are highly specialized cells that surround all hollow organs including blood vessels, airways, stomach, bladder, uterus and intestines. In blood vessels, VSMC's main function is the regulation of blood pressure and regional blood flow distribution. VSMC's within adult blood vessels proliferate at extremely low rates, however they express a unique collection of contractile proteins, ion channels and signalling molecules required for the cell's contractile function, which is unique when compared to other cells type. VSMC's retain extreme plasticity in phenotype in response to changes in local environment; for example, morphogenesis of blood vessels in response to vascular injury. The main function of VSMCs is contraction. During contraction, smooth muscle shortens and the diameter changes, which propels organ contents. Smooth muscle cells are not striated (as opposed to cardiac or skeletal muscle) giving rise to their smooth appearance.

Activation of smooth muscle cells occurs in response to external stimuli such as hormones, paracrine signalling molecules and changes in local environmental factors, including PCO_2, PO_2, pH and ROS. Contractile force is therefore determined by variations of activation of the contractile system in all coupled cells. Smooth muscle filaments are composed of primarily alpha-actin (α-actin) which are anchored to dense bodies. As with all smooth muscle, contraction arises due to cross bridge cycling between actin and myosin.

1.2.1 Organisation of the Contractile Fibres

The contractile apparatus of smooth muscle is composed of actin and myosin filaments. Myosin itself has a molecular weight of 520kDa and is formed of six polypeptide chains, two heavy chains and 2 pairs of light chains. The light chains can be further divided into "regulatory/functional" light chains 20kDa in size and "essential" light chains 17kDa in size.

Actin is a globular multifunctional protein that forms part of the microfilaments, found in all eukaryotic cells. There are currently four known isoforms identified within smooth muscle; α and γ actin associated with "contractile" phenotype while β and γ are associated with "cytoskeletal" actin. Actin monomers are 43kDa globular proteins (g-actin) which contains binding sites for 2 actin monomers, thereby creating filamentous actin or F-actin. F-actin is a double stranded helical structure where the actin monomers are orientated in the same direction. Contractile microfilaments such as stress fibres contain alpha actinin, which ensures actin fibres are bundled together in parallel and creates space between them into which myosin fibres fit. Actin monomers are also polar which is vital as it contributes to their assembly but also in establishing the movement of myosin relative to actin.

Two other proteins, calponin and caldesmon are key components of actin cytoskeleton and bind actin proteins. They are able to regulate actin filaments by crosslinking actin into networks as well as interacting with other structural proteins. Calponin and caldesmon can also inhibit the ATPase activity of myosin in smooth muscle.

1.2.2 Smooth muscle contraction and regulation

A key event that is essential for initiating smooth muscle contraction is the rise of intracellular calcium ($[Ca^{2+}]_i$). This can occur via release from intracellular stores such as the sarcoplasmic

reticulum (SR) [17] or via influx through voltage independent or dependent membrane channels [18].

Ca^{2+} release from stores occurs in response to activation of G-protein coupled receptor (GPCR) contractile agonists. This results in the activation of phospholipase c-β (PLCβ), and subsequent inositol triphosphate (IP_3) and 1,2-diacyglycerol (DAG) mediated Ca^{2+} increase[19],[20]. Increase in $[Ca^{2+}]_i$ can also occur via capacitive Ca^{2+} entry otherwise known as store operated calcium entry[21,22]. Voltage independent pathways can also involve agonist-induced Ca^{2+} release through the activation of ryanodine receptors (RyR) found on the SR. This can occur via calcium induced calcium release, a process whereby calcium influx activates RyR and promotes release from the SR [23-25]. Voltage dependent pathways occur via depolarisation (through attenuation of K^+ channel conductance) of the plasma membrane resulting in the activation of voltage operated calcium channels (VOCCs) such as L-type Ca^{2+} channels[26,27].

Ca^{2+} can then form a complex with calmodulin. The Ca^{2+}/calmodulin complex activates myosin light chain kinase (MLCK) which phosphorylates myosin light chain (MLC_{20}) at position serine 19. Myosin light chains are 20-kD regulatory subunits, that when phosphorylated, activate myosin. More specifically, this phosphorylation activates the myosin ATPase that provides the energy required to move the myosin head and promote cross bridge cycling between actin and myosin filaments and thereby contraction.

The degree of force generated during smooth muscle contraction is determined by the net phosphorylation of MLC. This is a balance between MLCK and myosin light chain phosphatase (MLCP). MLCP dephosphorylates P-MLC converting it back to the inactive MLC (Fig 1.1). Following contraction, $[Ca^{2+}]_i$ returns to basal levels which causes relaxation via plasma membrane Ca^{2+} ATPases (PMCA), sodium calcium exchangers (NCX), cytosolic binding

proteins and re uptake of Ca^{2+} into the SR via sarco/endoplasmic reticulum Ca^{2+} ATPase (Serca) [28].

Ca^{2+} Sensitization

Ca^{2+} sensitization is a process whereby there is an increase in contractile force in response to contractile stimuli independent of changes in free cytosolic calcium [29].

Ca^{2+} sensitization was initially observed in smooth muscle permeabilized with bacterial α-toxin [30]. This study revealed that $[Ca^{2+}]_i$ does not always mirror the degree of MLC phosphorylation and contractile force. Therefore, contraction in smooth muscle can be enhanced by events that are independent of changes in $[Ca^{2+}]_i$..

Somlyo *et al* [31] suggested that MLCP is a G protein-regulated enzyme. This was based on Ca^{2+}-independent contractile effect of guanosine 5′-*O*-(3-thiotriphosphate) (GTPγS) on permeabilized smooth muscle. Subsequently, this was confirmed by demonstrating that GTPγS and agonists increased MLC phosphorylation independently of changes in $[Ca^{2+}]_i$, by inhibiting dephosphorylation of MLC[12,30]. These findings, along with demonstrating that pre-treatment of smooth muscle with adenosine 5′-*O*-(3-thiotriphosphate) (ATPγS) under Ca^{2+}-free conditions caused thiophosphorylation of MYPT1 and increased the Ca^{2+} sensitivity of contractile force [32], focused attention on MYPT1 as a Rho-Kinase substrate [33] and a key factor in Ca^{2+} sensitization.

MLCP is a trimeric holoenzyme composed of three subunits, 38kDa catalytic subunit (PP1c), 110 kDa non-catalytic myosin phosphatase targeting subunit (MYPT-1) and a 20kDa non-catalytic subunit [34,35]. There are three main ways in which MLCP is regulated; dissociation of its heterotrimeric structure, inhibition of inhibitory proteins such as CPI-17 and phosphorylation of MYPT-1 [36]. Phosphorylation of MYPT-1 is a major regulatory mechanism of MLCP. There are at least two known phosphorylation sites, which are related to the inhibition

of MLCP [36]. Phosphorylation of MYPT-1 at Thr 696 (thr-697 in rat), is associated with MLCP inhibition [37]. Kimura *et al* [33] first demonstrated that Rho-Kinase phosphorylates this site however a number of other kinases can also do this. These include zipper-interacting kinase (ZIPK) [38] and integrin-linked kinase (ILK) [39]. Phosphorylation of MYPT-1 at Thr-850 is associated with MLCP disassociation and another key target of Rho-Kinase [40,41].

In vascular smooth muscle, it has been suggested that phosphorylation of MYPT-1 at thr-850 is the more significant site at inhibiting the actions of MLCP [41,42]. Phosphorylation at this site has been shown to be sensitive to Rho-Kinase inhibition [41,43].

DAG or Ca^{2+} can also activate protein kinase C (PKC) which in turn can also phosphorylate CPI-17 thereby inhibiting MLCP activity [44,45].

Inhibition of MLCP is now known to occur primarily via activation of the RhoA / Rho-Kinase pathway in response to GPCR activation and plays a key role in Ca^{2+} sensitization [29,46,47] (Fig 1.1). This will be explored in more detail in sections 1.6 and 1.7.

Crosstalk between RhoA/ROCK and cytosolic Ca^{2+}

RhoA/ROCK and cytosolic Ca^{2+} have distinct actions at promoting and enhancing VSM contraction. Until recently, Rho and Rho-kinase activation were considered to occur as a consequence of agonist binding. However, this assumption has been challenged, Mita *et al* used high K^{+} to depolarize the caudal artery and found the contraction to be Rho-kinase sensitive and associated with inhibition of MLCP [48]. A number of other studies have confirmed this observation and shown the activation of Rho-kinase by depolarization is Ca^{2+}-dependent in vascular smooth muscle [49-52] . Thus it appears that Rho and Rho-kinase are activated by two pathways, one Ca^{2+}-independent and one Ca^{2+}-dependent. The exact mechanism of how Ca^{2+} activates Rho-Kinase remains to be elucidated however number of studies have provided some

clues as to potential mechanisms of Rho-Kinase regulation via membrane depolarisation and Ca^{2+} signalling.

A study performed by Liu *et al* [53] recently reported that membrane depolarization causes a direct activation of G protein-coupled receptors leading to local Ca^{2+} release in smooth muscle. The authors demonstrate that membrane depolarization can induce RyR-mediated local Ca^{2+} release, leading to an increase in the activity of Ca^{2+} sparks and contraction in airway SMCs. The increased Ca^{2+} sparks are independent of VDCCs and the associated extracellular Ca^{2+} influx. This local Ca^{2+} release is attributed to direct activation of G protein-coupled M_3 muscarinic receptors in the absence of a ligand, which causes activation of Gq proteins and phospholipase C, leading to the generation of inositol 1,4,5-triphosphate (IP_3). Subsequently promoting an initial Ca^{2+} release through $IP_{(3)}$ receptors and then further Ca^{2+} release via RyR_2 due to a local Ca^{2+}-induced Ca^{2+} release process. These findings demonstrate an important mechanism for Ca^{2+} signalling but also has the potential of not only activating G_q signalling but also other heterotrimeric G proteins such as $G_{12/13}$.

Further evidence provided by Sakurada *et al* [54] demonstrated that depolarization with high KCl induced Rho activation and Rho kinase–dependent contraction, which are both Ca^{2+}dependent in rabbit aortic VSM. Furthermore, a Ca^{2+}dependent Rho activation also operates in VSM stimulated with noradrenalin and U46619, coupled to G_q and $G_{12/13}$. The authors suggest that Rho activity is likely regulated by both $G_{12/13}$ and G_q/Ca^{2+} and suggest that the Ca^{2+}-dependent Rho activation may involve Ca^{2+} and calmodulin stimulation of RhoGEF as Rho activation was inhibited by the calmodulin inhibition. Furthermore, there are known examples for calmodulin regulation of GEFs of the other small GTPases such as the Ras-GEFs Ras-GRF 1 and 2 which possess an IQ motif that act as calmodulin-binding site, were shown to be activated by Ca^{2+}-influx in an IQ motif-dependent manner [55]. It is therefore entirely possible that calmodulin may also activate RhoGEFs.

More recently, Janssen *et al* [56] sought to examine the contribution of voltage-dependent Ca^{2+} influx and Rho/ROCK signalling in the responses to high-millimolar KCl, making comparisons between TSM and BSM as well as among porcine, bovine, and human airways. The authors show that KCl caused substantial contractions in tracheal preparations which were sensitive to the removal of external Ca^{2+} or the selective L-type Ca^{2+} channel blocker nifedipine; porcine bronchial preparations were much less sensitive, and bovine bronchi were unaffected by 1 μM nifedipine. Interestingly, the authors demonstrate that KCl-induced contractions were also sensitive to two structurally different ROCK inhibitors: Y-27632 and HA-1077. Furthermore, the inhibitory effects of nifedipine and the ROCK inhibitors were not additive suggesting that they are art of the same pathway. KCl also stimulated Rho and ROCK, which was suppressed by nifedipine or by removal of external Ca^{2+}. KCl-induced $[Ca^{2+}]_I$ influx was not affected by Y-27632 but was reversed by $NiCl_2$ or by BAPTA-AM. The authors conclude that KCl acts through stimulation of Rho and ROCK, secondary to voltage-dependent Ca^{2+} influx. The authors speculate that depolarization and/or Ca^{2+} influx increases the activity of Rho GTPase-activating protein which in turn would result in activation of ROCK [29]. Other groups have also shown that ion channels to form large complexes with a wide variety of kinases and these complexes promote the interactions between the channels and enzymes is a prerequisite for signalling via those enzymes[57].

Conversely, it has also been suggested that RhoA/Rho-kinase signalling affects agonist-induced Ca^{2+} mobilization. This was shown by Ito *et al* who demonstrate that receptor-operated Ca^{2+} influx is inhibited by Rho-Kinase inhibition [58]. In another study, Shabir *et al* reported that Rho-Kinase activity without agonist stimulation, modulates myogenic contraction in both a Ca^{2+} dependent and independent manner [59].

What all these studies show is the diverse and highly complex nature of signalling events over and above the canonical signalling events demonstrated in figure 1. Further investigation will

be required to elucidate the mechanism(s) underlying this voltage- and/or Ca^{2+} dependent activation of the Rho/ROCK signalling pathway.

Figure 1.1:

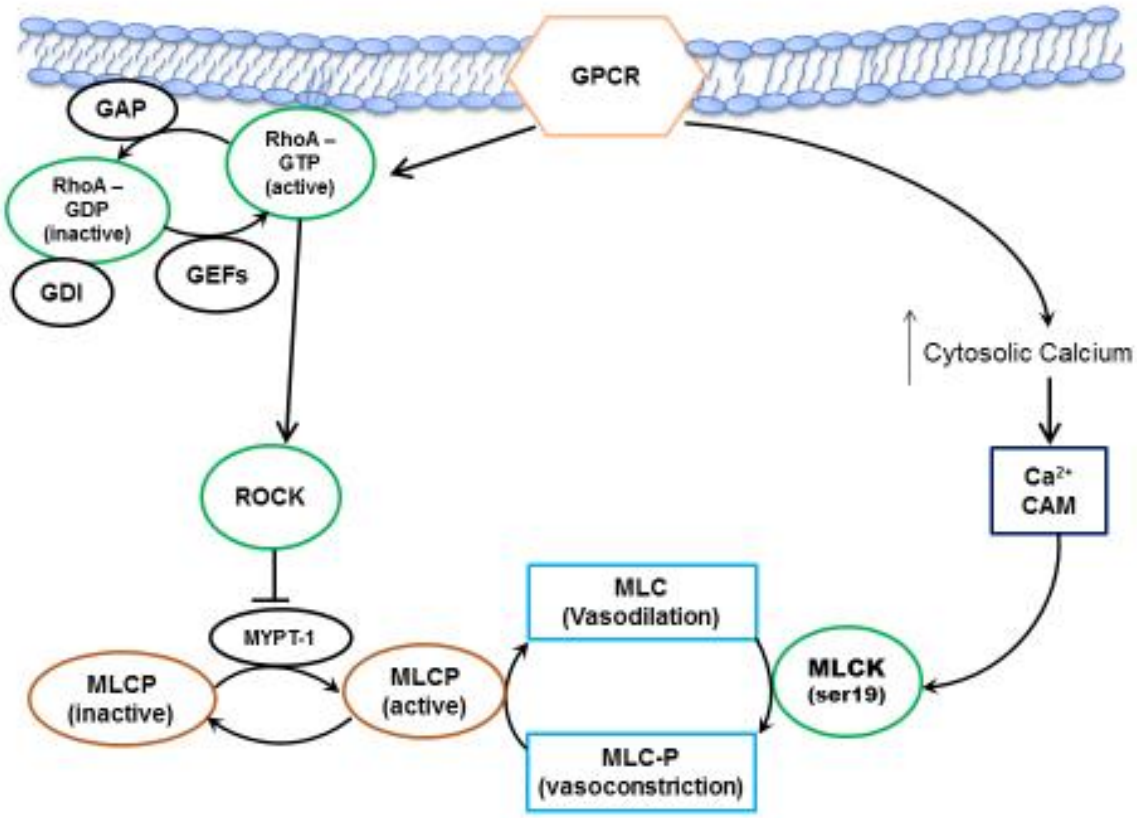

Figure 1.1: The major pathways involved in smooth muscle contraction.
Upon agonist stimulation of GPCRs, contraction occurs due to an increase in free cytosolic Ca^{2+}. Furthermore, sensitivity of the contractile machinery via activation of the RhoA/Rho-Kinase pathway can also occur, thereby, enhancing contractile force without the associated rise in free cytosolic Ca^{2+}. How these pathways are activated can be found in the main text.

1.2.3 Non-receptor tyrosine kinase in vascular function

Non-receptor tyrosine kinases (NRTKs) are cytoplasmic enzymes which act as important intermediates following activation of receptor tyrosine kinases (RTK) and G protein-coupled receptors (GPCR). These pathways are vital for contractile function, differentiation, survival, apoptosis and proliferation [60]. There is also strong evidence linking NRTK signalling to regulating vascular tone, increased intracellular Ca^{2+} levels [61] and Ca^{2+} sensitization [62].

A number of reports have linked NRTKs in modulating levels of free cytosolic Ca^{2+} and membrane potential. Touyz *et al* [63] demonstrated that in VSMC from human resistance arteries, angiotensin II induced a transient rise in $[Ca^{2+}]_i$, which was shown to be associated with a rise in IP_3 via tyrosine phosphorylation of phospholipase γ1 (PLC-γ1) [64,65]. Furthermore, L-type voltage-gated Ca^{2+} channel in VSMC are believed to be activated by tyrosine phosphorylation [66]. Wijetunge *et al* [67] was able to demonstrate that voltage-gated Ca^{2+} current is blocked by the tyrosine kinase inhibitors tyrphostin 23 and genistein. Liu and Sperelakis[68] also demonstrated that genistein, decreased the open time and increased the closed time of single L-type Ca^{2+}channels in rat portal vein cells.

NRTK have been implicated in regulating Ca^{2+} activated K^+ (BK_{Ca}) current in VSM. Genistein and lavendustin A both enhance BK_{Ca} current in rat tail artery cells, and tyrphostin A25 inhibit single channel currents during inside out patches[69]. More recently, Nagaraj *et al*[70] proposed that the Src-family kinases (SrcFK) is a crucial factor controlling potassium channels, acting as a cofactor for setting a negative resting membrane potential in hPASMCs. Taken together, these results demonstrate that NRTK have multiplicity of functions in regulating Ca^{2+} levels and membrane potential.

Several early studies, before the development of specific NRTK inhibitors, have also suggested that NRTK play an important role in Ca^{2+} sensitisation. These studies often used inhibitors

such as genistein to determine the role of tyrosine phosphorylation in smooth muscle contractility [71,72]. Subsequently, genistein reversibly inhibited contraction in alpha-toxin permeabilized smooth muscle preparations, demonstrating a role for protein tyrosine phosphorylation in Ca^{2+} sensitization[73]. Alpha-toxin permeabilization allows for the control of intracellular concentrations of some important factors required for the contraction, particularly calcium. By clamping the Ca^{2+} concentration at a constant level, factors that affect the sensitivity of the contractile machinery to Ca^{2+}, such as MLCP can be investigated. Skinned smooth muscle preparations effectively performs the same function as clamping Ca^{2+} concentration, except, the plasma membrane no longer maintains the ionic gradient necessary for maintaining the membrane potential. This allows for the control of calcium and other ions, therefore, intracellular signalling can be investigated without the influence of transmembrane currents [74].

Further evidence for the role of NRTK in Ca^{2+} sensitization has been shown in studies carried out by Toma *et al* [75] who demonstrated the effects of tyrosine kinase inhibitors on the contractility of rat mesenteric resistance arteries. Ohanian *et al* [76] demonstrated the involvement of tyrosine phosphorylation in endothelin-1-induced calcium-sensitization in rat small mesenteric arteries and Matinez *et al* [77] who investigated the involvement of protein kinase C, tyrosine kinases, and Rho-Kinase in Ca^{2+} handling of human small arteries. Furthermore, Sasaki *et al* [78] also demonstrated that TKIs, inhibited agonist- and GTPγS-enhanced Ca^{2+} sensitisation in skinned rabbit mesenteric artery.

GTPγS is a non-hydrolyzable G-protein-activating analog of guanosine triphosphate (GTP) and can mimic the Ca^{2+} sensitizing effects of receptor agonists. This prevents the GTP binding proteins from being inactivated, and allows the cellular processes and regulation to be investigated [79-81].

More recently, a number of studies using SrcFK specific blockers PP1 and PP2, have demonstrated a direct role of SrcFKs in contractile function [7,41,82,83]. Nakao *et al* [82] first provided evidence for the role of the SrcFK member, Fyn, in Ca^{2+} sensitization of coronary artery contraction mediated by the sphingosylphosphorylcholine (SPC)-Rho-Kinase pathway. Knock *et al* [41] demonstrate for the first time that agonist-mediated, Rho-Kinase-dependent Ca^{2+} sensitization but not basal Rho-Kinase activity in rat pulmonary artery requires SrcFK activity. Knock *et al* [7] further demonstrated a direct role of SrcFKs in the acute contractile response to hypoxia in small pulmonary arteries of rat. Finally, Shaifta *et al* [83] recently showed that SrcFKs mediates Ca^{2+} sensitization in airway smooth muscle (ASM), while Src and focal adhesion kinase (FAK) together and individually influence multiple Ca^{2+} pathways. SrcFKs will be dealt with in more detail in sections 1.4, 1.5 and 1.6.

1.3 Reactive oxygen Species

Section overview

Reactive oxygen species (ROS) are generated through the incomplete reduction of molecular oxygen. ROS are produced in healthy vascular tissue in response to a range of vasoconstrictor agonists and under hypoxic conditions which contribute to cellular functions. During hypoxic challenge, pulmonary arteries tend to constrict, a term commonly known as hypoxic pulmonary vasoconstriction (HPV). HPV is beneficial if it is short lived and highly localised, minimising the shunt effect. Global hypoxia throughout the lung can lead to pulmonary hypertension as this will cause constriction of the whole pulmonary circulation, thus increasing total pulmonary artery pressure and putting strain on the right heart.

This section will detail: what ROS are, how ROS are produced and the key players involved in their regulation. It will briefly detail why ROS are believed to act as key secondary messenger molecules mediating vascular smooth muscle contraction in response to multiple stimuli. This

will be followed by section 1.4, where I describe the evidence for protein kinases, in particular tyrosine kinases, as redox sensitive intermediates, in response to ROS production.

What are ROS?

Reactive oxygen species (ROS) are reactive molecules derived from molecular oxygen. They are diffusible, short-lived molecules that can reversibly oxidise proteins, lipid, ion channels and transcription factors within biological systems [84]. Initially, ROS were thought to occur solely as damaging bi-products of metabolism, however, they are now being recognised as bona fide second messengers in normal cellular function. ROS mediate responses such as gene expression, growth, survival/apoptosis, migration, adhesion and inflammation. However, ROS also modulate smooth muscle contractility [85], which will be the main focus of my PhD thesis.

There are several ROS species including superoxide ($O_2^{\bullet-}$), hydrogen peroxide (H_2O_2), peroxynitrite ($OONO^-$), and the hydroxyl radical ($OH^{\bullet}$), which are produced in biological systems. $O_2^{\bullet-}$ also reacts with NO, forming peroxynitrite ($ONOO^-$). It has been suggested that peroxynitrite ($ONOO^-$), modifies proteins through nitration or S-nitrosylation[86], although this is thought to be too indiscriminate to be of physiological relevance [87]. $O_2^{\bullet-}$ can pass through the membrane via anion channels and is believed to act as a major intermediate in contractile function and Rho-Kinase activation [88,89]. Knock *et al* [88] have shown that superoxide has very specific targets in pulmonary artery, independently of H_2O_2, namely activation of Rho-Kinase.

$O_2^{\bullet-}$ is converted to H_2O_2 by superoxide dismutase (SOD) [90]. H_2O_2 can also be produced by NADPH oxidase enzymes directly before $O_2^{\bullet-}$ leaves the enzyme [91]. H_2O_2 has received the most attention because of its higher stability compared to $O_2^{\bullet-}$ and due to its membrane permeability. It is important to note that not only does H_2O_2 act on adjacent targets, but because it is relatively stable, it can also serve paracrine functions. H_2O_2 is destroyed by catalase or glutathione peroxidise (by reduction to H_2O), but can be converted to hydroxyl radical ($OH^{\bullet}$) by the Fenton

reaction (catalysed by $Fe2^{+}$). As with peroxynitrite, hydroxyl radical is not thought to play a physiological role due to its extremely short half-life and highly reactive nature [87,92] .

1.3.1 How are ROS produced?

ROS production is tightly controlled by cytosolic or membrane-bound oxido-reductase enzymes including; NADPH oxidase, xanthine oxidase, cyclooxygenase, lipoxygenase, nitric oxide (NO) synthase, heme oxygenase, peroxidases and within the mitochondrial electron transport chain (complex I/III) (ETC). The main function of the ETC is to transfer electrons along the chain thus creating a proton gradient for the formation of ATP. However, when protons "leak" from the ETC, mainly from complex III, this generates ROS which mediates hypoxic pulmonary vasoconstriction (HPV) [93,94]. As mentioned, ROS can be produced by a variety of means, however I will focus specifically on NADPH oxidase and mitochondrial ETC ROS production.

1.3.2 NADPH Oxidase

NADPH Oxidases (NOX) proteins are a family of 7 membrane-associated, multiunit enzymes that catalyse the reduction of molecular oxygen using NADPH as an electron donor. Electrons are transferred from NADPH down an electrochemical gradient first to flavin adenine dinucleotide (FAD), then through the NOX heme groups and finally across the membrane to oxygen, forming $O_2^{\bullet -}$ [95,96]. In addition to these subunits, certain NOX enzymes contain EF-hand motifs at the N-terminus, allowing for the binding of Ca^{2+}. A limited number of NOX enzymes also contain a membrane-spanning region and a peroxidase-like domain at the N-terminus.

Expression of NOX

There are a number of NOX family members. However their expression, structure and ROS species produced varies between each NOX. The following table (Table 1.1) details this information:

Table 1:

NOX Isoform	Expression	Main Structure (reviewed in [97,98])	$O_2^{\bullet-}$ or H_2O_2
NOX1	Smooth Muscle [98,99] Endothelium [98] Osteoclasts [98]	- NOX1 - $p22^{phox}$ - NOXO1 (organiser) - NOXA1 (activator) - Rac1 (co-factor) - $p47^{phox}$ - $p67^{phox}$	- $O_2^{\bullet-}$ [100]
NOX2 (Phagocytic)	Phagocytes/Granulocytes [101] Endothelial Cells [102] Cardiomyocytes [103] Smooth Muscle[104]	- NOX2 - $p22^{phox}$ - $p47^{phox}$ (organiser) - $p67^{phox}$ (activator) - Rac2 (co-factor)	- $O_2^{\bullet-}$ [102]
NOX3	Fetal Kidney [98] Liver [105] Lung and Spleen [105]	- NOX3 - $p22^{phox}$ - NOXO1 (organiser) - NOXA1 (activator) - Rac (co-factor) - $p67^{phox}$ - $p47^{phox}$	- $O_2^{\bullet-}$ [106]
NOX4	Smooth Muscle [98] Endothelial Cells [107] Fibroblasts [108]	- NOX4 - $p22^{phox}$	- H_2O_2 [100]
NOX5	Lung [109] Skeletal muscle [109] Heart [109]	- NOX5 - Ca^{2+} (activator)	- H_2O_2 [110] - $O_2^{\bullet-}$ [110]
DUO 1	Thyroid [111] Cerebellum [111] Lungs [111]	- Duo1 - Ca^{2+} (activator) - $p22^{phox}$	- H_2O_2 [112]
DUO 2	Tracheal [113] Bronchial Epithelium[113] Thyroid [114]	- Duo2 - Ca^{2+} (activator) - $p22^{phox}$	- H_2O_2 [115]

Table 1.1: NOX Isoforms

Details NOX isoforms, expression, subunits present and what species of ROS each subunit is believed to produce.

General Mechanism of NOX activation

ROS are produced in healthy tissue in response to a wide variety of vasoconstrictor agonists including angiotensin [116], endothelin [117,118] and thrombin [119].

NOX activation occurs via calcium or protein–protein interactions and involves all NOX enzymes, with the exception of NOX4, which is constitutively active [120] and NOX5 and the DUOX enzymes which are directly calcium dependent [121,122]. Therefore control of NOX1, NOX2, and NOX3 is primarily achieved through alterations of the cytosolic proteins in response to stimuli such as GPCR activation.

In short, the activity of NOX1-3 in response to constrictor stimuli promotes translocation of $p67^{phox}$ [123] which binds to its NOX subunit. This binding is not strong and requires the adaptor proteins, active $p47^{phox}$ bound to $p22^{phox}$ [124,125] to augment $p67^{phox}$ to its NOX subunit. This function of $p47^{phox}$ is governed by phosphorylation, which occurs during activation of the oxidase [124,126]. The small GTPase Rac also binds to $p67^{phox}$ [127], thereby allowing for full NOX activity. In the case of NOX1 and 3, these are most highly activated by the $p47^{phox}$ and $p67^{phox}$ homologues, NOXO1 and NOXA1.

NOX4 is generally thought of being constitutive active therefore protein levels determine NOX4 activity and ROS production [128]. A growing number of studies suggest that NOX4 might also be acutely activated in response to agonist stimulation, but analysis of these papers show very mixed picture.

Finally, the physiological functions of NOX5 and DUOX1-2 are just emerging [129]. Due to the presence of EF hand motifs, the first stimulus identified to increase NOX5 activity was calcium.

Due to expression profile data already shown in table 1, NOX1, 2 and 4 are expressed in smooth muscle. NOX1 is known to be activated by angiotensin II (AngII) [130] and upregulated in Dahl

salt-sensitive rats[131]. More recently, Shaifta *et al* [99] demonstrated that NOX1 is essential in the generation of ROS for the contraction potentiating actions of sphingosylphosphorylcholine (SPC) in mesenteric arteries. Here, using mice lacking $gp91^{phox}$ (NOX2) or $p47^{phox}$, the organizer subunit for NOX2 and NOX1, potentiation was the same in vessels from WT and $gp91^{phox}$2/2 mice, it was absent in mice lacking $p47^{phox}$. NOX4 is thought to be constitutively active and responsible for basal ROS production [132,133]. This strongly suggests that activation of NOX1 and consequent generation of ROS are essential for the potentiating actions of SPC. Similar activation of NOX1 also occurs in response to the thromboxane analogue U46619 [134,135].

1.3.3 Mitochondria

The Mitochondria acts as another major source of cellular $O_2^{\bullet-}$ produced as a by-product of incomplete oxidative phosphorylation [136]. In particular, complexes I [137], II [138] and III [139] of the mitochondrial respiratory chain "leak" electrons during respiration to form $O_2^{\bullet-}$. From complex I and II, $O_2^{\bullet-}$ is released into the matrix where due to the high concentration of antioxidants, ROS is rapidly broken down, whereas complex III[139] can release $O_2^{\bullet-}$ from both sides of the inner mitochondrial membrane (figure 1.2). Antioxidants such as SOD2 (MnSOD) and catalase found in the mitochondria, rapidly breakdown or sequester $O_2^{\bullet-}$ and H_2O_2 to reduce reactivity to reduce the reactivity of these radicals (figure 1.2). This is detailed in figure 1.2:

Figure 1.2:

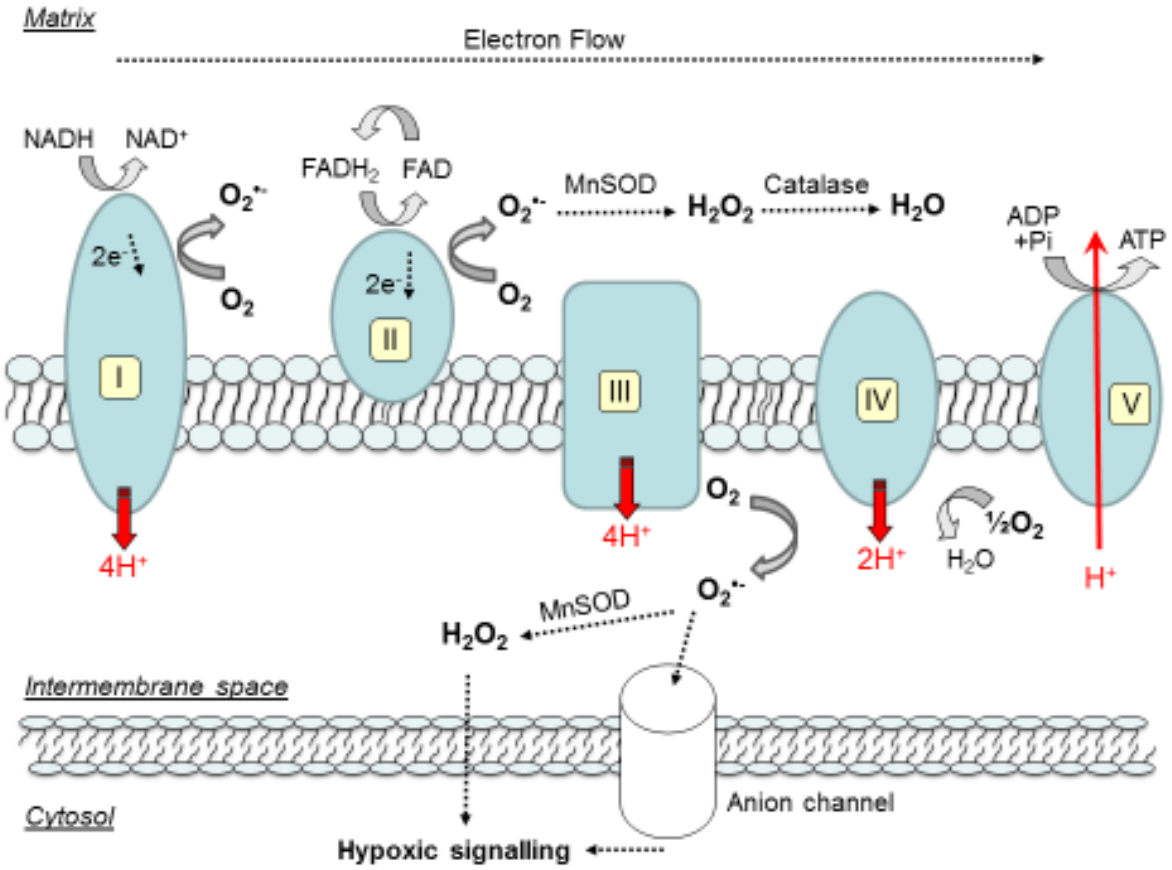

Figure 1.2: Mitochondrial ETC complexes can generate superoxide from multiple sites
Complex I and II release ROS primarily into the matrix compartment, where manganese superoxide dismutase (MnSOD) converts superoxide to hydrogen peroxide (H_2O_2). Hydrogen peroxide is further broken down by catalase to water. Complex III can generate ROS which is rapidly released into the intermembrane space. Superoxide can enter the cytosol via anion channels or converted to hydrogen peroxide and diffuse across the membrane.

Hypoxia

It is believed that hypoxia promotes ROS production from the mitochondria. This is known as the ROS hypothesis[140,141]. At first glance, this seems counter-intuitive, since the production of superoxide is dependent on the availability of O_2 as an electron acceptor. However, there are a number of factors which favour the release of ROS from the mitochondria.

Activation of mitochondrial potassium channels have been described to enhance ROS production. Marshall *et al* [102] first described the activation of NAD(P)H Oxidase (NOX) and increased superoxide production under hypoxic conditions. More recently, a link between NOX and the mitochondria has been described in endothelial cells. Here, Dikalov *et al* [142] describe how angiotensin II activates NOX2 which enhances ROS production subsequently activating ROS sensitive PKCε. PKCε phosphorylates and activates the mitochondrial ATP-sensitive potassium channels (mitoK$_{ATP}$) which increased the production of mitochondrial ROS [143,144] via reverse electron flow[102].

Recently, the Rieske iron-sulphur protein (RISP), which transfers one electron from ubiquintol at the outer ubinquintol-binding site to cytochrome c forming ubisemiquinone, which subsequently transfers an electron to cytochrome b. Ubisemiquinone has been shown to transfer electrons to molecular oxygen and produce superoxide. Knockdown or over-expression of RISP has been shown to inhibit or increase hypoxia induced ROS production[94,145,146].

The degradation of ROS is tightly regulated by antioxidant enzymes and cellular REDOX buffers [87] which rapidly breakdown ROS thereby reducing the chance of oxidative damage.

1.3.4 Antioxidant enzymes

The redox state of vascular tissues is controlled by oxidative stimuli and antioxidant enzymes such as SOD, catalase and glutathione redox buffers. The cell is normally kept in a reduced state however when this balance is shifted in favour of oxidation (oxidative stress)[147], this can affect cellular signalling pathways and promote disease states such as hypertension [116] and reperfusion injury [148]. These proteins are key in preventing damage from oxidative stress. It is important to note, that antioxidant enzymes/proteins also function beyond protecting the cell from oxidative damage. They are also key in 'normal signalling', being involved in the

termination and localisation of normal ROS bursts which could be involved in regulating oxidative signalling.

In response to physiological stimuli there is an increase in ROS production which is regulated and occurs in specific micro domains. This is different from oxidative stress as during oxidative stress there is an imbalance between the production of free radicals and the ability of the body to counteract or detoxify their harmful effects.

Superoxide dismutase (SOD)

There are 3 SODs found in mammalian cells, (SOD1, SOD2, and SOD3). SODs convert $O_2^{\bullet-}$ to H_2O_2. SOD1, a Cu/Zn SOD, is expressed in the cytoplasm, SOD2 (manganese containing) is also known as mitochondrial manganese SOD because of its localization. Finally, SOD3 (also Cu/Zn containing), which is secreted and then bound to the outer plasma membrane. Deletion of SOD has been implicated in a number of disease states [149].

Catalase

Catalase, catalyses the breakdown of H_2O_2 to water and O_2. Catalase contains 4 heme groups. The heme-iron is initially oxidized by H_2O_2 to form molecular oxygen and water [150]. Catalase expression is high in many tissues however catalase null mice develop normally [151].

Cellular Redox Buffers

Cellular redox buffers are buffer systems located within the cell that control levels of ROS thus protecting the cell from oxidative damage e.g. oxidative modification of proteins. There are three main redox buffers: Glutathione (GSH), Thioredoxins (Trx) and Peroxiredoxins (Prx).

Glutathione

GSH is considered the main redox buffer in a cell because of the large amount of reducing equivalents supplied by GSH [152] (glutathione present in cells at mM concentrations). GSH

molecules are easily oxidized to form GSH disulfide (GSSG), which is then reduced back to GSH by the reaction with GSH reductase (GR).

Reduced glutathione (GSH) can donate H^+ and e^- to ROS such as $O_2^{\bullet-}$ but forms a reactive GS. But 2 GS react together to form GSSG (oxidised glutathione). Glutathione peroxidase catalyses $2GSH + H_2O_2 \rightarrow GSSG$. 2 GSH are regenerated from GSSG by glutathione reductase, utilising NADPH as a reducing agent

The intracellular thiol redox status is described as the ratio of reduced to oxidized forms, GSH/GSSG, showing 100 or more at the steady state but decreasing to 10 or less under oxidative stress conditions [153,154].

Thioredoxins

Thioredoxins (Trx) are a group of ubiquitous antioxidant enzymes, found in organisms ranging from archae to mammals which contains two cysteines in the redox active centre [155]. They regulate the function of target proteins through oxidoreductase activity. Trx couples with Trx-dependent peroxidases (Prxs) to scavenge hydrogen peroxide (H_2O_2) and peroxynitrite along with catalyzing the reduction of disulfide bonds [156-158]. Organisms have developed their specialized subset of Trxs, which are located in various cellular compartments. For instance, some Trxs are abundant in the cytosol [159], while others are translocated to the nucleus [160,161] or mitochondria, associated with the cell membrane [162] or secreted to the extracellular environment [163].

Peroxiredoxins

Peroxiredoxins (Prx) are thiol-specific antioxidant proteins, also termed the thioredoxin peroxidases. Prxs exert their protective antioxidant role in cells through their peroxidase activity via redox-active cysteines whereby scavenging hydrogen peroxide, peroxynitrite and a wide range of organic hydroperoxides (ROOH) which are reduced and detoxified [164-168]. Along with

Trx, Prx are also able to catalyse the reduction of disulphide bonds. Although located primarily in the cytosol, Prxs are also found within mitochondria, peroxisomes, nuclei and membranes, and, in at least one case, exported [164] . Prxs are produced at high levels in cells and compose 0.1–0.8% of the soluble protein in other mammalian cells [169].

Glutathione Peroxidase (GPX)

Gpx promotes the breakdown of H_2O_2 and lipid hydroperoxides to water or corresponding alcohols using reduced glutathione (GSH) [170]. Gpx is thought to play a more critical protective antioxidant role in the cardiovascular system than catalase [171]. Gpx knockout mice exhibit increased susceptibility to ischemia–reperfusion injury [172].

These systems along with enzyme systems already discussed, offer a powerful antioxidant defence mechanisms.

1.4 Oxidative modification of Tyrosine Kinases in Vascular Function

Section Overview

Protein function can be altered by oxidative modification of amino acid residues, especially cysteine. At "physiological" levels of ROS, this oxidative modification may be limited to specific cysteine residues found on key proteins involved in cellular signal transduction which may alter their function and interactions with other proteins. Some of these include membrane channels such as K^+ channels and Ca^{2+} channels, tyrosine phosphatases and protein kinases.

Amongst the latter are the Src family of non-receptor tyrosine kinases (SrcFK) which may be activated through direct oxidative modification, while tyrosine phosphatases are inhibited leading to a net increase in phosphorylation. The eponymous member of the kinase family, Src, is of particular interest as a signalling molecule involved in proliferation and migration along with regulating multiple signalling pathways in smooth muscle contraction.

In this section, I will describe the relationship between ROS production (agonists and hypoxia) and activation of NRTK, specifically SrcFK, and how this relates to smooth muscle contraction.

Introduction

Non-receptor tyrosine kinases (NRTKs) are cytoplasmic enzymes which act as important intermediates following activation of receptor tyrosine kinases (RTK) and G protein-coupled receptors (GPCR).

Although both types of tyrosine kinases are primarily known for their roles in cell growth and proliferation, studies by Di Salvo *et al* [173,174] and Hollenberg's *et al* [72,175] suggested that NRTK also play an important role in vasoconstriction in response to G protein coupled receptors (GPCR) activation. This idea was suggested from observations that tyrosine kinase inhibitors (TKI) attenuated vasoconstrictor-induced contraction. Furthermore, activation of GPCR caused

tyrosine phosphorylation of multiple cellular proteins.There is now an increasing body of evidence indicating that tyrosine phosphorylation is an important proximal signalling mechanism following contractile stimuli, many of which also increase ROS production, including angiotensin II (Ang II), endothelin-1 (ET-1), and thrombin [84,116,118,119]. While most of the above involve activation of NADPH oxidase, there is evidence that ROS derived from mitochondria play an important signalling role. A specific example of the latter is hypoxic pulmonary vasoconstriction (HPV), where it has been proposed that the initial stimulus is hypoxia-induced elevation of mitochondrial ROS production [94,140,176] as discussed in section 1.3.3.

Furthermore, increased ROS levels have been shown to increase tyrosine phosphorylation in vascular tissue [72,177,178]. Evidence for a role of NRTK in GPCR-mediated vasoconstriction has come from numerous studies which have shown that TKI or tyrosine phosphatase inhibitors such as sodium orthovanadate can inhibit or enhance vasoconstriction. Furthermore, two previous studies using broad-spectrum tyrosine kinase blockers (genistein and tyrphostin) suggested that tyrosine kinases were involved in HPV[179,180], however due to the non-specificity of these TKI, the kinase involved was unknown.

Finally, a number of early studies using non-specific TKI such as lavendustin A and tyrphostin 47 been reported to see an increase rather than inhibit tyrosine phosphorylation. This disparity is due to the poor selectivity of these early non-specific TKI, and explains how using non-specific TKIs can exert opposing effects [181-184]. More recent, selective SrcFK inhibitors such as PP1, PP2, and SU6656 have demonstrate a high efficacy for SrcFK with very little non-specific effects [185-187].

1.4.1 Non-receptor tyrosine kinase (NRTK)

Many NRTKs are localised in the cytoplasm however some are anchored to the cell membrane via myristoylation and palmitoylation. In general, NRTKs contain SH2 and SH3 domains which are examples of non-catalytic domains involved in protein-protein interaction[188]. The Src Homology 2 (SH2) interacts with phospho tyrosine residues and Src Homology 3 (SH3) which interacts with proline rich sequences. The majority of NRTKs have a catalytic domain which is held in an inactive state through intramolecular bonds. However, the catalytic domain can be activated via auto-phosphorylation or via phosphorylation by another kinase [189], thereby opening the kinase domain. An example of this being activation of integrins, which bind ECM ligands subsequently activating SrcFK via activation of focal adhesion kinase (FAK) leading to further downstream signalling [190].

1.4.2 Kinase regulation by ROS

Protein kinases modify the function of target proteins by catalysing phosphorylation of tyrosine, threonine and/or serine residues. There are a number of protein kinases implicated in smooth muscle constriction, including receptor tyrosine kinases (e.g., epidermal growth factor-receptor [EGF-R] and platelet-derived growth factor-receptor [PDGF-R]), SrcFK, PKC, mitogen-activated protein kinases (MAPKs), and Rho-Kinase [191], many of which are prime targets for redox regulation.

Importantly, responses to physiological stimuli and changes in protein kinase activity are blocked by antioxidants. This suggests that ROS act as intermediate signalling molecules between stimulus and downstream effectors, such as kinases. This is consistent with the knowledge that exogenously applied ROS from xanthine/xanthine oxidase or quinones such as LY83583 [88,151] promote vasoconstriction. Vascular beds where externally applied ROS promote constriction include aorta[192] , pulmonary artery[88,193,194] and coronary artery[195]. ROS-mediated

vasoconstriction is inhibited by nonspecific tyrosine kinase inhibitors (e.g., genistein)[192], specific inhibitors of SrcFK [41,196] and Rho-Kinase inhibitors [88,192,197].

Exogenous ROS can also cause relaxation, depending on the vascular bed and the nature of any pre constriction [88,198]. Snetkov *et al* [89] demonstrated that $O_2^{\bullet-}$ promotes Rho-Kinase-dependent Ca^{2+} sensitization in pulmonary but not mesenteric arteries. In both arterial types, $K_{(V)}$ channels are shown to be open, however this only results in relaxation in mesenteric. This indicates that Rho-Kinase mediated Ca^{2+} sensitization is having an overriding effect in the pulmonary arteries which is not mirrored in the mesenteric arteries. Suggesting, a fundamental difference in what signalling pathways have a greater influence over vascular tone in different vascular beds.

It is clear that ROS play an important role in vascular function. As mentioned, there are a number of ways in which kinases can be activated or inhibited by oxidation. This can occur through oxidation or nitrosylation of redox-sensitive cysteines found within the kinase or via regulatory proteins such as tyrosine phosphatases[87,199]. It has also been suggested that nitration or nitrosylation of tyrosine residues by peroxynitrite may also prevent tyrosine phosphorylation [86], it is unknown how tightly regulated this process is [87].

1.4.3 Src-Family Kinases (SrcFK)

SrcFKs are a group of closely related NRTKs including the eponymous member Src [200]. SrcFKs have a molecular weight between 52-62kDa possessing six distinct and functional domains [201] (Figure 1.3). There are nine members of SrcFKs which have been well characterised in mammalian cells [200]. The most widely expressed members of the Src family include c-Src, Fyn, Yes, Lyn, Hck, Blk, Fgr and Frk [202]. Our laboratory has shown that Src, Fyn and Yes are highly expressed in rat intra-pulmonary arteries (IPA) and cultured pulmonary arterial smooth muscle cells (PASMCs) at both the mRNA and protein levels[41]. Furthermore, Src has been shown to be highly expressed in human tracheal smooth muscle cells[202].

Figure 1.3

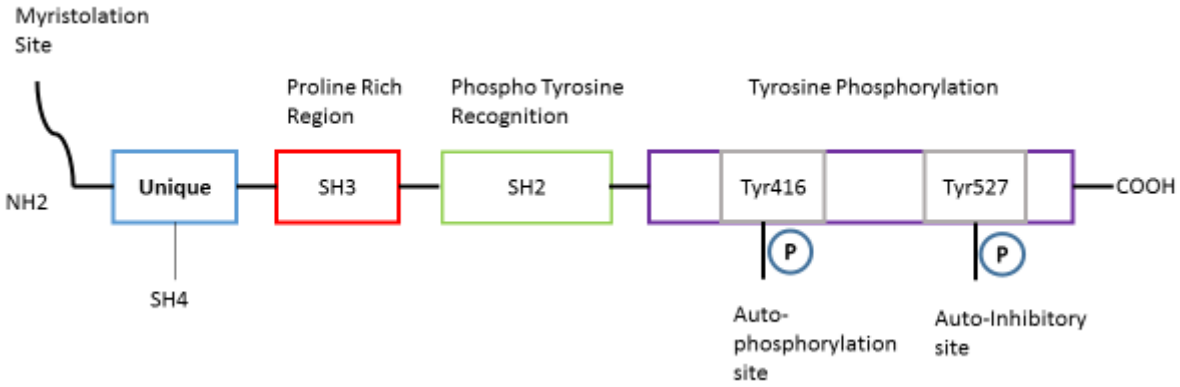

Figure 1.3: SrcFK Structure
The domain structure of Src family kinases. The Src kinase architecture consists of four domains: the unique region, which varies among family members, followed by the SH3 (protein-protein interactions), SH2 (binds to phospho tyrosine residues on other proteins or within same protein. The auto inhibitory site (Tyr 527) is required to be de phosphorylated followed by phosphorylation at (Tyr 416) for Src to be activated unless another protein disrupts the internal SH2 (tyr527) binding). These sites are indicated. Finally the SH4 domain is important for membrane targeting.

SrcFK exists either in a folded inactive form or an open active form. Src contains two important phospho-tyrosine residues, one in the kinase activation loop (tyr-416 in humans) and one in the C-terminal regulatory domain (tyr-527 in humans). The inactive form is kept folded by binding of the Src Homology 2 (SH2) domain with the phosphorylated tyr-527. This is stabilized by internal binding of the Src Homology 3 (SH3) domain with the proline-rich linker region [203]. Src is activated by de-phosphorylation of tyr-527 or by proteins binding to the phospho-tyrosine residues or proline-rich regions, such as the platelet-derived growth factor-receptor (PDGF-R) [203]. This results in the autophosphorylation of tyr-416 in the kinase domain, thereby fully activating the kinase. Tyr-416 may be further phosphorylated within the SH2 domain, by PKC, further destabilizing internal binding and activating Src [203]. Src inactivation occurs through either de-phosphorylation of tyr-418 or re-phosphorylation of tyr-527 by C-terminal src kinase (CSK)[203].

1.4.4 SrcFK regulation by ROS

SrcFK can be a target for either direct redox regulation and/or regulation indirectly through redox modification of associated proteins, such as tyrosine phosphatases.

Contractile stimuli that generate ROS have been shown to activate SrcFK. This has been demonstrated in studies that measure Src activity directly, or use tyr- 418 phosphorylation as a measure of activity. These stimuli include hypoxia/reoxygenation [7,204,205], stretch [195], growth factors [206], and GPCR agonists [99,116-118,207]. Activation of Src in response to GPCR agonists is linked to NOX activity [193,208] and in response to hypoxia, mitochondrial ROS [204]. Src is also activated by exogenous H_2O_2 in various tissues including vascular smooth muscle, at concentrations believed to be within the physiological range [209-211]. However, Src has been shown to be inactivated by H_2O_2 [212]. The latter study used 20 mM H_2O_2 as an oxidizing agent, which would be considered higher than physiological range of ROS. Therefore, Src may be activated by physiological levels of ROS however inactivated at higher concentrations.

In addition, since the primary trigger for HPV is believed to be an increase in mitochondrial ROS production [94], it is interesting to note that hypoxia enhances Src activity [7,204], while Src inhibition, inhibits HPV [7]. Thus, SrcFKs are prime targets for hypoxia-induced ROS as part of the mechanism of HPV.

Direct Redox Regulation of SrcFK

SrcFK proteins contain cysteine residues, cys-245 in the SH2 domain and cys-487 in the kinase domain, which have been shown to be redox sensitive to lipoxygenase-derived ROS at focal adhesions [213]. This study showed that Src activation was bi-phasic, the first phase involving dephosphorylation of tyr-527 mediated by protein tyrosine phosphatase (PTP), and the second phase involving oxidation of cys-245 and cys-487, resulting in enhanced Src activation.

Alternatively, SrcFK may also be activated through oxidation of as yet unidentified cysteine residues by either H_2O_2 or NO [211].

Indirect Redox Regulation of SrcFK

Exogenous ROS, peroxynitrite, and stimuli that can increase ROS production, increase cellular tyrosine phosphorylation, indicating that either PTP are inhibited or kinases are activated, or both [177,214]. All PTPs contain cysteine residues in their catalytic domains that are essential for catalytic activity. These cysteine residues has low pKa values and are therefore more sensitive to oxidation than cysteine residues of most other proteins[199].

PTPs can reverse tyrosine phosphorylation of downstream targets and are able to de-phosphorylate both tyr-527 and tyr-418 of Src. Therefore, the redox state of the cell and sensitivity of PTPs expressed will affect tyrosine phosphorylation. Currently, the PTPs that regulate SrcFK are unknown, however tyr-527 has been shown to be de-phosphorylated by the cytosolic phosphatases PTP1-B, SHP-1, SHP-2 PTP-a and CD45, with some reports also suggesting that PTP-BL and CD45 can de-phosphorylate Src at tyr- 418 [212,215,216].

Positive feedback between Src activation and ROS production

Src has been implicated as part of a positive feedback loop involved in enhancing ROS production [217-219]. Src has been shown to be upstream of serine phosphorylation of $p47^{phox}$ in response to angiotensin II, suggesting an intermediate kinase such as PKC [220]. In endothelial cells, Src mediates tyrosine phosphorylation of $p47^{phox}$ [126]. Furthermore, Ang II activates NOX which subsequent activates Src in a ROS-dependent manner, subsequently through transactivation of the EGF-R, activates rac-1, which is required for assembly and activation of NOX [219]. Finally, as discussed in the section 1.3.3, Dikalov *et al* [142] has shown the role of PKC and SrcFK in ROS induced ROS release. Interestingly, PKC and Src are themselves redox-

sensitive, giving rise to the possibility of positive feedback-mediated amplification and further signalling[92].

1.5 G-protein coupled receptors and smooth muscle regulation

Section Overview

Ca^{2+} sensitization in response to constrictor stimuli occurs primarily through the activation of the monomeric G protein RhoA and its principle effector Rho-Kinase. Rho-Kinase enhances constriction by phosphorylating the myosin phosphatase targeting subunit (MYPT-1), thereby inhibiting myosin phosphatase activity and enhancing myosin light chain phosphorylation. Previous studies have shown that constriction induced by agonists and hypoxia in pulmonary arteries involves activation of both RhoA and Rho-Kinase. Furthermore, it has been suggested that SrcFKs contributes to constriction though activation of RhoA/Rho-Kinase. The key proteins involved in RhoA/Rho-Kinase activation that are phosphorylated by Src are unknown. Logical targets are guanine nucleotide exchange factors (RhoGEFs) which promote exchange of GDP to GTP on RhoA, causing activation.

So far, I have outlined the evidence for ROS being produced in response GPCR stimulation but also under hypoxic conditions. Here, I discuss the evidence for SrcFK being a key component of GPCR signalling.

Introduction

Contraction occurs in response to a number of stimuli, one such stimuli is agonist-induced activation of GPCR. Heterotrimeric G proteins (Gα, Gβ/Gγ subunits) are molecular switches that turn on intracellular signalling cascades in response extracellular stimuli.

There are approximately 460 non-olfactory receptors encoded in the mammalian genome [221] which are activated by a broad spectrum and diverse ligands including neurotransmitters and hormones[222,223]. Upon activation, GPCRs undergo a conformational change which activates

heterotrimeric G proteins by promoting the exchange of GDP/GTP associated with the Gα subunit. This leads to the dissociation of Gβ/Gγ from Gα. These become free to act upon their downstream effectors and thereby initiate unique intracellular signalling responses. After the signal is terminated (via intrinsic GTPase activity, RGS proteins or ligand disassociation), GTP of Gα-GTP is hydrolysed to GDP and Gα becomes inactive (Gα-GDP), which leads to its re-association with the Gβ/Gγ dimer to form the inactive heterotrimeric complex[224].

1.5.1 Heterotrimeric G Proteins

GPCRs are characterised by having a seven-transmembrane domain containing an extracellular N terminal and a cytoplasmic c terminal [225]. The characteristics and class of GPCRs will not be described here in extensive detail. There are four basic families of guanine nucleotide-binding proteins (G-Proteins) involved in smooth muscle contraction. These are characterised depending on their G-protein α-subunit; $G\alpha_s$, $G\alpha_{I/}G_o$, $G\alpha_{q/}G_{11}$ and $G\alpha_{12/13.}$ [226].

There are three main classes of G-proteins which are involved in mediating smooth muscle contraction; $G_{I/}G_o$, $G_{q/}G_{11}$ and $G_{12/13}$. Receptors which are coupled to $G_{q/}G_{11}$ activate PLCβ, stimulate IP_3 mediated release of $[Ca^{2+}]_i$ from the SR and DAG mediated Ca^{2+} influx from membrane bound channels [227]. Activation of receptors coupled to $G_{I/}G_o$ can promote contraction due to inhibition of adenylyl cyclase and decreased protein kinase A (PKA) signalling [29]. This counteracts smooth muscle relaxation promoted by activation of G_s which stimulates the PKA pathway by enhancing the activity of adenylyl cyclase which increases levels of cyclic AMP (cAMP) which in turn activates PKA and promotes relaxation [228]. Finally, receptors coupled to $G_{12/13}$ act via Rho guanine nucleotide exchange factors (RhoGEFs) specifically the RGS domain containing RhoGEFs (p115 RhoGEF, PDZ-RhoGEF and LARG-RhoGEF) [229,230] (these will be discussed in greater detail in section 1.7.4). This results in the activation of RhoA via exchange of GDP to GTP and subsequent activation of Rho-Kinase mediated calcium sensitization

[29,46,231]. Rho-Kinase can also promote actin polymerization [232] as well as play a pivotal role in a number of other functions.

1.5.2 SrcFK activation by Heterotrimeric G-proteins

Activation of Src by G-proteins is just one of the many events following receptor stimulation [233]. Activation of Src by GPCRs can be direct, via association with the intracellular receptor domain of the GPCR or indirectly via other means, such as oxidative modification [234].

During my project, I used an agonist called U-46619 (U46). U46 is a thromboxane mimetic that induces vasoconstriction via activation of the TP receptor. This has been previously shown to involve Ca^{2+} sensitization[231,235,236] as well as increase intracellular calcium [231,237,238]. TP receptors are widely distributed in a variety of cell types including smooth muscle[239-242]. The TP receptor is known to be coupled to G_q and stimulate DAG/IP_3 secondary messenger system[243]. More recently, the TP receptor has also been found to be coupled to $G_{12/13}$[244]. Activation of $G_{12/13}$ is known to regulate RhoGEF proteins which are upstream of RhoA/Rh-Kinase [245]. U46 is a potent vasoconstrictor in IPA's and highly efficient at promoting vasoconstriction in IPA.

An essential question is how SrcFK are being activated by U46, which G-protein is involved and how it activates SrcFK?

Early experiments demonstrated that SrcFKs could be activated by a number of G-protein-coupled-receptors (GPCRs), including the lysophosphatidic acid (LPA_1, LPA_2, LPA_3)[246-248], α2A adrenergic[249], M1 muscarinic [249], M2 muscarinic[250], PAR-1[251] and PAR-2[252], ET_A[253] and AT_1[254] . Src activation by GPCRs coupled has predominantly been shown to be linked to pertussis toxin-sensitive Gi/o family G proteins, like the LPA, and is inhibited by proteins that sequester Gβγ subunits. However, Gq/11-coupled receptors like the AT_1 receptors can also mediate Gα subunit-dependent Src activation.

Several GPCRs including the TP receptor[255] contain consensus SH3 domain-binding motifs within their third intracellular loops or C-terminal tails. The β3 adrenergic receptor is an example where receptor activation promotes the formation of a complex between Src and the receptor [256]. Similar result have also been demonstrated with the purinergic P2Y2 receptor [257]. Direct interactions between Src and the TP receptor have not been shown. However, it is entirely possible Src can directly interact with the TP receptor due to the presence of its SH3 domain binding motifs found on both proteins.

Numerous studies also suggest that direct interactions between Src and Gα subunits may regulate SrcFK activity. Incubation of Src with GTP-γS-bound $G\alpha_s$ and $G\alpha_I$ results in a significant increase in Src activation [258]. $G\alpha_{12}$ has also been shown to activate Src via recruitment of HSP90 which increased paracellular permeability in response to thrombin [259]. Furthermore, overexpression of $G\alpha_{11}$ enhanced SrcFK activity leading to enhanced JNK and p38 MAPK activity which is blocked by the SrcFK inhibitor, PP2 and CSK overexpression [260]. Finally, the Gβγ complex which was originally believed to act as docking proteins for Gα subunits has been found to act as a key intermediate responsible for the activation of Src [246,261]. These findings suggest that SrcFK may function as G-protein-regulated effectors particularly with receptors that are bound to these subunits.

Signalling through GPCRs is regulated by arrestins. Arrestins bind to the receptors which prevents further G-protein activation. β-arrestins have been shown to function as signal transducers whereby β-arrestin 1 and β-arrestin 2 can bind directly to Src and recruit it to agonist-occupied GPCRs. The formation of β-arrestin:Src complexes on desensitized GPCRs appears to promote a 'second wave' of GPCR signalling [262].

ROS have also been implicated in signalling pathways initiated by other vasoconstrictor agonists, including angiotensin II and endothelin[263] coupled to PLC via G_q. Activation of G_q/PLC is known to be coupled to enhanced Src and PKC activity.

SrcFK has not been shown to be regulated directly by Ca^{2+} however other kinases such as protein-tyrosine kinase 2 (PYK2) [264] or PKC[92], which associate with SrcFK, are regulated by Ca^{2+}. As mentioned, the TP receptor is known to be coupled to G_q and stimulate DAG/IP_3 secondary messenger system[243] and increase Ca^{2+}, therefore it is possible that this increase in calcium can activate PYK2 or PKC to further activate SrcFK and promote signalling.

1.6 Rho-associated coiled-coil Kinase protein family (Rho-Kinase)

Section Overview

Rho-Kinase is a serine/threonine kinase and a member of the AGC family of kinases, activated by the monomeric G-protein, RhoA [16]. Leung and colleagues were the first to identify Rho-Kinase as an effector for the GTPase Rho[265]. Rho-Kinase has since emerged as an important factor in organisation of the actin-myosin cytoskeleton as well as an important regulator of cell contraction, motility, morphology, cell division, metabolism and gene expression [16,266,267].

Until now, I have detailed the evidence for SrcFK acting a ROS-sensitive intermediate and key component of GPCR signalling. This section, I will primarily describe the evidence implicating SrcFK as an upstream mediator of Rho-Kinase.

1.6.1 Expression of Rho-Kinase

There are two known isoforms of Rho-Kinase expressed in the mammalian system: ROCK1 and ROCK2. Rho-Kinase proteins are ubiquitously expressed however, ROCK2 is highly expressed in the brain and skeletal muscle [268-270]. Both ROCK1 and ROCK2 are expressed in

VSM[271]. ROCK2 predominantly regulates VSMC contractility by directly binding to and phosphorylating the myosin-binding subunit of myosin phosphatase [272].

1.6.2 Structure and activation of Rho-Kinase

Rho-Kinase is comprised of an amino-terminal or (N-terminal) catalytic domain, a central coiled-coil domain, a Rho-Binding domain (RBD) and a carboxyl-terminal (C-terminal) domain. The C-terminal has a pleckstrin homology (PH) domain containing a cysteine rich region of which the function is unknown [16,273]. The PH domain is involved in protein localisation and serves as a site for protein-protein interactions [274] (Figure 1.4).

Figure 1.4

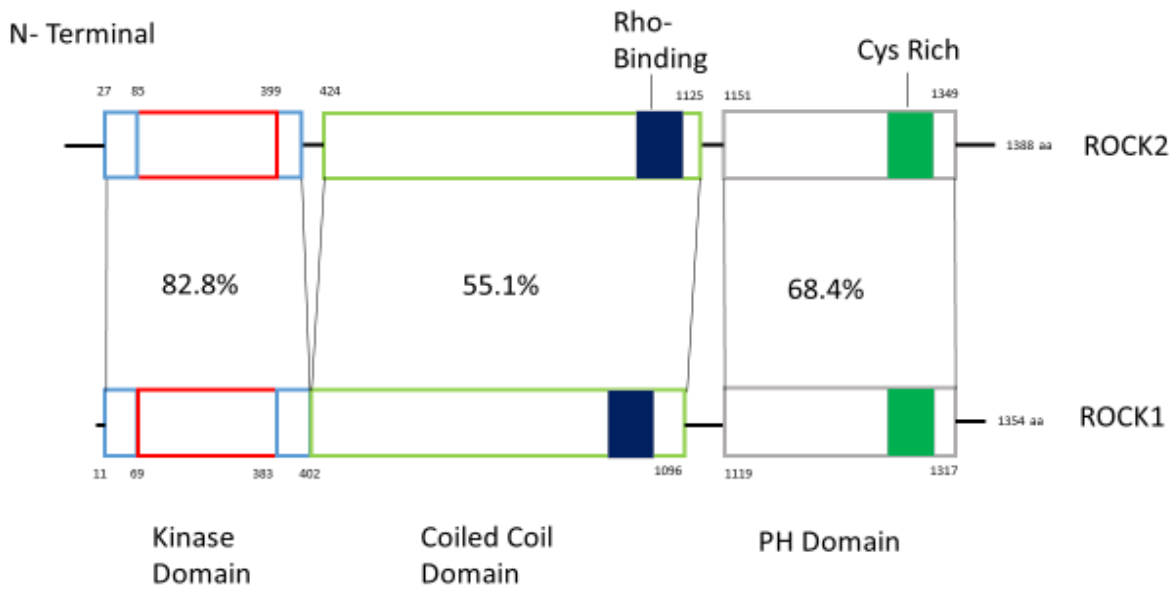

Figure 1.4: Rho-Kinase structure
Structure of Rho-Kinase. The structure of Rho-Kinase comprised of a Kinase domain, coiled coil domain containing a Rho-Binding domain and a pleckstrin homology (PH) domain containing a cysteine rich area.

The structure of Rho-Kinase is such whereby the coiled-coil domain acts as an auto inhibitory domain and the PH domain targets the protein to the membrane. This setup ensures that the kinase domain of Rho-Kinase is inhibited when unstimulated. Rho-Kinase is activated by GTP-bound RhoA which binds to the coiled-coil domain, compromising the binding between the c-

terminal region and the kinase domain thereby freeing/activating the kinase [16]. Rho-Kinase is not known to be directly regulated by other kinases or ROS.

1.6.3 Evidence for SrcFK Upstream of Rho-Kinase

There is an increasing amount of evidence implicating SrcFKs in agonist- induced Ca^{2+} sensitization. Many contractile stimuli, including various GPCR agonists, hypoxia and exogenous ROS activate RhoA/Rho-Kinase in VSM and there is pharmacological evidence that this is partly mediated via SrcFK[7,41,82,264].

Nakao *et al* [82] first demonstrated that crosstalk between NRTK and Rho-Kinase may underlie Ca^{2+}sensitisation. In this report, sphingosylphosphorylcholine (SPC) enhanced contraction of pig coronary artery strips with a minimal rise in $[Ca^{2+}]_i$. SPC-induced contraction was blocked by the SrcFK inhibitor PP1 and by the *S*-palmitoylation inhibitor EPA, which inhibits *S*-palmitoylation of SrcFKs thereby inhibiting their ability to anchor to the cell membrane. These VSMC preparation expressed both Src and Fyn, and SPC was able to promote translocation of Fyn, but not Src, to the plasma membrane. SPC was also able to enhance translocation of Rho-Kinase to the membrane, which was again inhibited by PP1 and EPA. This suggests a direct role for Fyn in promoting membrane translocation of Rho-Kinase, thought to be a crucial step in which it promotes Ca^{2+} sensitisation.

More recently, Knock *et al* [41] evaluated the role of SrcFK in Ca^{2+}-sensitization-dependent prostaglandin $F_{2\alpha}$ ($PGF_{2\alpha}$)-mediated contraction in rat small distal pulmonary arteries. This report demonstrates that the SrcFK -selective inhibitors, SU6656 and PP2, both selectively inhibit $PGF_{2\alpha}$-induced but not direct Ca^{2+}-induced contraction in α-toxin-permeabilized rat pulmonary artery. Also, SU6656 and PP2, inhibited $PGF_{2\alpha}$-mediated but not basal MLC_{20} phosphorylation at ser-19, suggesting the involvement of SrcFK only during stimulation of G-protein-coupled receptors. Furthermore, $PGF_{2\alpha}$ enhanced MYPT-1 phosphorylation at thr-855 (target for Rho-Kinase) was inhibited by SU6656 although

phosphorylation was unaffected, again suggesting that the involvement of SrcFK only during stimulation of G-protein-coupled receptors. Existing kinase inhibitors cannot easily distinguish between Src, Fyn, or Yes, all 3 of which are highly expressed in IPA. To distinguish which family member is involved in Ca^{2+} sensitization, these kinases do differ in the way that they are post-translationally modified, Src is dual myristoylated, whereas both Fyn and Yes are also palmitoylated[275]. Knock *et al* demonstrate that the non-selective acylation inhibitor 2-bromopalmitate, but not the selective palmitoylation inhibitor EPA [41,276], inhibited PGF2α-mediated Ca^{2+} sensitization. Subsequently, this report tentatively suggested that the eponymous member Src is in fact involved in $PGF_{2\alpha}$-mediated Ca^{2+}-sensitization in rat IPA and not Fyn as suggested by Nakao *et al*[82]. Finally, this study concludes by demonstrating that SrcFKs act upstream of Rho/Rho-Kinase in response to $PGF_{2\alpha}$. The SrcFK inhibitor SU6656 and the Rho-Kinase inhibitor Y27632 were not additive with respect to both inhibition of $PGF_{2\alpha}$-induced MYPT-1 and MLC_{20} phosphorylation and inhibition of the associated $PGF_{2\alpha}$-induced contraction. Furthermore, translocation of Rho-Kinase in PASMC, a process that is important for its activation, was reversed by pre-treatment with SU6656, indicating that the movement of Rho-Kinase in response to stimulation by $PGF_{2\alpha}$ was likely to be mediated by SrcFK. This study for the first time demonstrated that agonist-mediated, Rho-Kinase-dependent Ca^{2+}-sensitization, but not basal Rho-Kinase activity, in rat pulmonary artery requires SrcFK activity.

Another study by Knock *et al* [7] investigated the role of SrcFK in HPV. Prior to this investigation, a specific role of SrcFKs in HPV and the contractile pathway was unknown. This study provides the first direct evidence for a role or roles of SrcFKs in HPV and supportive evidence for the importance of Ca^{2+} sensitization in the sustained phase of the contraction. This study confirms that hypoxia both activates SrcFK and enhances PP2-sensitive tyrosine phosphorylation of multiple protein targets, coupled with the inhibition of HPV by both SU6656 and PP2, are suggestive of an active role of these kinases in HPV. In this study, Rho-Kinase-

mediated MYPT-1 phosphorylation was inhibited by SU6656, and hypoxia-induced translocation of Rho-Kinase in PASMCs was completely prevented by siRNA knockdown of Src and strongly inhibited by knockdown of Fyn. Therefore, SrcFKs are clearly involved in the upstream regulation of hypoxia-mediated Rho-Kinase activity. In addition to an involvement in Ca^{2+} sensitization, it was also found that the SrcFK inhibitor PP2 blocks the hypoxia-mediated $[Ca^{2+}]_i$ response in IPAs. The results suggest a direct role for SrcFKs in the acute contractile response to hypoxia in small pulmonary arteries of rat. Since SrcFK inhibitors block both hypoxia-mediated Rho-Kinase-dependent MYPT-1 phosphorylation and the hypoxic $[Ca^{2+}]_i$ response in IPAs, we may speculate that SrcFKs may act upstream of both key pathways to MLC_{20} phosphorylation and contraction.

Currently, the direct link between agonists/hypoxia and ROS through SrcFK has not yet been made.

1.7 Ras Homolog gene family member (RhoA)

Section Overview

In addition to heterotrimeric G-proteins as discussed above, another class of G-proteins exist classified as monomeric G proteins. These are structurally different from heterotrimeric G proteins as they are composed of one unit rather than α, β and γ subunits.

This section, I will discuss the Rho GTPases (RhoA) family, giving an overview of their expression, activation and regulation potentially via NRTK such as SrcFK.

1.7.1 RhoA Expression and activation

The Rho GTPases form a subgroup of the Ras superfamily of 20- to 30-kD GTP-binding proteins that have been shown to regulate a wide spectrum of cellular functions. These proteins are ubiquitously expressed comprise at least 10 distinct proteins: RhoA, B, C, D, and E; Rac1 and 2; RacE; Cdc42Hs, and TC10 and are involved in a number of signalling pathways such as cell proliferation, cytoskeletal dynamics and contraction[277].

RhoA in particular has been shown to be highly expressed in smooth muscle [278,279] and mediate its effects primarily through Rho-Kinase [280-282]. RhoA is activated in smooth muscle in response to multiple stimuli including G-protein coupled receptors [218,283-285], growth factors [286,287], cytokines and chemokines [288], extracellular matrix [289] and hypoxia [117,290,291] and mediates a number of cellular processes such as growth and proliferation [292,293], migration [292,294], inflammation [293] and excitation contraction coupling[29,47,295].

It is because of this multiplicity of functions in addition to having an important role in normal vascular homeostasis, dysregulation or over activation of the RhoA/Rho-Kinase pathway has been shown to be involved in disease processes [296,297].

Although much is known about the proteins that are immediately upstream of RhoA, these are numerous and varied and form a large network of signalling pathways in response to numerous stimuli. Key components are tyrosine kinases [298,299], tyrosine phosphatases [300] and reactive oxygen species (ROS) [207,301].

1.7.2 Regulation of RhoA activation and inactivation

Although our understanding is still incomplete, much is now known about how RhoA activity is controlled. Like all G-proteins, RhoA acts as a molecular switch, i.e. RhoA is inactive when bound to guanosine diphosphate (GDP) and active when bound to guanosine triphosphate

(GTP). RhoA is therefore activated by stimuli that promotes the exchange of GDP for GTP and inhibited upon stimulation of intrinsic GTPase activity.

The activity of RhoA is determined by 3 types of regulatory proteins: Guanosine nucleotide dissociation inhibitors (GDIs) [302,303], guanosine nucleotide exchange factors (GEFs) [29,304,305] and GTPase activating proteins (GAPS) [306].

Activation of RhoA is associated with its translocation from the cytosol to the membrane in response to contractile agonists [46,197]. RhoA then inserts into the membrane which is achieved through post-translational modification whereby a lipid tail is added by acyltransferase enzymes [307] and GDP is exchanged for GTP. Inactive cytosolic RhoA-GDP is bound to GDIs [302,303] which prevent RhoA activation in 2 ways, firstly, by covering the lipid tail preventing its insertion into the plasma membrane and secondly, preventing nucleotide exchange by competing for the nucleotide binding site with GEFs[303]. At the membrane, GEFs catalyse the exchange of GDP to GTP by increasing the rate of nucleotide dissociation, this allows the binding of the more abundant GTP [306,308] (Fig 1.5). Finally, all G-proteins contain intrinsic GTPase activity, which cleaves the bound GTP, generating GDP and inorganic phosphate. This activity is enhanced by GAPs [306]. It has also been suggested that GDIs may also prevent GAPs from binding to active RhoA-GTP [302,309] (Fig 1.5).

Figure 1.5

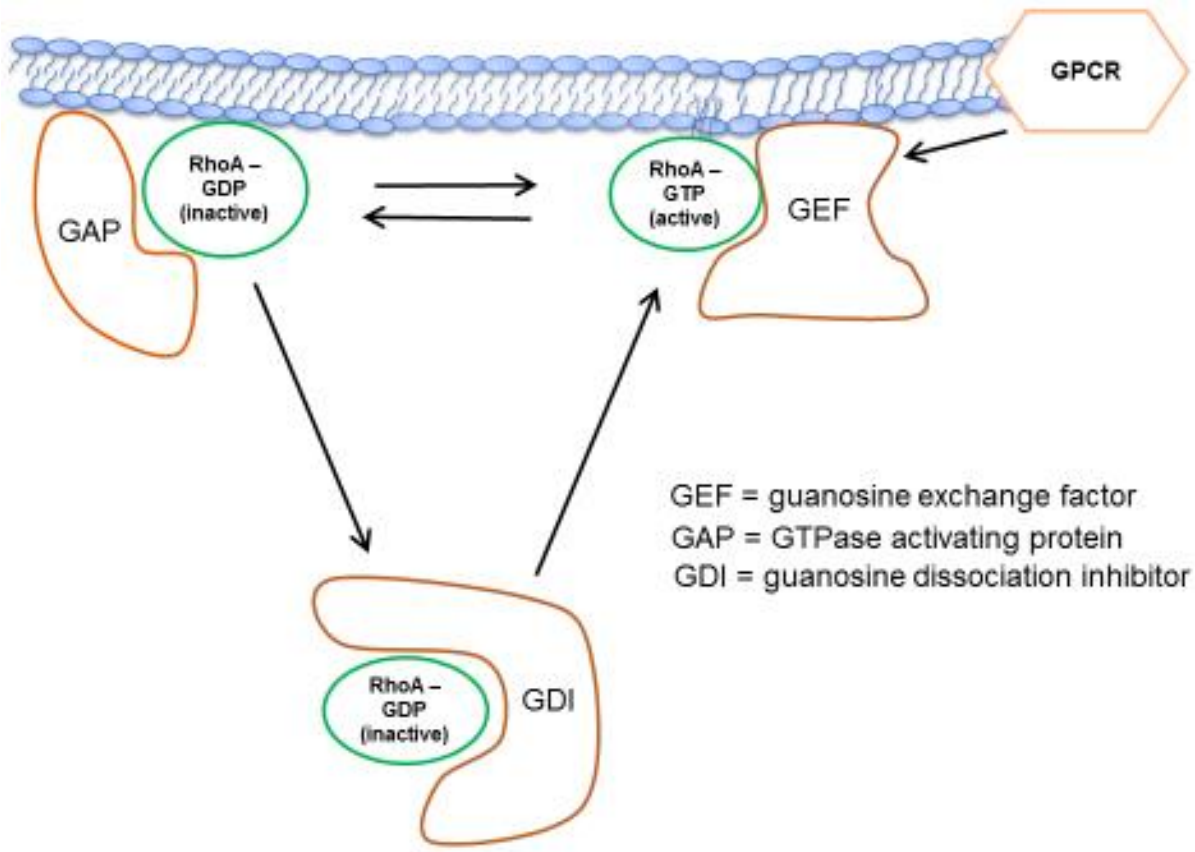

Figure 1.5: Canonical regulation of RhoA.
Cyclical activation/inaction of RhoA by nucleotide exchange, GTPase activity and cytosolic segregation. The details of which can be found in the text.

Understanding how Rho proteins are activated and inactivated has largely focused on regulatory proteins such as GEFs and GAPs. However, recent *in vitro* studies have indicated that GTPases may also be directly regulated by redox agents. Lander *et al* [310] were the first to show this with another monomeric G-protein, Ras; NO treatment of recombinant Ras increased the proportion of GTP-bound Ras and endogenous NO activated Ras in human T cells. Furthermore, Campbell's group also identified a distinct redox-active motif located in the phosphoryl-binding loop of the Rho family (RhoA, Rac1, and Cdc42) [311]. More recently, Aghajanian *et al* [312] demonstrated that RhoA can be directly activated by ROS in cells and that ROS-mediated activation of RhoA can induce cytoskeletal rearrangement. By using cysteine to alanine mutants, Aghajanian *et al* demonstrate that ROS-mediated activation of RhoA is dependent on

cysteines 16 and 20. Taken together, these findings indicate that ROS-mediated RhoA activation is another potential regulatory mechanism for the control of VSM function.

1.7.3 GAPS + GDI's

Expression and function of RhoGAPs in arteries have been poorly investigated probably because RhoGEFs are considered as primary and major regulators of Rho GTPase activity. However, in the absence of any stimulus, siRNA-mediated silencing of ARHGAP35 (also known as p190-RhoGAP or p190-A), ARHGAP1 (p50-RhoGAP), MYO9B (Myr5), or ARHGAP26 (GRAF) in vascular smooth muscle cells leads to an increase RhoA activity, indicating the expression and the function of these RhoGAPs [313].

GDIs inhibit RhoA activity by preventing the insertion of the C-terminal lipid tail into the plasma membrane. There are three GDI isoforms in mammals (RhoGDI1, RhoGDI2 and RhoGDI3) with RhoGDI1 being the most widely expressed [314]. Like GAPS, GDIs have not been widely studied in VSM.

RhoGDIs were initially characterized as simply Rho GTPase inhibitors; however, recent work indicates their function is a lot more complex[309]. A number of signalling pathways which lead to the phosphorylation of either the Rho GTPase or to RhoGDI have been shown to regulate RhoGDI–Rho GTPase interactions [315,316]. An example being, phosphorylation of Ser96 on the C terminus of GDI-1 by PKC [317], stimulates RhoA dissociation. Additionally, Src phosphorylation of RhoGDI, appears to decrease in the ability of RhoGDI to form a complex with Rho GTPases leading to enhanced Rho GTPase activity [318]. Subsequently, these reports point to an important role of RhoGAPs and RhoGDI in the regulation of RhoGTPase signalling.

1.7.4 RhoGEFs

RhoGEFs are a highly diverse group of proteins with at least 70 expressed in the human genome compared to 22 different Rho proteins. This discrepancy suggests that in response to environmental changes, the preferential activation of certain RhoGEFs may occur, subsequently activating RhoA. A number of possibilities have been described, 1) RhoGEFs have tissue-restricted expression and function more efficiently in a particular environment; 2) different upstream signals use different RhoGEFs to activate Rho proteins, therefore the RhoGEFs involved are probably different according to upstream stimuli and 3) RhoGEFs not only activate Rho proteins but may also, influence the downstream pathways which are activated depending on where in the cell the Rho protein is activated by the GEF, which may in turn depend on where that particular GEF was located [319]. The potential tissue-restricted expression of RhoGEFs suggests that they may also be involved in different functions of Rho-proteins such as cell cycle progression, migration, actin polymerisation, cell-cell adhesion and exo/endocytosis [299,304-306,320-325]. Expression profiles have established that a number of these RhoA-specific GEFs are expressed in the vasculature[319] with VSM-RhoGEF (ARHGEF15) being specific to vascular smooth muscle[320]. Selective targeting of tissue-specific GEFs therefore may be of therapeutic benefit.

Most RhoGEFs are of the DBL-RhoGEF family and contain two conserved domains, DBL homology (DH domain) which is the site of catalytic activity and a pleckstrin-homology (PH domain) which acts as an auto inhibitory domain [306,326]. The PH domain may direct localization of the GEF by associating with phosphatidylinositol-phosphatase (e.g. PIP_3). There are also RhoGEFs that are known to activate nucleotide exchange by structurally unrelated non-DH protein domains [323,327].

The signalling pathways which activate RhoGEFs are determined by their binding domains. Some GEFs can be activated directly by heterotrimeric G-Proteins through their RGS domain, others such as the Vav family possess a src-homology-2 (SH2) and/or src-homology-3 (SH3) domain. This allows for interactions with tyrosine kinases (resulting in tyrosine phosphorylation of the GEF).

RhoGEFs can be considered key molecules in RhoA activity. The following descriptions will be limited primarily, but not exclusively, to RGS domain containing RhoGEFs known to activate RhoA and be tyrosine phosphorylated.

There are three RGS domain containing RhoGEFs, ARHGEF1 (p115-RhoGEF), ARHGEF11 (PDZ-RhoGEF), and ARHGEF12 (LARG which are expressed in both conductance and resistance arteries of rat or mouse [328,329]. However, the most abundant RhoGEF in arterial smooth muscle cells is the specific RhoA GEF p63RhoGEF (ARHGEF25, GEFT) [319,330,331].

The first link between heterotrimeric G-proteins and the monomeric small GTPase Rho was established when ARHGEF1 (p115RhoGEF) was initially discovered [230,332]. Two additional RhoGEFs, ARHGEF11 (PDZ-RhoGEF) and ARHGEF12 (LARG) (leukaemia-associated RhoGEF) were identified as members of the p115RhoGEF family according to sequence similarity[229,333-335]. ARHGEF1 (p115-RhoGEF) localizes throughout the cytosol, and rapidly translocates to the plasma membrane upon GPCR-activation of $G\alpha_{12/13}$, or expression of constitutively active $G\alpha_{12/13}$mutants [308,336]. ARHGEF12 (LARG) is reported to be distributed throughout the cytoplasm in most cells. ARHGEF11 (PDZ-RhoGEF) also localizes to the cytosol in some cell types also in the cytosol, but in others at the cell periphery or near the plasma membrane where it interacts with cortical actin. Activation of ARHGEF11 (PDZ-RhoGEF) and ARHGEF12 (LARG) by $G\alpha_{12/13}$ induces their translocation to the plasma membrane [337-339].

ARHGEF1, ARHGEF11 and ARHGEF12 are directly activated by $G_{\alpha 12}$ or $G_{\alpha 13}$ which are coupled to a wide range of vasoconstrictor receptors [304,319,325,340,341]. More recently, ARHGEF1 has been shown to play a major role in $G_{\alpha q}$ linked Ang II-induced RhoA activation in vascular smooth muscle cells and Ang II-induced regulation of arterial tone and hypertension in rats or mice [325]. Whereby, ARHGEF1 is activated by phosphorylation by the non-receptor tyrosine kinase, Janus kinase 2 (JAK2), downstream of AT1 receptor stimulation. Interestingly, in this study, ARHGEF1 was not activated by ET-1, U46619 or noradrenaline, which is surprising since this GEF has also been shown to be activated directly by $G_{\alpha 12/13}$ which is coupled to ET_A and ET_B, TXA_2 and adrenergic receptors (α_1) [342]. Ang II has also been shown to activate ARHGEF1 in human peripheral blood mononuclear cells[304]. The authors conclude that ARHGEF1 may mediate Ang-II induced RhoA activation in humans. Additionally, ARHGEF12 has also been shown to be activated by $G_{\alpha q}$ [343] and ARHGEF25 (p63RhoGEF) is also responsible for the activation of RhoA by $G_{\alpha q}$ protein in response to phenylephrine (PhE) and endothelin (ET-1) [330]. Furthermore, activation of RhoA by 5-HT and sphingosine 1-phosphate in vascular smooth muscle cells is mediated by ARHGEF12 [344]. Activation of ARHGEF11 (PDZ-RhoGEF) and ARHGEF12 (LARG) has also been also been shown to be associated with tyrosine phosphorylation [324,345]. Finally, the Vav sub-family of GEFs, are the only GEFs that possess a SH-2 domain which allows their binding to tyrosine kinases such as Janus Kinase (JAK) or SrcFK leading to tyrosine phosphorylation [322]. Until recently, [325], they were the only GEFs to demonstrate that tyrosine phosphorylation was a requirement for activation.

It has been hypothesised that SrcFKs may be involved in Ca^{2+} sensitization through upstream regulation of RhoA via GEF phosphorylation [346], but this currently has not been shown. Several RhoA-specific GEFs (ARHGEFs) are expressed in VSM [319] that are activated by $G_{12/13}$ and/or by tyrosine phosphorylation which may be promoted by ROS[347]. Indeed, RhoGEFs are known

to be phosphorylated and activated by three other non-receptor tyrosine kinases, focal adhesion kinase (FAK), protein tyrosine kinase 2 (PYK2) or Janus kinase (JAK) [299,325,348]. There is no evidence to suggest that these three kinases are themselves directly ROS sensitive however they are activated by GPCR agonists in a NOX dependent manner as well as exogenous ROS [349-351] and through Src mediated tyrosine phosphorylation [352,353]. JAK also required ROS-dependent activation of PYK2[354].

Although the function of the RhoGEFs expressed in arteries is unknown for most of them, it should be noted that they are shown to be involved in vasoconstrictor-induced RhoA signalling activation.

1.8 Global Aims

Vascular function can be altered by oxidative modification of key proteins involved in cellular signal transduction, thereby altering their functions and interaction with other proteins. Amongst these, Src Family Kinases (SrcFK) which may be directly activated by oxidative modification, while opposing tyrosine phosphatases are inhibited, may contribute to net increases in tyrosine phosphorylation and altered vascular function. Previous results within my group has shown that prostaglandin–$F_{2\alpha}$ and hypoxia enhance total tyrosine phosphorylation, activate Src and cause SrcFK-dependent constriction. Combining these observations with the ROS-sensitivity of Src lead to the proposal that the interaction between SrcFK and ROS makes a central contribution to vascular smooth muscle function.

Overall my objective is to determine the role of agonist induced ROS generation in the physiological regulation of vascular tone and the signalling pathways in pulmonary arteries. Specifically, I will test the following hypotheses:

(1) ROS are key secondary messenger molecules mediating vascular smooth muscle contraction in response to multiple stimuli and Src-family kinases have a critical role as ROS-sensitive intermediaries in these signalling pathways.

(2) The GPCR agonist U46619 and exogenous ROS activate SrcFK, which subsequently activates RhoA and Rho-Kinase. This involves interactions with Rho guanine nucleotide exchange factors, notably ARHGEF1.

The following schematic (Figure 1.6) indicates potential pathways that will be investigated during this study.

Figure 1.6

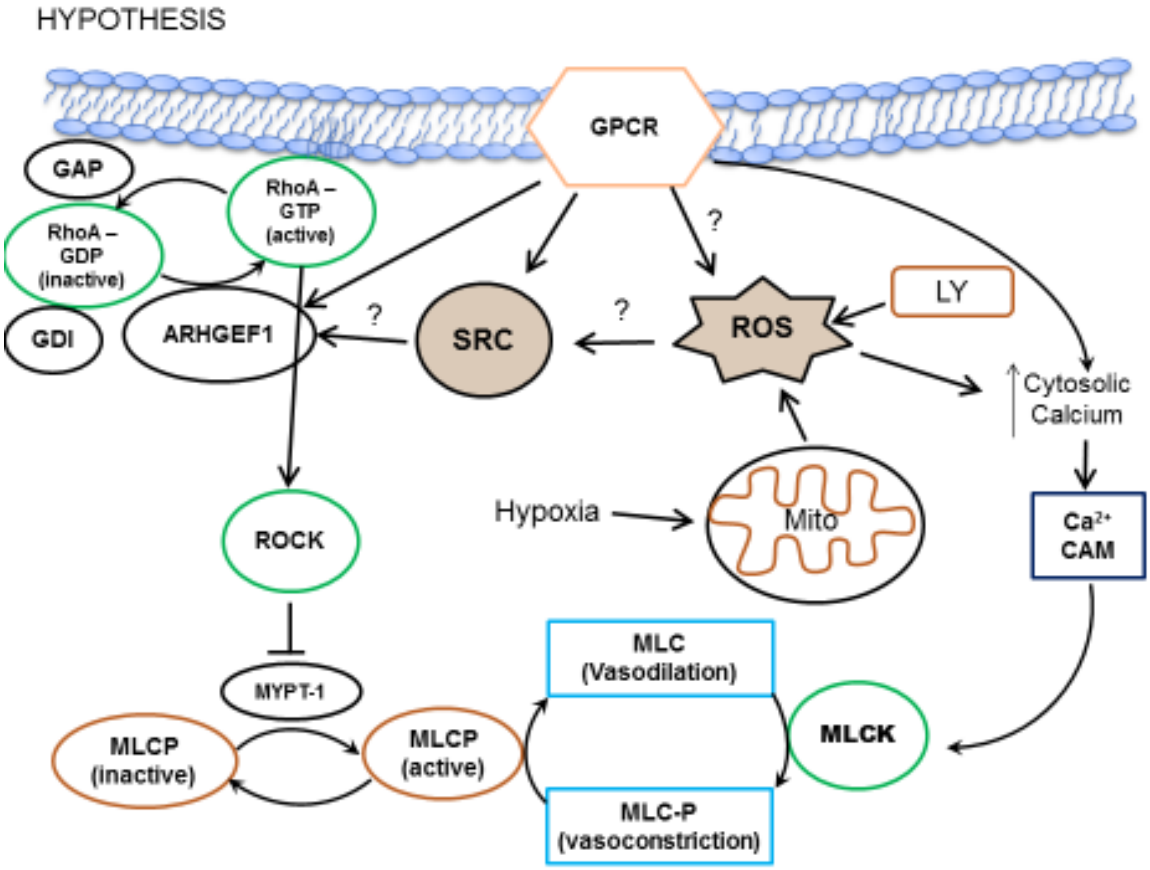

Figure 1.6: Schematic of the signalling pathways that I investigated during my PhD.
I demonstrated that the NRTK, Src, will act as a ROS sensitive intermediate potentially activating the RhoA/Rho-Kinase pathway via direct or indirect interactions with ARHGEF1.

2. Materials and Methods

2.1 Introduction

This chapter will detail the methodologies used throughout my PhD. Suitable techniques were used to measure contractile response in rat intra pulmonary arteries (IPA). In addition, luminescence was used to measure reactive oxygen species (ROS) production and suitable molecular techniques were used to investigate interactions between ROS, Src-FK, RhoA, Rho-Kinase and ARHGEF1.

2.2 Source of tissue

Small Pulmonary arteries were dissected from Rat lung tissue.

Small Intra Pulmonary arteries (IPA) were used in functional studies to measure functional responses to contractile agonists (see section 2.4). IPAs were also used in immunoprecipitation/co-immunoprecipitation and immunoblotting studies to investigate protein interactions as well as target protein activity (see section 2.6).

Pulmonary arterial smooth muscle cells (PASMCs) were generated by digesting the complete pulmonary arterial tree and then used to measure ROS production (see section 2.7.5 – 2.7.11) or visualise eGFP-tagged RhoA or eGFP-tagged ARHGEF1 translocation in live cells (see section 2.8).

2.2.1 Tissue Isolation for functional studies

Male Wistar rats (~250g) were sacrificed by lethal overdose of sodium pentobarbital (100mg/Kg), intraperitoneal (ip).

Lungs were dissected from the thorax of the rat and immediately placed into cold physiological saline solution (PSS) pH 7.4. PSS composition (mM): 118NaCl, 24 $NaHCO_3$, 1 $MgSO_4$, 4 KCl, 5.56 D-glucose, 0.434 NaH_2PO_4, 1.8 $CaCl_2$. IPAs were dissected from either the upper or middle lobes on the right side of the lung, or the upper lobe on the left side of the lung and

cleaned of any parenchyma and surrounding tissue. Subsequently, IPAs were cut into segments approximately 1mM in length and placed immediately in ice-cold PSS solution.

Maintaining tissue in a viable state for in vitro contraction experiments

Following tissue extraction, it is important to maintain the tissue in a viable state. The tissue is therefore kept in a solution that is both isotonic and within physiological pH range (pH7.35-pH7.45). Throughout my studies using intact tissue, I used Physiological salt solution (PSS). However, Phosphate-Buffered Saline (PBS) was used when investigating ROS measurements in pulmonary arterial smooth muscle cells (PASMCs).

PSS is a bicarbonate buffer that closely resembles blood serum for both pH and tonicity. PSS usually contain 0.9% NaCl dissolved in one litre of water, because NaCl dissociates completely into two ions – sodium and chloride – 1 molar NaCl is 2 osmolar. Therefore, PSS usually contains 154 mOsmol/L of Na^+ and Cl^- equating to 308 mOsmol/L. It has a slightly higher degree of osmolarity (i.e. more solute per litre) than blood which has a normal range between 270-290 mOsmol/L. However, this difference is not great enough to affect the osmotic pressure gradient.

pH is also another key factor which has to be maintained within the system. Blood pH is between 7.35 - 7.45 therefore this has to be maintained within our buffer. In normal physiology, blood pH is maintained primarily by the lungs via CO_2 regulation and the kidneys by bicarbonate (HCO_3^-) regulation.

The buffer has a pH of 7.4 and is maintained at this by gassing with 95% air, 5% CO_2. The CO_2 reacts with H_2O to form H_2CO_3 (carbonic acid). Carbonic acid will disassociate to produce HCO_3^- and H^+ ion. Since the buffer contains bicarbonate, any excess H^+ from tissue metabolism will react with bicarbonate to form carbonic acid. This is fully reversible with a high capacity to maintain pH so small changes will not have a great effect on pH.

2.2.2 Agonist, ROS generator and inhibitor Selection

U-46619 (U-46) and LY83583 (LY) were used to elicit contractile responses in functional studies or enhance phosphorylation responses/protein interactions of key proteins in immunoblotting studies. As well as promoting reversible translocation of key proteins in PASMCs.

U-46619 (U-46) was used throughout my investigations as it is a stable analogue of thromboxane A_2 (TXA_2), and a T Prostanoid receptor (TP receptor) agonist[243,355]. In our hands is a more effective vasoconstrictor in IPA than phenylephrine (PE), angiotensin II, (Ang II) or endothelin, (ET-1) [356].

LY83583 (6-anilino-5,8-quinolinequinone) (LY) is a quinolinedione[357] which has previously been used by our group as an intracellular superoxide generator [88,89]. Here, 10µmol/L LY83583 was shown to be inhibited by dicoumarol (10µmol/L), a blocker of the intracellular NADPH:quinone oxidoreductase enzyme diaphorase, in both MA and PA [89]. LY83583 ROS production was also shown to be sensitive to superoxide dismutase (SOD) and not catalase, suggesting that the ROS produced is superoxide as measured by changes in luminescence. This is important as there are opposing theories about the role of superoxide and H_2O_2 in smooth muscle function (see introduction).

Tempol (4-hydroxy-2,2,6,6-tetramethylpiperidine-N-oxyl) is an antioxidant which was selected as it is a cell-membrane permeable, water-soluble compound belonging to the nitroxide class of SOD mimetics[358]. It is able to dismutate superoxide catalytically, hydrogen peroxide by catalase-like actions, and limit the formation of hydroxyl radicals by Fenton reactions [358]. Tempol has been shown to reduce oxidative stress in obese rats [359], and other models where oxidative stress is prevalent [360].

Ebselen (2-phenyl-1,2-benzisoselenazol-3(2H)-one) is another antioxidant selected as it is a structurally different from tempol however contains similar potent anti-oxidant properties. Ebselen has been described as a lipid soluble organo-selenium compound which mimics glutathione peroxidase activity [361,362]. It has also been shown to react with the thioredoxin system and has been described as an excellent substrate for thioredoxin reductase (TrxR)[363]. Furthermore, ebselen has been shown to rapidly react with ROS generated during ischemia or reperfusion [364,365].

PP2 was selected as it is a well-known SrcFK inhibitor used extensively within our laboratory [7,41,83].

2.3 Functional Measurements

Contractile measurements were carried out using a single channel Mulvany-Halpern small vessel wire myograph (Figure 2.1)

Figure 2.1:

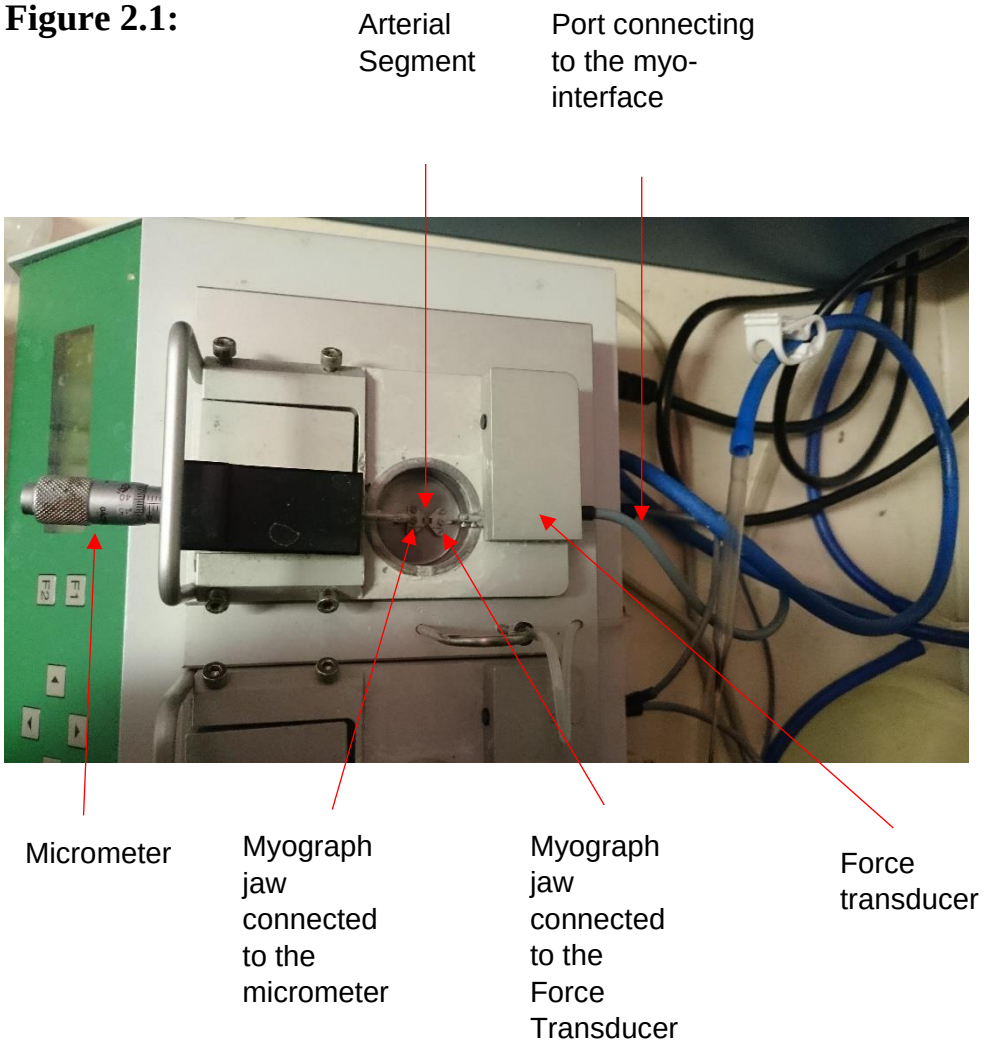

Figure 2.1: Main components of a Mulvany-Halpern small vessel wire myograph
Shows a single channel Mulvany-Halpern small vessel wire myograph (Model 320A) used throughout my studies. Vessels are mounted on wires and compounds added while tension is being measured.

2.3.1 Theory behind Force Measurement (Myography)

Background

Until the mid-1970s, most information about the mechanical, morphological and pharmacological properties of vascular smooth muscle was investigated using large vessels, the smallest being rat tail. Information about smaller vessels could only be investigated in perfusion

experiments and histological examinations. Due to the size of smaller vessels this discouraged investigators from undertaking mechanical experiments.

Myography was first developed by Mulvany and Halpern [366-369] and allowed small vessels to be mounted on a myograph. This allowed measurements of isometric responses particularly in investigating contractile properties of vascular vessels [7,88,89,191]. This differs from other methods as both ends of each mounting wire will be secured under tension without having to manipulate the vessels segment with dissecting equipment.

The arteries of interest used throughout my studies are the lateral side branch small IPA, approximately 150–500 μm internal diameter. These arteries were used as they constrict in response to hypoxic stimulus [7,370,371], an important determinant for pulmonary arteries. Furthermore, these arteries contain high VSM content of VSM therefore allowing for measureable responses on a wire myograph. Finally, from a technical aspect, these arteries are large enough to mount on a myograph with minimal damage thus maximising responses to stimuli.

Key component parts of a Myograph

The myograph itself is an instrument used to investigate contractile properties of small proximal resistance vessels. It comprises of two metal jaws, one of which is attached to a force transducer the other to a micrometer arm. A force transducer converts tension into voltage. The myograph force transducer is a strain gauge connected to a Wheatstone bridge, amplifier and interface connected to a PC. This allows the force generated by the vessel to be recorded in real time e.g. In response to U46619, the artery contracts, this alters the electrical resistance of the strain gauge which is shown in real time on the PC using myodaq software. Finally, there are 100 points measured per second however this is averaged 100 to 1 so there is 1 point per second showing. This helps reduce signal to noise ratio.

A micrometer arm is also attached and can be adjusted manually. This allows us to manually stretch the vessel over small distances to achieve a desired tension. The myograph is also kept at $37^{O}C$ by a built-in heater. Each preparation has its own individual gas inlet and suction for solution replacement.

Measuring Isometric Force

In smooth muscle, Ca^{2+} dependent phosphorylation of MLC_{20} promotes cross bridge cycling between actin and myosin filaments. This results in greater force generation and shortening of smooth muscle [29].

If a muscle is prevented from shortening when activated, the muscle will express its contractile activity by pulling against its attachments and developing force in response to stimuli. This type of contraction is termed isometric (meaning "same length"). When conditions are arranged so the muscle can shorten and exert a constant force while doing so, the contraction is called isotonic (meaning "same force").

2.4 Mounting of IPA's

IPA's were mounted onto a wire myograph by carefully inserting stainless steel wires (40µm) through the lumen of the arteries. During this period, arteries were immersed in PSS. The wires were tightly secured to mounting jaws by 4 screws. The wires were kept parallel at all times. The wires were wrapped clockwise around the screws, the screws were then tightened thereby tightening the wires. The jaws were adjusted using the micrometer arm and force measure by the transducer (Figure 2.2). IPAs were then gassed with 95% air and 5% CO_2.

Figure 2.2:

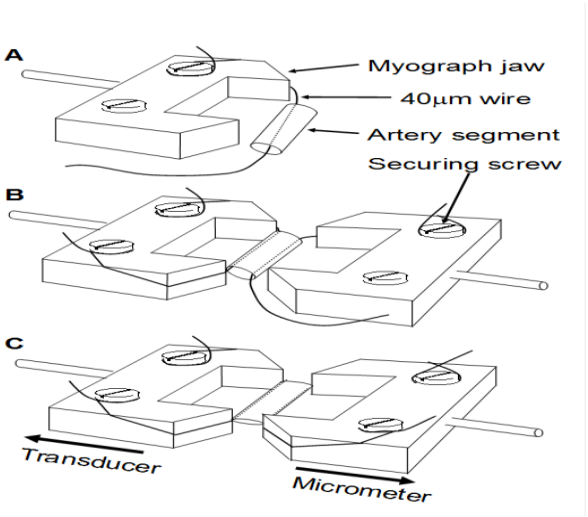

Figure 2.2: Shows the mounting of Pulmonary arteries onto a wire myograph
IPAs were mounted using stainless steel wires kept parallel at all times. These were secured by 4 screws. IPAs can be stretched using the micrometer and the force measured by the transducer.

2.4.1 Length Tension relationship and Normalization

Length tension relationship is the relationship between a muscles length and the isometric tension (force) which is generated when fully activated. During muscle activity, particularly at longer lengths, tension depends on passive stretch of the tissue along with active force generated by muscle fibres when stimulated. When the passive contribution is subtracted and only the active force generated is considered, the relationship between force and length will depend on active cross bridge cycling between actin and myosin.

Therefore before the start of any experiment it is important to perform a “Normalisation” step. There are 3 main reasons why this is important, the first being that elastic vessels size has to be clearly defined, the sensitivity to agonists or indeed antagonists is dependent on the amount ofstretch, finally any active responses is dependent on stretch which is why it is important to set the preparation of internal circumference to give a maximal response.

The aim of the "normalisation procedure" is to stretch the segment to the optimum of the length tension curve thereby maximising cross bridges between actin and myosin. Therefore, maximising the effect of stimulus on contraction.

2.4.2 Stretching and challenging with KPSS

IPA's were stretched until a tension of ~3.0mN was maintained for each vessel. This stretching procedure was required for determining the 'active' length tension relation in IPA's. This has been examined previously within the laboratory [88,89,372] . For rat IPA of the size used in this study, it was determined that a resting tone of ~3.0mN is approximately at the point on the length tension relationship curve that is optimum for the generation of active tension upon pharmacological stimulation. Active tension was tested after periods of incrementally increased stretch by repeatedly challenging IPA's with KPSS treatment for ~3minutes (KPSS is made by equimolar substitution of KCl for NaCl in PSS). This process occurred at least 3 times, the arteries were then allowed to rest before the start of the experiment. This process is demonstrated in figure 2.3:

Figure 2.3

(A)

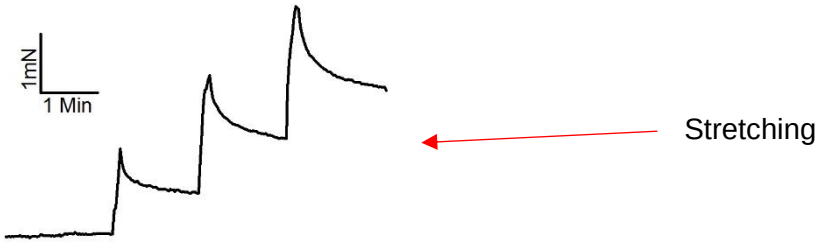

(B)

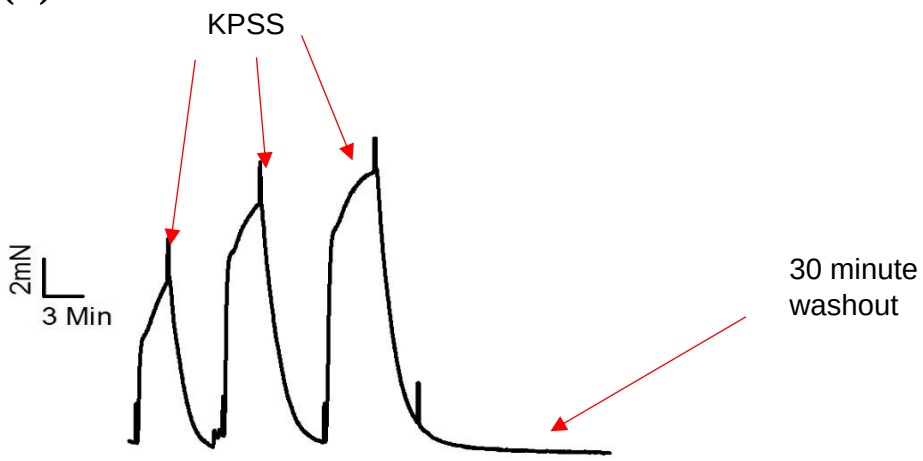

Figure 2.3: Illustration of Normalization Procedure and KPSS challenges
(A) A stepwise normalization procedure and (B) three challenges with KPSS. Following the third challenge with KPSS, IPAs were washed and left to rest for ~30 minutes.

2.4.3 Antioxidant and Kinase inhibitor dose response to KPSS and U46619 contractile responses

In order to determine the contribution of endogenous ROS to agonist-induced contraction, I examined the effects of the ebselen, tempol on sub-maximal contractile responses induced by the TP receptor selective agonist U46619 in IPA. I also confirmed that U46619-induced contraction is partially dependent on SrcFK activity using the SrcFK antagonist, PP2. In order to confirm the potential effects of DMSO alone, cumulative dose responses were performed with DMSO only. Furthermore, cumulative dose responses were performed using ebselen,

tempol and PP2 in the presence of KPSS. This ensured that the concentration of drugs used along with the volume of vehicle control had no non-specific effect on contractile function.

Following a series of stretches, three KPSS challenges were performed in IPAs. A resting period of ~30 mins was given to allow each IPA to return to basal tonic levels. IPA's were then challenged with a fourth KPSS challenge and the contraction was allowed to plateau after ~25 minutes incubation. A cumulative dose response to ebselen (0.1-10μM), tempol (0.1-3mM), PP2 (1-30μM) or (d) DMSO (0.5-14.5μL) was performed.

The above protocol was then performed, but the IPA's were challenged with U46619 (100nM) instead of a fourth KPSS. A cumulative dose response to (a) ebselen (0.1-10μM), (b) tempol (0.1-3mM), (c) PP2 (1-30μM) or (d) DMSO (0.5-14.5μL) was performed.

2.4.4 Effect of antioxidants and kinase inhibitor in IPA on exogenous ROS contractility

LY83583-derived superoxide has been shown to directly constrict IPA at 10μM [88]. However, the concentration of LY83583 (1μM) used in this study does not itself cause contraction of IPA[88] but causes an enhancement of 2nM U46619 response which is approx. 10% of KPSS in amplitude. The effect of antioxidants, ebselen (10μM), tempol (3mM), SrcFK inhibitor PP2 (30μM) and DMSO (5μL) (as a vehicle control) were investigated on contractile responses to exogenous ROS enhanced contractile responses.

Following the initial normalisation procedure, a control response was performed whereby U46619 (~2nM) was incubated with IPA for 10 minutes. 1μM LY83583 was added to the IPA for 10 minutes resulting in an enhancement of contraction. IPAs were then washed 3 times in PSS and allowed to rest for ~30 minutes. This was then repeated again. This controls for any potential run-down with time which could potentially influence the responses to U46619 and LY83683.

In separate IPAs, an initial control response was performed. This was followed by pre-incubation of ebselen (10μM), tempol (3mM), PP2 (30μM) or DMSO (5μL) with IPAs for 10 minutes before re applying U46619 and LY83583. Incubation with DMSO allowed me to control for any potential effect DMSO could have on contractile function thus ensuring any effect seen was due to the presence of the drug and not due to the presence DMSO.

2.4.5 Effect of inhibiting NOS on agonist induced and ROS enhanced contractile responses

In order to eliminate the role of nitric oxide in the effects of antioxidants and PP2 on U46619-induced contraction and to eliminate the possibility that the enhancing effect of LY83583 on U46619-induced contraction was as a result of nitric oxide scavenging response by superoxide, these experiments were repeated in the presence of L-NAME.

A normalisation procedure was initially performed followed by a resting period of ~30 mins. L-NAME (300nM) was then incubated with IPAs for ~20mins. U46619 (100nM) was subsequently added and a cumulative dose response to antioxidants, PP2 or DMSO was performed as discussed in an earlier section.

The effect of L-NAME on exogenous ROS was also investigated. An initial control response was performed and IPA's were subsequently allowed to rest. L-NAME (300nM) was then incubated with the IPAs for ~20mins followed by U46619 (100nM) and 1μM LY83583 exposure.

2.4.6 Effect of Mitochondrial inhibitors on U46 induced contraction

In order to determine that myxothiazol and rotenone were acting downstream of mitochondrial electron transport chain, U46619 induced contractile responses were performed in the presence and absence of myxothiazol, rotenone and DMSO.

Following stretching, challenging with KPSS, IPAs were given a rest period for 30 minutes. A first control response was carried out whereby U46619 (100nM) was incubated with the IPA for 10 minutes. The IPAs was then washed 3 times in PSS and left to rest for 30 minutes. IPAs were then pre-incubation with DMSO (5µL), myxothiazol (100nM) and rotenone (100nM) for 15min. U46619 (100nM) was then re-applied.

2.5 Immuno/ Co-immunoprecipitation

Background

Immunoprecipitation (IP) is a commonly used technique for antigen detection and purification. Co–immunoprecipitation (CO-IP) is an extension of IP and is based on the potential of IP reactions to capture a target i.e. antigen as well as other molecules that are bound to the target. Therefore depending on the focus of the experiment, the experiment could be immunoprecipitation (primary target - antigen) or co-immunoprecipitation (secondary targets – interacting proteins).

The principle is straightforward: the antibody can be crosslinked onto a beaded support where an antibody-binding protein is immobilized (such as protein A or G which are high affinity IgG ligands and bind to the Fc region of antibodies effectively immobilising the antibody capture site outward).

The lysate is then added to the antibody complex and the antigen is captured along with any other attached macromolecules. Any proteins not captured are then washed away. After capturing the antigen, the antigen complex is eluted from the support (the antibody may also be eluted from the support depending on the denaturing buffer). The solute is then analysed by SDS-PAGE followed by western blot detection to verify the identity of the antigen and other macromolecules (see sections: 2.6.7 and 2.6.9).

2.5.1 Pulmonary artery isolation for CO-IP and immunoblotting studies

Homogenates were prepared from IPAs. The complete arterial tree was dissected from the upper lobes from the right and left side of the rat lung. All parenchyma and any other surrounding tissue was cut free. The tissue was completely submerged in cold PSS throughout the entire dissection process. Dissection was performed on a Sylgard dissecting dish.

For western blot samples, the arterial tree was cut longitudinally through the main branch thereby ensuring an equal number of side branches for each sample. For IP samples, a complete arterial tree was used per sample to ensure enough protein was extracted. After dissection, the arterial trees were immediately transferred into a 1.5ml eppendorf tube containing 1mL of PSS and kept on ice.

2.5.2 Protein extraction consideration

Protein was extracted from IPA to measure phosphorylation responses or protein-protein interactions in response to stimuli/inhibitors.

Due to the structure of tissue compared to cells e.g. tissue samples, which contains higher levels of extracellular proteins such as collagen and elastin, mechanical force as well as the addition of a lysis buffer was required to extract protein.

Another issue is that membrane proteins are hydrophobic therefore a detergent is required to extract these proteins [373]. The choice of detergent will vary between CO-IP and western blot analysis and will be discussed in the next section.

Furthermore protein degradation by protease enzymes during extraction will occur therefore the addition of a protease inhibitors to the lysis buffer is required.

Many of the proteins that I investigated were phosphorylated (indicating their activity) therefore phosphatase inhibitors were also added to stop any de-phosphorylation by phosphatases which may also be present during extraction.

2.5.3 Lysis buffers

The choice of lysis buffer depends upon the type of tissue, where the protein is situated and whether you want to maintain protein interactions. For protein extraction in tissue for western blot analysis, SDS lysis buffer was used. SDS is anionic and a very effective surfactant that can solubilise almost all proteins. It disrupts non-covalent bonds within and between proteins; completely denaturing proteins.

Non-ionic detergents (NP-40 or Triton) were considered however nonionic detergents are considered mild surfactants as they break protein-lipid, lipid-lipid interactions but not protein-protein interactions. They do not denature proteins. This means that proteins are solubilised in their native and active form and retain their protein interactions. Non-ionic detergents are used mainly for immunoprecipitation and co-immunoprecipitation.

I used a Triton based buffer instead of NP40 for IP/CO-IP studies. I did initially try extracting protein with NP-40 but was unable to extract enough protein for western blot analysis. I therefore used Triton which allowed me to extract enough protein from my samples.

2.5.4 Sample Tissue Treatment and protein extraction

Treatment and protein extraction method was performed differently which is detailed below.

Western blot Analysis

Arteries were equilibrated for a 15 minute period during which they were incubated in PSS (pH 7.4) and maintained at a temperature of 37^{o}C while being continuously gassed with 5%CO_2/95% air. Following equilibrium, U46619 (100nM) and 1μM LY83583 time controls

were performed. This was followed by investigating the effect of 15 minute pre-incubation with ebselen, tempol, PP2 or DMSO on U46619 induced phosphorylation responses.

Hypoxia

The effect of hypoxia on protein phosphorylation was also investigated. Following equilibration, arteries were pre incubated with 1nM U46619 for 15 minutes. The gassing was subsequently changed to 1% O_2/5% CO_2/Nitrogen for 1 or 5 minutes depending on the protein of interest. This was again followed by investigating the effect of pre-incubating myxothiazol (100nM), rotenone (100nM) or DMSO (5µL) for 15 minutes prior to U46 or 1 or 5 minute hypoxic exposure.

Immuno Precipitation

Arteries were equilibrated for a 15 minute period during which they were incubated in PSS (pH 7.4) and maintained at a temperature of 37^{o}C while continuously gassed with 5%CO_2/95% air. Following equilibrium, IPA's were then treated with U46619 (100nM) for 15 minutes.

Following treatment, IPA's was immediately snap frozen in liquid nitrogen. The frozen tissue was pulverised using a Bessman Tissue Pulveriser (Spectrum Laboratories), which was cooled in liquid nitrogen.

Samples prepared for western blot analysis: Pulverise tissue was transferred into 70µl of 1xSDS lysis buffer containing 0.1M Tris HCl (pH6.8), 2% SDS, 1% phosphatase inhibitor cocktails 2 and 3 (Sigma) and 1% protease inhibitor (Sigma). This was immediately vortexed mixed for 1 minute at room temperature to extract protein from the tissue. The resulting mixture was then centrifuged at 10g for 3 minutes, the supernatant was collected and pipetted into a clean Eppendorf.

Samples prepared for IP/CO-IP studies: Pulverise tissue was transferred into 70µl of 1% Triton X-100 lysis buffer containing 20 mM Tris HCl (pH8.0), 1% Triton X-100, 137mM NaCl,

2mM EDTA, 1% phosphatase inhibitor cocktails 2 and 3 (Sigma) and 1% protease inhibitor (Sigma). This was immediately vortexed mixed at room temperature for 10 seconds at room temperature followed by 50 seconds kept on ice. This was repeated 12 times and ensured enough protein was extracted from my sample. The resulting mixture was then centrifuged at 13g for 10 minutes at $4^{O}C$, the supernatant was collected and pipetted into a clean Eppendorf.

2.5.5 IP/CO-IP

Protein was extracted as previously discussed for immediate western blot, however for IP/Co-IP a triton based lysis buffer was used to extract protein from tissue.

IP/CO-IP was performed using a Pierce™ Crosslink Magnetic IP/CO-IP Kit (8805) was used. Initially a 1X modified coupling buffer was prepared for each IP reaction. 25µL of Pierce protein A/G Magnetic Beads were then aliquoted into a microcentrifuge tube and the beads were then collected using a magnetic stand for 1 minute at room temperature. The storage solution was discarded and 500µL of 1X modified coupling buffer was added to each tube gently mixed and incubated for 1 minute at room temperature on a rotating platform. The beads were collected using a magnetic stand and this stage was repeated.

An antibody solution was then prepared. The antibody was diluted 1:20 in coupling buffer, +lysis buffer and ultrapure water giving a final antibody concentration of 5µg per IP.100µL of prepared antibody solution was added to the beads, mixed and incubated on a rotating platform for 15 minutes at room temperature with vortex mixing every 5 minutes. The beads were then collected using a magnetic stand.

1X modified coupling buffer was then added to each tube, gently mixed and the beads collected using a magnetic stand. The supernatant was then discarded and 1X modified coupling buffer was added to each tube and gently vortexed. The beads were then collected using a magnetic stand, the supernatant discarded, and this stage was repeated.

Bound antibodies were then crosslinked to protein A/G using a cross linker solution containing 2.5µL of 20X coupling buffer, 4µL of 0.25mM DSS and 43.5µL of ultrapure water. This was added to the beads and incubated for 30 minutes at room temperature on a rotating platform. The beads were then collected using a magnetic stand and the supernatant discarded. Elution buffer was then added to the beads and gently mixed for 5 minutes at room temperature on a rotating platform. The beads were then collected using a magnetic stand and the supernatant discarded. This was repeated 2 more times. Cold IP lysis/wash buffer was then added to the beads and gently vortex mixed. The beads were then collected with a magnetic stand and the supernatant was discarded. This was repeated one more time.

The lysate solution was diluted to 210µL with IP lysis/wash buffer. 70µL of diluted lysate solution was added to each tube containing crosslinked magnetic beads and incubated overnight at 4^{o}C on a rotating platform. The beads were then collected using a magnetic stand the unbound sample (supernatant) was saved for analysis. The beads were then washed three times using IP lysis/wash buffer followed by a single wash using ultrapure water. The beads were then collected using a magnetic stand and elution buffer was added to each mixture and left to incubated for 5 minutes at room temperature on a rotating platform. The elution buffer has a low pH (pH2.0), the low pH condition allows the disassociation of the antibody-antigen interactions however if left for prolonged periods of time can disassociated the antibody and protein A/G interactions. Therefore, 7µL of neutralizing buffer is added.

2.5.6 Measurement of Protein content by Bicinchoninic Acid Assay

Following protein extraction, a bicinchoninic acid assay was performed. This ensured the amount of protein loaded into a polyacrylamide gel is standardized across all my samples.

A bicinchoninic acid assay (BCA) also known as a Smith assay was performed on each tissue homogenate as described by Smith *et al* 1985 [374]. This is a popular colorimetric detection

method for quantifying total protein which combines the reduction of Cu^{2+} to Cu^{+} by protein in an alkaline medium with the highly selective and sensitive colorimetric detection of the cuprous cation (Cu^{+}) by Bicinchoninic Acid.

The BCA assay was chosen because it has a number of advantages of other colorimetric assays such as Lowry [375] and Bradford [376] assays. These include greater reagent stability, increased sensitivity, decreased protein: protein variation and it is compatible with samples that contain up to 5% detergent (surfactants).

The Lowry method [375] involves the reaction of copper ions with peptide bonds and the oxidation of aromatic protein residues under alkaline conditions (Biuret test). This method was not used because the reaction method is not well understood. Also the method is intolerant towards compounds such as Mg^{2+}, K^{+}, EDTA and Tris [376].

The Bradford assay is a more sensitive method than the Lowry method with less drawbacks [376]. However, the main disadvantage the Bradford assay has is that it is incompatible with the percentage of detergent used to solubilise proteins. This will cause the reagent to precipitate even at low levels. Furthermore, the coomassie dye present is highly acidic therefore a small number of proteins cannot be measured due to poor solubility. Coomassie dyes also offer greater protein variation.

The BCA method is also not perfect as it is not compatible with high concentrations of SDS. To overcome this, tissue homogenates were diluted in cell lysis prior to performing a BCA assay.

Protein samples (tissue homogenates including the unbound fraction of IP/CO-IP samples but not the bound fraction) were diluted 1:4 in 1x lysis buffer (Invitrogen). This ensured that the protein concentration remained within the standard curve range of the BCA protein (0 – 2mg/ml). Homogenates were then mixed 1:1 with cell lysis buffer. Protein standards were made

using ddH_2O and mixed 1:1 with cell lysis buffer. BCA reagent was added to protein samples (standards or homogenates) in a 96 well plate (Thermos scientific) and incubated at $37^{O}C$ for 30 minutes. After incubation, a purple/blue colour forms due to the reaction of BCA with the cuprous cation which was subsequently read at 562nm.

2.5.7 Sample preparation for Gel Loading

Tissue homogenates (containing between 15 - 40µg of protein) were prepared in (4x) NuPAGE LDS ® Sample Buffer (Invitrogen) (pH 8.4). A standard laemmli buffer usually contains 106mM Tris HCl, 141mM Tris base, 4% SDS, 20% Glycerol, 0.51mM EDTA, 0.2mM Serva Blue G250, 0.175mM Phenol Red.

SDS is a detergent that solubilises all the protein but also makes proteins negatively charged meaning that proteins will run towards the positive end on the gel. As all the proteins are negatively charged, the only factor that affects the rate of travel through the gel is molecular weight. Glycerol increases the density of the protein sample and thereby ensures that the sample stays in the well. EDTA is present as it is a strong chelator of metal (e.g. Mg^{2+}) necessary for enzymatic activity. This therefore helps inhibit protease and phosphatase enzymes found in the samples. Serva Blue and Phenol Red act as tracking dyes.

An appropriate volume of 1x cell lysis buffer was added to each sample, ensuring the same volume and protein concentration remained the same in each sample. The samples were then boiled at $95^{o}C$ for 5 minutes, denaturing of proteins. The samples were immediately placed on ice followed by centrifugation for ~30s using a top table centrifuge prior to being loaded into a gel. A molecular marker (Precision Plus Protein All Blue Standard, Bio-Rad) is also added into an adjacent well to the samples. The molecular marker or ladder is a mixture of protein of known molecular weight/size. This is used to determine the relative size of proteins which are

subject to gel electrophoresis. Proteins of interest can matched to know weights found in the protein marker.

2.5.8 Polyacrylamide gel electrophoresis and protein blotting

Gel electrophoresis is routinely used to analyse protein mixtures quantitatively and qualitatively. It enables high resolution of proteins, some of which may on vary in size by a few hundred Daltons. As the proteins carry the same negative charge, their migration can be initiated by an electric field and their mobility will dependent on their size. The most commonly used system is sodium dodecyl sulfate polyacrylamide gel electrophoresis or SDS-PAGE for short.

Proteins of a molecular size between 15 – 125kDa were separated using gel electrophoresis in the presence of 1x MOPS running buffer (Invitrogen). The running buffer contains 25mM Tris base, 190mM glycine and 0.1% SDS. Protein samples were pre-loaded onto a 4-12% precast Tris-Glycine polyacrylamide (PAGE) gel (Invitrogen) and resolved at 180v for 90minutes using the Xcell Surelock Mini-Cell Electrophoresis system (Invitrogen). A 4-12% gradient gel was used as we were separating a mixture of proteins with different molecular weights.

Once the proteins have been separated by electrophoresis, they must be transferred onto an appropriate membrane. The most common method is electroblotting, first described by Towbin *et al* 1979 [377]. An electric field is applied perpendicular to the plane of the gel for 1 hour at 40V using a wet electro blotting system XCell II Blot Module (Invitrogen), this causes the proteins to migrate to a charged protein binding membrane, nitrocellulose membrane (Amersham). The membrane is in direct contact with the PAGE gel and a 'sandwich' is created between the electrodes with the addition of filter paper and sponges. This is submerged in 1x transfer buffer/ conducting solution (25mM Tris, 192mM glycine, 20% methanol) to allow the protein to move readily from the Page gel to the membrane. Transfer of proteins can be visualised by staining the membranes with reversible dyes such as Ponceau S.

2.5.9 Blocking

Prior to antibody treatment, the membrane is blocked for 1 hour at room temperature using 5% non-fat milk solution (Marvel) in Tris Buffered Saline with Tween (TBST) (Sigma). This is crucial as it helps prevent non-specific binding of antibodies (primary and secondary) to the nitrocellulose membrane.

Bovine Serum albumin (BSA) is another commonly used blocking solution that can be used instead of milk. It is believed to work better especially when probing using phospho antibodies as albumin is a secreted protein and tends not to be phosphorylated. Milk also contains a protein called phospho casein. This phosphoprotein can lead to higher background due to non-specific recognition of the phospho motifs. However studies carried out previously in our laboratory have found that milk provides less background than BSA.

2.5.10 Detection of Protein of Interest

In order to detect our proteins of interest, the membranes have to be probed using a primary antibody that recognises the specific epitope found on our protein. The primary antibody is not detectible, instead a secondary antibody which is raised against the IgG of the same species of primary antibody will be used. The following table (Table 2.1) demonstrates primary and secondary antibody protein targets, dilutions factors and expected molecular weight of protein target.

Table 2.1:

Target Protein	Molecular weight (kDa)	Primary Antibody (Dilution)	Secondary Antibody (Species and Dilution)
P-MYPT1 (thr 850)	125	1 in 3000	Goat Anti Rabbit (1 in 3000)
MYPT1	125	1 in 1000	Goat Anti Rabbit (1 in 3000)
P-MLC (ser 19)	20	1 in 1000	Goat Anti Mouse (1 in 3000)
MLC	20	1 in 1000	Goat Anti Rabbit (1 in 3000)
P-Src (tyr 416)	60	1 in 500	Goat Anti Rabbit (1 in 3000)
Src	60	1 in 1000	Goat Anti Rabbit (1 in 3000)
Phospho Tyrosine		1 in 1000	Goat Anti Rabbit (1 in 3000)
ARHGEF1	115	1 in 1000	Goat Anti Rabbit (1 in 3000)
GAPDH	37	1 in 4000	Goat Anti Mouse (1 in 2000)

Table 2.1: Primary and Secondary antibodies and dilutions
Shows the dilutions of primary and secondary antibodies for all target proteins detected using western blot. The species of the secondary antibody is also mentioned.

The secondary antibody is linked to an enzyme called horseradish peroxidase (HRP). When mixed with an appropriate chemiluminescent substrate, the resulting reaction emits light which can be detected by light sensitive film or camera. HRP is commonly used as it is able to amplify a weak signal and allow the detection of low levels of target proteins.

Antibody dilutions are prepared using a wash buffer containing a low percentage of blocking reagent. This helps prevent background and non-specific staining. The wash buffer used is Tris Buffered Saline with Tween (TBST) (SIGMA). It contains Trizma base, NaCl (0138M),

distilled water and Tween-20 (0.05%) which acts as a detergent. Washing the membrane also helps remove and minimise nonspecific binding.

All antibodies were made up in TBST and 5% non-fat milk. The majority of the antibodies have been used previously within the group[7,41,83,88]. Furthermore, p115 RhoGEF antibody has also been used by other groups [230,308], therefore I was confident in the dilutions and specificity of the antibodies used.

Nitrocellulose membranes were incubated with primary antibody overnight at 4^{o}C with constant agitation. Membranes were then washed 3 times in TBST, 10 minutes per wash. The appropriate HRP-secondary antibody was applied for 1.5 hours at room temperature with constant agitation. Following incubation with the secondary antibody, the nitrocellulose membranes were subsequently washed a further 3 times in TBST, 10 minutes per wash. In order to detect our protein of interest, membranes were exposed to an appropriate enhanced chemiluminescent (ECL) substrate.

Phospho-proteins have a much weaker signal and require a much stronger ECL. Therefore all 3 of our phospho proteins were detected using SuperSignal West Femto chemiluminescent substrate (Thermo scientific). This substrate, as described by Thermo scientific, is ultra-sensitive an able to detect low-femtogram levels of protein by Western blot analysis with horseradish peroxidase (HRP) enzyme.

Membranes were initially probed 1st for phospho-proteins due to their weak signal. Following detecting of phospho-protein, membranes were rinsed with TBS to remove any excess ECL. The same membrane was then stripped of antibody using 10ml of Restore Western Blot stripping buffer (Thermo scientific) for 1 hour at room temperature under constant agitation. The membrane were then rinsed using TBS and blocked again in 5% non-fat milk solution for 1 hour at room temperature and then re-probed with an appropriate total antibody in 5% non-

fat milk overnight at 4^{o}C again under constant agitation. This protocol was performed for each membrane.

The total antibody detects the total amount of non-phosphorylated and phosphorylated forms of its protein. This is used as an internal control and allows the ratio of phosphorylated: non-phosphorylated protein to be determined. GAPDH was used during IP/CO-IP studies as a loading control because it is stable and constitutively expressed and considered a housekeeping gene.

Membranes were then incubated with an appropriate secondary antibody for 2 hours at room temperature. As total proteins have a stronger signal a weaker ECL was used e.g. ECL plus or ECL prime (Amersham, GE healthcare). This also helped limit any bleed through by any phosho signal that has not been removed during the stripping process.

Detection of proteins was carried out using Biorad ChemiDoc XRS+ gel imaging system. Bands were detected using a high resolution protocol suitable for the distinction of bands that are close together.

On each gel there were at least 3 controls. The average of these controls was calculated and an average of their phospho-protein: total protein ratio was used as the control values. The effects of all the treatments were expressed as a percentage increase or decrease of the average control response.

2.6 Pulmonary artery smooth muscle cell (PASMC) Studies

2.6.1 Pulmonary artery Smooth Muscle Cell Line Generation

PASMCs were isolated by digestion of the pulmonary arterial tree. The digestion process targets the connective tissue and not the cells. Arterial trees were dissected as previously described (in section 2.1.1), then cut into small pieces and added to a glass tube containing (~2mL) of filtered PSS solution (Gibco). The pieces of tissue were cleaned using filtered PSS (3X) and then added to the enzymatic solution.

The enzymatic solution contained HEPES buffer (pH7.4) which was composed of (mM): 120 NaCL, 4 KCL, 1 $MgCl_2$, 10 HEPES (no Ca^{2+}, no EGTA and 1gl/L glucose) and an enzymatic composition of 4mg of collagenase Type XI (0.2%w/v) (Sigma), 2mg of papain (0.1% w.v) (Sigma), 2mg of trypsin inhibitor (0.1%w/v)(Sigma) and 20µL of DL-Dithiothreitol (1mM)(Sigma). This solution was vortex mixed at room temperature for 2 minutes, filtered through a 0.2µM filter (Millex) and then incubated at 37ºC for 30 mins (inverting the tube several times to ensure a thorough mixing).

The cell suspension created was centrifuged at 200g for 1 minute at room temperature, the supernatant was aspirated and ~2mL of warm filtered HEPES solution was added. The tube was inverted (3x) before being centrifuged at 200g for 1 minute. This stage was repeated 2 more times with HEPES buffer. The washing stage was continued using warm media a further 3 times.

The media was aspirated and 5mL of fresh media was added. The solution was dispersed into individual cells by vigorously pipetting up and down (~30x) using a glass pipette and rubber bulb. This was incubated in a T25 flask at 37ºC, 5% CO_2.

2.6.2 Cell Culture medium

Primary smooth muscle cells lines were cultured using, Dulbecco's Modified Eagle Medium (DMEM) (500ml) containing Foetal Bovine Serum (FBS heat inactivated) (50ml), Sodium Pyruvate (100mM) (5ml), Non-essential amino acids (MEM NEAA 100x) 5ml, PSG (100x) 5mL (penicillin 10,000 U/ml, streptomycin 10mg/ml, l-glutamine 200mM). A detailed composition of supplements and their function can be found in table 2.2 below:

Table 2.2:

Supplements added to DMEM: Normal Cell culture	**Function**
Fetal Bovine Serum	Provides growth factors to support growth and satisfy metabolic needs of the cells during culture
Glucose	Acts as an energy source for cells in a reduced environment
L-Glutamine	Acts as an alternative energy source for cells that are not efficient at metabolising glucose. Supports Cellular growth where there are high energy demands and large levels of protein and nucleic acid synthesis
Sodium Pyruvate	Additional Energy Source
Non-essential Amino Acids	Supplement to increase cell growth and viability
penicillin and streptomycin	Used to prevent bacterial contamination from gram positive and gram negative

Table 2.2: Cell Culture media Supplements

Details the supplements present in Dulbecco's modified Eagle Medium (DMEM) used for PASMC culture.

2.6.3 Smooth Muscle Cell Line Culture

Cells were initially seeded into 1xT25 (passage 1) however after reaching 80% confluency, the cells were then seeded at approximately 1 in 3 dilutions e.g. 1xT25 into 1xT75 flask (passage 2) and from 1xT75 flask into 3xT75 (passage 3). Cells were grown in appropriate size flasks until used for experimental procedures usually after passage 3. Each passage on average took 4 days.

In order to split the cells, media was aspirated and the cells washed with sterile 1XPBS thereby removing all the cell debris. Trypsin ethylenediaminetetraacetic acid (EDTA) (0.05%) was added to the flask containing cells and left to incubate at $37^{O}C$ for 3 minutes. Trypsin is an enzyme that acts by severing peptide bonds which hold the cells together as well as keep them attached to the flask. EDTA is an important component which aids trypsin as this acts as a chelator of Ca^{2+} and Mg^{2+} which inhibits trypsin activity.

The flask was tapped horizontally several times to ensure all of the cells had detached and separated from each other. The appropriate volume of warm media was then added and mixed with the cells (FBS in the media inhibits the activity of trypsin). The cells were then centrifuged for 5 minutes (200g) at room temperature. The supernatant was aspirated and the cells were re-suspended in the appropriate volume of fresh media (DMEM).

After enough cells were grown, these were required to undergo growth arrest or serum starvation for 24 hours. Serum starvation forces the cells (mostly) into G0 arrest [378] but also ensures that the cells return to a contractile phenotype as contractile protein levels are dramatically reduced during proliferation. PASMCs take ~12hours to divide in our hands, therefore 24 hours allows the cells to finish diving and all be at the same growth arrest point. Furthermore all other proliferative signals which may interfere with signalling events will have been silenced.

During serum starvation, the cells are still alive and functioning properly, they just lack the necessary proteins to undergo cell division. In order to growth arrest cells, cells were incubated in DMEM containing all the necessary supplements except FBS. The composition of supplements used can be found in table 2.2 but without FBS.

2.6.4 Verification of PASMC as smooth Muscle (Detection of Smooth Muscle Markers)

There are 2 key markers that are used for the detection of vascular smooth muscle; calponin and α-actin. Staining for these markers was carried out at a low and later passage number thereby ensuring no cell differentiation.

Calponin binds to actin and myosin Ca^{2+} binding proteins and inhibits actomyosin ATPase as well as the movement of actin filaments over myosin. α-actin is a cytoskeletal actin-binding protein localized in dense bodies which stabilizes the muscle contractile apparatus. Therefore both proteins are considering to be an integral in smooth muscle function [379,380] and good markers of smooth muscle. This is demonstrated in Figure 2.4, where staining for both proteins can be clearly seen and is evidence that the cells are indeed smooth muscle cells.

Figure 2.4

(A) **(B)**

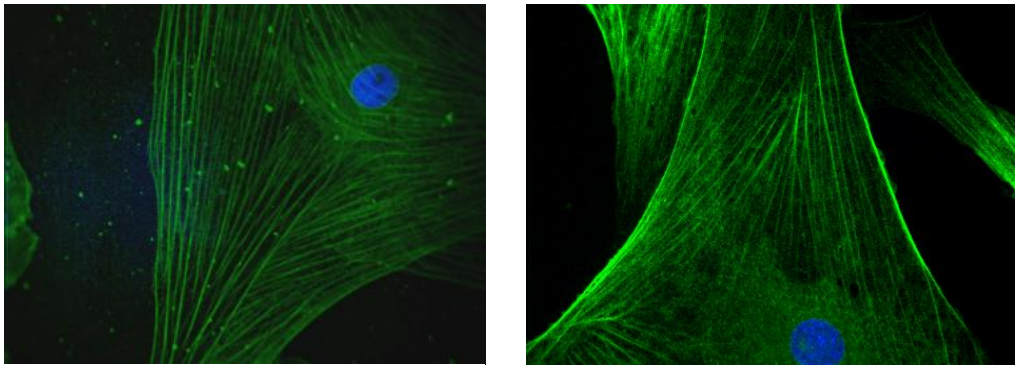

Figure 2.4: Staining for VSMC markers
Staining for (A) α-actin and (B) calponin staining, confirming that these cells are smooth muscle cells. Hoechst, which stain for DNA show the presence of the nucleus.

2.6.5 Reactive Oxygen Species (ROS) measurement in PASMC and tissue

Reactive oxygen species (ROS) measurement was investigated in both PASMCs and IPAs. As discussed in the introduction section, ROS are believed to act as signal moieties at physiological levels but dysregulation is associated with numerous diseases.

2.6.6 Choice of 96 well plate for ROS measurements

White or black solid bottom and white or black clear bottom plates are available in which to perform these experiments. Clear bottom plates provide and an advantage of being able to examine cells by microscope during the course of an experiment. However, there is an essential difference between white and black plates and that is their reflective properties. White plates reflect light and maximise light output signal whereas black plates absorb light and reduce background and crosstalk. For these reasons, white plates are used when measuring luminescence while black plates are used for fluorescence.

2.6.7 Luminescent and fluorescent probes used

Luminescence

Luminescence is a general term used to describe the emission of light by a substance that is not due to heat (**Incandescence** is light from heat energy). Luminescence is "cold light" that can be emitted at room or lower temperatures and involves the release of an electron from its lowest energy "ground" state into a higher energy "excited" state. The electron then returns the excess energy in the form of light so it can return back to its "ground" state. With few exceptions, the excitation energy is always greater than the energy (wavelength, colour) of the emitted light.

Luminescent studies were performed primarily using the dye L-012 (8-amino-5-chloro-7-phenylpyrido [3,4-d]pyridazine-1,4-(2H,3H) dione) (Wako Pure Chemical Industries). L-012, a modified form of luminol, has been described as a specific probe for $O_2^{\bullet -}$ [381-384] producing a much stronger signal than other CL probes. There are a number of reasons I chose to use

L-012, the first being is that it is not subject to redox cycling and has been described as being reliable for detecting NOX-derived $O_2^{\bullet-}$ using high throughput screening (HTS) assays[384,385]. L-012 is much more sensitive than other probes such as luminol and lucigenin and produces a signal at least 100 times stronger. The procedure is inexpensive, easy to perform, quick and unlike luminol is not pH dependent. Furthermore when performing control experiments, L-012 produced much higher and consistent results when compared to other luminescent dyes. The main drawback is that L-012 primarily detects superoxide but may also detect $ONOO^-$ and probably other ROS [383,385-387].

Lucigenin (bis-*N*-methylacridinium nitrate) was also use briefly when determining which probe to use throughout my studies. It is the most widely used chemiluminescent probe used extensively to detect superoxide[102,388-392] in enzymatic and cellular systems. For example, lucigenin has been used to detect superoxide production from NADPH-oxidase in phagocytic cells, NADH-dehydrogenase in mitochondria, NADPH-cytochrome P_{450} reductase in microsomes, and from xanthine oxidase and NAD(P)H oxidases in endothelial and vascular smooth muscle cells [84,389,393-396]. Lucigenin's main strengths are that it is specific for superoxide ($O_2^{\bullet-}$), cell permeable and inexpensive. I did not use lucigenin due to it being involved in redox cycling and able to generate superoxide ($O_2^{\bullet-}$). Furthermore, in control experiments I found that the lucigenin signal is only slightly above background meaning normal chemiluminescence plate readers or luminometers that we use within the laboratory are not sensitive enough to detect a strong enough signal that I would be confident with. I would have also had to of run substantially more plates than L-012 to obtain significant results.

Luminol was also briefly used during preliminary experiments. Luminol is one of the oldest used chemiluminescent probes[397]. It can be oxidized by a variety of ROS, including H_2O_2[398], hydroxyl radical [399], hypochlorous acid[400], and peroxynitrite [401,402]. The main advantage to using

luminol is that it can detect intracellular and extracellular ROS, is not involved in redox cycling and inexpensive to perform. Luminol in not specific for a certain ROS species, require the presence of peroxidases and is also pH dependent with optimal pH being 9-10. Furthermore as with lucigenin, I found luminol to produce a very weak signal and found the signal to only be above background.

Fluorescence

Fluorescence is the emission of light by a substance that has absorbed light. The emitted light has a longer wavelength, and therefore lower energy, than the absorbed light. Therefore allowing for an accurate reading of results.

The main fluorescent probe used throughout this investigation is Amplex Red (N-acetyl-3, 7-dihydroxphenoxazine) which has been used in the detection of extracellular hydrogen peroxide (H_2O_2)[403,404]. Amplex Red involves the measurement of H_2O_2 by horseradish peroxidase-catalysed oxidation of the Amplex Red to resorufin which when excited at 530nM emits strongly emits light at 590nM.

Amplex Red has a number of advantages, it has low background fluorescence, high specificity for H_2O_2, resorufin is also stable with the excitation and emission maximum wavelengths that are far enough apart to stop autofluorescence also Amplex Red can also be used in a wide range of different cell types [403,404].

Amplex Red assay does have a number of drawbacks, the first being that resorufin is a substrate of HRP and can be further oxidised resulting in fluorescence [405]. Furthermore the stability of Amplex Red may be an issue at high pH values (>8.3)[405]. Also like other HRP methodologies, it is susceptible from interference with substances which that oxidize this enzyme.

2.6.8 ROS measurement in cell free system

As discussed above, each probe has their own advantages and disadvantages. Therefore a control experiment was performed for each probe in a cell free system to determine which probe gave an accurate, readable (far greater than baseline) and a more stable signal.

Lucigenin (10μM) and NADPH (100μM), luminol (10μM), L-012 (50μM), Amplex Red (50μM) and 0.1U/ml horseradish peroxidase (HRP) were aliquoted individually into 20ml of PBS (GIBCO). Amplex Red solution was prepared in dim light. Xanthine oxidase (Sigma) (0.5-2mU/ml) and its substrate hypoxanthine (Sigma) (250μM) were added to each mixture at room temperature or to PBS alone. 150μL of the resulting mixtures were added to the corresponding 96 well plate. Changes in luminescence was measured at 5 minute intervals with 5 readings taken, while fluorescent readings was measured every minute for 10 minutes. This was performed using Promega GloMax Discover: Multimode detection system at 37^{O}C.

Xanthine oxidase caused no marked increase in luminescence in the presence of lucigenin + NADPH (Fig 2.5A) or luminol (Fig 2.5B). Lucigenin is shown to produce a low luminescent reading with virtually no difference between blanks and samples containing xanthine oxidase at any time point. In the presence of luminol, samples containing xanthine oxidase actually reduced luminescence levels below the blank readings at each time point. In the presence of L-012, 2mU/ml of xanthine oxidase did cause a marked increase in luminescence at 5 minutes (Fig 2.6A). This signal did decrease over time to plateau ~25minutes, however the signal produced was still much greater than what was obtained from blank readings. Finally, xanthine oxidase at the concentrations used, produced a large increase in fluorescence in the presence of Amplex Red (Fig 2.6B). The fluorescent signal increased over time and did not appear to plateau with the exception of 1mU/ml of xanthine oxidase.

Xanthine oxidase is an enzyme known to produce ROS, therefore changes in luminescence/Fluorescence correspond to changes in ROS production. Lucigenin produced a very weak signal which would require an extremely large n number to be able to gain statistical significance. Luminol signal actually decreased in the presence of xanthine oxidase when it should have increased. For these reasons I decided not to use these probes for future experiments.

L-012 and Amplex Red produced measurable results much greater than blank values at all time points. Furthermore, both probes are structurally different and each offer a different method of measuring ROS (L-012 = luminescence, Amplex Red = fluorescence). Therefore, these probes were chosen to measure ROS in future experiments in cells and/or tissue. Previous work within my group using Amplex Red found no measurable responses in cells when stimulated, therefore this probe would be used primarily for tissue studies.

Figure 2.5

(A)

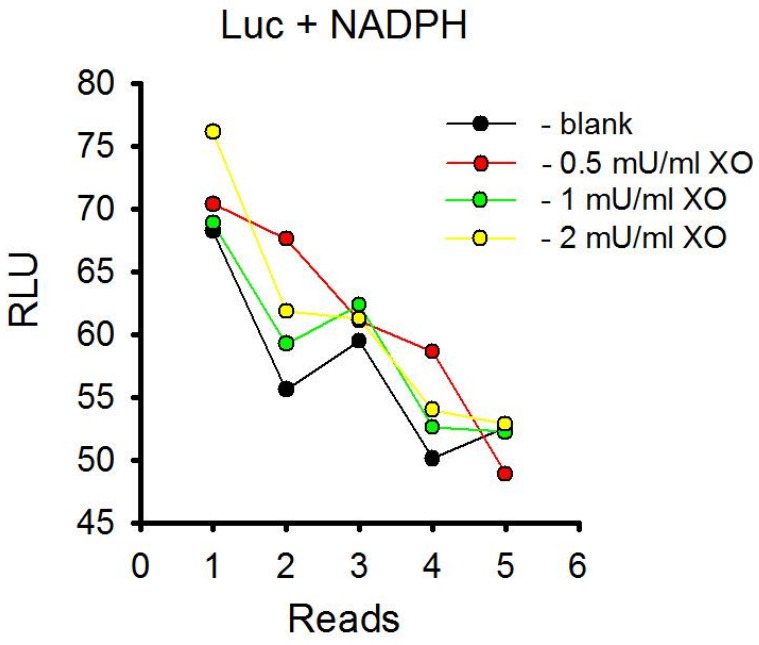

(B)

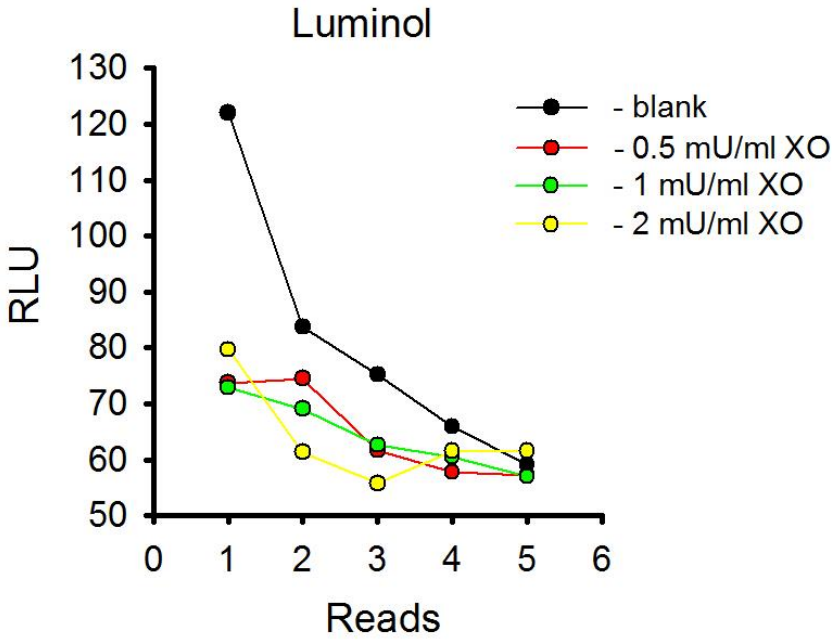

Figure 2.5: Effect of xanthine oxidase on ROS production in the presence of lucigenin and luminol

Luminescent results from **(A)** Lucigenin (10µM) and NADPH (100µM) (upper panel) and **(B)** Luminol (10µM) (lower panel) in the presence and absence of 0.5 – 2mU/ml xanthine oxidase and its substrate hypoxanthine (250µM). Line graphs represent reads at every 5 minutes (n = 1) for each condition.

Figure 2.6

(A)

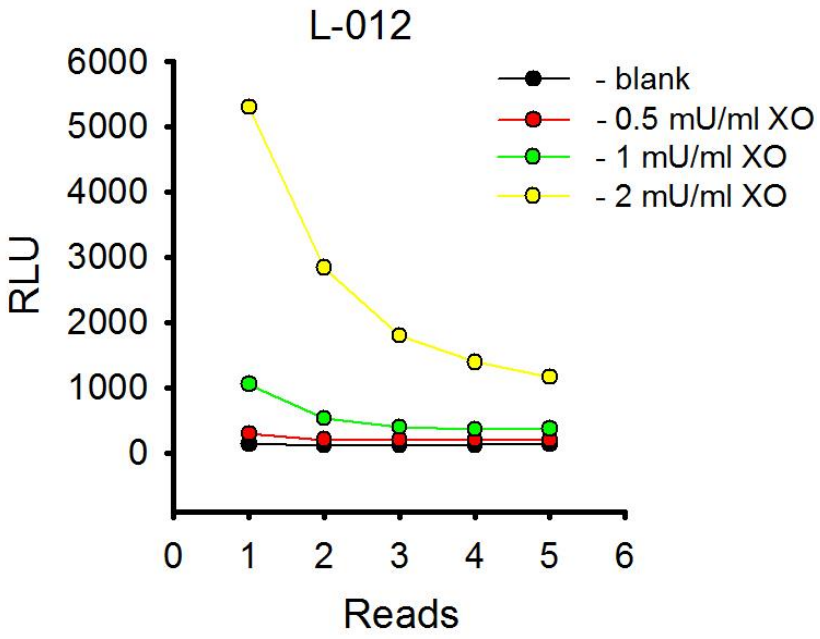

(B)

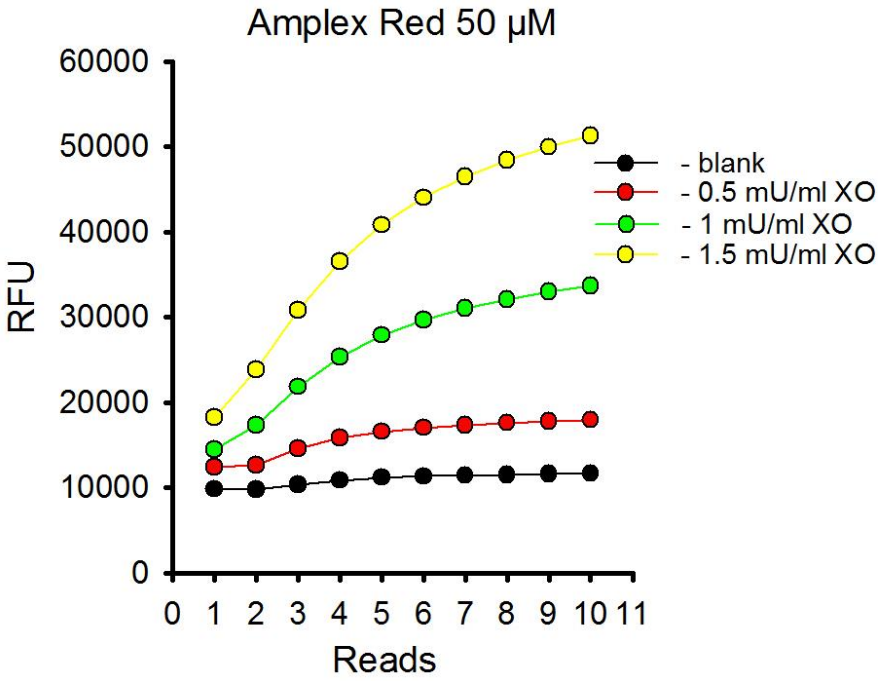

Figure 2.6: Effect of xanthine oxidase on ROS production in the presence of L-012 and Amplex Red

Shows luminescent results from **(A)** L-012 (50µM) (upper panel) and fluorescent results for **(B)** Amplex Red (50µM) (lower panel) in the presence and absence of 0.5 – 2mU/ml xanthine oxidase and its substrate hypoxanthine (250µM). Line graphs represent reads at every 5 minutes (n = 1) for L-012 and reads at every minute for Amplex Red.

2.6.9 Buffers used during studies

While investigating ROS production in cells and tissue, it was important to choose the right buffer in which to perform my experiments. Phosphate Buffered Saline (PBS) and Hanks Balanced Salt Solution (HBSS) were deemed to be suitable buffers as they are stable at room temperature and at $37^{O}C$, maintain cell osmolarity and maintain a neutral pH in order not to destroy the cell or tissue sample. Furthermore, bubbling with CO_2 is not required as this is not a bicarbonate buffer and would be extremely difficult to perform using Promega GloMax Discover: Multimode detection system.

I therefore performed a control experiment to determine which buffer would be used along with L-012.

L-012 (50μM), xanthine oxidase (2U/ml) and its substrate hypoxanthine (Sigma) (250μM) were added to each buffer at room temperature. 150μL of the resulting mixtures were added to the corresponding 96 well plate. ROS production was then measured at 5 minute intervals at $37^{O}C$ using Promega GloMax Discover: Multimode detection system (Figure 2.7).

Results indicate that L-012 and PBS give the highest signal over the shorter time point. Therefore PBS will be used as the buffer for measuring ROS production

Figure 2.7

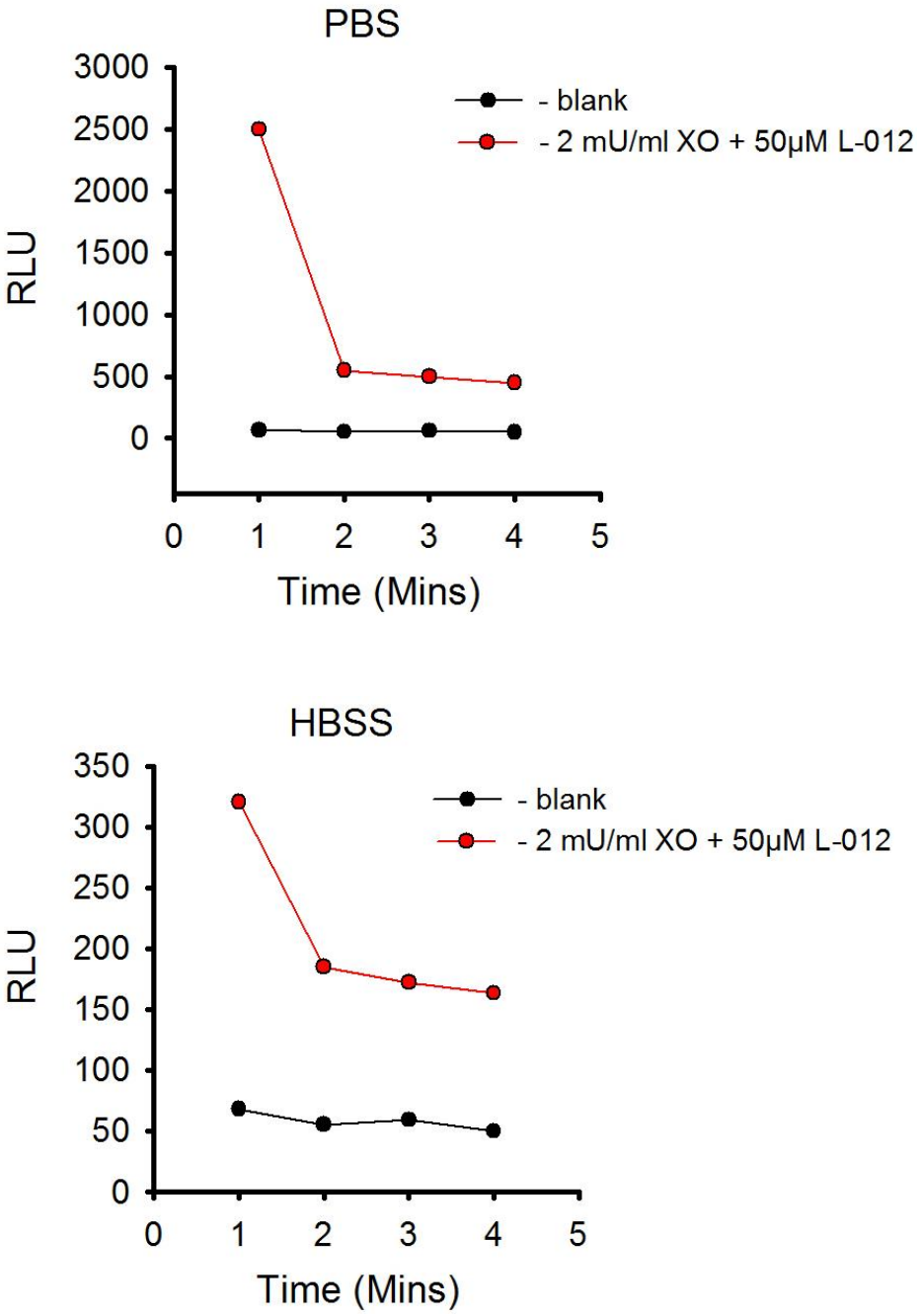

Figure 2.7: Effect of PBS and HBSS on xanthine oxidase ROS production in the presence of L-012

Shows luminescent results from L-012 and xanthine oxidase in PBS (upper panel) and HBSS (lower panel). Line graphs represent reads at every 5 minutes (n = 1) for each condition

2.6.10 ROS measurement in PASMCs

Following initial growth of PASMCs cell lines, PASMCs were seeded into a 96 well white solid bottom plate at a density of between 5.0 – 10.0x10^4 cells per well. Cells were allowed to attach overnight at 37^{o}C in DMEM + 10% FBS (as described in 2.6.1). Following ~24 hour incubation, media was subsequently aspirated and fresh media added. Cells were then left to incubate until they were 90% confluent. The media was then aspirated and replaced with serum free media (as described in 2.6.3), cells were then incubated for ~24 hours. Following serum starvation, media was aspirated and replaced with PBS containing luminescent dyes: L-012 (50μM). 150μM of solution was added to the appropriate wells as a control or in the presence of U46 (100nM), U46 and tempol (3mM), U46 and ebselen (10μM), tempol (3mM) or ebselen (10μM). As a positive control, this was also carried out in the presence of our superoxide generator LY83583 (1 or 10μM). LY83583 (1μM) ROS was also measured in the presence of antioxidants tempol (3mM), ebselen (10μM). ROS production was then measured at 5 minute intervals from 0 – 30 mins at 37^{O}C using Promega GloMax Discover: Multimode detection system.

2.6.11 ROS measurement in Tissue

L-012 Measurement

Rat Intra-pulmonary artery were cut into 2 pieces, added to a well in a 96 well plate and incubated for 30 minutes. Initially 150μM of solution containing solely L-012 (50μM) was added to each well for 10 minutes followed by the addition of U46619 (0.1 or 1 μM) for 10 minutes finally with the addition of superoxide dismutase (SOD) (200U/ml) or tempol (3mM) for the final 10 minutes. Chemiluminescence was then measured at 1 minute intervals from 0 – 30 mins at 37^{O}C.

U46619 (0.1 or 1μM) did not enhance chemiluminescence as measured by L-012 (Fig 2.8) in IPA with control and treated samples appearing to follow a similar pattern of luminescence.

Furthermore, SOD and tempol were able to marginally reduce chemiluminescence suggesting they are inhibiting basal ROS production in control and treated samples. However, as there was no difference between U46619 treated and control samples, I therefore did not use L-012 to measure ROS production in tissue.

Figure 2.8

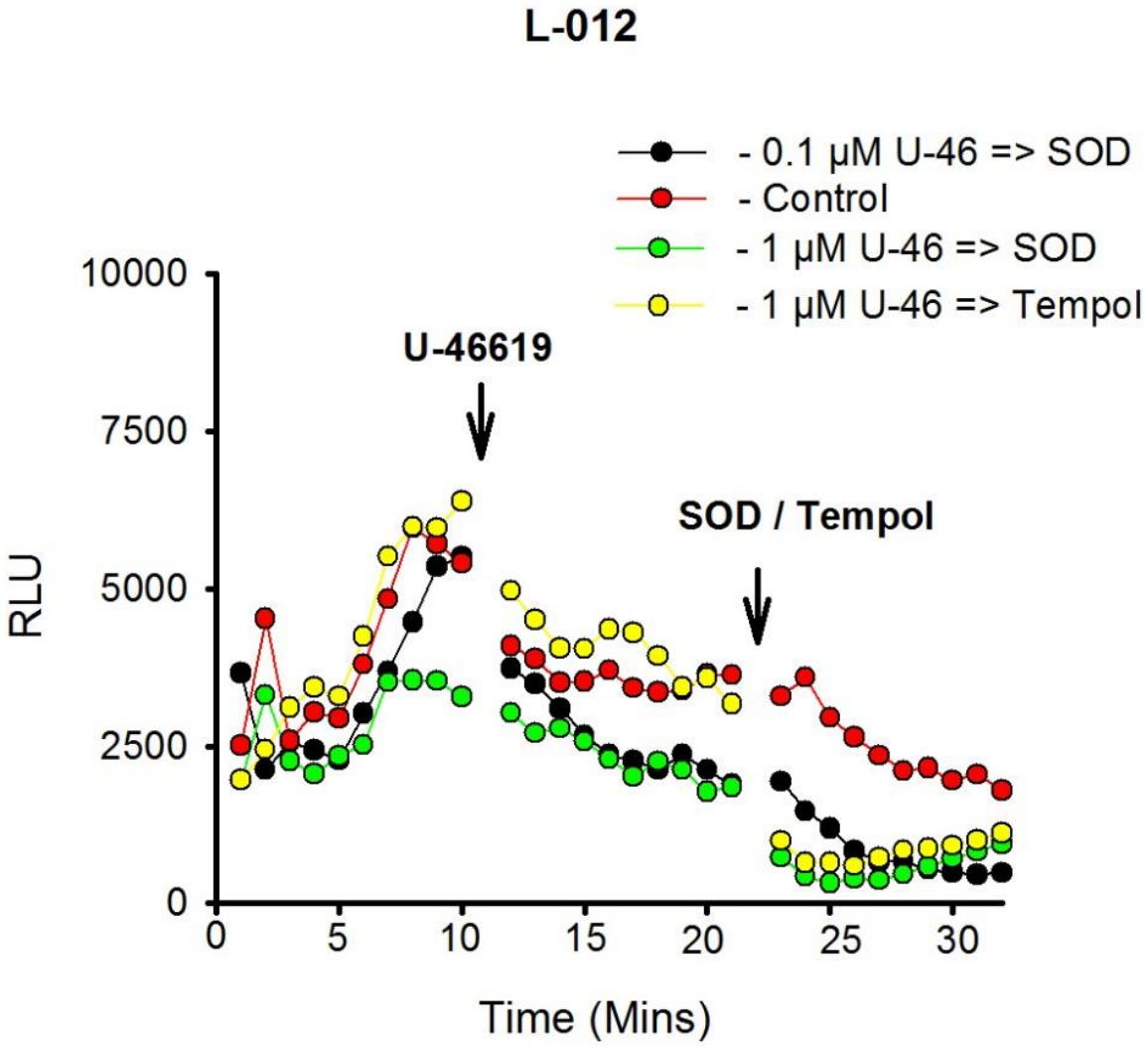

Figure 2.8: Effect of U46619 and antioxidants on ROS productions in the presence of L-012 in IPA

Shows luminescent results from ROS production in tissue. Line graphs represent reads at every 1 minutes (n = 1) for each condition. There was no significant increase in ROS production with U46619 or compared to control.

Amplex Red Measurement

Rat Intra-pulmonary artery were cut into 2 pieces and incubated at $37^{O}C$ in the dark for 3 hours in 1.5ml eppendorf tubes containing 1ml PBS, Amplex Red (10µM), 0.1U/ml HRP and U46619 (0.1 or 1 µM) with or without SOD (200U/ml) or ebselen (10µM), Phospho 12-13-dibutyrate (PDBU) (0.1 or 1µM) (Sigma), SOD (200U/ml) and ebselen (10µM). Following 3 hour incubation, 150µl of supernatant from each condition was pipetted into a solid clear bottom black plate, and read using Promega GloMax Discover: Multimode detection system at room temperature.

PDBU was used as a positive control during this set of experiments. PDBU is a known activator of PKC [406] which activate NOX production via phosphorylation of the $p47^{phox}$ subunit thus enhance ROS production[125].

U46619 and PDBU were unable to increase fluorescence using Amplex Red, rather both stimuli were shown to decrease the fluorescent signal. U46619 in the presence of ebselen and SOD showed similar results to U46619 alone whereas ebselen had no effect vs control however SOD marginally increase luminescence. The variety of results obtained along with the knowledge that U46619 and PDBU were unable to increase fluorescence, I therefore did not use Amplex Red to measure ROS production in tissue (Fig 2.9).

Figure 2.9

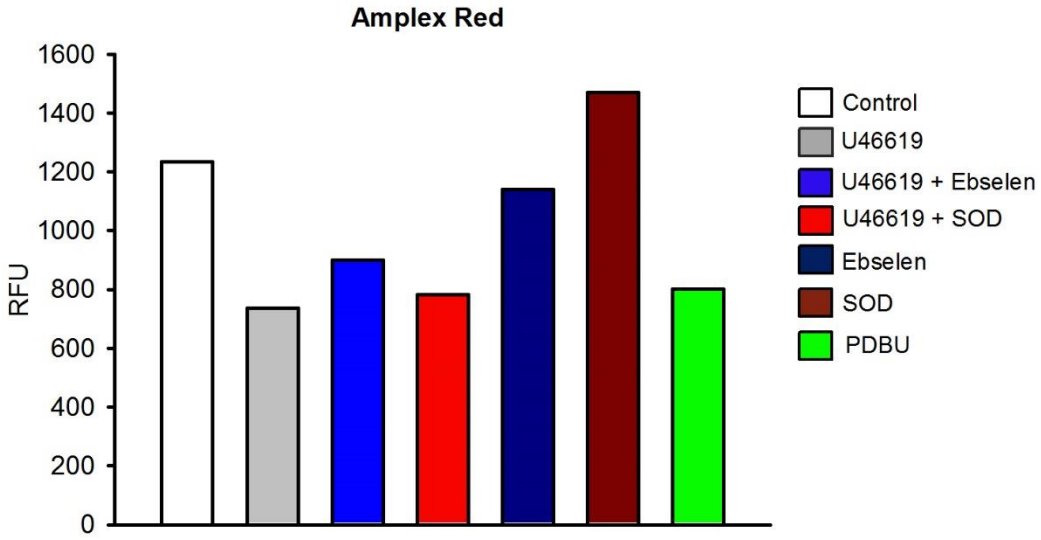

Figure 2.9: Effect of U46619 and antioxidants on ROS productions in the presence of Amplex Red in IPA

Shows fluorescent results from ROS production in tissue. Bar chart represent the mean (n = 2) per condition. There was no significant increase in ROS production with U46619 or PDBU compared to control.

2.7 Transfection of PASMC's for visualising Protein Translocation

PASMC's were transfected in order to visualize protein movement within the cell in response to stimuli and/ or inhibitors. As discussed in the introduction section, RhoA and ARHGEF1 are located in the cytosol in an inactive form however upon stimulation, translocate to the cell periphery where they are believed to be activated.

Green Fluorescent protein (GFP)

GFP has been used extensively during fluorescent microscopy. GFP is composed of 238 amino acids that exhibits bright green fluorescence with a major peak at 395 nm and a minor peak at 475 nm when exposed to light in the blue wavelength [407-409]. GFP can be tagged along with other proteins such as RhoA or ARHGEF1. This creates a fusion protein which are proteins created through the joining of two or more genes that originally coded for separate proteins but

code for both proteins from 1 promoter site. Creating a fusion protein such as eGFP-tagged RhoA or eGFP-tagged ARHGEF1, allows us to combine the functionality of both proteins. Due to the fluorescent properties of GFP, this allows us to visualise protein movement throughout the cell. GFP was therefore excited at 395nm and emission was captured at 509nm during my experiments.

2.7.1 Cloning of rat RhoA and ARHGEF1 into a C-terminal GFP vector

Plasmid design and generation was carried out by Dr Yasin Shaifta prior to the initiation of my research and the full protocol can be found in the appendix. However the whole process can be broken down into several important steps.

Initially our genes of interest to be isolated, cloned and over-expressed are RhoA and ARHGEF1. RhoA cDNA product was made and purified "in house" while ARHGEF1 was obtained and verified from Source Bioscience (Source BioScience UK Limited) cDNA library.

RhoA mRNA was obtained from rat PASMCs. This was then reverse-transcribed to produced complimentary DNA (cDNA). RhoA forward (start) and reverse (finish) primers were then designed using the known RhoA DNA sequence to serve as start and finish points for transcription, thus ensuring accuracy and limiting non-specific transcription.

Polymerase chain reaction (PCR) was then performed to amplify the DNA product to generate millions of copies of our DNA sequence. The PCR samples were then run on a 1% agarose gel, with enough sample left to perform the following cloning procedure. GeneRuler^{TM} 1kb DNA Ladder or λ DNA/ EcoRI+HindIII Marker were run alongside the samples to determine the size of the PCR product to determine semi-quantitatively that we have the correct product.

The band at the correct molecular weight was cut from the gel, and cloned into PCR®2.1-TOPO vector using DNA ligase. This vector was initially used as it was a cheaper alternative to using pcDNA™6.2/C-EmGFP/TOPO® which will be used when we have obtained a purified product.

The reaction mixture was then chilled on ice before proceeding to One Shot® Chemical Transformation of competent *E .coli* cells (Invitrogen Life Technologies, UK). The reaction mixture and *E .coli* cells were incubated to allow the plasmid to enter the cells. The resulting mixture of bacterial cells were spread onto pre-warmed LB-agar-ampicillin (100 μg/ml) selection plates and left to incubate. Cells have not been transfected with the plasmid will be unable to grow as they do not have the antibiotic resistance gene found on the plasmid. The clones that had grown were then lysed, protein was precipitated, DNA was captured in a column, eluted, precipitated and then re-dissolved. This stage was performed to purify the DNA product.

Once we have the correct product, this process was again carried out for both RhoA and ARHGEF1 except the DNA product was cloned into pcDNA™6.2/C-EmGFP/TOPO®. TOPO® TA cloning allows cloning of the PCR insert in the forward and reverse orientation, due to identical overhangs in the insert and in the vector. The occurrence of both orientations should theoretically be of equal chance. Therefore, to identify the clones which have the RhoA PCR insert ligated in the forward orientation, clone was assessed for their restriction endonuclease sites.

2.7.2 Cell Transfection

PASMCs were grown until confluency and then detached as previously described. Transfection was carried out using Amaxa™ Basic Nucleofector™ Kit for Primary Smooth Muscle Cells (LONZA). For each transfection, $1.3x10^6$ cells was used.

Initially a transfection mix was prepared at room temperature, consisting of 19μL supplement and 85.5μl nucleofector (protects cells). Cells were then centrifuged at room temperature for 5 minutes at 200g, the media was then aspirated. 4μg of eGFP tagged-RhoA or eGFP-tagged ARHGEF1 plasmid was then added into a transfection tube. The nucleofector and supplement

mixture was added to the cell pellet and thoroughly mixed. This cell mixture was then added to the plasmid and thoroughly mixed. This was subsequently added to a nucleofector corvette (Lonza). Transfection was then performed by electroporation using a Nucleofector™ 2b Device (Lonza).

Electroporation was used due to the higher transfection rate and cell survival when compared to lipofection. This works by shocking the cells with an electrical pulse which disrupts the phospholipid bilayer of the membrane, creating temporary pores. This also raises the electrical potential across the membrane allowing charged molecules such as DNA to pass through the pores [410].

Immediately after transfection, cells were added to warm media. 1ml of media containing the transfected cells were added to round 19mm glass coverslips (VWR international) and left to incubate until the following day were the media was aspirated and fresh media was added. Cells were left to grow until ~50% confluent. This allowed imaging of a single cell to be carried out with relative ease, furthermore if there was a greater confluency, then cells would be grown on top of each other making imaging difficult. It also allowed cells to grow and spread out again making it easier to see translocation from the perinuclear region to the cell periphery.

When cells reached ~50% confluent, media was aspirated and replaced with serum free media and left to incubate at 37^{O}C for 24 hours and then imaged.

2.7.3 Live Cell Imaging

Live cell imaging was performed using a Zeiss Axiovert 200 Microscope and visualized using BD™ CARV II Confocal Imager. The light source used was a 120W Metal Halide light source which allows a full-spectrum (360nm–700nm) imaging through filter sets which are matched to the excitation and emission requirements of our fluorescent sample.

Therefore in order to image proteins tagged with eGFP, light emitted from our light source passes through our excitation filters which is matched to the UV wavelength. This is then focussed onto our sample which emits a green fluorescence which is filtered through the emission filters matched to green fluorescence and enables visualisation of our protein as illustrated in figure 2.10.

Figure 2.10

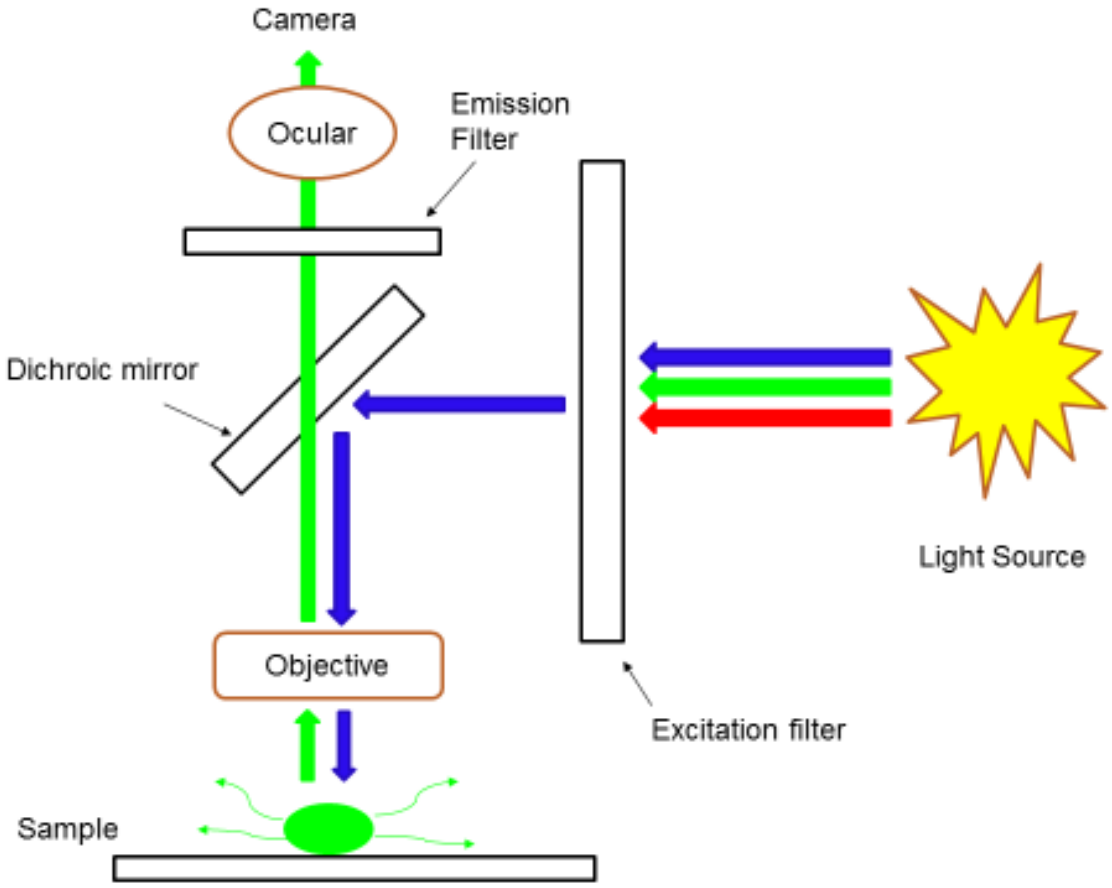

Figure 2.10: Overview of the excitation light path from the light source to the sample and the emission light emitted from the sample toward towards the camera.
Shows the excitation light path from the light source, where it is filtered by the excitation filter, and reflected towards the sample via a dichroic mirror. The emitted light from the sample passes through the dichroic mirror where it is filtered by an emission filter, finally reaching the camera.

Images were taking using a digital camera built into the imaging system. The images itself were constructed by binning of pixel intensities. Each pixel has a specific number and this number

relates to what colour the pixel is. Binning allows the combination of adjacent pixel to create one single pixel in the recorded image. In this experiment, I used a 3 x 3 binning factor optimised previously by others within the laboratory. This allowed me to gather information from 9 pixels (in a square), thereby increasing the pixel intensity by 9. This does increase the signal to noise ratio but reduces resolution. Each image was exposed to light for 65.0ms. I varied the frame rate during the experiment to reduce photo-bleaching of eGFP. This occurs when the fluorophore, in this case eGFP permanently loses its ability to fluoresce due to photo induced chemical damage and covalent modification.

Media was aspirated and replaced with PSS which is continuously bubbled with 5%CO_2/95% air. Coverslips were mounted onto the microscope and visualised at X40 magnification at 37^{O}C. Initially 5-10 frames were taken of the coverslip every 5 seconds were no treatment was applied as a control run. U46619 (100nM) or LY83583 (1µM) was then applied and frames were taken every 2 seconds for 30 seconds. The coverslip was then washed with PSS and left to incubate for 10 minutes during which time 5 frames were taken over 10 minutes, 1 frame every 2 minutes. Following incubation period, U46619 (100nM) or LY83583 (1µM) was then reapplied to control cells and frames were taken every 2 seconds for 30 seconds. In non-control cells, inhibitors ebselen (1µM), tempol (3mM), or PP2 (1µM) was added to the coverslip and left to incubate for 10 minutes with 5 frames being taken, 1 frame every 2 minutes. U46619 (100nM) or LY83583 (1µM) was then reapplied to control cells and frames were taken every 2 seconds for 30 seconds. The software used for image building was Metafluor and Metamorph (Molecular Devices) (7.8.12.0).

Translocation image Analysis

Image J software was used to measure puncta formation or changes in background intensity in the presences of our stimuli and inhibitors. The image was loaded into image J and a line scan was performed. This was carried out by drawing a line through 3 separate points in the image

at opposite ends of the cell where puncta appeared or background region. The line was drawn from the inside of the cell to the outside. The profile of the line was plotted and the greyscale value of intensity is shown. This process is demonstrated below in Figure 2.11. The values were then plotted into Microsoft excel.

Figure 2.11:

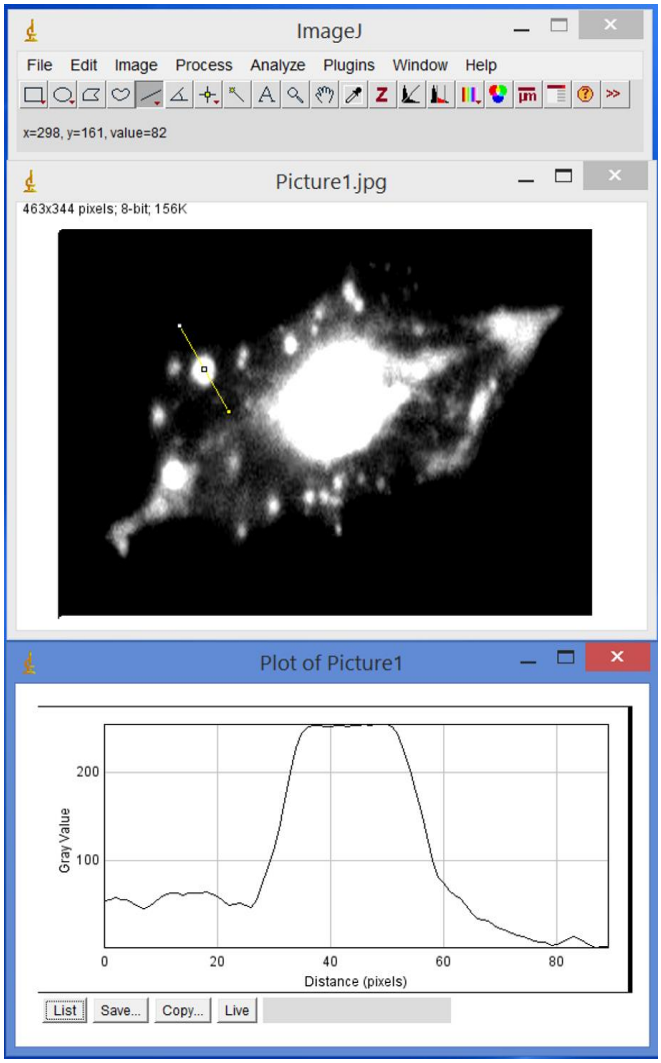

Figure 2.11: Analysis of a transfected PASMC picture while stimulated using Image J software.

Shows Measurement of puncta Using Image J. The top panel shows the line scan function that was used for measurements. The second panel shows how the line scan function was applied to our image. The bottom panel shows the greyscale profile that was generated from the analysis. As illustrated in the bottom panel, the initial grayscale readings corresponds to cytosol grayscale value, the subsequent increase in grayscale value corresponds to the appearance of spots/patches and the final grayscale values correspond to outside grayscale value. The grayscale values obtained from the readings inside the cell periphery next to their corresponding spots were used as background measurements. The average of 3 points was obtained and subsequently subtracted from the measurements of spots/patches. The reversible appearance of peripheral spots or patches was associated with a reversible darkening of adjacent background level cellular fluorescence. This change was also measured by performing a lines scan function adjacent to where the spots/patches appeared.

2.8 Statistical Analysis

Data were statistically analysed using Sigmastat (version 3.5; Systat Software Inc., USA). All values were expressed as means +- SEM, n = number of arteries / cells, N = number of animals/cell lines which will be detailed for each experiment. Results were considered significant if $p < 0.05$, actual levels of significance are detailed for each experiment.

Simple paired comparisons of 'before and after treatment' in the same tissue sample and unpaired comparisons of independent or unpaired samples were performed using a paired/unpaired Student's t test. Multiple comparisons were performed using analysis of variance (ANOVA). One-way ANOVA with a Holms Sidak post-hoc test was used where there was a single independent variable, for example differences in mean phosphorylation in IPAs for control, agonist/hypoxia, agonist/hypoxia + inhibitor conditions and SrcFK, MYPT-1 and MLC_{20} time controls.

Two-way ANOVA with a Holms Sidak post-hoc test was used to compare results with multiple independent variables and/or time series where multiple measurements were made from each preparation, for example to investigate interactions between 'time' and 'treatment' factors on ROS measurements.

The power of each test of the overall ANOVA will be detailed within the figure legends for each experiment.

Variation of n Numbers

Throughout my studies, there is some variability in n numbers particularly with regards to phosphorylation data such as figure 3.12. In this figure, the n number for LY1μM treatment at 30 seconds is higher than treatment at 30 minutes. This variation was due to data that had already been generated within the laboratory (at 30 seconds) being added to data that I generated.

Other examples where n numbers varied include figures 3.13, 3.17 and 3.18. The variation between control and treated samples in these figures arose due to how the data was originally going to be presented. Initially, the data was going to be presented as untreated, U46 treated, U46+ebselen/tempol or PP2 with ebselen/tempol or PP2 vs basal levels. Thus presenting the data as 3 graphs/blots for each protein.

I then decided that the data should be presented as untreated, U46 treated, U46 +ebselen, U46 +tempol and U46 +PP2 with a separate set blot for ebselen, tempol, PP2 vs basal. I was therefore able to combine all untreated and U46 data from each set of data but not for U46 + inhibitor. I subsequently had ~3 times the amount of controls and U46 treated samples vs U46 + inhibitor. This consequently gave rise to the variation in n numbers but allowed me to present the data as two graphs/blots per protein.

Variation of n numbers within other figures was due to variance between samples. Therefore by repeating the experiment, I was trying to distinguish whether the variance was due to the treatment or from random variance caused by underlying differences between rats or vessels and errors in measurement.

2.9 Reagents

Invitrogen, Paisley, U.K

Non-essential amino acids

Sodium Pyruvate

L-glutamine

Dulbecco's modified Eagle's Medium

Fetal Bovine serum

Trypsin EDTA

Hank's Balance salt solution

MOPS running buffer

NuPAGE transfer buffer

Nitrocellulose membrane (0.2µM pore)

NuPAGE Bis-Tris Gel 4-12%

NuPAGE sample buffer

Sigma-Aldrich Company Ltd, Poole, U.K

Bovine Serum Albumin

Protease inhibitor Cocktail

Phosphatase inhibitor cocktail 2 and 3

TBS Tween

TBS

Tween 20

DMSO

NADPH

Lucigenin

Luminol

Horseradish peroxidase

Tempol

Ebselen

Merck/Millipore, Hertfordshire, UK

PP2

Phospho MYPT-1 (thr 850)

Cell signalling, MA United States

Phospho-Src (Tyr 416) antibody

Src antibody

Phospho MLC_{20} antibody

MLC_{20} antibody

MYPT-1 antibody

Other

Super Signal West Femto Chemiluminescent substrate (Thermo Scientific)

Restore western blot stripping buffer (Thermo Scientific)

Amplex Red (Thermo Scientific)

ECL Plus western blotting detection system (GE healthcare)

ECL Prime western blotting detection system (GE healthcare)

BCA Protein assay kit (Pierce, Northumberland, U.K)

GAPDH primary antibody (Abcam, Cambridge, U.K)

Ethanol (BDH Merck Ltd, Poole, U.K)

Methanol (BDH Merck Ltd, Poole, U.K)

L-012 (Wako Pure Chemical Industries, VA, USA)

GloMax®-Multi Detection System (Promega)

Axiovert 200 Microscope (Zeiss)

BD™ CARV II Confocal Imager (BD Bioscience)

Chapter 3

SrcFKs act as ROS sensitive intermediates in Pulmonary Vascular Smooth Muscle contraction

3.1 Background

ROS are generated through incomplete reduction of molecular oxygen by oxido-reductase enzymes, such as NADPH-oxidase (NOX) [98,205,411] or the mitochondrial electron transport chain [412,413]. Oxidant stress has long been associated with cardiovascular diseases such as ischemic reperfusion injury [205], atherosclerosis [414] and pulmonary hypertension [117,411,415]. It is only relatively recently that reactive oxygen species (ROS) have been implicated as physiological signalling moieties that modulate cellular functions including vascular tone in health. ROS are produced in healthy tissue in response to a wide variety of vasoconstrictor agonists including thromboxane[416], angiotensin [116], endothelin [117,118] and thrombin [119] leading to increased $[Ca^{2+}]_i$ concentration and Rho-Kinase mediated vasoconstriction. ROS are also believed to be increased by acute hypoxia and are implicated in hypoxic pulmonary vasoconstriction [301,412,413].

Protein function can be altered by oxidative modification of key amino acid residues, especially cysteine. Therefore, physiological levels of ROS may modify specific cysteine residues of key proteins involved in cellular signal transduction altering their functions and interaction with other proteins[87]. An example being protein kinases[92]. Amongst these, SrcFK may be directly activated by oxidative modification [92,213] while opposing tyrosine phosphatases are inhibited, leading to a net increase in tyrosine phosphorylation[199,417]. The eponymous member of the SrcFK, c-Src is of particular interest because it is a signalling molecule involved in smooth muscle proliferation and migration in response to various stimuli [205,213,418], and as discussed previously, in contractile responses.

In addition to evidence for ROS-mediated activation of Src in oxidative stress-associated with hyper-contractile states [204,205], as discussed, many vasoconstrictors generate ROS under physiological conditions and activate tyrosine kinases. Previous results within my group have shown that prostaglandin – $F_{2\alpha}$ and hypoxia enhance total tyrosine phosphorylation, activate

Src and cause SrcFK-dependent constriction [7,41]. Similar relationships have been seen in other vascular beds [82,419,420]. Combining these observations with the proposed ROS-sensitivity of Src leads me to propose that the interaction between SrcFK and ROS makes a central contribution to vascular smooth muscle function. 3.2 Hypothesis

I hypothesise that SrcFK will act as a ROS sensitive intermediate acting as an upstream signalling moiety involved in vasoconstriction and activation of the RhoA/Rho-Kinase pathway. SrcFK will act as a link between agonist induced ROS production and vasoconstriction via activation of Rho-Kinase. SrcFK is therefore a requirement in agonist induced ROS mediated vasoconstriction.

3.3 Experimental Design

The following methods were adopted in order to help address my chapter hypothesis.

ROS Measurement

ROS measurements were performed in PASMC's using the luminescent dye L-012 (50μM). PASMCs were grown until 80-90% confluent, followed by 24 hour serum starvation. Following 24 hours, media was aspirated and L-012 or L-012 + U46619 / LY8383 or L-012 + U46619 / LY83583 + inhibitor was added to all wells in a row. The cells were immediately read on a Promega GloMax Discover: Multimode detection system with a reading being taken every 5 minutes with a 5 minute incubation in-between reads. An average of eight wells in a row was calculated, and changes were expressed as a % change from control at each time point. Data was expressed as means +- SEM and statistical analysis was carried out using 2 way ANOVA in sigma stat (version 3.5). As time was found not to be a factor for ROS production, rather whether the presence of stimulus plus inhibitor, representative graphs plotted were at 15 minutes as this was deemed to present the most stable and accurate data.

Functional Studies

Functional studies were performed in Intra Pulmonary arteries (IPA's) to investigate whether: (1) ROS-induced contraction is SrcFK dependent and to investigate the ROS dependency of U46619 in tissue on the myograph, (2) U46619 induced contraction is SrcFK and ROS dependent, (3) LY83583 enhanced, U46619 contraction is not due to the removal of NO instead of increased ROS production, finally, (4) the concentrations of ebselen, tempol and PP2 used have any non-specific contractile effects (using KPSS contractile responses).

Although inhibitors of ROS and SrcFK have previously been used within our laboratory, it was essential to carry out an inhibitor cumulative dose responses to KPSS contractile responses. As discussed in the introduction, recent data has shown that Rho-Kinase signalling can be induced by membrane depolarisation. Therefore, to ensure that the inhibitor concentration used is not acting as a Ca^{2+} channel antagonist or MLCK inhibitors, these inhibitors were tested against KPSS contractile function believed to be predominant Ca^{2+} mediated contraction. This will clarify that the effects seen using these inhibitors will be predominantly via Rho-Kinase signalling and not Ca^{2+} signalling.

In addition, ROS and SrcFK inhibitors are poorly water soluble and are therefore diluted in our vehicle DMSO. I therefore investigated whether DMSO had any effect on contractile responses. Dose responses were carried out in the presence of (A) inhibitor plus vehicle and (B) vehicle control only. IPA's were dissected from the same vascular tree, mounted onto a wire myograph so that for each experiment, there was at least 1 vessel from the same arterial tree which was treated with inhibitors and DMSO or DMSO only.

IPA were pre-constricted with KPSS or U46619 (100nM) to achieve ~70% of KPSS. This was allowed to plateau. Subsequently, a cumulative concentration response was performed using either ebselen (0.1µM - 10µM), tempol 0.1mM – 3mM), PP2 (1µM – 30µM) or DMSO (0.5 -

6µL which is the same volume present in the solution of inhibitor plus DMSO). Each concentration was allowed to incubate for 10 minutes. Following the final concentration, IPA were washed at least 3 times in PSS and contractile force was allowed to return to baseline. When investigating the effect of NOS inhibition of U46629 induced contraction, L-NAME (300nM) was added to the chamber and allowed to incubate for 15 minutes before the addition of U46619 and cumulative concentration response with inhibitors.

The effect of DMSO, ebselen (10µM), tempol (3mM) and PP2 (30µM) was investigated in response to U46619 induced, LY83583 enhanced contractile responses. An initial control response was performed whereby U46619 (2nM) was initially added to IPAs for 10 minutes to achieve ~10% of KPSS. This was immediately followed by the addition of LY83583 (1µM) and incubated for a further 10 minutes. IPA's were subsequently washed three times in PSS and allowed to rest until a steady baseline was achieved. Inhibitors of either ROS: ebselen (10µM), tempol (3mM), SrcFK: PP2 (30µM), NOS: L-NAME (300nM) and DMSO were then added to the chamber and allowed to incubate for ~15 minutes before conducting a second response in their presence. IPA were then washed at least 3 times in PSS following treatment and contractile force was allowed to return to baseline.

Phosphorylation studies

Phosphorylation studies were performed to determine, if SrcFK does act as ROS sensitive intermediate upstream of Rho-Kinase. If so, inhibition of ROS should decrease SrcFK activity and inhibition of both ROS and/or SrcFK should decrease the activity of Rho-Kinase. SrcFK activity will be measured by SrcFK autophosphorylation (Tyr416), Rho-Kinase via phosphorylation of MYPT-1 (Thr850) and MLCK activity via MLC_{20} phosphorylation (ser19).

Secondly, SrcFK autophosphorylation (Tyr416) was investigated in the presence of LY83583 (1µM) as LY is a verifiable source of ROS therefore confirming the ROS sensitivity of SrcFK.

As the largest peak responses from U46 time control occurred at 0.5 min and 30 min (for SrcFK autophosphorylation) these time points were investigated using LY83583 (1µM) treatment. The effect of LY83583 (1µM) on MYPT-1 (Thr850) or MLC_{20} phosphorylation was not investigated in this study as previous studies from our group have explored this [88,89].

Finally, phosphotyrosine was also investigated in the presence of LY83583 and PP2. Phosphotyrosine shows a rage of proteins of various molecular weights which are tyrosine phosphorylated. If there is an increase in band intensity in response to LY83583 and this is inhibited by PP2, I can infer that the protein is tyrosine phosphorylated in response to SrcFK activation either directly or indirectly via a SrcFK sensitive intermediate.

The ratio of phosphorylated SrcFK, MYPT-1 and MLC_{20} was calculated by dividing phospho levels by total level of protein thus giving an indication of protein activity.

Initially, time control experiments for SrcFK autophosphorylation, MYPT-1 and MLC_{20} phosphorylation was investigated in the presence of U46619 (100nM). IPA's were dissected and treated with U46619 for 0.5, 2, 5 and 30 minutes or left untreated. The highest phosphorylation responses and therefore activation for all 3 proteins was 30 minutes. This time point was therefore used in future investigations with inhibitors.

IPA were dissected and initially incubated with our inhibitors for 15 minutes, U46619 (100nM) was then added for 30 minutes. Simultaneously untreated samples were prepared. The lysate was then prepared and analysed as previously discussed (see chapter 2, section 2.6.5).

Strength of experimental design (Chapter 3)

During this chapter, one of the main strengths was that during each experiment a control vascular was always included amongst a set of rings isolated from a single rat, each would then receive a specific treatment e.g. U46, ebselen, tempol, PP2 etc. Therefore, an effects seen can be compared to its control preparation.

Although the n numbers are variable, for most experiments throughout my thesis the n numbers are high. This helps ensure that the results I am obtaining are a genuine. It also helps reduce the risks or type 1 or 2 errors while performing statistical analysis.

The samples are from multiple sets of rats, again this ensures that the effects seen are not due to a homogenous group but rather across a population. Making any results obtained more genuine.

3.4 Results Section

3.4.1 ROS and SrcFK are Key intermediates contributing to U46619-induced contraction

Initially, I examined whether the selective TP receptor agonist U46619 stimulated endogenous ROS production and whether the glutathione peroxidase mimetic ebselen (10μM) or the SOD-mimetic 4-hydroxy-TEMPO (tempol) (3mM) were acting as antioxidants in PASMCs using the luminol-derived ROS-sensitive chemiluminescent probe L-012 [385]. U46619 enhanced chemiluminescence which was abolished by prior incubation with ebselen or tempol (Fig 3.1). Basal chemiluminescence was significantly reduced by ebselen, however, tempol abolished basal chemiluminescence, suggesting tempol to be a better basal ROS scavenger in this system (Fig 3.1). The data presented in this figure was at one time point (15 minutes as this was deemed to present the most stable and accurate data), whereas measurements were made at multiple time points and all of those data were entered into the statistical analysis (Fig 3.1).

I next wanted to determine the influence endogenous ROS production has on agonist-induced contraction. Contractile responses were measured using rat intra-pulmonary arteries. Sub-maximal contraction induced by U46619 (100nM) was inhibited by ebselen (10μM) (Fig 3.3) and tempol (3mM) (Fig 3.4) in a dose dependent manner, whilst, our vehicle showed no significant changes indicating U46619 induced contraction is partially ROS dependent (Fig 3.2). U46619-induced contraction was also shown to be is partially dependent on SrcFK as the SrcFK antagonist, PP2, induced a concentration-dependent relaxation (Fig 3.5).

Representative traces show that treatment with our vehicle DMSO caused no significant changes in contractile force elicited by U46619 (Figure 3.2), this data taken together with data from KPSS contraction data (shown later) indicates that DMSO is a suitable solvent for use in my studies and that any inhibitory effect observed will be due to the presence of inhibitor and not DMSO.

A concentration of 30μM PP2, 10μM ebselen and 3mM tempol was used for future experiments. The PP2 concentration is approximately 15 times that of the IC_{50} (previous laboratory studies). This concentration is required as PP2 dose responses carried out previously in pulmonary artery homogenates demonstrate that a concentration of 30μM PP2 is required to fully inhibit SrcFK activity (measured by Tyr-416 phosphorylation). 30μM PP2 was shown to inhibit KPSS contractile responses by a small but significant amount (shown later) but as discussed in future sections, SrcFK play a role in regulating membrane potential and therefore I concluded that this concentration was suitable for subsequent experiments [70,421,422].

Figure 3.1

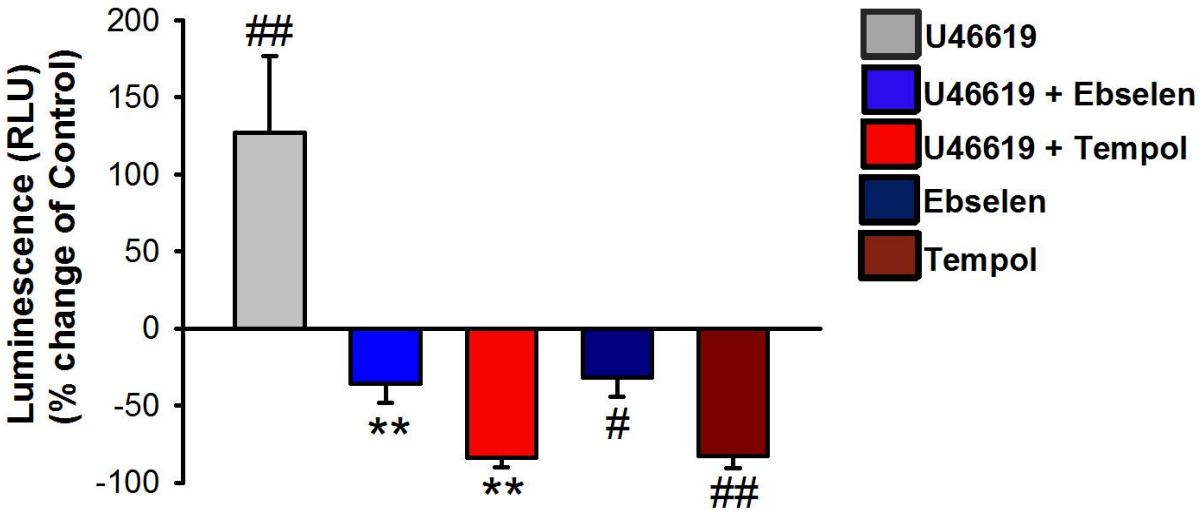

Figure 3.1: Effects of U46619, antioxidants on ROS production
Effects of ebselen (10μM) or tempol (3mM) on U46619-induced ROS production (15min, 100nM) or on basal ROS production in PASMC, measured by L-012 chemiluminescence. ##P<0.001 vs. control; #P<0.05 vs. control; **P<0.001 vs. U46619 alone (2-way ANOVA, factors: time and drug treatment), n=10 separate smooth muscle cell cultures passage 3, isolated from 7 different rats. Power of performed test 0.782.

Figure 3.2

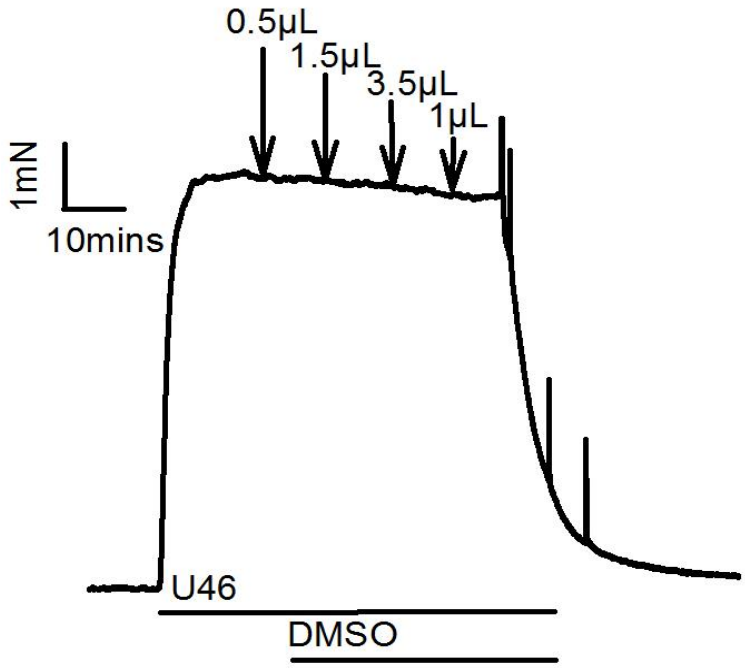

Figure 3.2: Effects of DMSO on U46619 induced contraction
Concentration-dependent relaxation responses to DMSO (n=5 arteries, isolated from 5 different rats) representative traces with arrows highlighting where each dose was added.

Figure 3.3

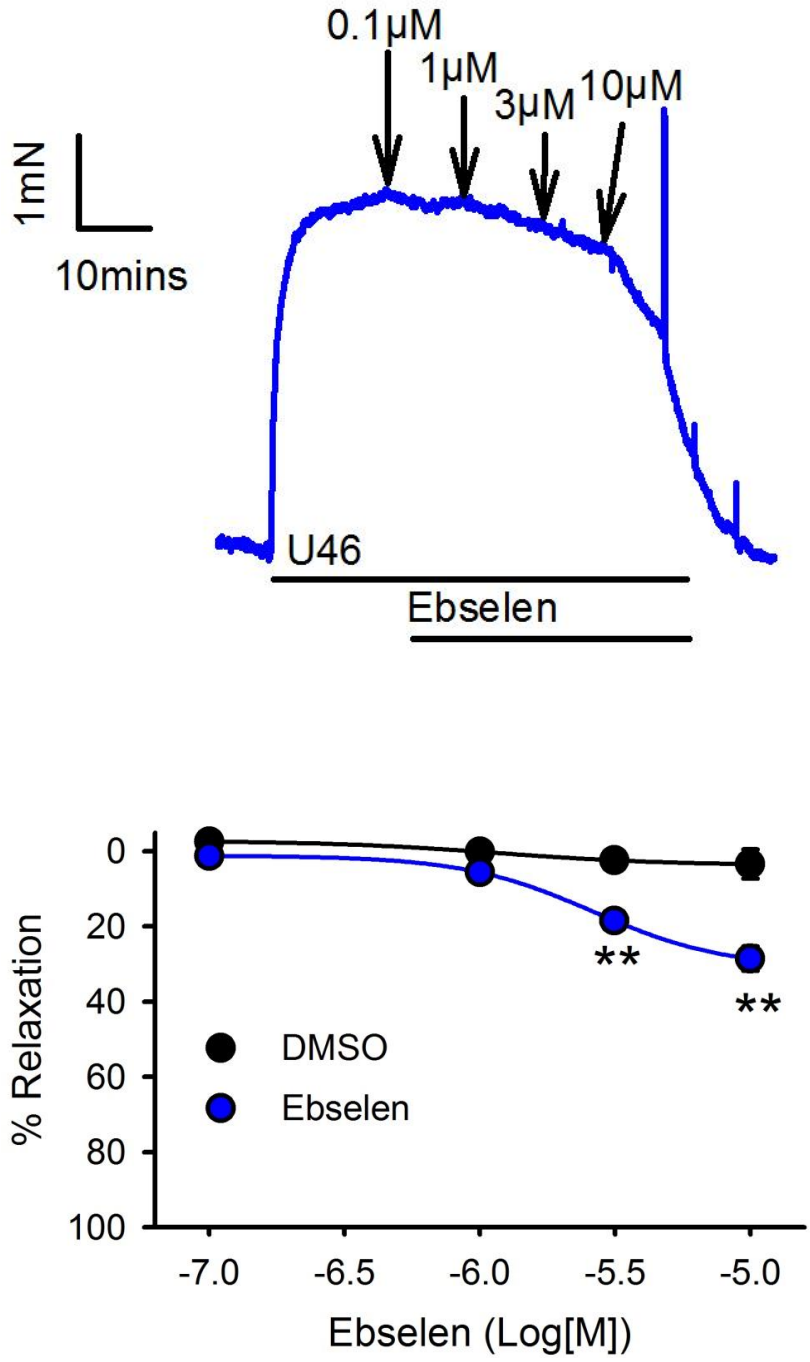

Figure 3.3: Effects of U46619 and ebselen on U46619 induced contraction
Concentration-dependent relaxation responses to ebselen (n=8 arteries, isolated from 7 different rats) in IPA pre-constricted with 100nM U46619. Upper panel: representative traces with arrows highlighting where each dose was added. Bottom panel: mean effects of inhibitors plotted against DMSO vehicle control (n=5 arteries, isolated from 5 different rats). **P<0.001 vs. DMSO control (2-way ANOVA, Factors: DMSO and drug treatment. Power of performed test 0.962).

Figure 3.4

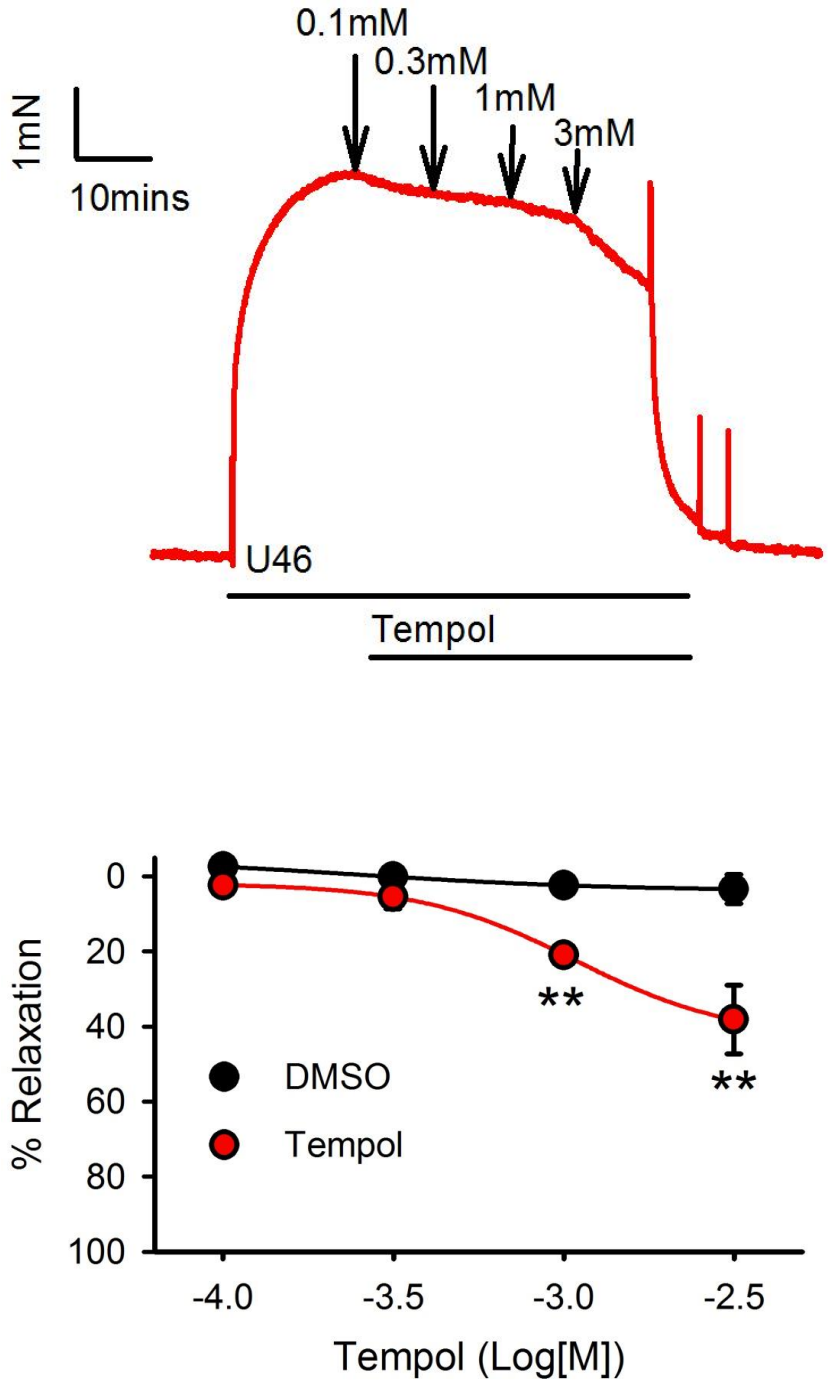

Figure 3.4: Effects of U46619 and tempol on U46619 induced contraction
Concentration-dependent relaxation responses to tempol (D, n=8 arteries, isolated from 7 different rats) in IPA pre-constricted with 100nM U46619. Upper panel: representative traces with arrows highlighting where each dose was added. Bottom panel: mean effects of inhibitors plotted against DMSO vehicle control (n=5 arteries, isolated from 5 different rats). **P<0.001 vs. DMSO control (2-way ANOVA, Factors: DMSO and drug treatment. Power of performed test 0.772).

Figure 3.5

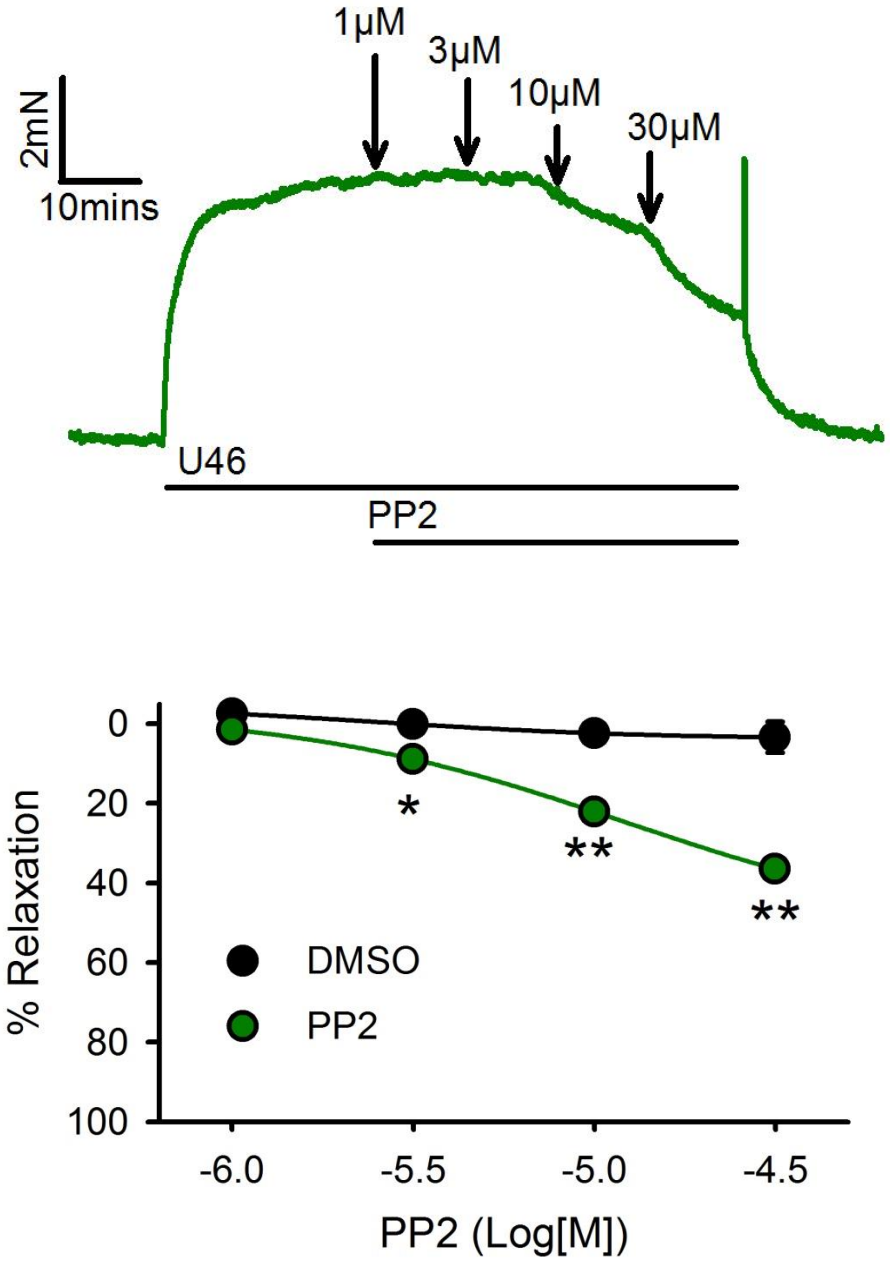

Figure 3.5: Effects of U46619 and PP2 on U46619 induced contraction
Concentration-dependent relaxation responses to PP2 (E, n=6 arteries, isolated from 6 different rats) in IPA pre-constricted with 100nM U46619. Upper panel: representative traces with arrows highlighting where each dose was added. Bottom panel: mean effects of inhibitors plotted against DMSO vehicle control (n=5 arteries, isolated from 5 different rats). **P<0.001 vs. DMSO control, *P<0.05 vs. DMSO control (2-way ANOVA, Factors: DMSO and drug treatment. Power of performed test 0.992).

3.4.2 LY83583-induced-ROS production augments U46619-induced contraction in a SrcFK and ROS dependent manner

Having established that U46619 enhances PASMC ROS production and IPA contractile responses in a ROS and SrcFK dependent manner, I next wanted to repeat these experiments using a well-known exogenous ROS source. This would allow us to confirm ROS production in my system but also show that ROS induced contraction is SrcFK dependent.

Using the membrane permeable quinolinequinone LY83583, a known generator of intracellular superoxide [423], LY83583 (1µM and 10 µM) increased L-012 chemiluminescence with 1µM showing a similar increase as 100nM U46619 (Fig 3.6A). Similarly, the effect of 1µM LY85683 was abolished by ebselen and tempol confirming that both drugs are acting as antioxidants (Fig 3.6B). Again, the data data presented in this figure was at one time point (15 minutes), whereas measurements were made at multiple time points and all of those data were entered into the statistical analysis (Fig 3.6A and B).

Previous work carried out within our laboratory has shown that 1µM LY85683 does not in itself promote constriction in IPA [88], however it can enhance the response to 2nM U46619 pretone which is ~10% of KPSS. Repeating this response but pre-incubating IPA with ebselen (Fig 3.8), tempol (Fig 3.9) or PP2 (Fig 3.10) along with increasing U46619 concentration to 8-10nM to match initial pretone levels, LY83583 contractile responses were significantly reduced, while DMSO vehicle had no effect (Fig 3.7).

Figure 3.6

(A)

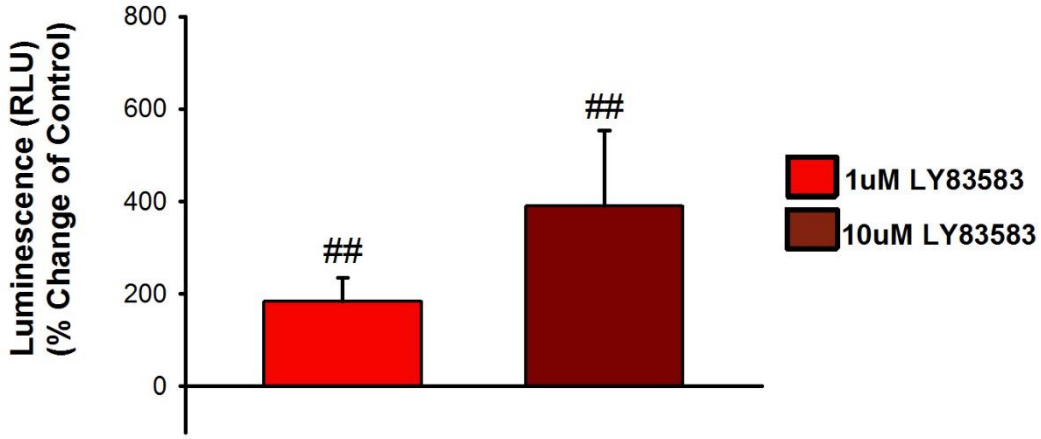

(B)

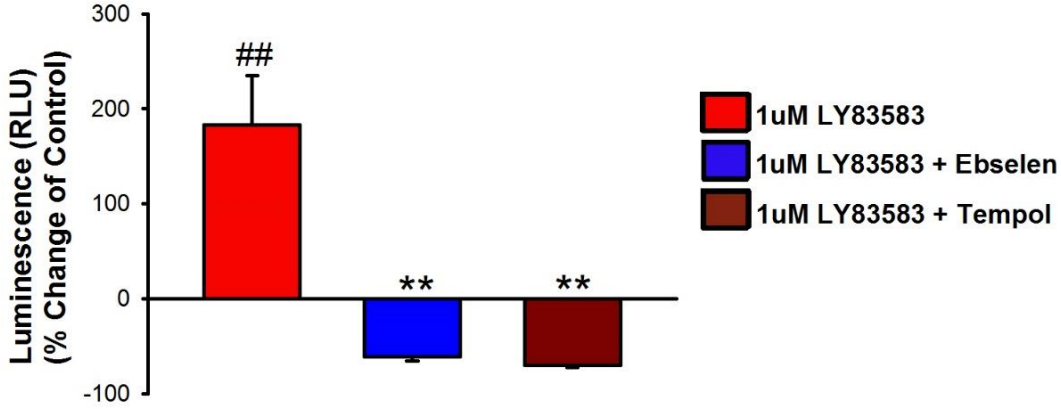

Figure 3.6: Effects of exogenous superoxide, ebselen and tempol on ROS production in PASMCs

A: LY83583 (LY, 1 and 10 µM, 15min, n=12 separate smooth muscle cell cultures passage 3, isolated from 9 different rats.) generates superoxide, in PASMC, as measured by L-012 chemiluminescence, ##P<0.001 vs. control, (2-way ANOVA, Factors: Time and Drug treatment, Power of performed test 0.653), which was **B:** subsequently inhibited by ebselen (ebs, 10µM, n=10 separate smooth muscle cell cultures passage 3, isolated from 7 different rats.) or tempol (temp, 3mM, n=10 separate smooth muscle cell cultures passage 3, isolated from 9 different rats.). **P<0.001 vs. LY alone, ##P<0.001 vs. control (2-way ANOVA, Factors: Time and Drug treatment, Power of performed test 0.853).

Figure 3.7

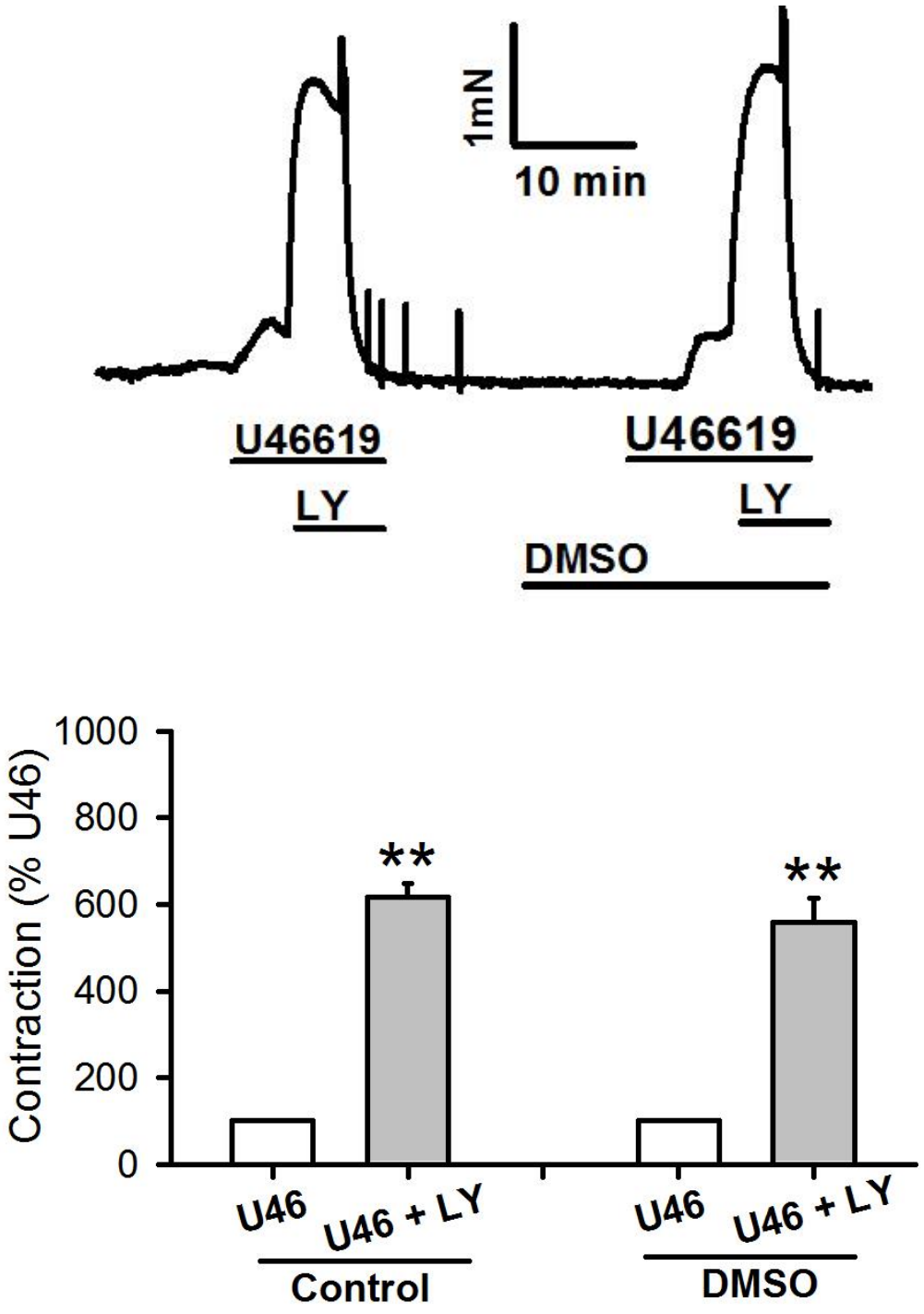

Figure 3.7: Effects of LY83583 and DMSO on U46619-induced contraction
U46619 concentration was adjusted to achieve ~10% of KPSS (U46). 1µM LY83583 was then added for 10min (U46+LY). This response was then repeated in the presence of DMSO vehicle (n=6 arteries, isolated from 5 different rats) Upper panel: representative traces. Bottom panel: mean ± SEM measurements of peak LY83583-induced contraction, expressed as a percentage increase of U46619 pre-constriction. **P<0.01 vs. U46, (2-way ANOVA, Factors: U46, U46+LY +- inhibitor drug treatment. Power of performed test: 1.000).

Figure 3.8

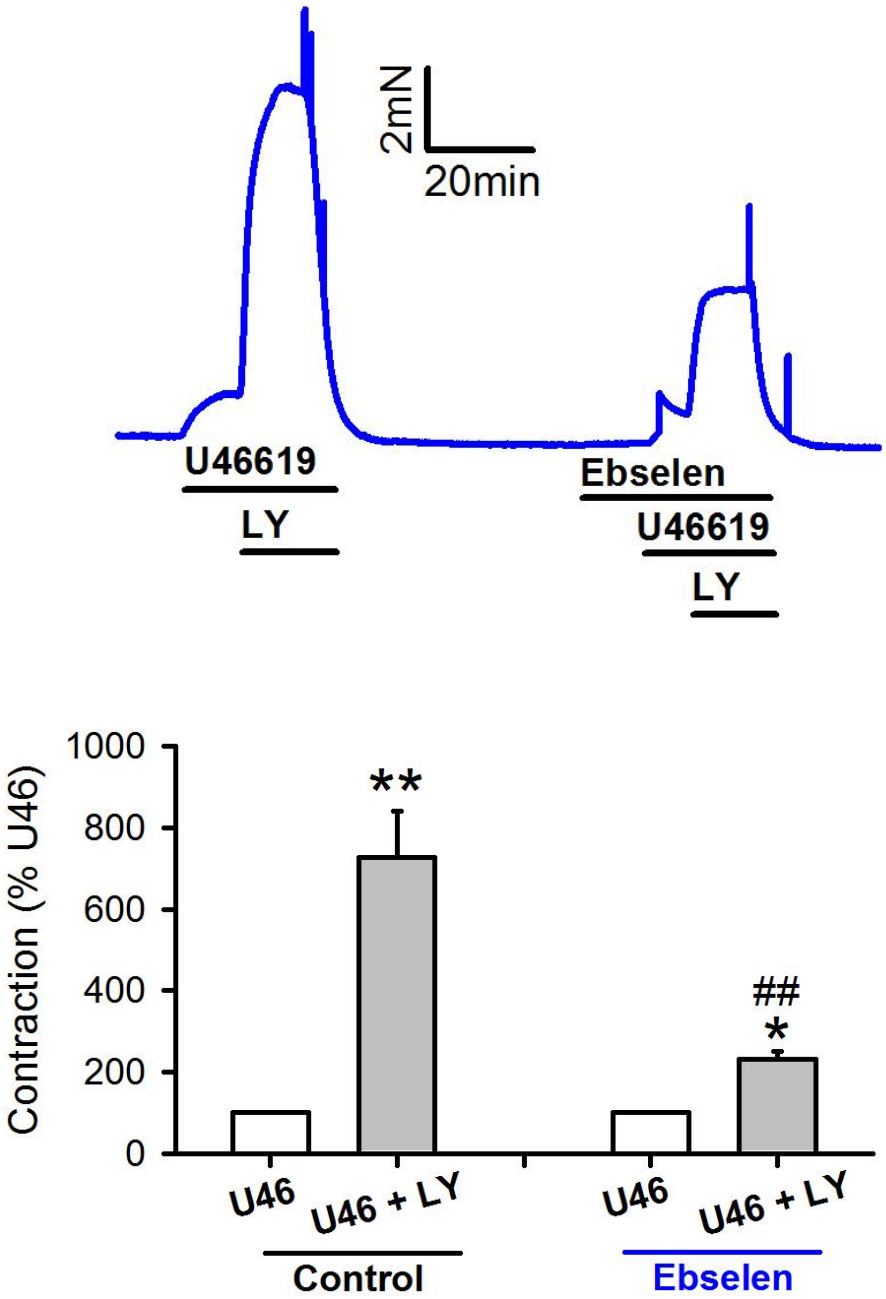

Figure 3.8: Effects of LY83583 and ebselen on U46619-induced contraction
U46619 concentration was adjusted to achieve ~10% of KPSS (U46). 1µM LY83583 was then added for 10min (U46+LY). This response was then repeated in the presence of ebselen (10µM, n=7 arteries isolated from 7 different rats). Upper panel: representative traces. Bottom panel: mean ± SEM measurements of peak LY83583-induced contraction, expressed as a percentage increase of U46619 pre-constriction. **P<0.001 vs. U46, *P<0.05 vs. U46; ##P<0.001 vs. control U46+LY (2-way ANOVA, Factors: U46, U46+LY +- inhibitor drug treatment. Power of performed test: 0.989).

Figure 3.9

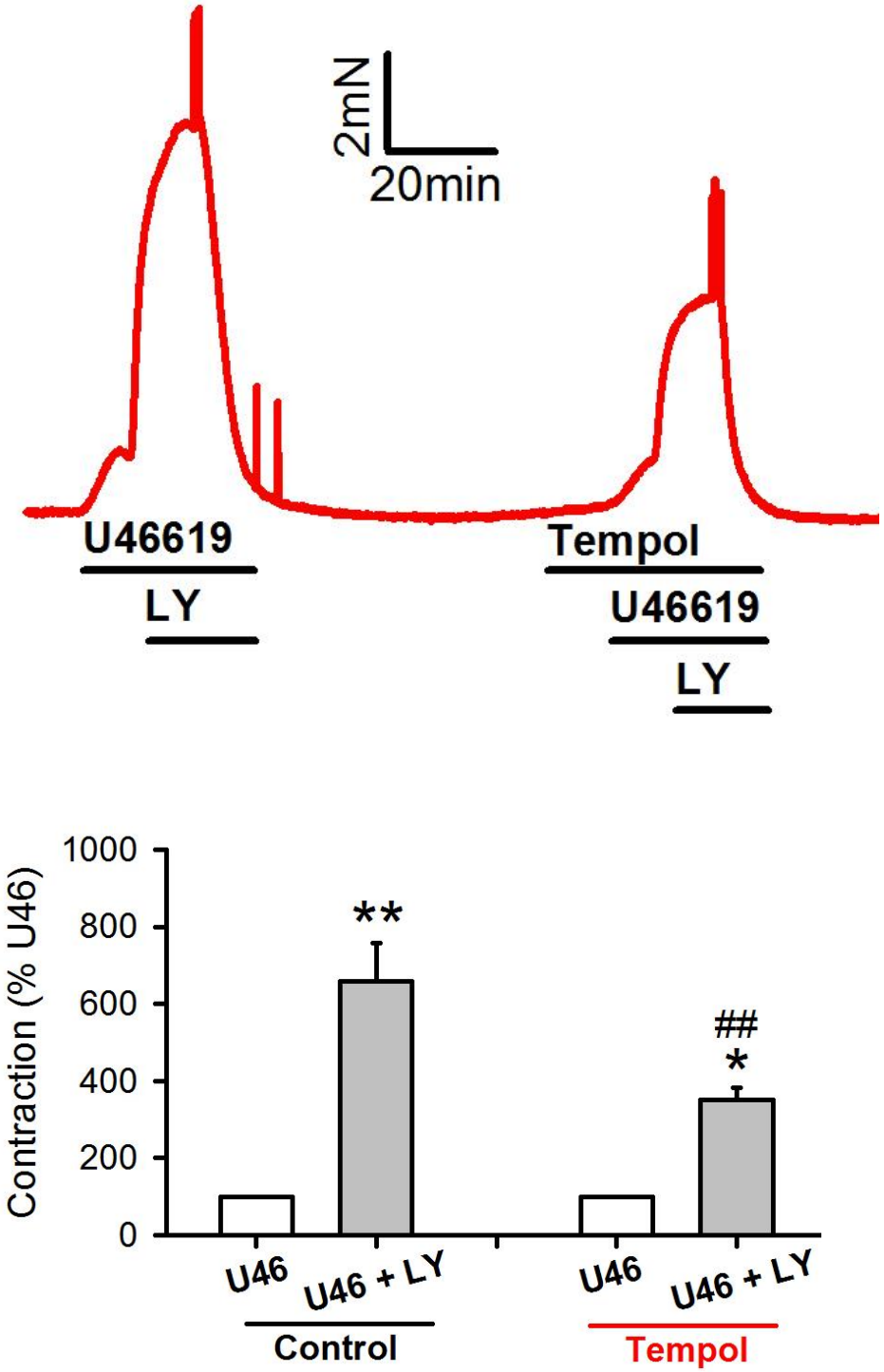

Figure 3.9: Effects of LY83583 and tempol on U46619-induced contraction
U46619 concentration was adjusted to achieve ~10% of KPSS (U46). 1µM LY83583 was then added for 10min (U46+LY). This response was then repeated in the presence of tempol (3mM, n=11 arteries isolated from 8 different rats) Upper panel: representative traces. Bottom panel: mean ± SEM measurements of peak LY83583-induced contraction, expressed as a percentage increase of U46619 pre-constriction. **P<0.001 vs. U46, *P<0.05 vs. U46; ##P<0.001 vs. control U46+LY (2-way ANOVA, Factors: U46, U46+LY +- inhibitor drug treatment. Power of performed test: 0.786).

Figure 3.10

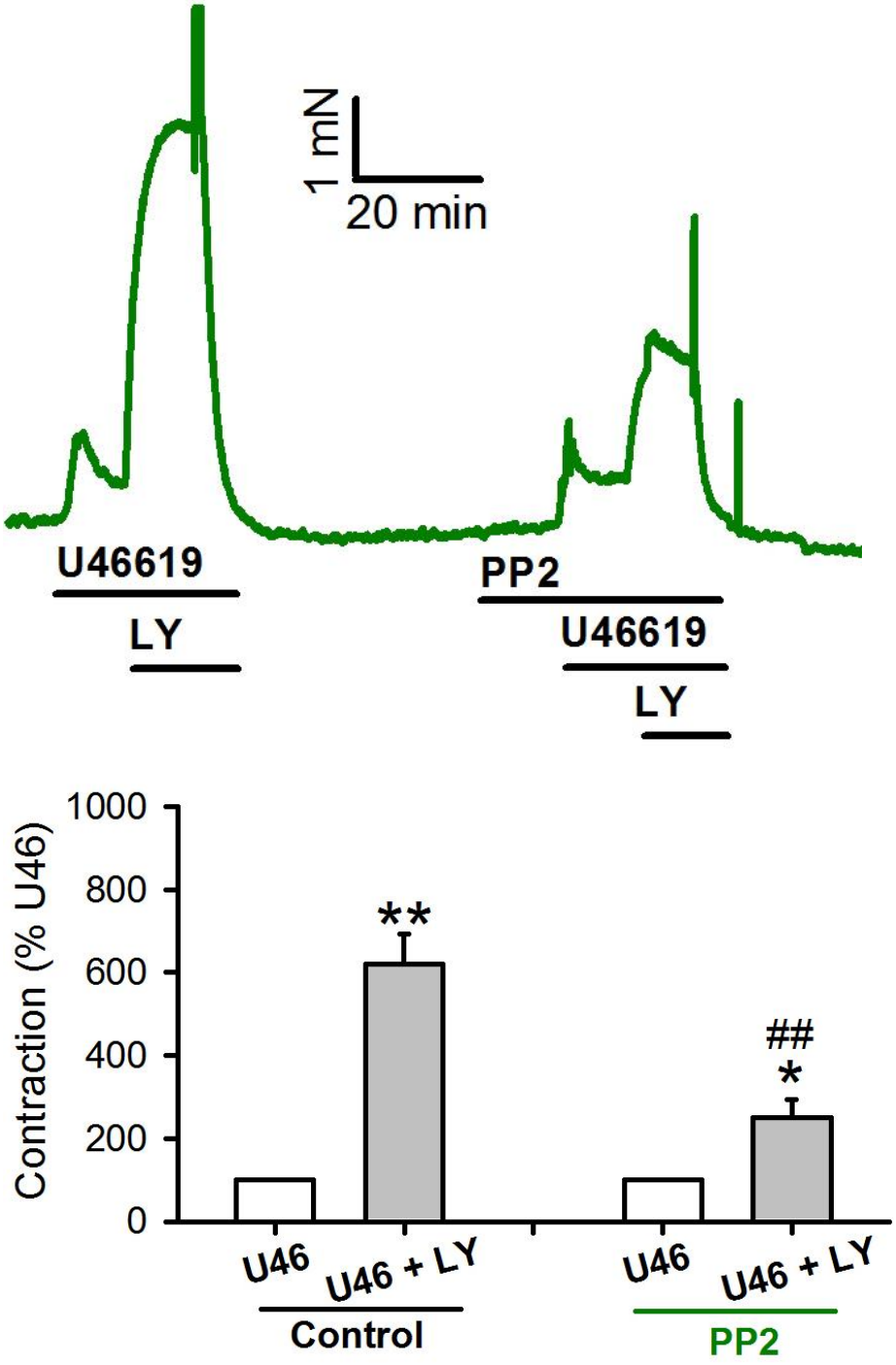

Figure 3.10: Effects of LY83583 and PP2 on U46619-induced contraction
U46619 concentration was adjusted to achieve ~10% of KPSS (U46). 1µM LY83583 was then added for 10min (U46+LY). This response was then repeated in the presence of PP2 (30µM, n=11 arteries isolated from 8 different rats) Upper panel: representative traces. Bottom panel: mean ± SEM measurements of peak LY83583-induced contraction, expressed as a percentage increase of U46619 pre-constriction. **P<0.001 vs. U46; *P<0.05 vs. U46; ##P<0.001 vs. control U46+LY (2-way ANOVA, Factors: U46, U46+LY +- inhibitor drug treatment. Power of performed test: 0.976).

3.4.3 U46619 and LY83583 promote SrcFK autophosphorylation in a time dependent, ROS dependent and SrcFK dependent manner

The data produced so far has shown that both U46619 and LY83583 increased ROS production and enhanced contractile responses which is sensitive to antioxidants and PP2. The next step is to investigate whether SrcFK activity is increased following U46619 treatment and blocked by antioxidants and SrcFK inhibitor PP2. This will help verify that SrcFKs are indeed ROS sensitive and also confirm I am indeed measuring Src-autophosphorylation. LY83583 stimulation will also be investigated as a control to confirm that SrcFK is indeed ROS sensitive. Src-FK activity can be measured by measuring its autophosphorylation site at Tyr-416 in response to stimulation.

U46619 enhanced SrcFK autophosphorylation in a biphasic time-dependent manner peaking at 0.5min and 30min (Fig 3.11). LY83583 (1μM) also enhanced SrcFK auto-phosphorylation without the presence of U46619, suggesting that SrcFK activity is ROS sensitive (Fig 3.12). SrcFK are indeed shown to be ROS sensitive, as prior incubation with antioxidants ebselen, tempol or PP2 inhibited U46619-induced increase in SrcFK autophosphorylation (Fig 3.13A). Basal SrcFK phosphorylation was unaffected by ebselen and somewhat reduced by tempol (Fig 3.13B) whilst PP2 significantly inhibited basal SrcFK phosphorylation (Fig 3.13B), which is explored further in the discussion.

When blots were further probed with anti-phospho-tyrosine (P-Y). LY83583 enhanced P-Y immunoreactivity at multiple bands, particularly bands at 80, 90 and 115 kDa. These bands along with another at approximately 140 kDa were sensitive to PP2, suggesting SrcFK-dependent phosphorylation (Fig 3.14).

Figure 3.11

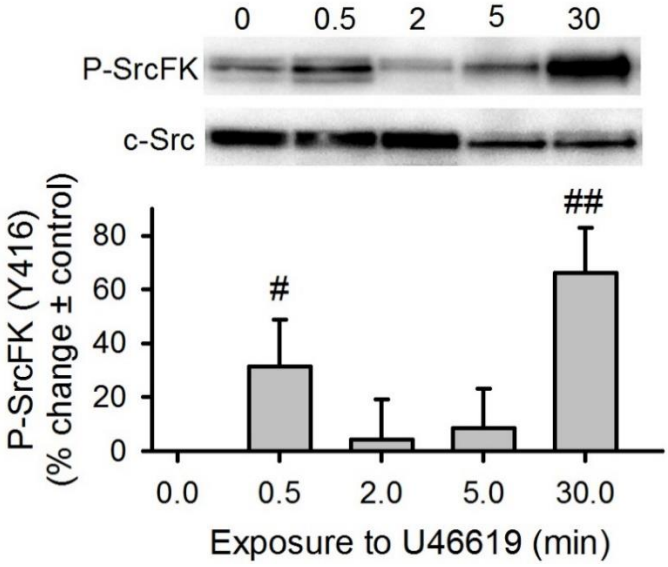

Figure 3.11: Effects of U46619 on SrcFK auto-phosphorylation in IPA
U46619 (U46, 100nM) enhances SrcFK auto-phosphorylation (Tyr-416) in IPA in a time-dependently manner (n=9 arterial samples isolated from 5 different rats, #P<0.05 vs. control, ##P<0.01 vs. control, 1-way ANOVA, Factor: time. Power of performed test: 0.691).

Figure 3.12

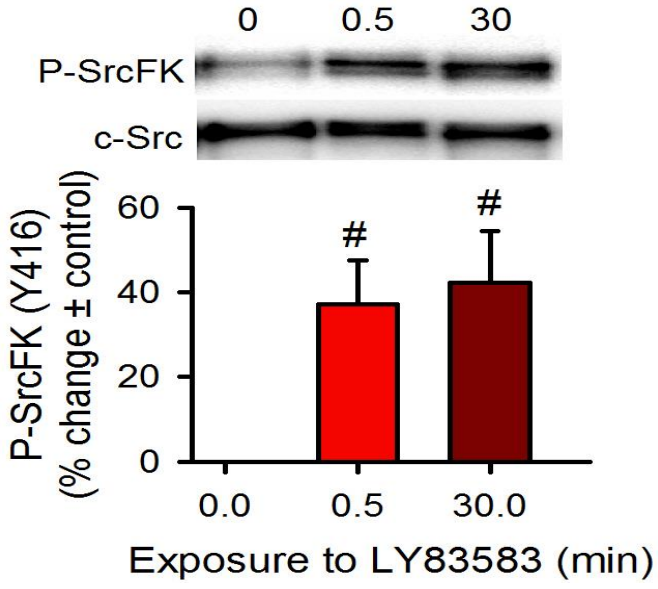

Figure 3.12: Effects of exogenous superoxide on SrcFK auto-phosphorylation in IPA
LY83583 (1µM) enhanced SrcFK auto-phosphorylation at 0.5min (n=16) and 30min (n=7 arterial samples isolated from 4 different rats), #P<0.05 vs. control (1-way ANOVA, Factor: time, Power of performed test 0.657)

Figure 3.13

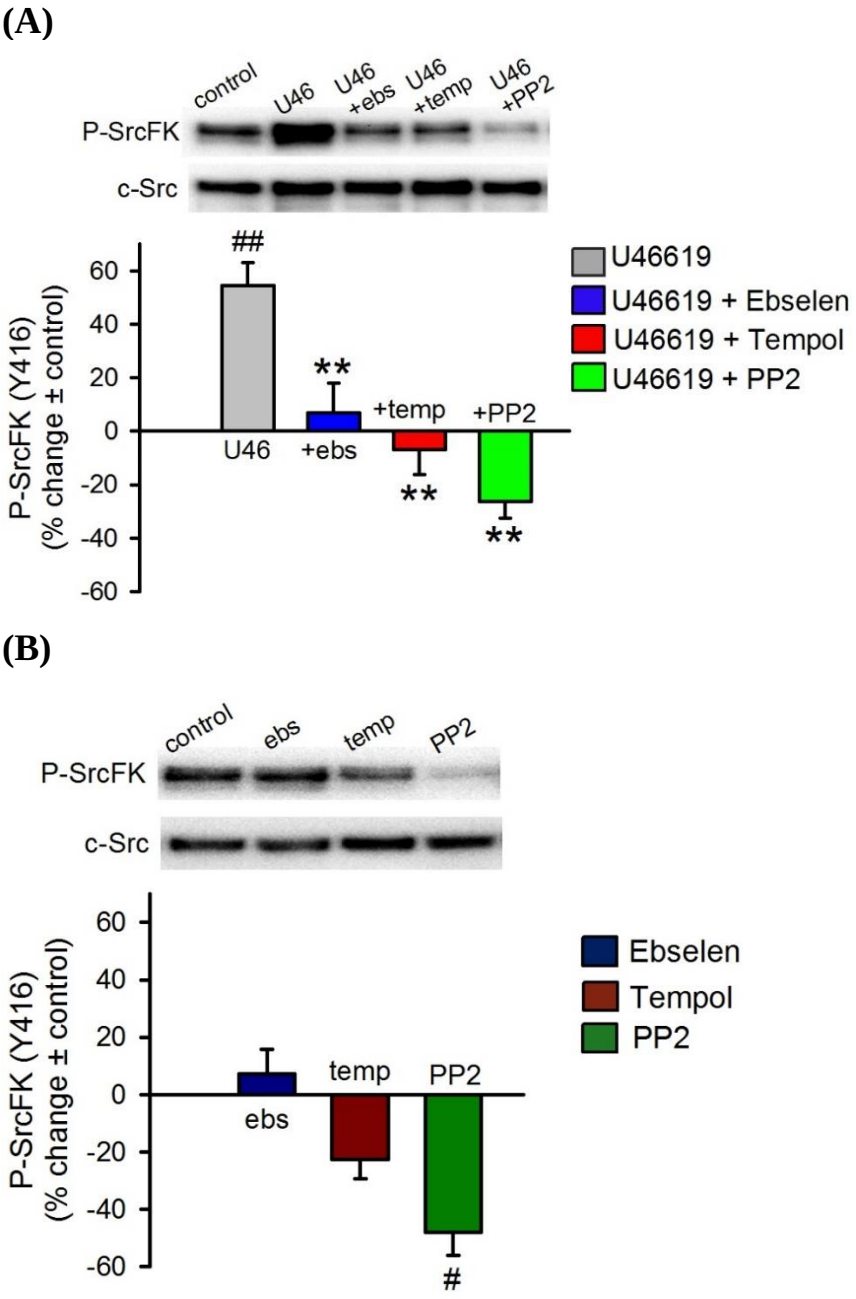

Figure 3.13: Effects of U46619 and antioxidants on SrcFK auto-phosphorylation in IPA

A: At 30 min, U46619-induced SrcFK auto-phosphorylation is inhibited by ebselen (ebs, 10µM, n=14 arterial samples isolated from 10 rats), tempol (temp, 3mM, n=11 arterial samples isolated from 9 rats) or PP2 (30µM, n=10 arterial samples isolated from 9 rats), ##P<0.001 vs. control, **P<0.001 vs. U46 alone, while in the absence of U46 (**B**), Basal SrcFK auto-phosphorylation is unaffected by ebselen (n=10 arterial samples isolated from 9 rats) or tempol (n=10 arterial samples isolated from 9 rats) but significantly inhibited by PP2 (n=8 arterial samples isolated from 6 rats), #P<0.05 vs. control, (2-way ANOVA, Factors: U46+inhibitor and inhibitor alone. Power of performed test 0.801).

Figure 3.14

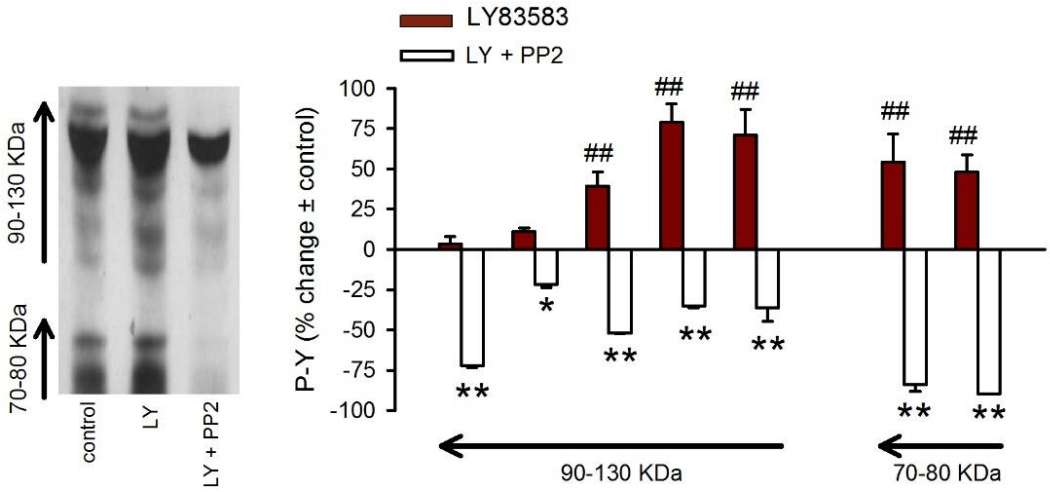

Figure 3.14: Effects of U46619, antioxidants and exogenous superoxide on SrcFK auto-phosphorylation in IPA

LY83583 (1µM) enhanced tyrosine phosphorylation of multiple proteins, including bands of approximately 80, 90, 115 and 140 kDa. These bands were sensitive to SrcFK inhibition with PP2 (30µM, n=4 Arterial samples isolated from 3 rats). ##P<0.01 vs. control, *P<0.05, **P<0.001 vs. LY alone (2-way ANOVA, Factors: control, LY +- inhibitor, Power of performed test 0.960).

3.4.4 U46619 promotes MYPT-1 and MLC_{20} phosphorylation in a time dependent, ROS dependent and SrcFK dependent manner

Previous work has shown that SrcFKs play a role in pulmonary contraction via activation of Rho-Kinase[7,41,82,83] and that exogenous ROS can activate Rho-Kinase [88]. Therefore, I investigated whether SrcFKs is a ROS sensitive intermediate acting upstream of Rho-Kinase.

I therefore investigated Rho-Kinase activity by measuring the phosphorylation of the Rho-kinase target myosin phosphatase targeting subunit-1 (MYPT-1) and of the MLCK target, the 20 KDa regulatory subunit of myosin (MLC_{20}). U46619 enhanced phosphorylation responses in a time-dependent manner of both MYPT-1 (Fig 3.15) and MLC_{20} (Fig 3.16). Prior incubation with either ebselen, tempol or PP2 inhibited the U46619-induced, 30 minute increase in phosphorylation responses (MYPT-1: Fig 3.17A, MLC_{20}: Fig 3.18A). Basal phosphorylation was not significantly affected by either of the three inhibitors ((MYPT-1: Fig 3.17B, MLC_{20}: Fig 3.18B).

Figure 3.15

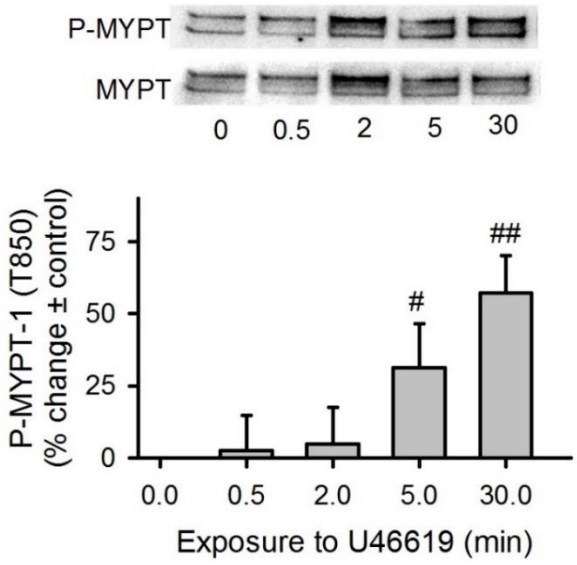

Figure 3.15: U46619-induced MYPT-1 phosphorylation is partly mediated via ROS and SrcFK in IPA

U46619 (U46, 100nM) enhances phosphorylation of MYPT-1(T850) (n=8 arterial samples isolated from 5 rats) in a time-dependent manner in IPA, #P<0.05 vs. control, ##P<0.001 vs. control, 1-way ANOVA, Factor: time. Power of performed test: 0.927).

Figure 3.16

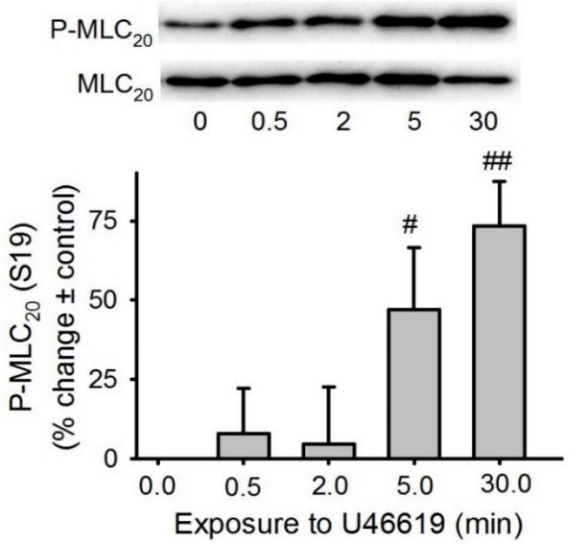

Figure 3.16: U46619-induced MLC_{20} phosphorylation is partly mediated via ROS and SrcFK in IPA

U46619 (U46, 100nM) enhances phosphorylation of MLC_{20} (S19) (n=10 arterial samples from 6 different rats) in a time-dependent manner in IPA, #P<0.05 vs. control, ##P<0.001 vs. control, 1-way ANOVA. Factor: time. Power of performed test: 0.966).

Figure 3.17

(A)

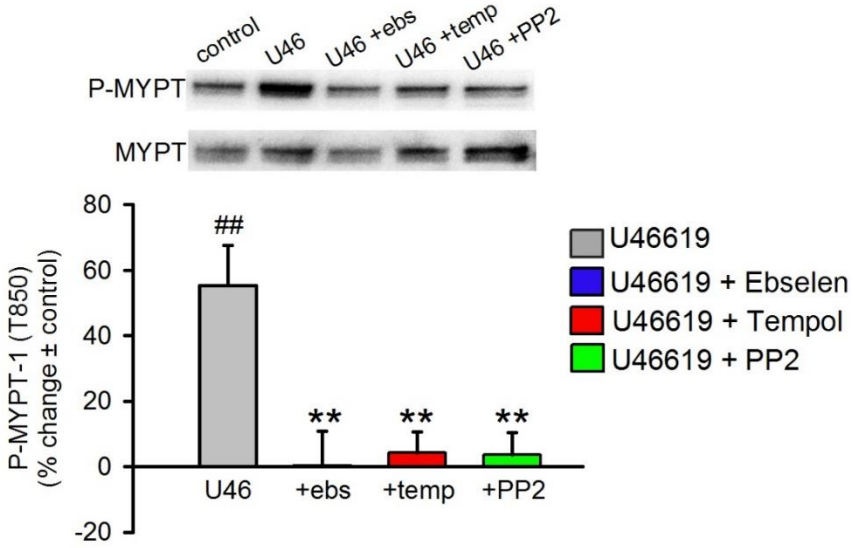

(B)

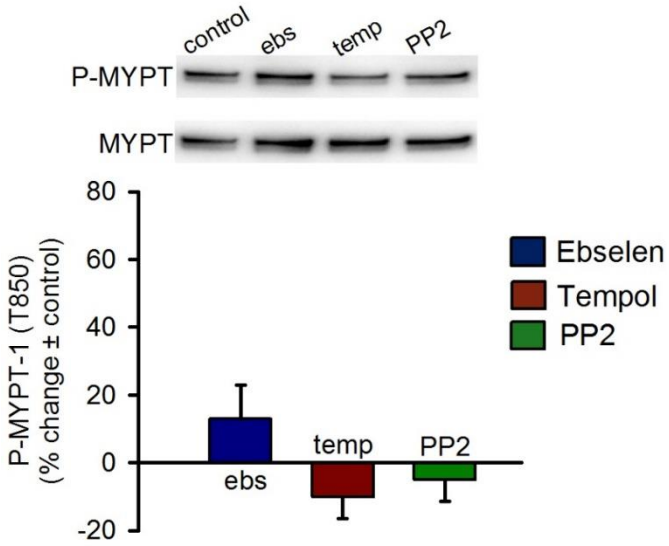

Figure 3.17: U46619-induced MYPT-1 and MLC_{20} phosphorylation is partly mediated via ROS and SrcFK in IPA

A: At 30 min, U46619-induced MYPT-1 phosphorylation is inhibited by ebselen (ebs, 10µM, n=8 arterial samples isolated from 8 rats), tempol (temp, 3mM, n=12 arterial samples isolated from 10 rats) and PP2 (30µM, n=18 arterial samples isolated from 13 rats) ##P<0.001 vs. control (n=27 arterial samples isolated from 16 rats), **P<0.001 vs. U46 alone, while, **B:** basal levels of MYPT-1 phosphorylation was unaffected by ebselen (n=11 arterial samples isolated from 11 rats), tempol (n=12 arterial samples isolated from 11 rats) or PP2 (n=18 arterial samples isolated from 13 rats) (2-way ANOVA, Factors: U46+inhibitor and inhibitor alone. Power of performed test 0.800).

Figure 3.18

(A)

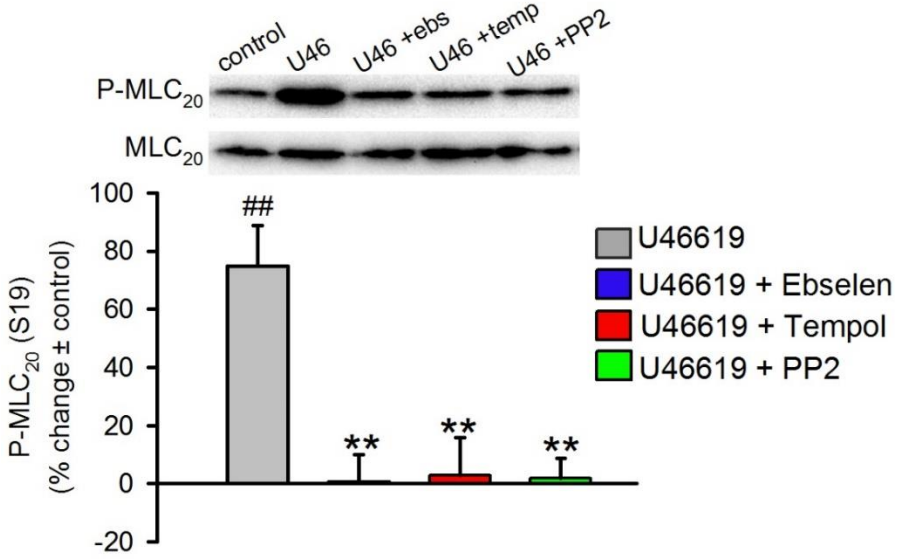

(B)

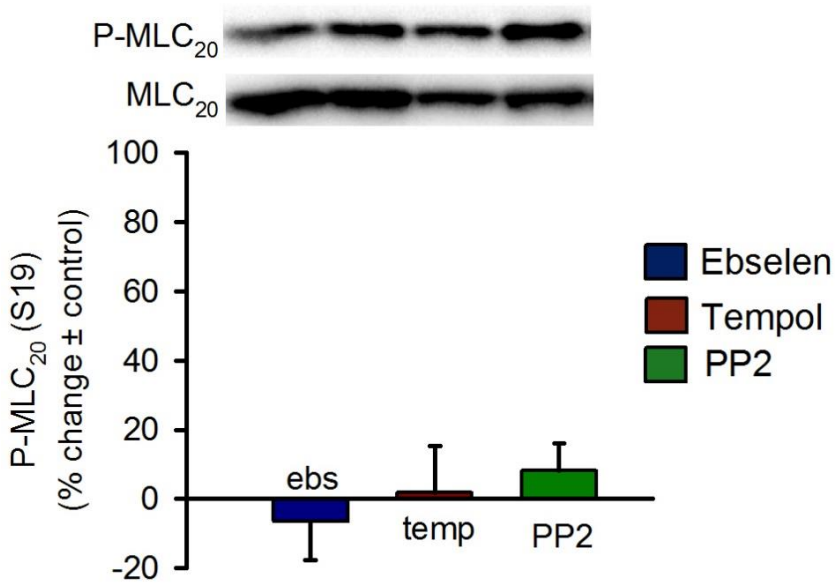

Figure 3.18: U46619-induced Rho-kinase activity and MLC_{20} phosphorylation is partly mediated via ROS and SrcFK in IPA.

A: At 30 min, U46619-induced MLC_{20} phosphorylation is also inhibited by ebselen (n=14 arterial samples from 12 rats), tempol (n=12 arterial samples from 11 rats) and PP2 (n=17 arterial samples from 14 rats) ##P<0.001 vs. control (n=27 arterial samples isolated from 16 rats), **P<0.001 vs. U46 alone, while, **B**: basal levels of MLC_{20} phosphorylation is unaffected by ebselen (n=13 arterial samples from 12 rats), tempol (n=12 arterial samples from 11 rats) or PP2 (n=18 arterial samples from 14 rats) (2-way ANOVA, Factors: U46+inhibitor and inhibitor alone. Power of performed test 0.697).

3.4.5 KPSS contraction is unaffected by ebselen, tempol, and marginally affected by PP2

This is a set of control experiments in order to show that ebselen, tempol or PP2 are not inhibiting contractile function via inhibition of VDCC or MLCK. Therefore, I performed a cumulative dose response of these inhibitors to investigate these drugs on a pure Ca^{2+} influx pathway such as KPSS induced contraction. As KPSS contraction involves the opening of voltage gated calcium channels, therefore allowing the influx of calcium and subsequent MLCK activation, significant inhibition of these contractile responses makes it difficult to interpret any results using that concentration of drug as the drug could simply be inhibiting the opening of calcium channels or MLCK activation.

Treatment with DMSO (Figure 3.19), ebselen (0.1μM - 10μM) (Figure 3.20), tempol (0.1 – 3mM) (Figure 3.21) had no effect on KPSS induced contraction whilst PP2 (30μM) (Figure 3.22) reduced KPSS contraction but only by 15-20%.

Figure 3.19

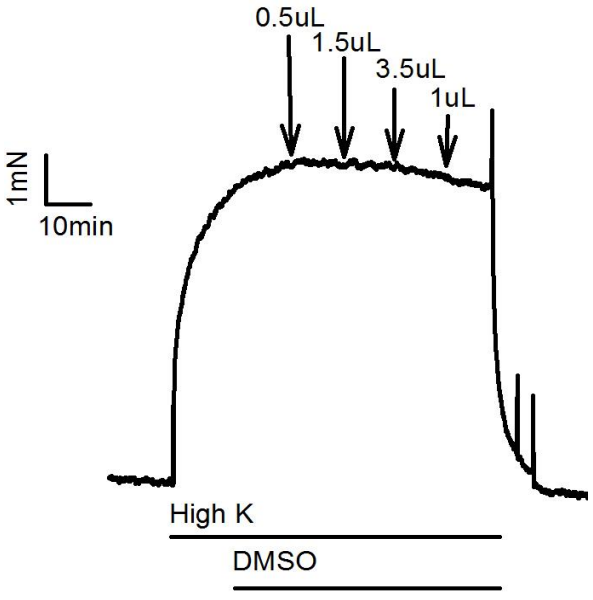

Figure 3.19: Effects of antioxidants and SrcFK inhibition on KPSS induced contraction in IPA

Effect of DMSO (0.5 – 6.0μL) on KPSS induced contraction in IPA. Panel: representative trace with arrows indicating where each dose was added (2-way ANOVA, Factors; DMSO and inhibitors, Power of performed test 0.970, n=7 arteries isolated from 7 rats).

Figure 3.20

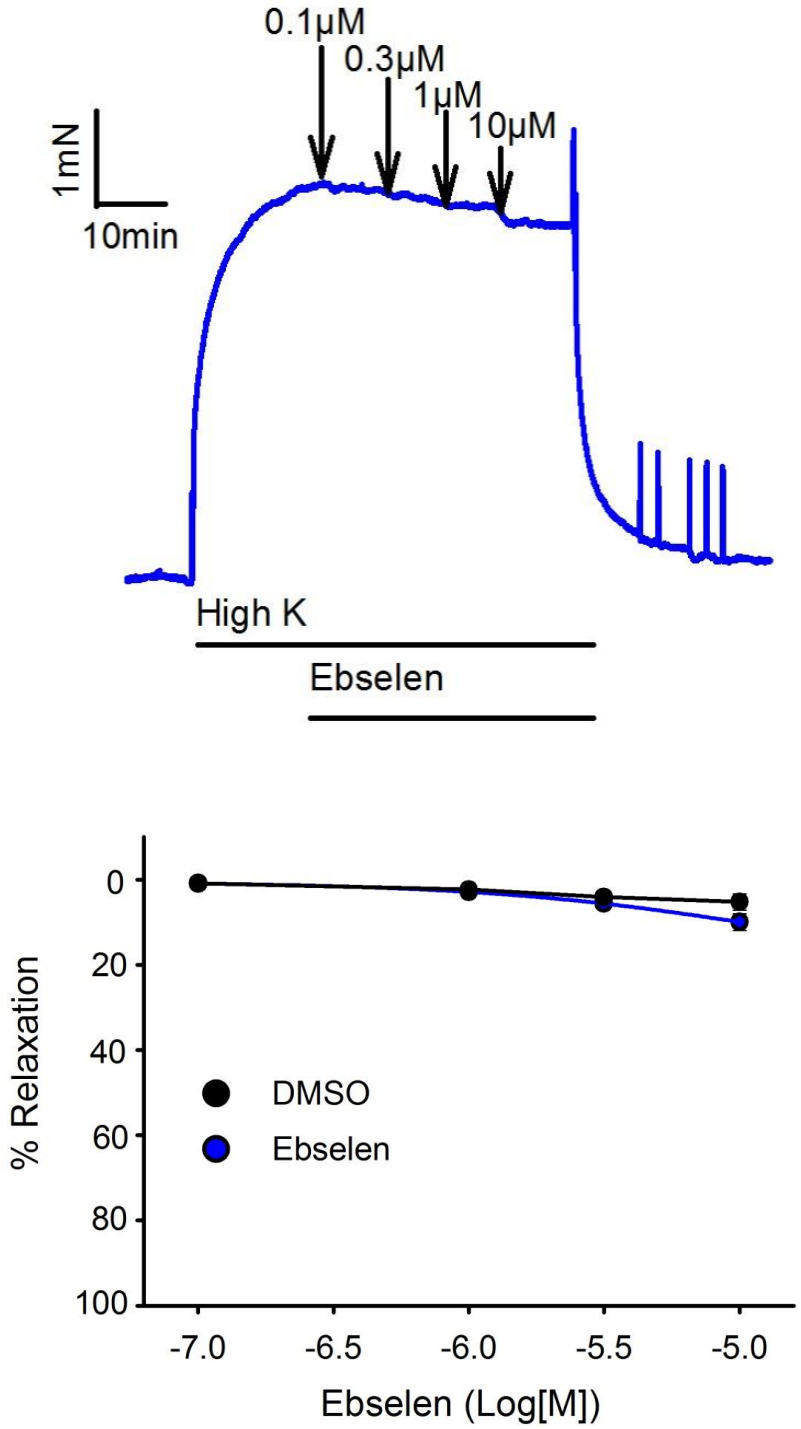

Figure 3.20: Effects of ebselen on KPSS induced contraction in IPA

Effect of ebselen (0.1µM - 10µM) on KPSS induced contraction in IPA. Upper panel: representative traces with arrows indicating where each dose was added. Bottom panel: mean relaxation ± SEM measurements. (2-way ANOVA, DMSO and inhibitors, Power of performed test 0.970, n=8 arteries isolated from 8 rats)

Figure 3.21

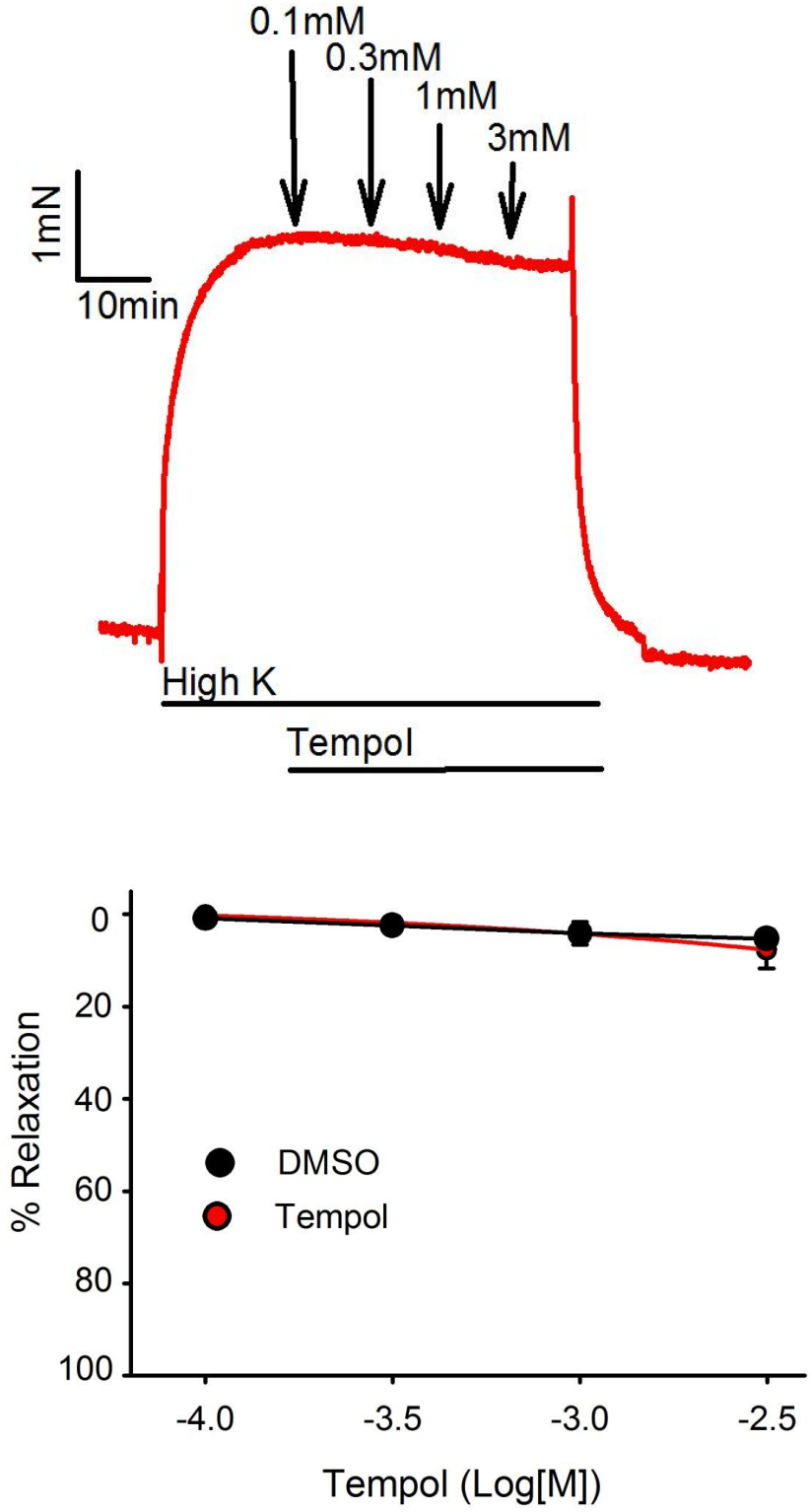

Figure 3.21: Effects of tempol on KPSS induced contraction in IPA

Effect of tempol (0.1mM – 3mM) on KPSS induced contraction in IPA. Upper panel: representative traces with arrows indicating where each dose was added. Bottom panel: mean relaxation ± SEM measurements. (2-way ANOVA, Factors: DMSO and inhibitors, Power of performed test 0.970, n=8 arteries isolated from 8 rats)

Figure 3.22

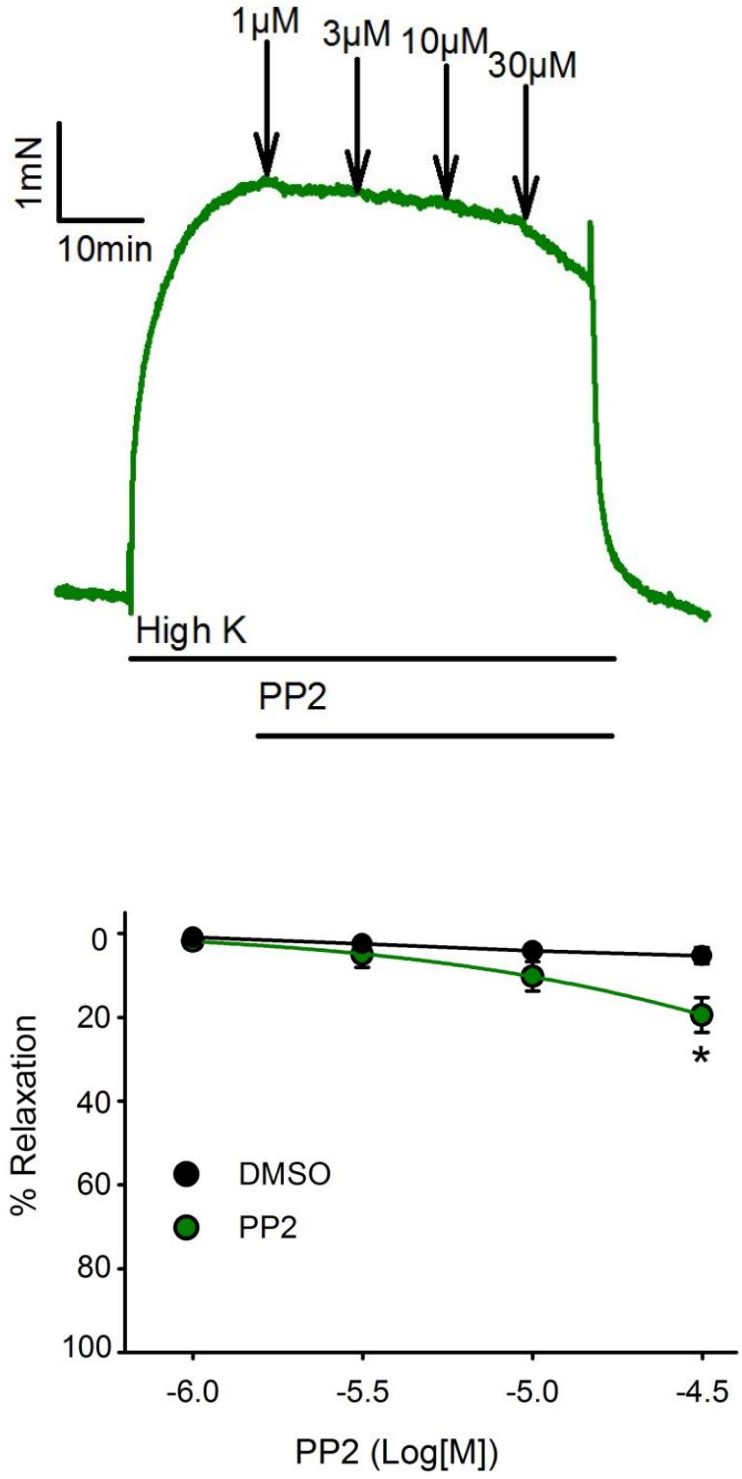

Figure 3.22: Effects of PP2 on KPSS induced contraction in IPA

Concentration-dependent relaxation responses to PP2 in IPA pre-constricted with KPSS. Effect of PP2 (1μM– 30μM) on KPSS induced contraction. Upper panel: representative traces with arrows indicating where each dose was added. Bottom panel: mean relaxation ± SEM measurements (*P<0.05 vs. KPSS, n=8 arteries isolated from 8 rats) (2-way ANOVA: Factors: DMSO and inhibitors, Power of performed test 0.970).

3.4.6: LY83583-induced enhancement of U46619-induced contraction is not nitric oxide dependent

N_{ω}-Nitro-L-arginine methyl ester hydrochloride (L-NAME) is an analogue of arginine (cell permeable) that is known to inhibit the production of endothelial NO. NO has an essential role in vasodilation via activation of Protein Kinase G (PKG) and also suppresses contractile responses to GPCR agonists [424-426]. I therefore investigated whether pre-incubation with L-NAME (300nM), a nitric oxide scavenging, enhanced contraction, also, to test whether the effect of LY83583 was via NO scavenging.

As shown previously, 1µM LY85683 enhanced contractile responses to 2nM U46619. When this response was repeated, but in the presence of L-NAME (300nM), U46619 concentration was lowered to 1nM to match pre-constriction amplitude, the LY83583-induced enhancement of the U46619-induced contraction was similar to what was seen without L-NAME (Fig 3.23). Therefore, the observed enhancing effect of LY on U46-induced contraction is not via scavenging of NO by LY-generated superoxide.

I also investigated whether prior removal of NO by L-NAME influenced inhibition of U46-induced contraction by antioxidants or PP2. Therefore, these experiments were repeated in the presence of L-NAME (300nM). U46619 concentration was lowered to 50nM to maintain sub maximal contraction. Under these conditions, relaxation responses to DMSO (Fig 3.24), ebselen (Fig 3.25), tempol (Fig 3.26) and PP2 (Fig 3.27) were essentially the same as without L-NAME (section 3.4.1). To further augment these results, the differences between L-NAME plus inhibitor and its paired DMSO control were also compared to the difference between inhibitor alone and its paired DMSO control. Relaxation responses were the same under both conditions, thus providing further evidence that ebselen, tempol and PP2 are not promoting relaxation via NO scavenging. This data can be found in the appendix section (Fig A.1). As

contractile function is significantly affected primarily by the highest 2 doses of each inhibitor, the comparisons shown in the appendix section only show the highest 2 doses.

Figure 3.23

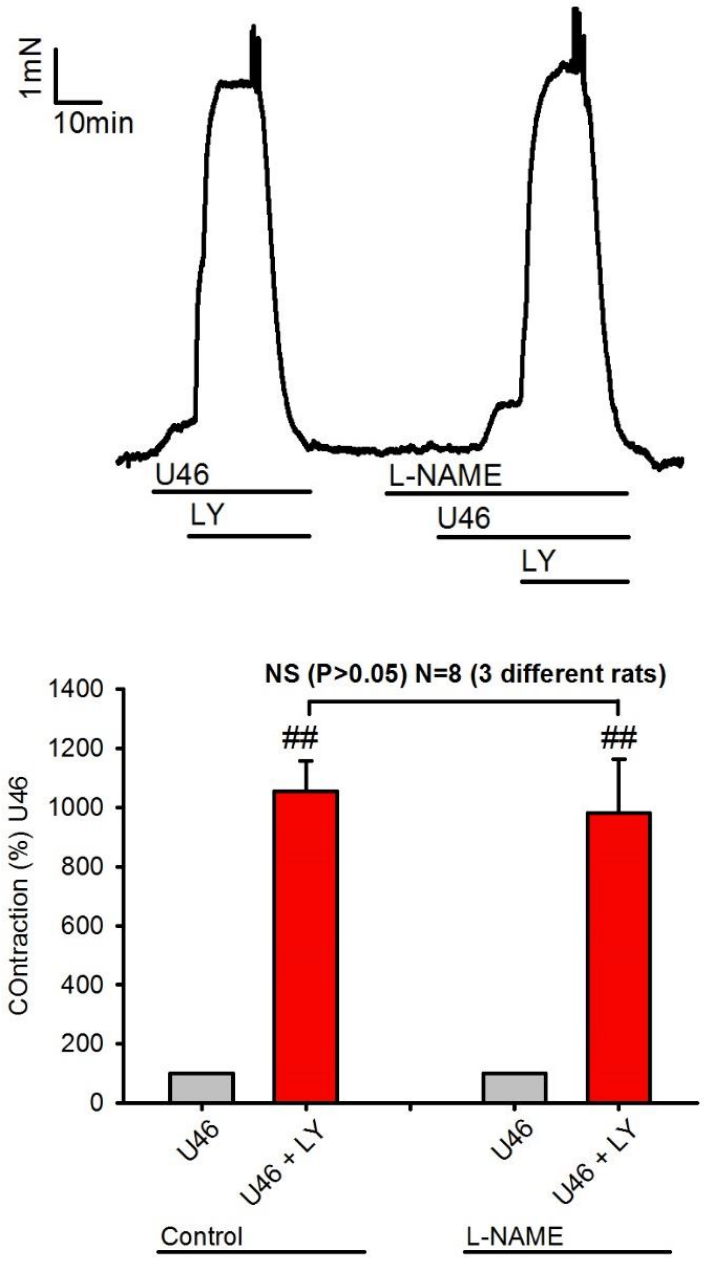

Figure 3.23: Effects of L-NAME on LY83583 enhanced U46619-induced contraction in IPA
U46619 concentration was adjusted to achieve ~10% of KPSS (U46). 1µM LY83583 was then added for 10min (U46+LY). This response was then repeated in the presence of L-NAME (300nM, n=8 arteries isolated from 4 rats). Upper panel: representative traces. Bottom panel: mean ± SEM measurements of peak LY83583-induced contraction, expressed as a percentage increase of U46619 pre-constriction. ##P<0.001 vs. U46 (2-way ANOVA, Factors: U46, U46+LY +- L-NAME treatment. Power of performed test: 0.754).

Figure: 3.24

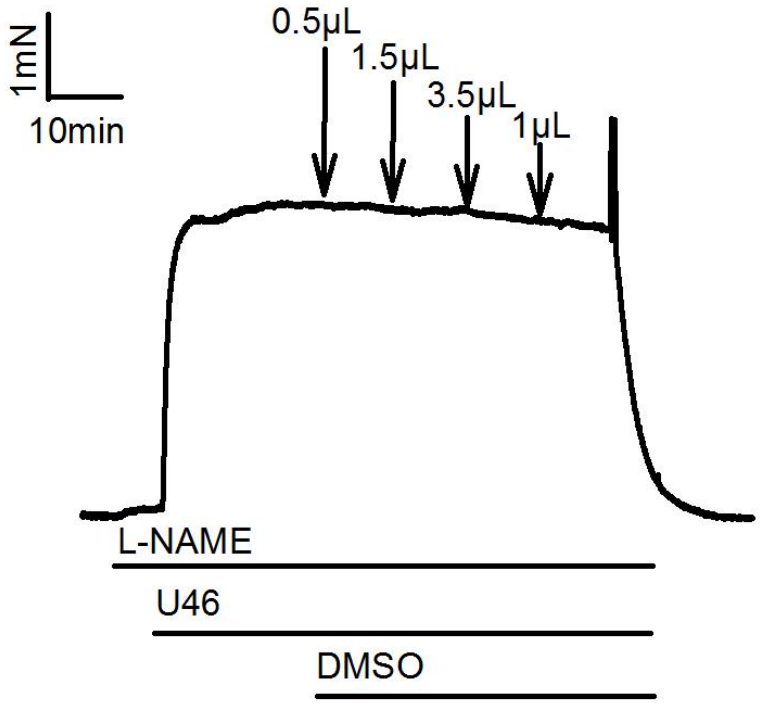

Figure 3.24: Effects of L-NAME and DMSO on U46619 contraction
Concentration-dependent relaxation responses to DMSO (B, n=8 arteries isolated from 8 rats) in IPA pre-constricted with 100nM U46619 in the presence of L-NAME (300nM). Panel: representative traces with arrows highlighting where each dose was added (2- Way ANOVA, Factors: DMSO and inhibitors, Power of performed test 0.999).

Figure 3.25

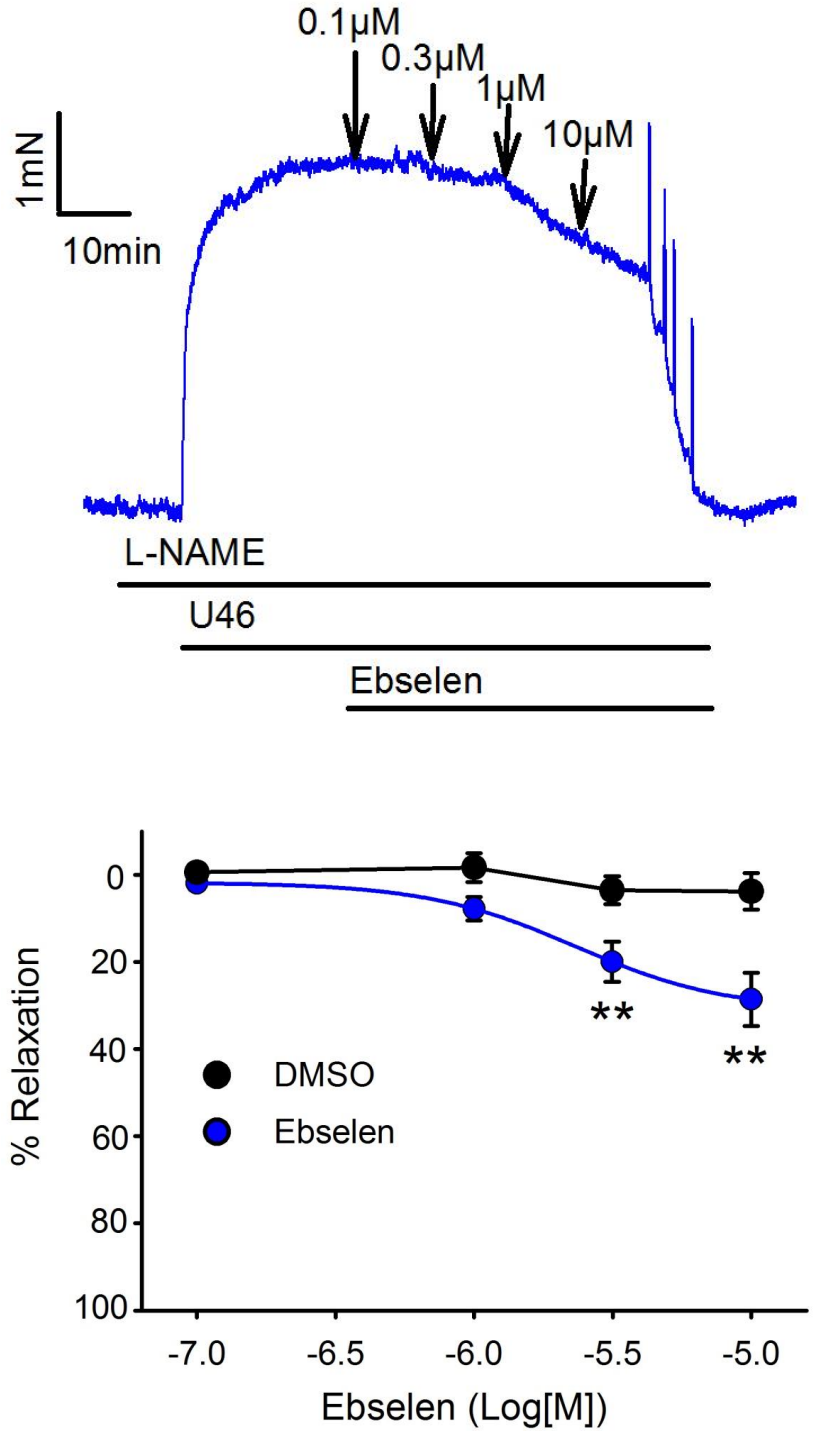

Figure 3.25: Effects of L-NAME and ebselen on U46619 contraction
Concentration-dependent relaxation responses to ebselen (C, n=7 arteries isolated from 7 rats) in IPA pre-constricted with 100nM U46619 in the presence of L-NAME (300nM). Upper panel: representative traces with arrows highlighting where each dose was added. Bottom panel: mean ± SEM measurements of peak LY83583-induced contraction, expressed as a percentage increase of U46619 pre-constriction. **P<0.01 vs. DMSO control (2-way ANOVA Factors: DMSO and inhibitors, Power of performed test 0.690).

Figure 3.26

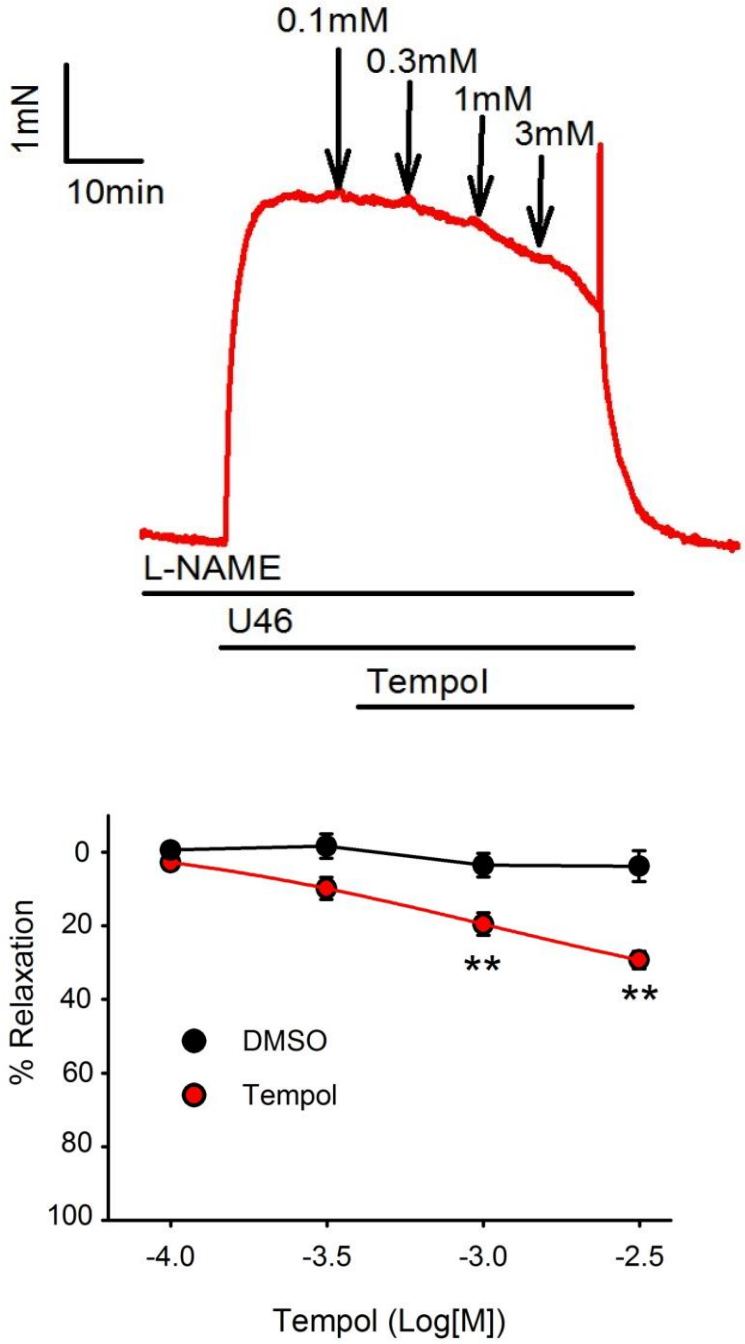

Figure 3.26: Effects of L-NAME and tempol on U46619 contraction
Concentration-dependent relaxation responses to tempol (B, n=6 arteries isolated from 6 rats) in IPA pre-constricted with 100nM U46619 in the presence of L-NAME (300nM). Upper panel: representative traces with arrows highlighting where each dose was added. Bottom panel: mean ± SEM measurements of peak LY83583-induced contraction, expressed as a percentage increase of U46619 pre-constriction. **P<0.001 vs. DMSO control (2-way ANOVA Factors: DMSO and inhibitors, Power of performed test 0.743).

Figure 3.27

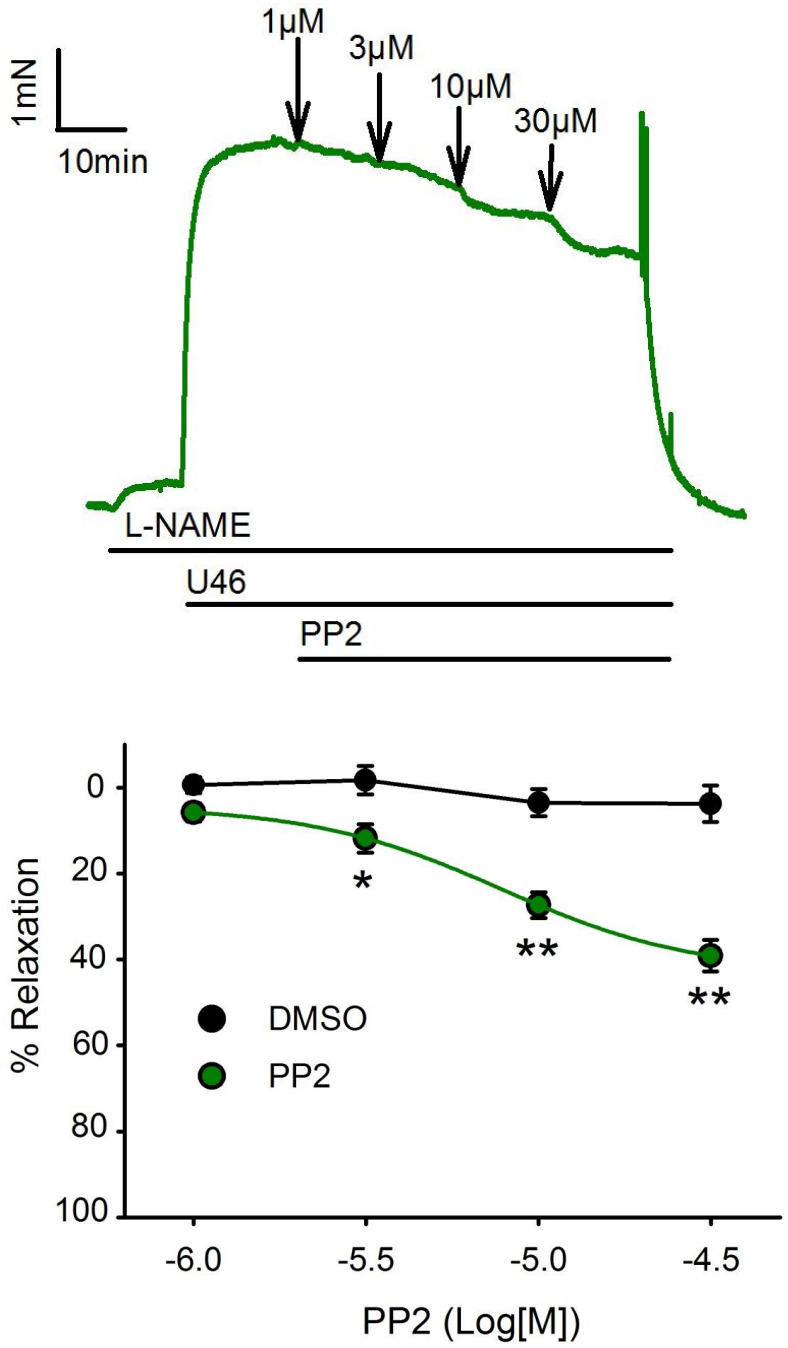

Figure 3.27: Effects of L-NAME on U46619 and PP2 contraction

Concentration-dependent relaxation responses to PP2 (E, n=8 arteries isolated from 8 rats) in IPA pre-constricted with 100nM U46619 in the presence of L-NAME (300nM). Upper panel: representative traces with arrows highlighting where each dose was added. Bottom panel: mean ± SEM measurements of peak LY83583-induced contraction, expressed as a percentage increase of U46619 pre-constriction. *P<0.05, **P<0.01 vs. DMSO control (2-way ANOVA Factors: DMSO and inhibitors, Power of performed test 0.705).

3.5 Summary of findings

The purpose of this chapter was to investigate the stated hypothesis of:

"ROS are key secondary messenger molecules mediating vascular smooth muscle contraction in response to multiple stimuli and Src-family kinases have a critical role as ROS-sensitive intermediaries in these signalling pathways".

The findings of this chapter are:

- U46619 and LY83583 induce ROS production in PASMCs which along with basal ROS production is sensitive to antioxidants ebselen and tempol.
- U46619 and LY83583 both directly constrict pulmonary arteries independently of nitric oxide and that these constrictions are sensitive to SrcFK inhibition with PP2 or antioxidants ebselen and tempol.
- U46619 and LY83583 enhance SrcFK autophosphorylation in a time dependent manner. In the case of U46619 responses, this is also ROS and SrcFK dependent.
- LY83583 enhance tyrosine phosphorylation of multiple protein targets in pulmonary arteries and this phosphorylation is sensitive to PP2.
- U46619 enhance MYPT-1 and MLC_{20} phosphorylation and that this is sensitive to SrcFK inhibition and ROS inhibition.

3.6 Discussion

It is well established that RhoA and its effector Rho-Kinase play an essential role in regulating smooth muscle contraction and Ca^{2+} sensitization. Agonist induced Ca^{2+} sensitization involves Rho-Kinase mediated phosphorylation of myosin light chain phosphatase (MLCP) thereby inhibiting MLCP activity [29,427], however the link between agonist and RhoA/Rho-Kinase activation in response to upstream mediation needs further investigation.

Many vasoconstrictors generate ROS under physiological conditions and also activate tyrosine kinases. Previous work within our group has shown that prostaglandin-$F_{2\alpha}$ and hypoxia enhance total cellular tyrosine phosphorylation, activate Src and cause Src-FK-dependent constriction [7,88]. Similar relations have been identified within other vascular beds [82,419]. These observations combined with the noted ROS-sensitivity of Src[213] suggest that interactions between SrcFK and ROS make a central contribution to vascular smooth muscle function.

This study was therefore designed to investigate the relationship between vascular ROS production, SrcFK activity and Rho-kinase activity in normal vasoconstrictor responses in IPA and to investigate whether SrcFK act as ROS sensitive intermediates acting upstream of RhoA/Rho-kinase.

3.6.1 U46 & LY induce antioxidant-sensitive ROS production

Key studies within my group have shown a role for SrcFK in HPV [7], interactions between SrcFK and Rho-Kinase in agonist induced Ca^{2+} sensitization[41] and the role of superoxide in pulmonary and systemic signalling pathways [89]. A key element missing was how agonists, hypoxia, exogenous ROS, SrcFK and Rho-Kinase activation are all linked together. I therefore investigated how ROS, SrcFK and Rho-Kinase are linked together to promote contraction in pulmonary arteries.

Firstly, I investigated ROS production in PASMCs. ROS are considered bona fide secondary messenger molecules which are produced within the cell in response to physiological and pathophysiological stimuli. The two main sources of ROS in VSM being NADPH oxidase (NOX) [98,428] and mitochondrial electron transport [94,413,429]. A number of studies have shown that vascular NOX activity is enhanced by a number of G-protein-coupled receptor (GPCR) such as angiotensin II, endothelin-1, thrombin, ATP, thromboxane and U46619 [134,430-433]. Indeed within this study I also show in our system, the TP receptor selective agonist U46619 is able to stimulate production of ROS in PASMCs and that this is inhibited by antioxidants ebselen and tempol.

Throughout the study, the membrane permeable quinolinequinone LY83583 was used as it is a verifiable source of ROS, that our group has previously used to compare the genuine effects of GPCR on endogenous ROS production[88]. This therefore helped validate methods and drugs used i.e. by acting as a positive control for measuring ROS production along with confirming that ebselen and tempol were indeed acting as anti-oxidants. The LY83583 results also mirrored results obtained from U46619. This helped support the conclusions that ROS are key secondary messenger molecules mediating vascular smooth muscle contraction and that SrcFK have a critical role as ROS-sensitive intermediaries in vascular smooth muscle contraction.

U46619 acts through thromboxane receptor, also known as the prostanoid TP receptor coupled to G_q [434 356]. Activation of receptors coupled to $G_{q/11}$-proteins activates phospholipase C (PLC) leading to the hydrolysis of phosphatidylinositol 4,5-bisphosphate (PIP_2) and generation of diacylglycerol (DAG) and inositol 1,4,5-trisphosphate (IP_3). This results in activation of PKC and Ca^{2+} release from intracellular stores [435]. The PKC family are well known too phosphorylate the p^{47}phox subunit of NOX thereby promoting its activity and ROS production [125,436]. On the other hand, LY83583 promotes ROS production by acting as a substrate for NADPH:quinone oxidoreductase diaphorase (see methods section) [89].

In the presence of ebselen or tempol, ROS production was inhibited with tempol more effective than ebselen. L-012 is known to measure $O_2^{\bullet-}$ [381-384], however may also detect $ONOO^-$ and probably other ROS[383,385-387]. Since tempol has been described as a SOD mimetic[131,437] and ebselen being a glutathione peroxidase mimetic [438], it makes perfect sense for tempol to be a more effective antioxidant in this system particularly if the primary ROS species being measured is superoxide.

The ROS that is being produced is believed to be from NOXs as previously described in this tissue [99], and coupled with the wealth of data already published which shows agonist-induced ROS production is via NOX activation by constrictor stimuli. The possible role of mitochondrial ROS will be addressed in chapter 4.

What is not made clear throughout this study is which NOX is involved in ROS production. However, the aim of the study was not to determine which NOX is being activated rather what the ROS being produced are acting on.

The use of specific inhibitors, knockout models or co-localisation studies could be used to determine which NOX is being activated. Published data has shown that the vasculature expresses NOX1, NOX2, NOX4 and NOX5 [439-442], which can be regulated by a number of factors including physical factors (stretch), contractile agonists such as angiotensin II (Ang II) and endothelin-1 (Et-1) as well as growth factors (e.g. EGF, PDGF)[443-446]. Furthermore, Shaifta *et al*[99] have recently shown that Sphingosylphosphorylcholine (SPC) mediates vasoreactivity via PLC and NOX1-mediated increase in ROS [99].

NOX1 has been shown to be responsible for $O_2^{\bullet-}$ production and redox signalling following agonist stimulation [99] and associated with pathological conditions, such as atherosclerosis, diabetes, and hypertension[447]. NOX1 regulation has also been accredited to phosphorylation [448].

Taken together, the activation of NOX is complex and that more than one NOX family member, alone or in association, may be involved in NAD(P)H oxidase–mediated ROS production.

3.6.2 Activation of SrcFK by endogenous and exogenous ROS

Contractile and phosphorylation studies were performed to investigate whether SrcFKs perform a critical role acting as ROS-sensitive intermediaries in smooth muscle contraction and whether this interaction leads to the activation of Rho-Kinase.

Previous studies carried out by Oda *et al* [449] and Sakai *et al* [200] demonstrated that SrcFK is highly expressed in vascular and airway smooth muscle. Previous work, investigating the role of tyrosine kinases in smooth muscle have used broad spectrum TKI's, tyrphostins and genistein which promoted relaxation [71,72]. However, these TKIs do not distinguish between receptor and non-receptor tyrosine kinases. Following the development of selective SrcFK inhibitors, PP2 [186] and SU6656 [450], the role of SrcFK has been studied in more detail particularly within our laboratory [7,41,83] along with other groups [82].

In this study, I demonstrate that U46619 -induced contraction and LY83583 enhanced U46619-induced pre-constriction is SrcFK and ROS dependent. In both cases, contraction is inhibited by the unrelated antioxidants ebselen and tempol and SrcFK inhibitor PP2.

U46619 and LY83583-induced SrcFK auto-phosphorylation on Y416, a recognised indicator of SrcFK activity, peaking at both 30 seconds and 30 minutes.

The biphasic response seen in these experiments was also noted by Knock *et al* in response to $PGF_{2\alpha}$[41] and as explained in Chapter 1 and discussed below, can be explained by direct and indirect redox regulation of SrcFK.

SrcFK is retained in an inactive state by binding of its SH2 domain to its own phosphorylated C-terminal regulatory domain at Tyr-527, this folding may be disrupted and lead to the

autophosphorylation of Tyr-416. The cysteine residue within the SH2 domain of Src (cys-245) may be directly oxidised by ROS, leading to the activation of Src [211]. Src may also be oxidised at both cys-245 and cys-487 [213]. This also causes unfolding of the Src protein and autophosphorylation of the tyr-416 residue [451]. ROS may also promote the activation of Src through oxidative modulation of the proteins involved in normal Src regulation. These 'indirect redox regulation mechanisms' involve the oxidation and pre-dominantly inhibition of both PTPs and C-terminal Src kinases (Csks) – an important kinase group involved with the phosphorylation, and inactivation, of Src at tyr-527 [92,452].

The disparity of activation levels between the two time points may suggest that ROS in this case may be activating SrcFK via different pathways. As mentioned, 'direct' oxidation mechanisms of SrcFK activation would be, faster and more instantaneous than those of the indirect pathways. Therefore, at 30 seconds, ROS may preferentially modulate SrcFK via these direct mechanisms, leading to faster, but more unstable active forms of Src, which may be quickly dephosphorylated. Alternatively, the activation of SrcFK by indirect redox regulation may be more predominant at 30 minutes particular PTPs that are oxidatively inactivated by ROS [92,213,418,451,453].

The U46619 (at 30 minute) increase in SrcFK phosphorylation is blocked by ebselen and tempol and SrcFK inhibitor PP2 but basal levels are not blocked by ebselen or tempol but are by PP2. This indicates that basal SrcFK autophosphorylation is not regulated by ROS but also confirms PP2 to be a SrcFK inhibitor. This also suggests interacts between ROS and SrcFK only during stimulation of G-protein-coupled-receptor. A possible explanation could be that GPCR stimulation, enhances interactions between ROS and SrcFK within the same microdomain. Without stimulation, it is likely that SrcFK and ROS will not significantly interact and are located within different microdomains therefore unable to interact. This perhaps explains why

tempol and ebselen inhibit basal ROS production but do not significantly affect basal phosphorylation in the absence of U46 or LY.

LY (1 and 10μM) enhanced ROS production in PASMCs however LY (10μM) enhanced ROS production to a greater level than LY (1μM) however there was no significant difference between each concentration. LY (1μM) was able to induced activation of SrcFK (at 30s and 30min) but is unable to alter tension without combining with another stimuli such as U46. Previous work within my group has shown that LY (at > 1 μmol/L), causes a sustained, reproducible, SOD- and Y27632-inhibitable constriction in small pulmonary arteries [88,89]. Similar to my results, Knock *et al* [88,89] also determined that LY at lower concentrations (<1 μmol/L) can enhance ROS production but is unable to alter tension but can do so when applied in combination with other stimuli such as $PGF_{2\alpha}$. It is believed that although both concentrations of LY can enhance ROS (albeit not significantly different from each other), LY (10μM) does enhance ROS to a greater level which reaches a threshold whereby the need for a secondary stimuli is not required to generate tension. Furthermore, LY (at > 1 μmol/L), is able to enhance rho-kinase activity but also increase intracellular Ca^{2+} concentration whereas LY at (<1 μmol/L) can only enhance rho-Kinase activity. As calcium is essential for contraction (see introduction) this will be why LY (at > 1 μmol/L) is able to generate tension. Finally, as LY (at > 1 μmol/L) can enhance Ca^{2+} whereas LY at (<1 μmol/L) is unable to can perhaps be explained by bursts of ROS generated in response to LY. Although as mentioned, there is no significant difference between 1 or 10μm LY, 10μm LY is still able to produce a higher concentration of ROS which could overwhelm the redox buffer systems within the microdomain. This could allow ROS to "escape" which may activate Ca^{2+} channels in the membrane or promote release from stores.

Furthermore, LY83583 enhanced SrcFK-dependent tyrosine phosphorylation of multiple proteins bands in IPA which are sensitive to SrcFK inhibition. One can therefore postulate that

the increased phosphorylation of these bands may be direct targets for SrcFK or regulated via another tyrosine kinases which in turn is mediated by SrcFK. What is of interest is the band ~115kDa. This which as discussed in chapter 5, could be ARHGEF1. These findings are not direct evidence for the tyrosine phosphorylation of ARHGEF1 by SrcFK, but phosphorylation has been shown to be a requirement for ARHGEF1 activation, albeit by JAK2 [325]. Furthermore, FAK, PYK2 and JAK2 have been shown to phosphorylate RhoGEFs which may be partly mediated via SrcFK interactions. The band located ~120kDa could be FAK, which Shaifta *et al* have recently shown to interact with SrcFK in airway smooth muscle [83].

My results demonstrate that SrcFK, act as ROS sensitive intermediates in IPA contractile responses. This correlates with previous published data by Knock *et al* [41] where the SrcFK selective inhibitors, SU6656 and PP2, both selectively inhibit $PGF_{2\alpha}$ but not Ca^{2+} induced contraction in α-permeabilized rat pulmonary artery, also $O_2^{\bullet-}$ constricts rat pulmonary arteries via Rho-Kinase-mediated Ca^{2+} sensitization[88]. Furthermore, functional data by liu *et al*[453] demonstrated that genistein had a profound effect on U46619 induced contraction in pulmonary artery, showing similar results to what I have seen using the SrcFK specific inhibitor PP2. The effects of SrcFK inhibition was also shown by Sakai *et al* [200], whereby in angiotensin-II (ANG-II)-induced hyper-responsiveness to carbachol which was blocked using the SrcFK specific inhibitor SU6656 in rat bronchi.

The general constrictor role for ROS has been explored using exogenously applied superoxide using xanthine/xanthine oxidase or quinones including LY83583 and menadione [88,151,423]. Furthermore, the internal stimuli for hypoxic pulmonary vasoconstriction (HPV) is believed to be an initial rise in mitochondrial ROS [94,140,176,412,413]. Importantly, physiological responses too many of the stimuli and changes in protein kinase activity described have been inhibited by antioxidants [117,119,290,454] and SOD [454,455] , correlating with the effects seen here using ebselen and tempol.

My data further contributes to the wealth of data that vasoconstrictor stimuli increase ROS levels and enhance tyrosine phosphorylation [41,88,456,457] subsequently promoting vasoconstriction. More specifically, that SrcFK act as ROS sensitive intermediates during this process.

It is important to note that vascular beds react differently to externally applied ROS. ROS promote constriction in a number of vascular beds including aorta [192], pulmonary artery [88,193,196,458], coronary artery [195] and mesenteric artery [192] and is associated with associated with numerous cardiovascular diseases, including systemic and pulmonary hypertension. However, ROS have complex constricting and relaxing actions on the systemic vasculature, depending on the size of the artery, nature of pre-constriction, amount and type of ROS present, and where the ROS is being generated [89,198,459]. The two principal ROS species, $O_2^{\bullet-}$ and H_2O_2 have unique actions on the vasculature. $O_2^{\bullet-}$ promotes contraction in both pulmonary and systemic arteries via nitric oxide scavenging [460,461] but also through activation of redox sensitive kinases [88]. Whereas, systemically, hydrogen peroxide mediates vasodilation and may act as an endothelium-derived hyperpolarizing factor (EDHF) via opening of K^+ channels [462] [89]. In pulmonary arteries, hydrogen peroxide is more likely to be pro-contractile [194] and EDHF not as important than it is systemically [463].

$O_2^{\bullet-}$ and H_2O_2 also contribute to endothelium-independent constriction through activation of multiple protein kinase pathways [196]. Previously, we showed that $O_2^{\bullet-}$ acts predominantly through Rho-kinase[88] whilst H_2O_2 mediates its actions via activation of PKC directly constricted rat PA[194]. Furthermore, hydrogen peroxide also causes Ca^{2+} release from ryanodine-sensitive stores[194]. However, a greater understanding is required to elucidate the differences exhibited by $O_2^{\bullet-}$ and H_2O_2 in different vascular beds.

3.6.3 Endogenous ROS production mediates activation of Rho-kinase via interactions with SrcFK

After establishing that SrcFK are ROS sensitive intermediates involved in mediating U46619 and LY83583 contraction in rat IPA, I extended my investigation to determine whether this occurred upstream of RhoA/Rho-Kinase.

If ROS and SrcFK are indeed upstream mediators of the RhoA/Rho-Kinase and form a signalling axis, then inhibition of either ROS or SrcFK should decrease Rho-Kinase activity.

Previous work has shown that Rho-Kinase inhibits MLCP activity via phosphorylation of MYPT-1, the regulatory subunit of myosin phosphatase, primarily at the thr-855 site [41] which is independent of changes in intracellular calcium [33]. Subsequently, leading to increased MLC_{20} phosphorylation via MLCP inhibition.

MYPT-1 and MLC_{20} phosphorylation responses follow a parallel time course in response to U46619 stimulation. This can be attributed to the activation of RhoA/Rho-Kinase pathway which as discussed, inhibits myosin light chain phosphatase thereby enhancing MLC_{20} phosphorylation. This is in line with a number of studies that have shown, measuring MYPT-1 phosphorylation, that agonists activate Rho-Kinase [7,41,43,89,281,464].

U46619 induced MYPT1 and MLC_{20} phosphorylation is inhibited in the presence of ebselen, tempol and PP2, however basal levels remain unaffected confirming that agonist-induced ROS, not basal ROS, is contributing to SrcFK and Rho-kinase activation (section 3.4.4).

The question arises as to whether ROS and SrcFK in response to U46619 is upstream of RhoA/Rho-kinase or enhances Ca^{2+}-sensitivity through a separate pathway. Previously, Knock *et al* [41] demonstrated that the SrcFK inhibitor SU6656 and the Rho-Kinase inhibitor Y27632 were not additive with respect to both inhibition of $PGF_{2\alpha}$-induced MYPT-1 and MLC_{20} phosphorylation and inhibition of the associated $PGF_{2\alpha}$-induced contraction, suggesting

that S*rc*FK and Rho-kinase may be part of the same pathway. Furthermore, Rho-kinase translocation was blocked by prior treated with SU6656, suggesting that SrcFK mediated rho-kinase translocation.

My data adds to these findings as both U46619 and LY enhance SrcFK (Tyr-416) and Rho-kinase (MYPT-1and MLC_{20}) phosphorylation responses which are sensitive to ebselen, tempol and PP2 whilst basal levels remain unaffected. As SrcFK activity is sensitive to antioxidants, whilst Rho-Kinase activity is sensitive to antioxidants and PP2, this suggests a signalling axis whereby in response to constrictor stimuli such as U46619 and LY, there is an increase in ROS production which enhances SrcFK activity subsequently activating Rho-Kinase.

Basal levels remain unaffected by antioxidants and PP2, suggesting there is little interactions between these molecules at the basal level and that prior stimulation is required for this signalling axis to occur. This further suggests that these molecules may be in different signalling microdomains under basal conditions but are then brought together to create this signalling axis following stimulation.

A further consideration is that this was not performed in calcium clamped conditions. Therefore, Ca^{2+} will play a role in MLC_{20} phosphorylation responses. Agonists cause contraction through a combination of Ca^{2+} responses such as DAG mediated activation of non-selective cation channels thereby promoting calcium influx and IP_3 mediated Ca^{2+} release from stores but also through Rho-Kinase activation. SrcFK has been implicated in both responses. Previous studies from our group confirmed a role for Src upstream of Rho-Kinase by clamping Ca^{2+} therefore I did not need to perform these experiments myself in calcium free condition[41],[88].

There is no evidence that Rho-Kinase is directly redox sensitive. Therefore activation of RhoA/Rho-kinase may be mediated further upstream by tyrosine kinases [88]. Since the SrcFK inhibitor PP2 is also shown to inhibit MYPT-1 and MLC_{20} phosphorylation, it is reasonable to

suggest that SrcFK are involved as ROS sensitive intermediates involved in the activation of RhoA/Rho-kinase in response to constrictor stimuli.

Taken together, inhibition of ROS and SrcFK or indeed enhancement can affect contractile responses via multiple pathways.

3.6.4 Control Experiments

Dose responses for ebselen, tempol and PP2 were initially conducted to KPSS in order to find the correct concentration of drug where there where minimal off target contractile effects. To investigate such effects, high K^+ was used to induce contraction. High K-induced contractions in healthy smooth muscle promotes depolarization of smooth muscle cell membrane and opens voltage dependent Ca^{2+} channels, resulting in an influx of extracellular Ca^{2+} and an activation of contractile machinery. As discussed in the introduction, membrane depolarisation can activate parallel contractile signalling pathways such as Rho-Kinase. However, this is believed to be a secondary response and the primary function of depolarisation is Ca^{2+} signalling. As ebselen and tempol were shown to have no affect at the concentrations used, this suggest at the concentrations used will have no non-specific effect on contractile machinery. PP2 at the highest concentration has a slight effect on high K^+ however previous data within our laboratory has shown PP2 to have no effect in human ASM high K responses. Lack of effect of PP2 on 80mM K+ (where Ca2+ channels are fully opened by depolarisation, suggests that PP2 is not a Ca2+ channel antagonist independently of its actions on Src. U46 induces ROS production via NOX, however there is little evidence to suggest that depolarisation can also activate NOX. Therefore, it is expected that U46 induced contraction will be more sensitive to antioxidants and PP2 vs high K^+ contraction.

In order to determine the role of nitic oxide in U46619 and LY83583 contractile responses, dose responses were repeated in the presence of L-NAME (a NO synthase inhibitor). What I

see from the results is that L-NAME enhances tissue sensitivity to U46619 which is why a lower concentration of U46619 was used to match contraction amplitudes In the presence of L-NAME. However, L-NAME did not alter the enhancing effect of LY83583 on U46619-induced contractile response. Therefore LY83583 is not enhancing contraction by removing NO.

In conclusion, the data in this chapter strongly suggests ROS are key secondary messenger molecules mediating vascular smooth muscle contraction in response to multiple stimuli and Src-family kinases have a critical role as ROS-sensitive intermediaries in these signalling pathways. The ability of ebselen and tempol inhibit SrcFK autophosphorylation and PP2 to inhibit both SrcFK and MYPT1 and MLC_{20} phosphorylation is strong evidence that ROS activates SrcFK which subsequently activates Rho-Kinase, as summarised in figure 3.28. The mechanisms involved in Rho-Kinase activation will be discussed in a later chapter (chapter 5).

Figure 3.28:

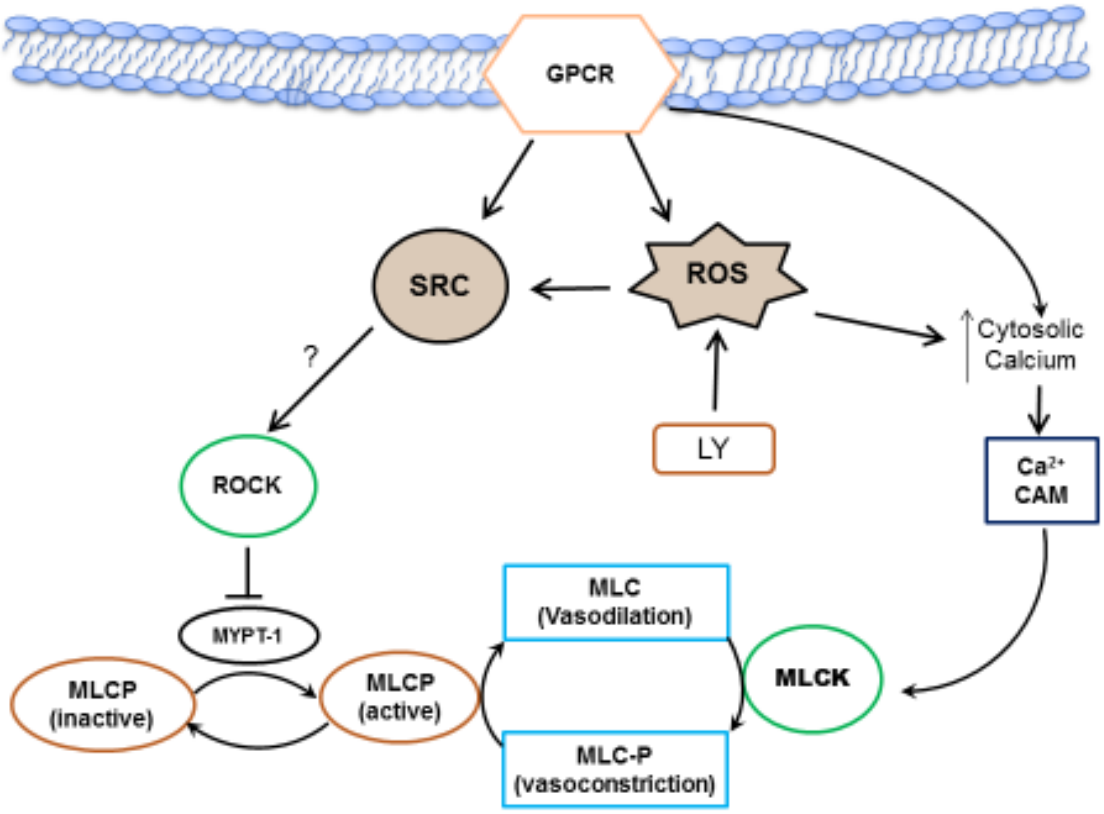

Figure 3.28: Shows the upstream regulation of the Rho-kinase pathway by ROS and SrcFK.

The data demonstrate that SrcFK are ROS sensitive intermediate in response to stimulation. The mechanism by which RhoA/Rho-Kinase is activated will be discussed in a later chapter.

Chapter 4

Hypoxia enhances SrcFK, MYPT-1 and MLC_{20} phosphorylation in a mitochondrial ETC-dependent manner

4.1 Background

Hypoxic pulmonary vasoconstriction (HPV) is a is a rapid and reversible contractile response to hypoxia, whereby blood flow is directed away from poorly ventilated areas of the lung to areas with higher oxygen content thereby maximising ventilation perfusion matching. HPV is typically bi-phasic in isolated pulmonary arteries, with a large transient first phase followed by a gradually developing second phase [372,465]. The first phase is associated with a large transient rise in intracellular calcium ($[Ca^{2+}]_i$) however phase 2 develops gradually with a stable but small and rapid increase in $[Ca^{2+}]_i$ [465], which is enhanced in a Rho-Kinase dependent Ca^{2+} sensitization manner [370] and is endothelium dependent [466,467].

As discussed in the introduction chapter, SrcFK's are a family of closely related non-receptor tyrosine kinases including Src, Fyn and Yes which are highly expressed in pulmonary arteries [41]. Tyrosine kinases are involved in cell growth but are also important in smooth muscle contraction [76,235]. Studies by this group and others have shown that SrcFKs play a critical role in agonist induced Rho-Kinase mediated Ca^{2+} sensitization [41,82]. Furthermore, Knock *et al* [7] have also implicated that SrcFK play a central role in HPV. Previously, SrcFK have been shown to play a direct role in contractile responses to hypoxia and that SrcFK inhibitors block hypoxia-mediated Rho-Kinase dependent MYPT-1 phosphorylation [7]. This along with evidence that hypoxia triggers an increase in ROS production[94,140,413] suggests that SrcFK act as ROS sensitive intermediate involved in hypoxia mediated Ca^{2+} sensitization.

A widely accepted view is that HPV is initiated via increased ROS production from complex three of the electron transport chain[412,468]. Due to the oxidative sensitivity of SrcFK and the perception that hypoxia increases ROS production, it is reasonable to assume that increased ROS production from the mitochondria can activate SrcFK to promote Rho-Kinase mediated Ca^{2+} sensitization.

4.2 Hypothesis

I hypothesise, that hypoxia will enhances SrcFK, MYPT-1 and MLC_{20} phosphorylation in a mitochondrial ETC-dependent manner. Furthermore, if SrcFK do act as ETC-dependent intermediates in Rho-Kinase mediated vasoconstriction, inhibition of the ETC should decrease the activity of SrcFK, as well as Rho-Kinase, of which the latter will be apparent by inhibition of MYPT-1 and MLC_{20} phosphorylation responses.

4.3 Experimental Design

The following methods were adopted in order to help address my hypothesis that hypoxia will enhance SrcFK, MYPT-1 and MLC_{20} phosphorylation in a mitochondrial ETC-dependent manner.

Phosphorylation Responses

In order to determine whether hypoxia-induced SrcFK and Rho-kinase activity in IPA is dependent on mitochondrial ETC ROS production, I investigated the effects of rotenone (100nM) and myxothiazol (100nM) (complex I and III inhibitors, respectively) on peak hypoxia-induced SrcFK (1min), MYPT-1 (5min) and MLC_{20} (5min) phosphorylation responses in IPA.

To achieve measurable responses to hypoxia, pre-tone is required. Therefore, ~2nM U46 was pre incubated for 15 minutes (achieves 10% of KPSS contraction) before making the sample hypoxic. Samples were then gassed in 1% O_2 for 1 minute (SrcFK) or 5 minutes (MYPT-1 or MLC_{20}) and protein extracted as previously described (see methods chapter, section 2.6.5). These time points were chosen as a previous study from out group[7] determined that SrcFK autophosphorylation was increased following 1 minute hypoxia while MYPT-1 and MLC_{20} was increased following 5 minutes of hypoxia [7]. To investigate the inhibitor effect, pre-incubating with either myxothiazol (100nM), rotenone (100nM) or DMSO (5µL) was performed for 15

minutes prior to exposing the samples to U46 (~2nM) for 1 or 5 minutes of hypoxia. Bands were then analysed by measuring the ratio of phosphorylated SrcFK, MYPT-1 and MLC_{20} total SrcFK, MYPT-1 and MLC_{20}. The data was expressed as a % mean change from control +- SEM.

Functional Studies

In order to ensure that complex I and III blockers rotenone (100nM) and myxothiazol (100nM) were primary targeting signalling events downstream of the ETC and not through enhanced activation of NOX signalling and to ensure that DMSO vehicle was have no effect on contraction, the effect of DMSO and inhibitors rotenone (100nM) and myxothiazol (100nM) was investigated on U46619 (100nM) induced contraction. An initial control response was performed whereby U46619 (100nM) was initially added to IPAs and allowed to incubate for 10 minutes. IPA's were subsequently washed three times in PSS and allowed to rest until a steady baseline was achieved. DMSO or Inhibitors rotenone (100nM) or myxothiazol (100nM) were then added to the chamber and allowed to incubate for 15 minutes before conducting a second response with U46619. IPA were then washed at least 3 times in PSS following treatment and contractile force was allowed to return to baseline. Data was expressed as mean % change from control +- SEM.

4.4 Results Section

4.4.1 Hypoxia enhances SrcFK, MYPT-1 and MLC_{20} phosphorylation in a mitochondrial ETC-dependent manner

Previous work within our laboratory has shown that hypoxia activates SrcFKs and triggers protein tyrosine phosphorylation in IPA. Furthermore, hypoxia-mediated Rho-kinase activation, Ca^{2+} sensitization, and Ca^{2+} responses are dependent on SrcFKs, suggesting that SrcFKs play a central role in HPV [7]. I therefore wanted to determine whether hypoxia-induced SrcFK and Rho-Kinase activity in IPAs is dependent on mitochondrial ETC ROS production. I

investigated the effects of rotenone (complex I inhibitor) or myxothiazol (complex III inhibitor) on hypoxia-induced SrcFK (1min), MYPT-1 (5min) and MLC_{20} (5min) phosphorylation responses. A small degree of pre-tone is required in order to achieve a full hypoxic response[372] similar to what was witnessed during contractile studies using LY83583 (chapter 3). Following 15 minutes pre-incubation with 2nM U46619, phosphorylation responses of all three proteins were investigated under hypoxic conditions. Hypoxia enhanced phosphorylation responses of all three proteins, which was subsequently abolished by either rotenone or myxothiazol (SrcFK: Fig 4.1A, MYT1: Fig 4.2A and MLC_{20} Fig: 4.3A). U46619-induced and basal phosphorylation responses were not significantly affected by either inhibitor (SrcFK: Fig 4.1B, MYT1: Fig 4.2B and MLC_{20}: Fig 4.3B).

Figure 4.1

(A)

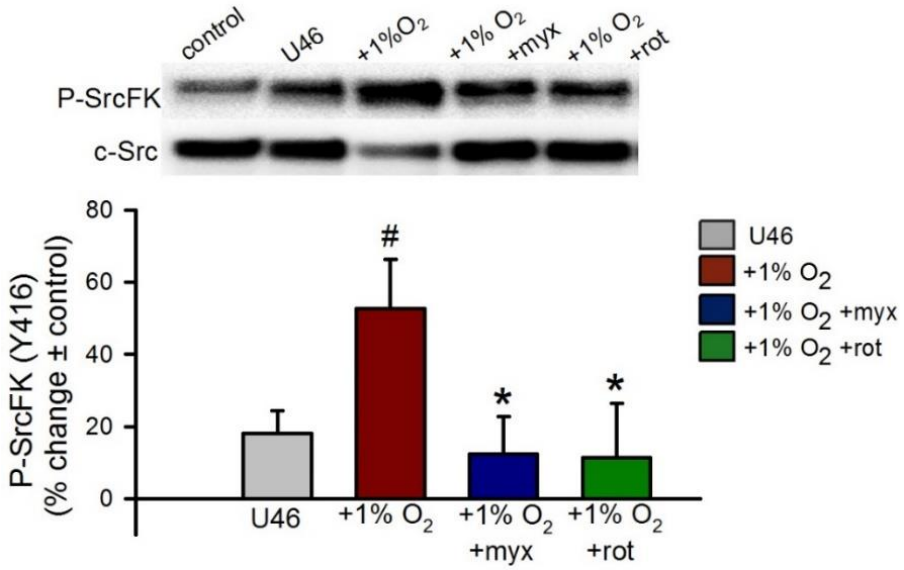

(B)

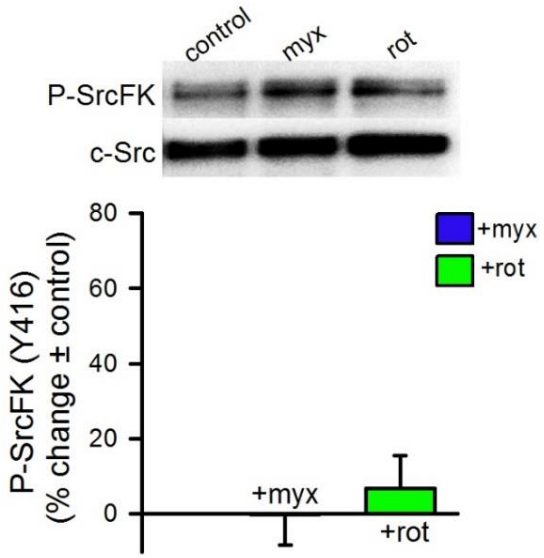

Figure 4.1: Effects of hypoxia and mitochondrial ETC inhibitors on SrcFK phosphorylation in IPA

A: Hypoxia (1% O_2, 1min) enhanced SrcFK auto-phosphorylation following U46619 (U46, 2nM, 15min) pre-tone, which was inhibited by myxothiazol (myx, 100nM) or rotenone (rot, 100nM). #P<0.05 vs. U46 alone, *P<0.05 vs. U46/1% O_2 (2-way ANOVA, Factors: Normoxia and hypoxia + inhibitors, Power of performed test: 0.540, n=9-10 arterial samples isolated from 7 rats). **B:** Myxothiazol or rotenone alone has no significant effect on basal SrcFK auto-phosphorylation (1-way ANOVA, Factor: Inhibitor alone, Power of performed test: 0.640 n=8-9 arterial samples from 5 rats).

Figure 4.2

(A)

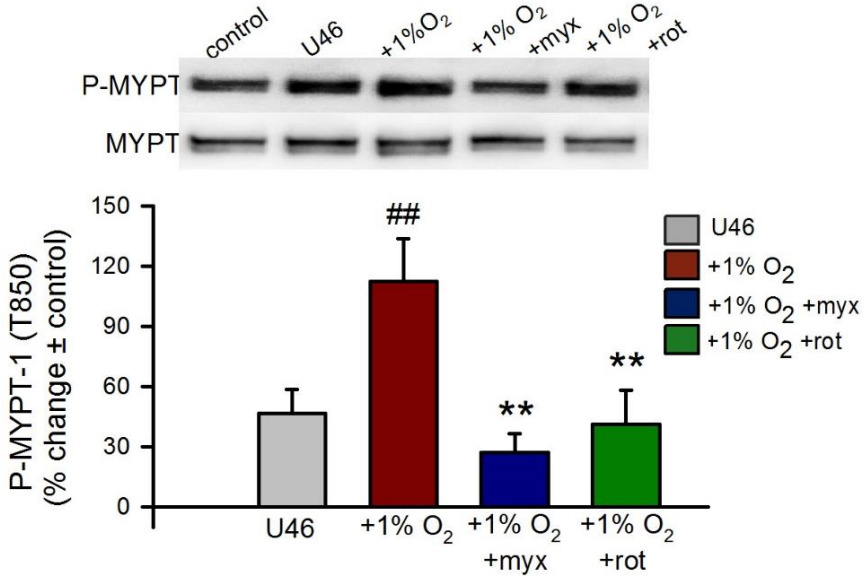

(B)

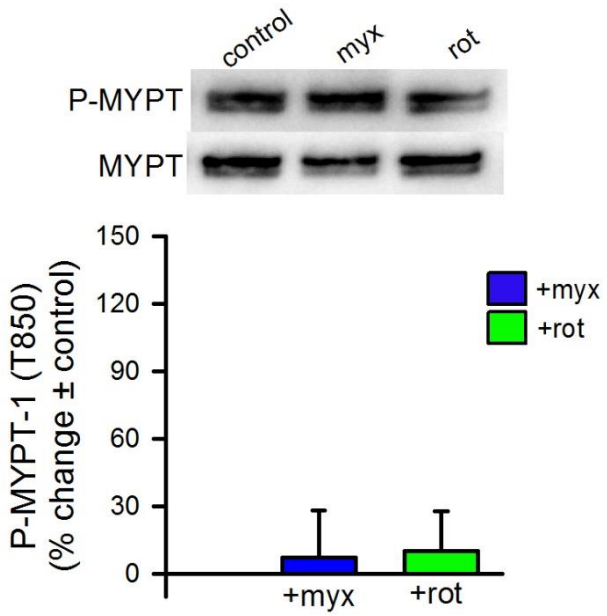

Figure 4.2: Effects of hypoxia and mitochondrial ETC inhibitors on MYPT1 phosphorylation in IPA

A: Hypoxia (1% O_2, 5min) enhances MYPT-1 phosphorylation following U46619 (U46, 2nM, 15min) pre-tone, and this enhancement is blocked by myxothiazol (myx, 100nM) or rotenone (rot, 100nM). ##P<0.01 vs. U46 alone, **P<0.01 vs. U46/1% O_2 (2-way ANOVA, Factors: Normoxia and hypoxia + inhibitors, Power of performed test: 0.756, n=9-10 arterial samples isolated from 7 rats). **B:** Myxothiazol or rotenone alone has no significant effect on basal MYPT-1 phosphorylation (1-way ANOVA, n=9-11, Factor: Inhibitor alone, Power of performed test: 0.930, n=8-9 arterial samples from 5 rats).

Figure 4.3

(A)

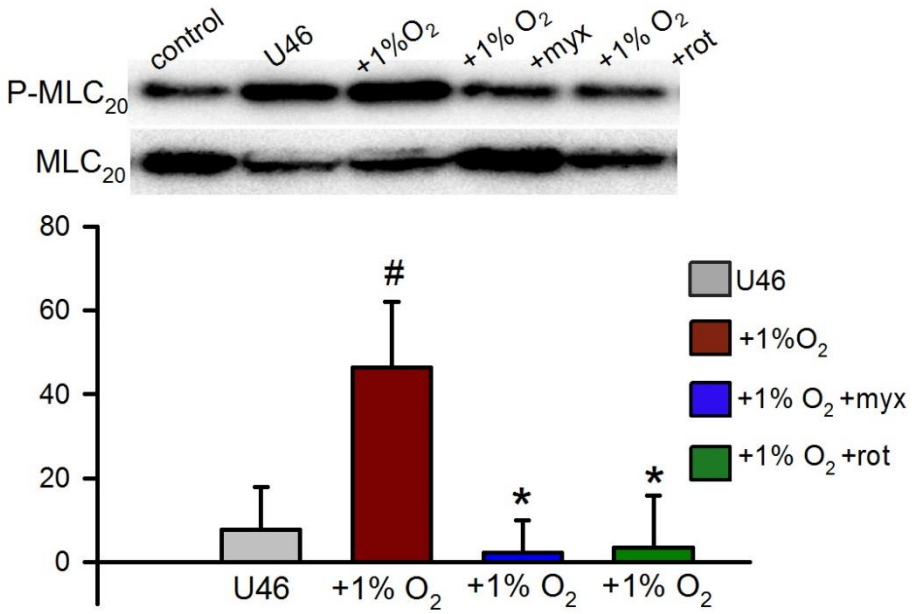

(B)

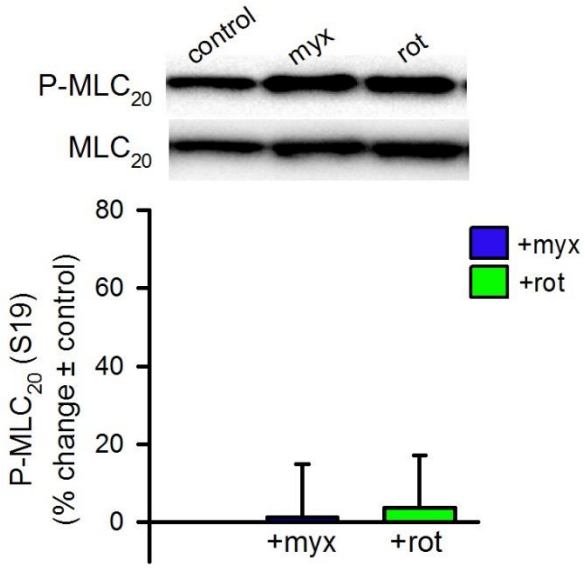

Figure 4.3: Effects of hypoxia and mitochondrial ETC inhibitors on MLC_{20} phosphorylation in IPA

A: Hypoxia (1% O_2, 5min) enhances MLC_{20} phosphorylation following U46619 (U46, 1nM, 15min) pre-tone, which was inhibited by myxothiazol (myx, 100nM) or rotenone (rot, 100nM) #P<0.05 vs. U46 alone, *P<0.05 vs. U46/1% O_2 (2-way ANOVA, Factors: Normoxia and hypoxia + inhibitors, Power of performed test: 0.595, n=9-10 arterial samples isolated from 7 rats n=9-10). **B:** Myxothiazol or rotenone alone has no significant effect on MLC_{20} basal phosphorylation (1-way ANOVA, Factor: Inhibitor alone, Power of performed test: 0.502, n=9-10 arterial samples from 5 rats).

4.4.2 U46619 induced contractile response is not mitochondrial ETC-dependent

ROS, as previously discussed, can be derived from a number of sources such as NOX and mitochondria (see introduction, section 1.3). Previous studies, have suggested that ROS induced via NOX promotes increased ROS production from the mitochondria which is subsequently involved in signalling, so called ROS induced ROS release and vive vesa [102,144,469].

ROS induced ROS release (RIRR) overview

As discussed, a number of investigations have indicated that ROS participate in regulating vascular function in both normal vessels or as part of an adaptive response during disease [470,471]. The concentration and localisation of oxidant-generating and quenching enzymes indicate a high compartmentalization within the cell. As ROS are ubiquitous and are known to be involved in signal transduction and cell injury, their accumulation must be controlled. RIRR is an example of this control.

Lee et al [472] demonstrated that complete serum withdrawal in human 293T cells increased mitochondrial ROS production. Mitochondria ROS then stimulated phosphoinositide 3-kinase followed by translocation of Rac1, allowing its interaction with NOX1. ROS generation in this model is such that initial ROS production from mitochondria is relatively transient, but the evoked activation of NOX1 is more prolonged [472]. This study therefore demonstrated *1*) How a transient ROS signal (from mitochondria) can be converted into a more sustained ROS release (from NADPH oxidase), and *2*) it also describes a pathway by which ROS generated at one subcellular site triggers ROS production in a different site through signal transduction.

Conversely, ROS generation from mitochondria can be triggered from ROS produced by NADPH oxidase. Hawkins et al [473] demonstrated in pulmonary microvascular endothelial cells that the activation of NADPH oxidase produces extracellular $O_2^{\bullet-}$. The $O_2^{\bullet-}$ produced can then be transported intracellularly through a chloride channel-3, where it triggers rapid

Ca^{2+} mobilization followed by mitochondrial $O_2^{\bullet-}$ production. These findings not only demonstrate a link between two enzymatic sources of ROS but also establish a role for $O_2^{\bullet-}$ as a signalling molecule involved in RIRR where extracellular ROS stimulate intracellular ROS production, resulting in endothelial dysfunction and cellular apoptosis.

Furthermore, Kimura et al [474] identified a novel signalling pathway where ANG-II stimulation of ANG-I receptors activates NADPH oxidase in the heart by a protein kinase C-mediated mechanism. The NOX derived ROS are essential for the activation of mitochondrial ATP-sensitive K^+(K_{ATP}) channels, which elicit preconditioning through an increase in mitochondrial ROS release[474] . The findings of this study reveal how ROS generated in one region of the cell (membrane) coordinates ROS production in a separate compartment (mitochondria) to effect a physiological response. This mechanism was more recently demonstrated by Dikalov *et al* [102,142] in endothelial cells, whereby, angiotensin II activates NOX2 via PKCε which phosphorylates and activates the mitochondrial ATP-sensitive potassium channels leading to an increase in ROS production from the mitochondria which subsequently activates SrcFK. This increased SrcFK activity further activates NOX leading to a potential feed forward mechanism (Fig 4.4).

Stimuli that elevate ROS production may therefore cause tandem activation of PKC and SrcFK. It has been suggested that a reciprocal relationship between Src and PKC appears to exist at least in the context of ROS signalling[92]. Activation of Src may be enhanced by PKC-mediated phosphorylation of Src in the SH2 domain[203,475] whereas H_2O_2 promotes colocalization of several PKC isozymes with Src, followed by src-dependent phosphorylation and activation of PKC [476-479] (Fig 4.4).

Figure 4.4:

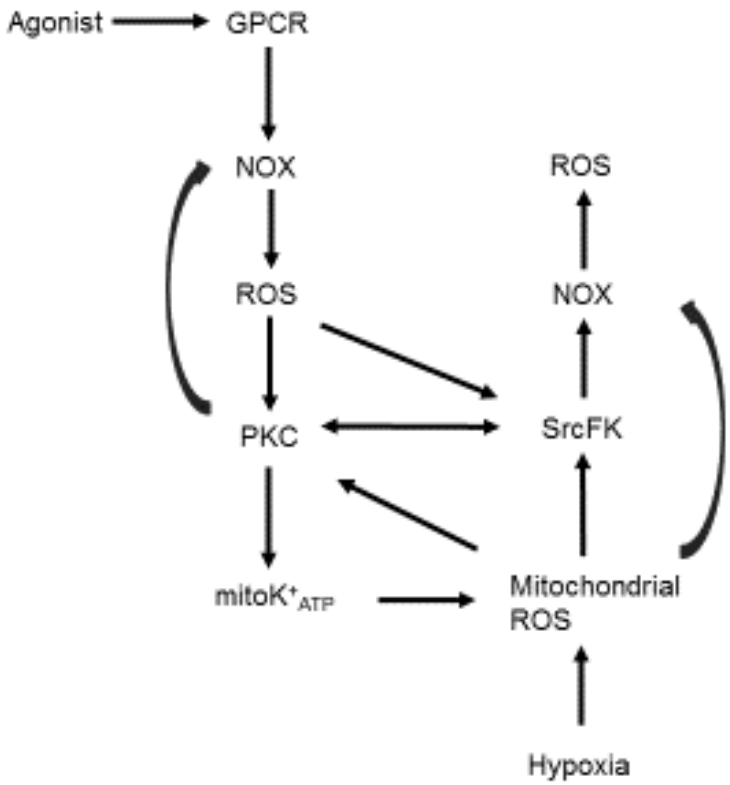

Figure 4.4: Schematic showing the potential signalling mechanisms involved during ROS induced ROS release.
Agonists acting via GPCRs can induce ROS production via NADPH Oxidase (NOX). The increase in ROS production can subsequently Activate PKC and SrcFK which either (1) Phosphorylate each other leading to tandem activation or (II) phosphorylate NOX leading to a further increase in ROS. PKC can enhance ROS production from the mitochondria via phosphorylation of mitoK$^{+}_{ATP}$ Channels. This increase in ROS may also (I) Further activate SrcFK and PKC which may lead to increased phosphorylation of NOX or (II) Activate NOX directly. This suggests a number of positive feedback loops which may be generated following NOX or mitochondrial activation leading to increased ROS production.

Due to the potential influence of RIRR in this system, I wanted to determine whether using rotenone (complex I inhibitor) and myxothiazol (complex III inhibitor) which primarily targets the mitochondria, affects signalling via mitochondria inhibition and not through enhanced activation of NOX signalling.

In order to investigate this question, I assessed the effects of rotenone (complex I inhibitor) or myxothiazol (complex III inhibitor) on U46619 induced contraction. An initial control response was performed whereby U46619 (100nM) was incubated with IPA for 15 minutes followed by 3 washes in PSS to achieve a stable baseline. Subsequently, IPA's were pre-incubation with DMSO (Figure 4.5), rotenone (100nM) (Figure 4.6) or myxothiazol (100nM) (Figure 4.7) for 10 minutes followed by a secondary dose of U46619 (100nM). Representative traces show that treatment pre-incubation with DMSO and rotenone had no effect on contraction whereas myxothiazol reduced the contractile response, but not significantly.

Figure 4.5

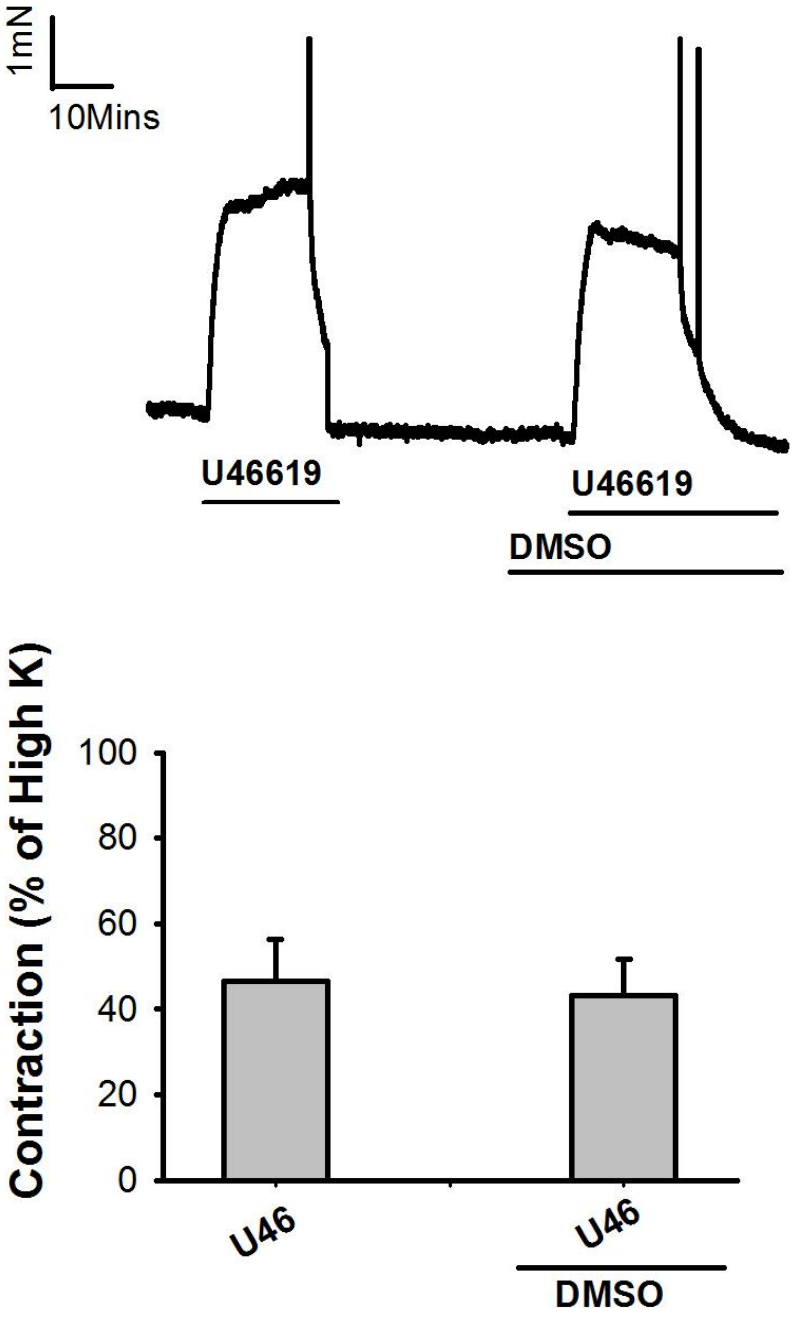

Figure 4.5: Effects of DMSO on U46619 induced contractile responses in IPAs
U46619 (U46, 100nM, 15min) was initially incubated with IPAs. This response was then repeated in the presence of DMSO. Upper panel: representative traces. Bottom panel: mean ± SEM measurements of peak U46619 induced contraction response (NS, n=6, paired T-test).

Figure 4.6

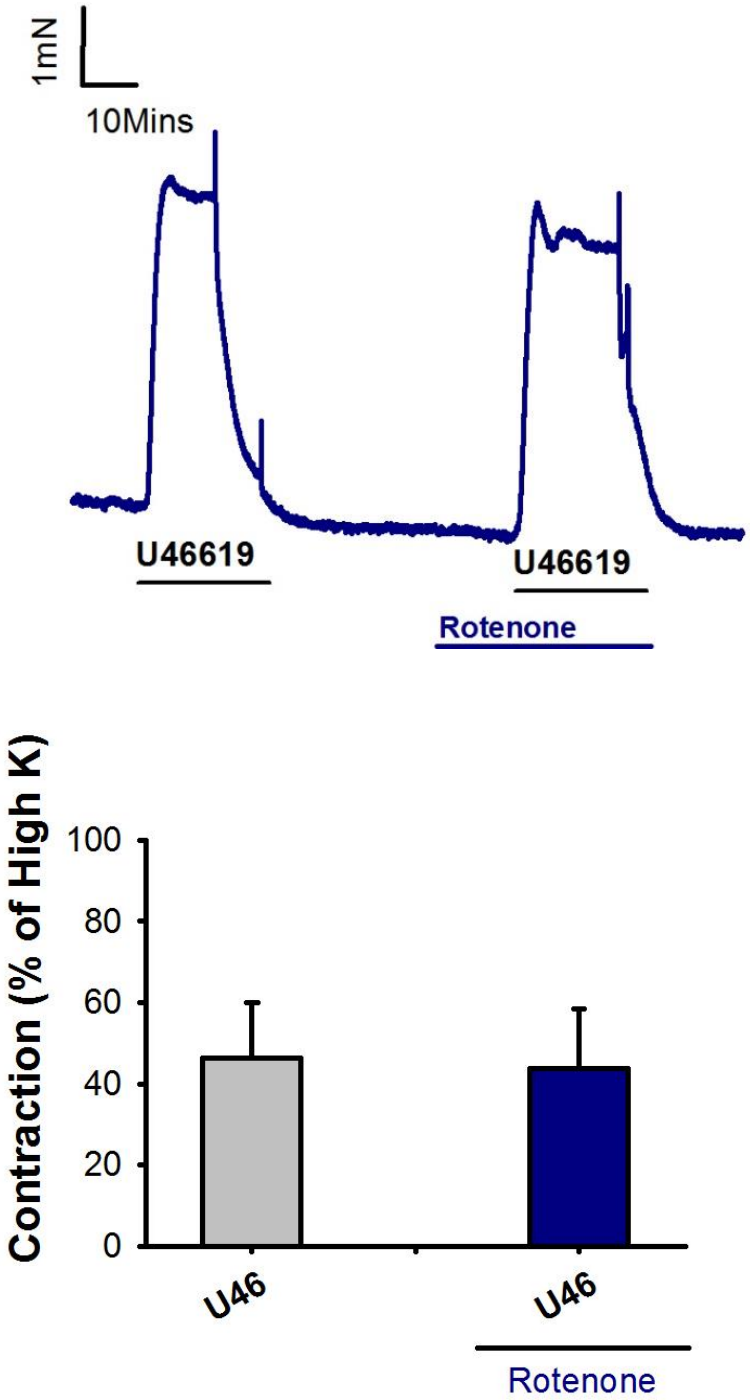

Figure 4.6: Effects of rotenone on U46619 induced contractile responses in IPA
U46619 (U46, 100nM, 15min) was initially incubated with IPAs. This response was then repeated in the presence of rotenone. Upper panel: representative traces. Bottom panel: mean ± SEM measurements of peak U46619 induced contraction response (n=6, paired T-test).

Figure 4.7

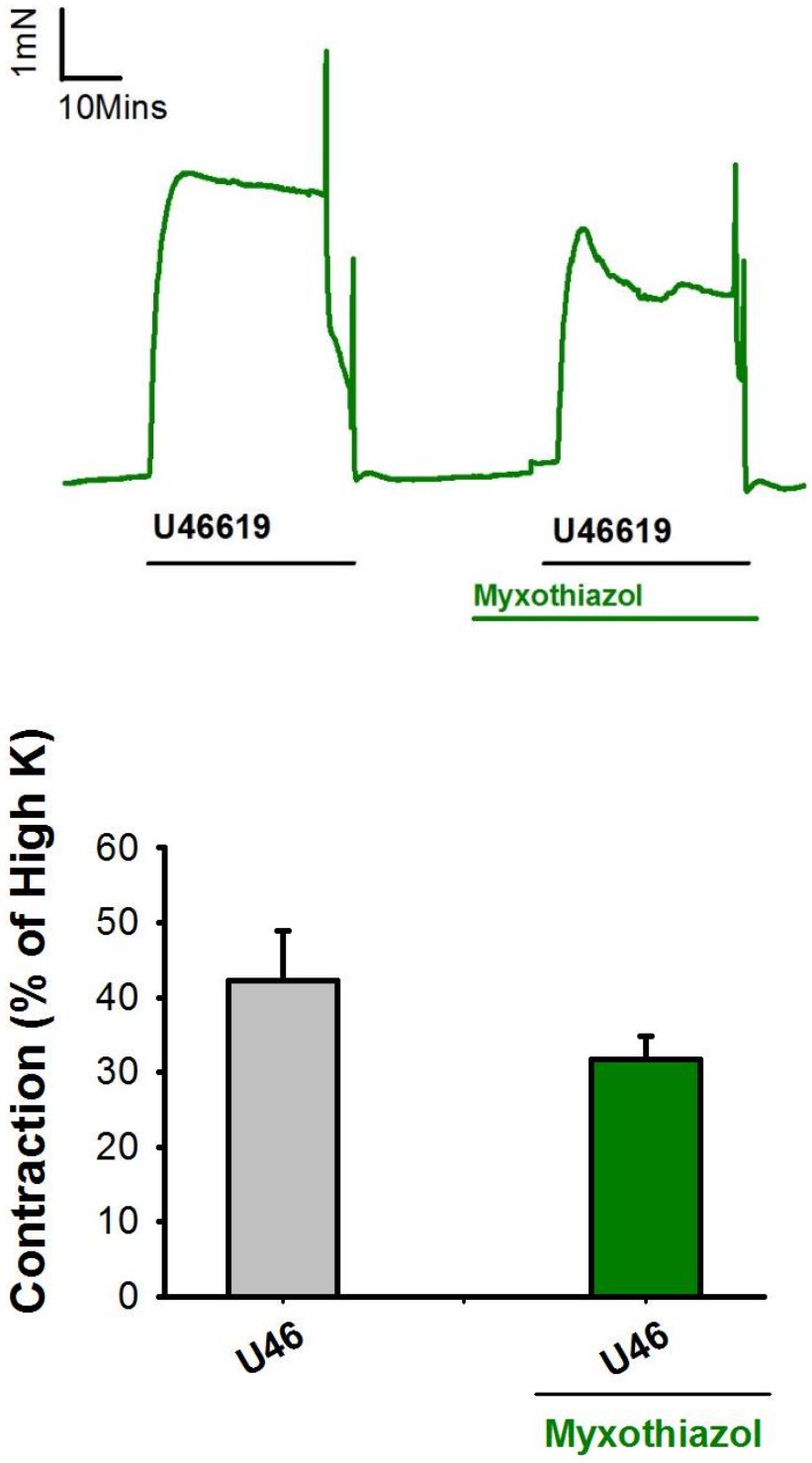

Figure 4.7: Effects of myxothiazol on U46619 induced contractile responses in IPA
U46619 (U46, 100nM, 15min) was initially incubated with IPAs. This response was then repeated in the presence of myxothiazol. Upper panel: representative traces. Bottom panel: mean ± SEM measurements of peak U46619 induced contraction response (n=8, paired T-test).

4.5 Summary of findings

The purpose of this chapter was to investigate the stated hypothesis of:

"SrcFK will act as a link between hypoxic induced ROS production and Rho-Kinase activation".

The findings of this chapter are:

- Hypoxia enhances SrcFK, MYPT-1 and MLC_{20} phosphorylation in a mitochondrial ETC-dependent manner.
- Rotenone and myxothiazol act primarily by target the mitochondrial ETC.

4.6 Discussion

This study provides complimentary evidence for a role of SrcFKs as a ROS sensitive intermediate in HPV and supportive evidence that SrcFKs act as upstream regulators of the Rho-Kinase pathway. Previous work performed within the laboratory[7] was used to help determine peak hypoxic phosphorylation responses.

Activation of the Src-Family Kinases is thought to occur through redox modification leading to autophosphorylation. Direct redox modification has been demonstrated whereby ROS generated from lipoxygenase, modulates SrcFK activity directly through oxidative modulation of cysteine residues; cys-245 in the SH2 domain and cys-487 in the kinase domain[92] at focal adhesions, contributing to cell movement and attachment to the extracellular matrix [213]. ROS may also promote the activation of Src through oxidative modulation of the proteins involved in normal Src regulation. These 'indirect redox regulation mechanisms' involve the oxidation and inhibition of both PTPs and C-terminal Src kinases (Csks) – an important kinase group involved with the phosphorylation, and inactivation, of Src at tyr-527[92]. Alternatively, SrcFK may also be activated without prior de-phosphorylation of tyr-527 through oxidation of as yet unidentified cysteine residues by either H_2O_2 or NO [211].

SrcFK and Rho-kinase have previously been shown to be activated by hypoxia in PA and act as major contributors to HPV [7]. Our findings demonstrate that hypoxia (in the presence of U46), activates SrcFK at 1 minute in IPA which compliments previous work by Knock *et al* [7] who also demonstrates that SrcFKs are activated in IPA in response to hypoxia. Furthermore, Seko *et al* [480] also show that hypoxia induced Fyn activation, a SrcFK member. Hypoxia (in the presence of U46) is also shown to enhance MYPT-1 and MLC_{20} phosphorylation at 5 minutes. This time point was chosen as it is primarily associated with Ca^{2+} sensitization pathway [370,465] (sustained phase).

U46619 is a prostanoid and promotes contraction via Rho-Kinase mediated phosphorylation [42]. It has been shown by Knock *et al* [41] that SrcFK are involved in $PGF_{2\alpha}$ mediated Ca^{2+} sensitization. Here, MYPT-1 phosphorylation was inhibited by the SrcFK inhibitor SU6656 and hypoxia induced translocation was inhibited by siRNA knockdown of Src and Fyn, providing strong evidence for SrcFK acting upstream of Rho-Kinase.

I cannot confirm the synergistic effect of U46619 and hypoxia on phosphorylation since I never looked at hypoxia alone on phosphorylation responses. However, since $PGF_{2\alpha}$ and hypoxia have been shown to have a synergistic effect [7] it is reasonable to assume that U46619 as a prostanoid (similar to $PGF_{2\alpha}$) and hypoxia will have a similar effect. Similarly, I did not look at calcium responses, therefore I cannot confirm any increases in intracellular calcium. Again, $PGF_{2\alpha}$ and hypoxia have been shown to increase intracellular calcium [7], there is no reason to think that U46619 and hypoxia will not accomplish the same. Since hypoxia (as discussed) has previously been shown to activate SrcFK and that U46619 (chapter 3) activates SrcFKs, which enhances MYPT-1 and MLC_{20} phosphorylation, the actions of hypoxia on phosphorylation or blockers of mitochondria are independent of pre-constriction events.

Hypoxia promotes increased leakage of electrons primarily from complex III of the electron transport chain (ETC), producing ROS, which enters the cytosol to cause contraction. This is supported by work performed by Leach *et al* [93] who concluded that complex III of the mitochondrial ETC acts as the hypoxic sensor in HPV. Furthermore, recent work performed by Waypa and colleagues demonstrated that in PASMC and lungs from adult mice with smooth muscle specific deletion of the Rieske iron-sulfur protein (RISP), which is required for superoxide generation at Complex III, attenuates hypoxia induced ROS signalling [94]. Here, I compliment these previous findings by showing that hypoxia-induced SrcFK auto-phosphorylation and hypoxia-induced MYPT-1 and MLC_{20} phosphorylation are inhibited by mitochondrial inhibitors rotenone and myxothiazol.

Pharmacological inhibitors such as rotenone and myxothiazol can block electron transfer at a specific site which can impact ROS generation (figure 4.8). As most of the ROS generated at the mitochondria comes from complex III, inhibition of complex III by myxothiazol will inhibit hypoxic signalling. Rotenone acts as a downstream inhibitor of complex 1, suppressing electron transfer to complex III subsequently inhibiting hypoxic signalling[481]. ROS can still be produced from complex 1[481,482], II [138] however unlike complex III where the ROS enters the intermembrane space and is rapidly ejected from the mitochondria[483], ROS produced in complex I and II is released primarily into the matrix compartments where it is rapidly broken down (figure 4.8).

Figure 4.7:

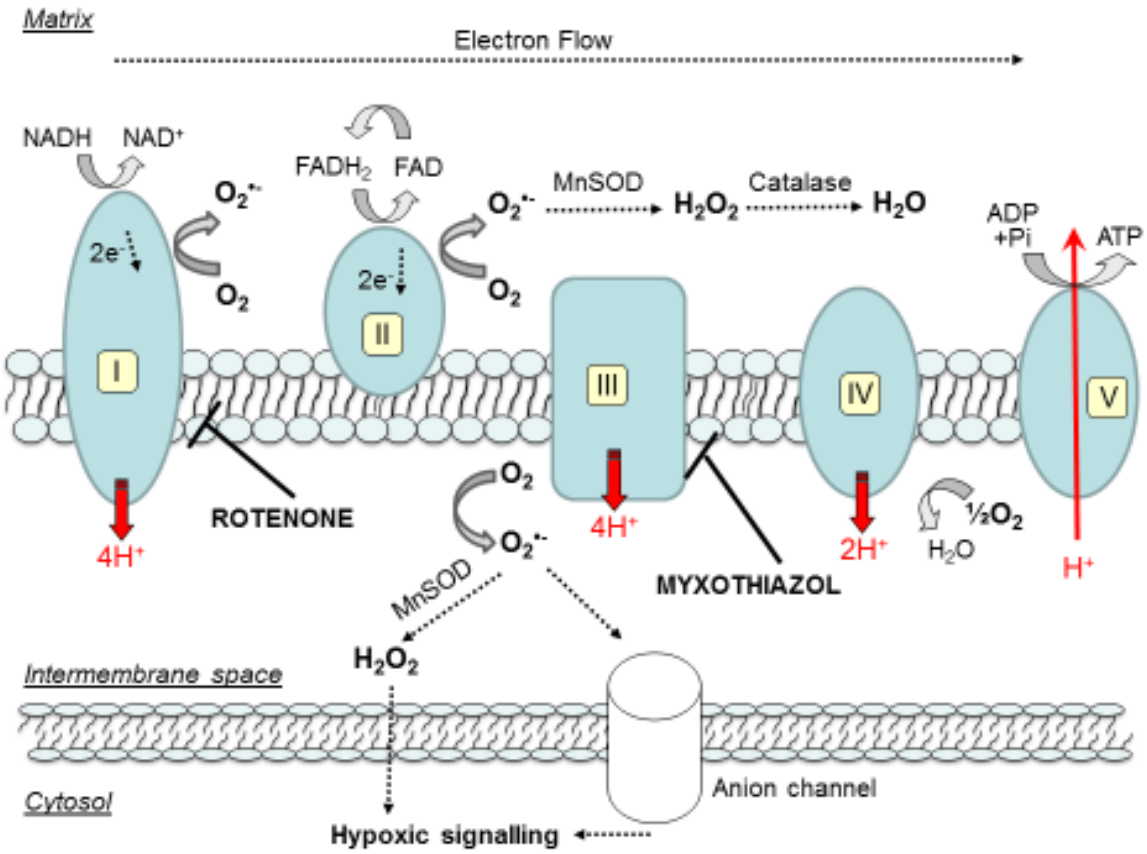

Figure 4.8: Inhibition of mitochondrial ETC complexes by rotenone and myxothiazol
Rotenone and myxothiazol work by interfering with the electron transport chain in the mitochondria. Rotenone acts by blocking electrons being transfered from complex I while myxothiazol also acts by blocking electron transfer from complex III. This creates a backup of electrons within the mitochondria. This will also lead to a decrease in ATP generation at ATP production is driven by the proton gradient which is itself set up by the transfer of electrons.

Furthermore, SrcFKs act as ROS sensitive intermediates that contribute to Rho-Kinase activation during hypoxic challenge. Rotenone and myxothiazol do not significantly inhibit the underlying basal phosphorylation of these proteins indicating that these inhibitors only influence protein activity during states of hypoxia.

I next investigated whether rotenone and myxothiazol act by primarily targeting the mitochondrial ETC and not through enhanced activation of NOX signalling. Since NOX and

mitochondria may interact via a phenomenon known as ROS induced ROS release (RIRR) (as discussed earlier in this section) [484], whereby ROS produced through activation of NOX (via GPCR activation) enhances ROS production from the mitochondria. Conversely, ROS produced from the mitochondria can initiate ROS production from NOX [472] thereby promoting a feed-forward amplification of ROS [144,473,474,485] and subsequently activating signalling events.

This mechanism was demonstrated by Dikalov *et al* [102,142] in endothelial cells, whereby, angiotensin II activates NOX2 thereby enhancing ROS production which subsequently activate PKCε. PKCε phosphorylates and activates the mitochondrial ATP-sensitive potassium channels (mitoK_{ATP}) which increased the production of mitochondrial ROS [143,144]. The enhanced ROS production from the mitochondria activates SrcFK. This increased SrcFK activity further activates NOX and leads to a potential feed forward mechanism involving Src, PKC, NOX and mitochondria leading to increased ROS production.

Here, I demonstrate that myxothiazol marginally but not significantly inhibited U46619-induced contraction whereas rotenone had no effect, indicating that myxothiazol and rotenone primary target signalling events downstream of the ETC, and that U46619-induced contraction occurs independently of this. Although myxothiazol does not significantly reduce U46 induced contraction, it still has a marginal effect. This could be due to a reduction in ATP by oxidative phosphorylation, which is required for cross bridge cycling. Roteneone does not have the same effect as electrons can still flow from complex 2.

There is still controversy that exists between whether hypoxia does indeed increase ROS generation, known as the ROS hypothesis, and whether hypoxia decreases ROS production, known as the Redox hypothesis.

Numerous studies exists which demonstrate that HPV involves an increase in ROS production from the mitochondria, either directly or indirectly [94,301,413]. Several reports indicate that

hypoxia increases mitochondrial ROS production in both freshly isolated and cultured rat PASMCs [176,486]. Further evidence for hypoxia-induced increases in ROS generation in the pulmonary circulation came from studies by Waypa *et al* who demonstrated that HPV required electron flux through complex III and that an increase in ROS were responsible for inducing a hypoxic contractile response [94,140,412]. Using the thiol redox sensor, roGFP (which does not have the serious limitations of commonly-used probes), targeted to the cytosol, intermembrane space (IMS) or the mitochondrial matrix, Waypa *et al* were able to compare basal and hypoxic changes PASMC[412]. The roGFP sensor is a mutant of GFP which contains outer surface cysteine residues [487]. Oxidation of these residues alters the fluorescent properties allowing for it to act as a thiol redox sensor furthermore as this is reversible, this can be used as an absolute measure of percentage oxidation [488]. Waypa *et al* demonstrated in PASMCs a 20% increase in cytosol and IMS oxidation while a decrease in matrix oxidation during hypoxia and similar changes in isolated systemic arterial smooth muscle cells [412]. Suggesting, that hypoxia elicits an oxidative signalling response. More recently, Waypa *et al* extended these finding by PASMC and lungs from adult mice with smooth muscle specific deletion of the RISP gene [94]. They observed a loss of hypoxia-induced changes in thiol redox state implicating mitochondrial complex III and ROS signalling in the oxygen sensing response underlying the acute HPV response.

Indirect evidence for the increased ROS hypothesis is also provided by observations that low concentrations of peroxide induce a sustained constriction of PA [194], and elevation of PASMC $[Ca^{2+}]_i$ via release from ryanodine sensitive stores[176,194,486]. Furthermore, ROS scavengers in cultured PAMSCs during hypoxia abolish the $[Ca^{2+}]_i$ increase induced by hypoxia in the cytosol, indicating that ROS signals are required for signal transduction linking hypoxia to contractile responses in these cells [140,413,489]. Finally, antioxidants or overexpression of

antioxidant mechanisms suppress HPV in perfused lungs [490] and hypoxia-induced elevation of $[Ca^{2+}]_i$ in PASMC [486].

Many proteins including SrcFK [7,204], PKC[194], mitogen-activated protein kinase (MAPKs) [192], FAK, PYK2 and JAK [299,325,348] are indeed activated by hypoxia or have at least been shown to be involved in ROS mediated vasoconstriction.

PKC is a family of cytosolic serine/threonine kinases family known to be activated by H_2O_2 or peroxynitrite in pulmonary artery smooth muscle and endothelium [491]. H_2O_2 has also been shown to trigger subcellular translocation of various PKC isozymes in PASMCs [492]. Both PKC and ROS have been implicated in HPV[493].

Acute HPV in rat IPA has been found to be biphasic [465]. In this study, the first phase is associated with a sharp transient rise in Ca^{2+} through intracellular stores from the SR (and some influx through membrane channels), with a PKC-dependent component and the subsequent prolonged phase which involves a smaller and more regulated increases in Ca^{2+}, and enhanced contraction through Ca^{2+} sensitisation [370]. PKC-mediated activation of SrcFK may also be involved in this process. Stimuli that elevate ROS production may cause a tandem activation of PKC and SrcFK. ROS signalling may also involve a reciprocal relationship between Src and PKC. Activation of Src may be enhanced by PKC mediated phosphorylation of Src in the SH2 domain, whereas H_2O_2 promotes colocalization of several PKC isozymes with Src, followed by Src-dependent phosphorylation and activation of PKC. In addition, both SrcFK and PKC may act upstream of the MAPKs [203,475-478].

However, a study by Robertson *et al* [465] investigating the effect of hypoxia on intracellular Ca^{2+} ($[Ca^{2+}]_i$) and tension in small rat intrapulmonary arteries (IPA), demonstrated that the first phase of the hypoxic constriction is associated with a transient rise in $[Ca^{2+}]_i$ via either Ca^{2+} influx and/or release, and may be associated with PKC-dependent component. Whereas, the

second phase involves a PKC-independent sensitization of the contractile machinery to Ca^{2+}. This suggests that PKC could be involved initially in the activation of hypoxic signalling events but is of less importance during more sustained hypoxic events [494].

MAPKs are key kinases involved in a number of signalling pathways triggered by G-protein-coupled receptors and receptor tyrosine kinases. MAPKs have been implicated in control of vascular function in response to cellular stresses such as hypoxia, oxidative stress, inflammation, vasoconstrictor hormones, integrins, and cytokines[177,495]. MAPKs are not directly redox-sensitive but instead rely on ROS-mediated activation of upstream pathways such as SrcFK and PKC. Phosphorylation of MAPKs is enhanced by peroxide and occurs through trans-activation of growth-factor receptors or SrcFK in tandem with PKC[496]. Reports vary over the importance of MAPKs to ROS-mediated smooth muscle constriction, however Ang II-mediated NADPH-dependent ROS production is required for p38 MAPK and MAPK activation [497].

A recent study by Morrell *et al* [498] investigating whether p38 MAP kinase mediates acute hypoxic pulmonary vasoconstriction in isolated rat pulmonary artery demonstrate that: (1) p38 MAP kinase inhibitor SB-203580 attenuates the delayed hypoxic contraction, (2) p38 MAP kinase inhibition does not have a significant effect on rat pulmonary artery under normoxic conditions, (3) p38 MAP kinase activation significantly affected vasodilation. The authors conclude that p38 MAPK is an important mediator of sustained hypoxia-induced vasoconstriction of the pulmonary artery and also plays a major role in phase I vasodilation. Furthermore, the authors suggest a signalling axis whereby hypoxia activates Rho-Kinase which phosphorylates p38 MAP kinase which subsequently phosphorylates heat shock protein 27 (HSP27) to promote actin filament stabilization which ultimately contributes to vasoconstriction.

Finally, FAK, PYK2 and JAK2 have been shown to phosphorylate and activate RhoGEFs[299,325,348]. These kinases are not known to be directly ROS sensitive, however they are activated by GPCR in a NOX dependent manner and by exogenous ROS[349-351]. This appear to occur through SrcFK mediated phosphorylation which will be explored further in chapter 5 [352,353].

The Redox hypothesis developed by Weir, Archer and colleagues describes hypoxia decreasing ROS generation in PASMCs [499,500]. This attenuation in ROS production would alter the redox state within the cell and chemically reduce K_v channels thereby closing these channels, resulting in membrane depolarisation and entry of extracellular Ca^{2+} leading to contraction[501]. This concept was supported by studies where they measured reciprocal changes in PA pressure and ROS levels during hypoxia and normoxia in perfused lungs using lucigenin or luminol chemiluminescence to detect ROS [502]. Furthermore, Reeve *et al*[503], reported that rotenone decreased chemiluminescence and increased vascular tone in isolated perfused lungs.

A recent study by Nagaraj *et al* [70] determined that the two-pore-acid-sensitive K^+ channel TASK-1, is phosphorylated and activated by SrcFKs at resting membrane potential. However during hypoxia, SrcFKs are inhibited thereby inhibiting TASK channel activity, promoting depolarisation and enhancing contraction. This is at odds with a report by Knock and co-workers who report that hypoxia increased SrcFK activity[504]. A potential explanation for this discrepancy relies on the importance of tyrosine kinases in the pathophysiology of Pulmonary Arterial Hypertension (PAH). It has recently been shown that treatment with dasatinib, a dual Bcr/abl and SrcFK inhibitor, for chronic myeloid leukaemia causes PAH which is resolved following discontinuation of dasatinib treatment [505-507]. Suggesting, that it may not due to marked cellular proliferation, but to chronic vasoconstriction. Furthermore, imatinib which is the first-line therapy for CML [508] and an effective inhibitor of the platelet-derived growth factor receptor, may improve haemodynamics in some PAH patients [509]. Nagaraj *et al* [70] suggest that

dasatinib initiated pulmonary hypertension may relate to their findings that SrcFK inhibition reduces potassium channel current and causes depolarisation of hPASMCs in response to hypoxia. However this is only consistent with the knowledge that SrcFKs are ROS sensitive if hypoxia inhibits ROS production therefore contradicting the work by Waypa *et al* 2007. In order to resolve the discrepancy, the relationship between ROS and K^+ in pulmonary VSM and the importance of K^+ channels in vascular tone would be required.

The discrepancy between the ROS hypothesis and the Redox hypothesis arises most likely due to the methods used to assess ROS generation. The studies by Archer and co-workers relied heavily on lucigenin- a chemiluminescent probe which interacts with superoxide [510] to detect primarily extracellular ROS. In contrast, intracellular generation of ROS during hypoxia, and chemical or genetic sensors of intracellular ROS detect small but significant reversible changes. It is therefore reasonable to conclude that at least some of the controversy regarding whether ROS is increased or decreased during hypoxia is due to probes or measurement systems used. Furthermore, a number of studies have shown that ROS generation within cells is regulated differently amongst subcellular compartments, therefore measurements in one compartment can be markedly different from another. Finally, on balance, recent reports strongly favour the ROS hypothesis.

My results show that although hypoxia does activate SrcFK upstream of Rho-Kinase, this has no effect on U46619 induced contractions. This also coincides with contractile and phosphorylation data (chapter 3) which clearly demonstrate that U46619 promotes contraction in a ROS and SrcFK dependent manner. My results also agree that hypoxia increases ROS production to activate hypoxic mediated cell signalling. The mechanism by which hypoxia enhances SrcFK activation and subsequent activation of Rho-Kinase are still not fully understood. However Rho-Kinase-mediated Ca^{2+} sensitisation of PA contraction is critical for sustained HPV and contributes to increased resistance in chronic hypoxic PH [511]. The

mechanism by which hypoxia activates Rho-Kinase was until recently unknown. Knock *et al*. have now shown in rat distal PA that Src-family kinases are involved in the activation of Rho-Kinase by both agonists[41] and hypoxia[7] and indeed also by superoxide (but not peroxide)[88],consistent with the ROS hypothesis of HPV. The link between ROS, SrcFK and RhoA/Rho-Kinase is still unknown but will be discussed further in chapter 5.

In Summary, my results in this chapter demonstrate that ROS production in response to hypoxia activate SrcFK upstream of Rho-kinase and acts as a key ROS sensitive intermediary. I also confirm that U46619 induced contractile responses are not dependent on mitochondrial ROS production (as illustrated in Fig 4.9).

Figure 4.9

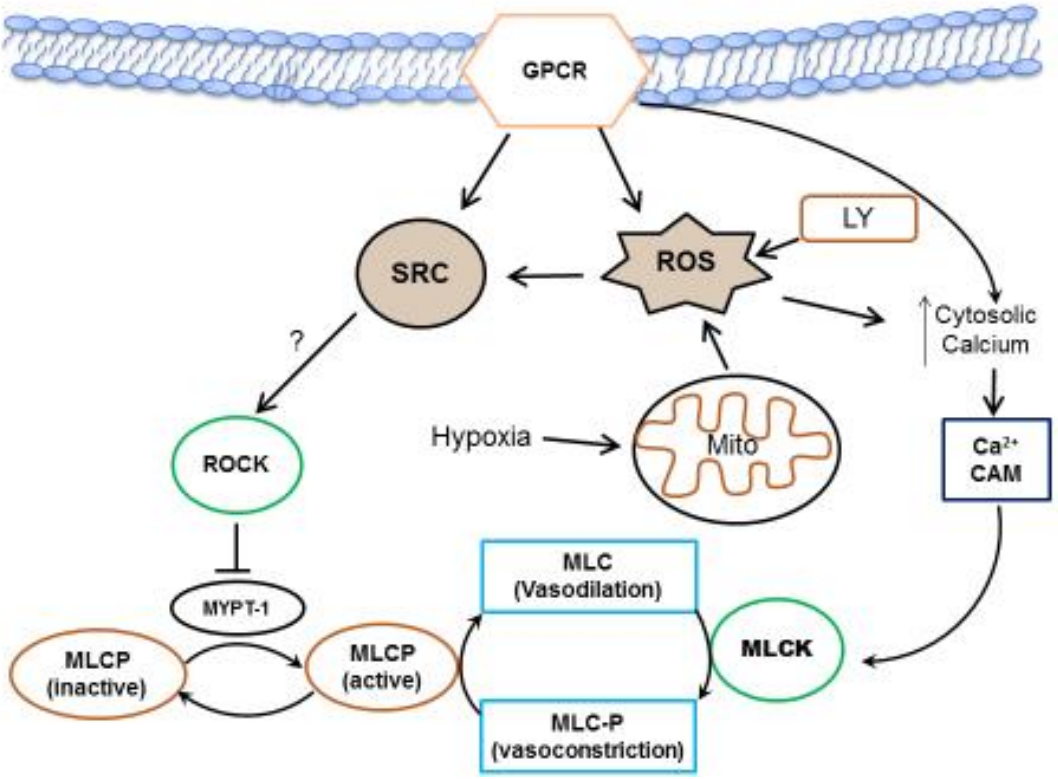

Figure 4.9: Shows the upstream regulation of the Rho-kinase pathway by ROS and SrcFK
The data demonstrate that SrcFK are ROS sensitive intermediate in response to hypoxia. The mechanism by which RhoA/Rho-Kinase is activated will be discussed in chapter 5.

Chapter 5:

Interaction between ROS, SrcFK, AHRGEF1 and RhoA

5.1 Background

Ca^{2+} sensitization occurs in response to constrictor stimuli, whereby there is increased contractile force without an increase in $[Ca^{2+}]_i$ [29]. This process is mediated primarily through the activation of the small monomeric G protein RhoA and its principle effector, the serine-threonine kinase Rho-Kinase [29,504]. Rho-Kinase enhanced constriction occurs primarily through phosphorylating the myosin phosphatase binding subunit (MYPT-1), thereby inhibiting myosin light chain phosphatase, subsequently enhancing myosin light chain phosphorylation [29,41,42].

Rho-kinase is activated by the monomeric G-protein RhoA, which tends to 'translocate' from the cytosol to the plasma membrane [512,513]. RhoA is a molecular switch that cycles between an inactive, GDP-bound form and an active, GTP-bound form[306,514]. The active, GTP-bound form triggers activation of its effector Rho-kinase.

Key proteins involved in RhoA/Rho-Kinase activation are unknown however logical targets are guanine nucleotide exchange factors (RhoGEFs). These are a highly diverse group of proteins, some of which include ARHGEF11 (PDZ-RhoGEF), ARHGEF12 (LARG) and ARHGEF1 (p115-RhoGEF) which are known to be tyrosine phosphorylated [324,325,345]. However, phosphorylation of GEFs is not an absolute requirement for the activation of RhoA, as GEFs can be activated through direct interactions with $G_{\alpha 12/13}$. The exception is the VAV family which does require phosphorylation to be activated. ARHGEFs, translocate in response to GPCR stimulation[308], subsequently exchanging GDP for GTP on RhoA, thereby activating RhoA.

I chose to examine ARHGEF1 because it has previously been implicated in AngII-induced hypertension, and shown to be tyrosine phosphorylated by JAK2 in mesenteric artery, an essential step in its activation by AngII[325].

We and others have also shown that constriction induced by agonists or hypoxia in PA and other vascular preparations involves activation of Rho-Kinase [41,235] and RhoA[46,117,504]. A number of studies have also suggested that SrcFK contribute to constriction via activation of RhoA/Rho-Kinase [7,41,82,515].

Previous studies have already shown that superoxide activates Rho-Kinase and causes Rho-Kinase dependent constriction in PA [88,89], SrcFK may also activate the RhoA/Rho-Kinase pathway in response to ROS via interaction with a RhoGEF such as ARHGEF1.

5.2 Hypotheses

Having established that Rho-kinase was a mediator of *endogenous* ROS-dependent and SrcFK-dependent U46619-induced phosphorylation responses, I further explored what SrcFKs are acting upon in order to activate Rho-Kinase.

I therefore hypothesised, that ROS and SrcFK may mediate eGFP- tagged RhoA and eGFP-tagged ARHGEF1 translocation. If SrcFK and ROS do mediate eGFP- tagged RhoA and eGFP-tagged ARHGEF1 translocation, inhibition of either SrcFK or ROS should inhibit translocation of these protein.

To further clarify the relationship between SrcFK and ARHGEF1, I also examined their co-localisation in IPA by immunoprecipitation, to test the hypothesis that prior treatment with U46619 will enhance co-immunoprecipitation between c-Src and ARHGEF1.

5.3 Experimental Design

The following methods were adopted in order to help address my hypotheses that "ROS and SrcFK may be mediating RhoA and ARHGEF1 translocation in PASMCs. Furthermore, U46619 will enhance co-immunoprecipitation between c-Src and ARHGEF1 in IPA".

Translocation studies

PASMCs generated from Pulmonary arteries (as described in the methods chapter) were transfected with either eGFP-tagged RhoA or eGFP-tagged ARHGEF1 and grown until confluent. Cells were subsequently serum starved for 24 hours in serum free media. Following 24 hour serum starvation, coverslips were mounted onto a zeiss axiovert 200 inverted fluorescent microscope and cells were imaged at x40 magnification. Cells were imaged by taking 5 frames every 5 seconds as a control run, U46619 (100nM) / LY83583 (1µM) was then added to the chamber and images were taken every 2 seconds for 2 minutes. The frequency and time of images taken was increased due to the quick initiation and quick nature of translocation. Cells were subsequently washed in PSS and allowed to rest for 10 minutes with an image being taken every 2 minutes. This process was then repeated in control cells otherwise cells were pre-treated for 10 minutes with inhibitor (ebselen 1µM, tempol 3mM and PP2 3µM) with an image being taken every 2 minutes for 10 minutes. U46619 (100nM) / LY83583 (1µM) was then added and images were taken every 2 seconds for 2 minutes. Data was expressed as % change from control means +- SEM.

Co-immunoprecipitation

CO-immunoprecipitation studies were performed in protein extracted from pulmonary arteries, untreated / treated with U46619. CO-immunoprecipitation was performed by immunoprecipitating c-Src and probing for the co-immunoprecipitated ARHGEF1. Protein levels of Src and ARHGEF1 are unaffected by U46619 treatment, therefore the levels of Src in treated and untreated samples will be similar, as this protein is being pulled down however, the

level of co-immunoprecipitated ARHGEF1 found in the bound fraction, should be enhanced by U46619 treatment.

For each sample condition, a full arterial tree was used. Arteries were gassed for 15 minutes prior to treatment to allow samples to equilibrate. Following 15 minutes gassing, control samples were immediately snap frozen, alternatively U46619 (100nM) was incubated for 15 minutes with the tissue after which the tissue was immediately snap frozen. The 15 minute time point was used as MYPT-1 phosphorylation was significantly increased at 5 and 30 minutes therefore a compromised time would offer the best chance of observing SrcFK and ARHGEF1 interactions particularly if this is acting upstream of RhoA/Rho-Kinase activation. Protein was extract from Pulmonary arteries using a 1% Triton based buffer. CO-IP was then performed as described in the methods chapter, section 2.6.5.

Strength of experimental design

During this chapter, the main strength was that multiple cell lines generated from different rat tissue, was used to investigate translocation responses. As multiple cell lines were used this ensures that the effects seen were genuine rather than seeing a response from 1 particular cell line which matched my hypothesis. Also each set of translocation data had at least 1 control to compare the effects of stimuli and stimuli plus inhibitor in the same cell, therefore paired.

5.4 Results Section

5.4.1 U46619 and LY83583 promote reversible eGFP-tagged RhoA translocation which is SrcFK and ROS dependent.

Data from previous chapters established that SrcFK contributes to ROS-mediated Rho-kinase activation in response to GPCR stimulation, exogenous ROS and hypoxia. I therefore further investigated the link between SrcFK and Rho-kinase.

Rho-kinase is activated by the monomeric G-protein RhoA. RhoA activation involves translocation from the cytosol to the plasma membrane. Therefore, using eGFP-tagged RhoA in live PASMC, I visualised and quantified translocation in response to U46619 and LY83583 as a corollary of activation [512,513]. In unstimulated PASMC, eGFP-tagged RhoA fluorescence was primarily located in the nucleus/perinuclear region. Exposure to U46619 (100nM) or LY83583 (1μM) brought about a rapid and reversible translocation (enhanced concentration of eGFP fluorescence into spots/patches) at the cell periphery or at cellular attachment points which was visible for several seconds (Fig 5.1- 5.7).

Following a successful response to the initial stimuli, cells were washed (10min) and then incubated either with ebselen (1μM, 10min), tempol (3mM, 10min) or PP2 (3μM, 10min) before being re-exposed to either U46619 or LY83583 (Fig 5.3-5.7). The second translocation responses were abolished by all three inhibitors (enhanced concentration of eGFP fluorescence into spots/patches was absent in the presence of inhibitor) i.e. ebselen and tempol inhibit ROS whilst PP2 is blocking SrcFK activity (Fig 5.3- 5.7), while in control cells, following washout, re-application of stimuli promoted a similar pattern and intensity as the first exposure, confirming that the responses are reproducible (Fig 5.1- 5.2). It was also noted that the addition of U46619 or LY83583, promoted a reversible redistribution of low level diffuse background fluorescence that surrounds the region where the spots (patches) appear, confirming a re-distribution of RhoA (Fig 5.1- 5.7). In the presence of inhibitor, this redistribution did not occur

(Fig 5.3 – 5.7). These changes were confirmed by quantification, further supporting the conclusion that eGFP-tagged RhoA translocation is ROS and SrcFK dependent.

Figure 5.1

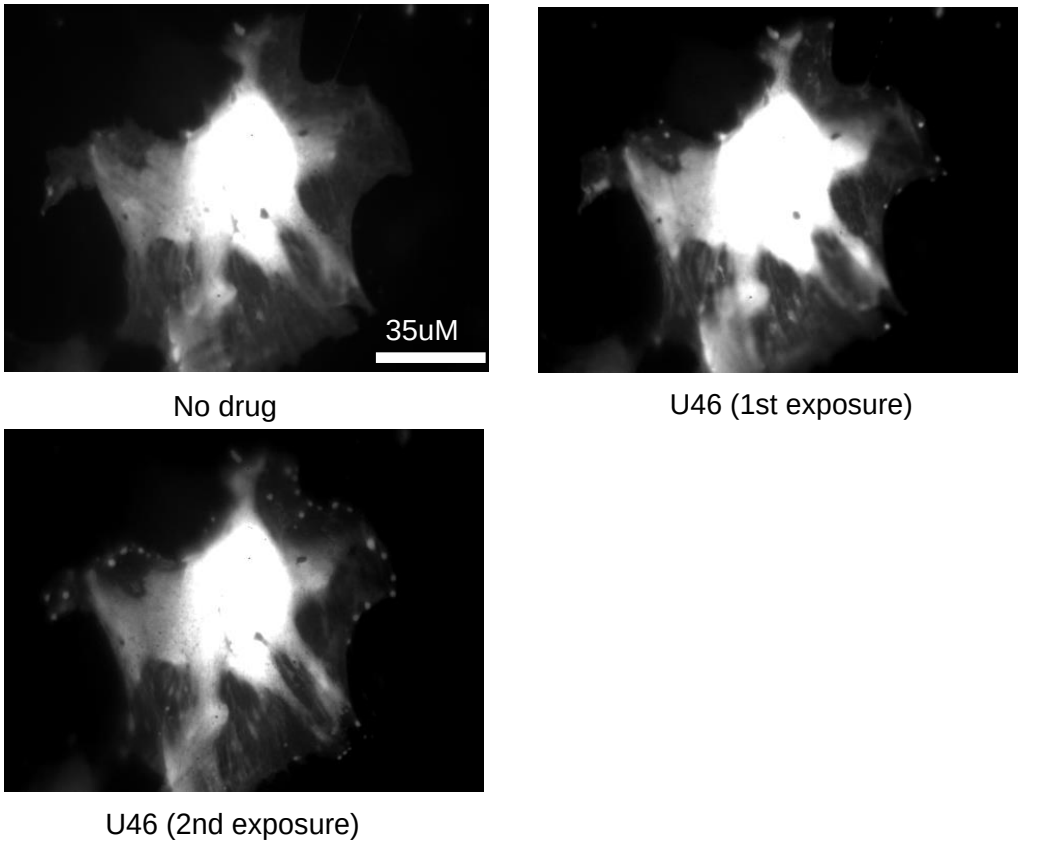

Figure 5.1: Effects of U46619 on eGFP-tagged RhoA translocation in PASMC.
Representative fluorescent images of PASMCs transfected with eGFP-tagged RhoA, unstimulated (top left panel), or in the presence of U46619 (top left, right and middle left panels) (U46619, U46, 100nM). Background measurements were made from readings inside the cell periphery next to the corresponding spots (top left, right and middle left panels). Quantification of spot/patch fluorescence intensity expressed as % change of control levels during U46619 stimulation (Bottom left and right panels). ##P<0.001 vs. baseline, 2-way ANOVA, Factors: U46 alone, U46+ DMSO, Power of performed test: 0.735, n=9 cells from a total of seven different cell lines. Each measurement is combined from at least 3 spots/patches from each cell.

Figure 5.2

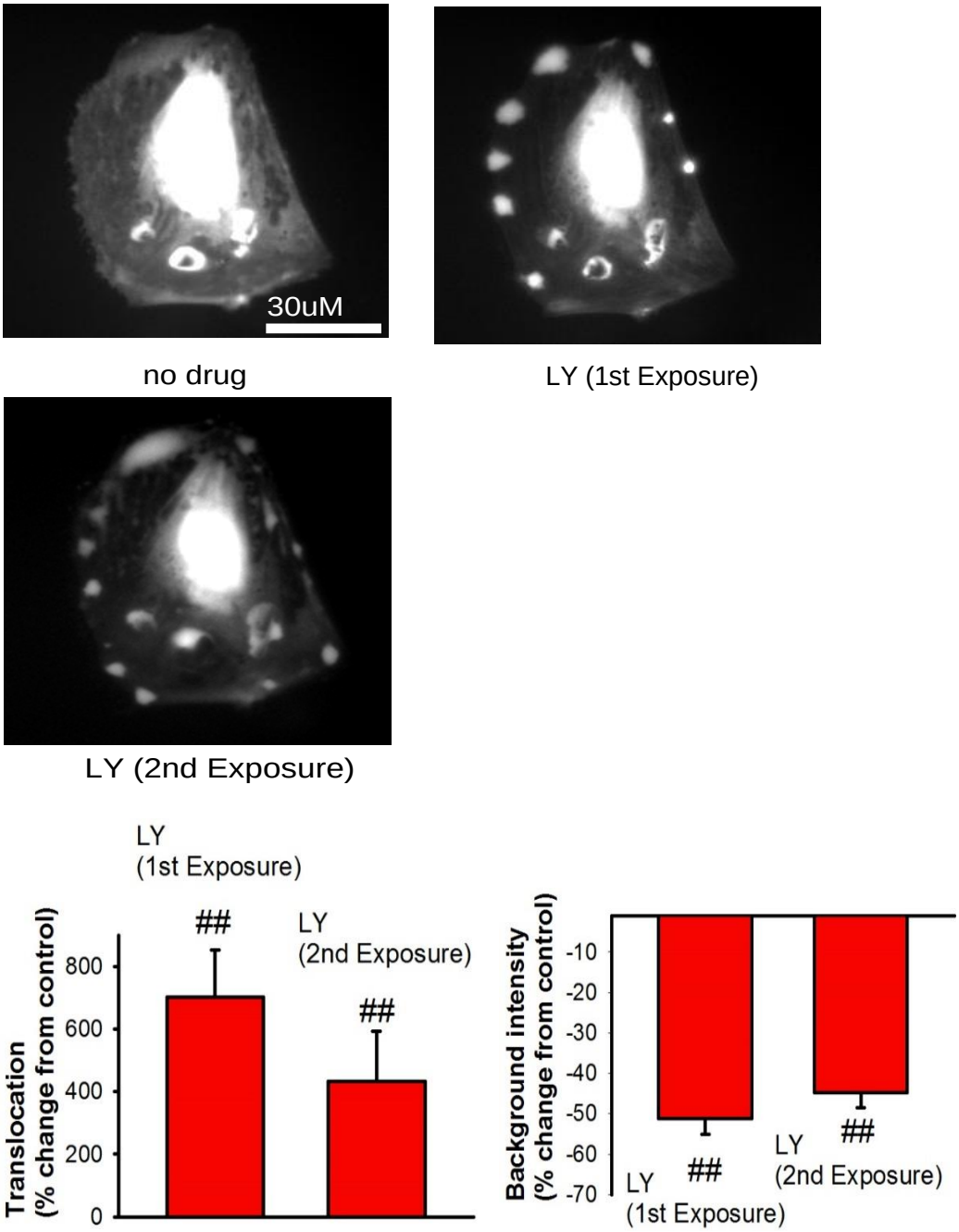

Figure 5.2: Effects of LY83583 on eGFP-tagged RhoA translocation in PASMC.
Representative fluorescent images of PASMCs transfected eGFP-tagged RhoA, unstimulated (top left panel), or in the presence of LY83583 (top right and middle left panels) (LY83583, LY, 1µM) Background measurements were made from readings inside the cell periphery next to the corresponding spots/patches (top left, right and middle left panels). Quantification of spot/patch fluorescence intensity expressed as % change of control levels during LY83583 stimulation (bottom left and right panels) ##P<0.001 vs. baseline, 2-way ANOVA, Factors: LY alone, LY+ DMSO, Power of performed test: 0.946, n=8 cells from a total of seven different cell lines. Each measurement is combined from at least 3 spots/patches from each cell.

Figure 5.3

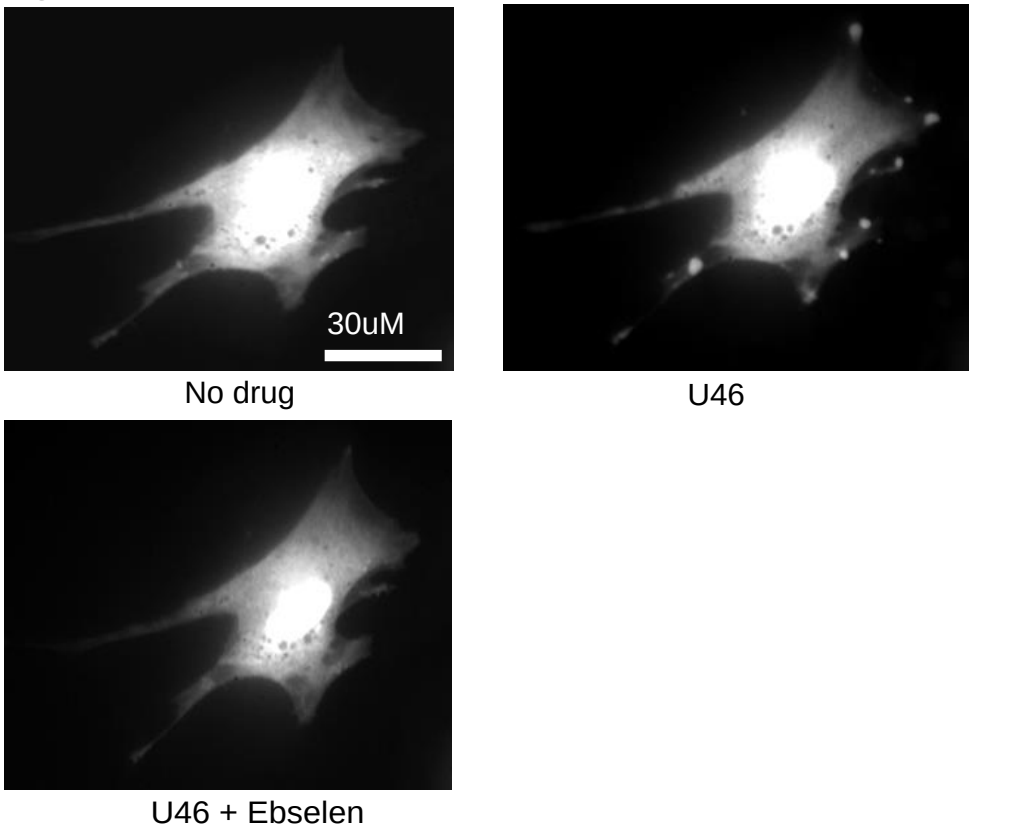

Figure 5.3: Effects of U46619 and ebselen on eGFP-tagged RhoA translocation in PASMC. Representative fluorescent images of PASMCs transfected with eGFP-tagged RhoA, unstimulated (top left panel), in the presence of U46619 (top right panel) and in the presence of U46619 plus ebselen (middle left panel) (U46619, U46, 100nM, ebselen, Ebs, 1µM). Background measurements were made from readings inside the cell periphery next to the corresponding spots/patches (top left, right and middle left panels). Quantification of spot/patch fluorescence intensity expressed as % change of control levels during U46619 stimulation and in the presence of U46619 plus ebselen (bottom left and right panels) ##P<0.001 vs. baseline, **P<0.001 vs. U46619 alone, *P<0.05 vs. U46619 alone, 2-way ANOVA, Factors: U46 alone, U46+ inhibitor, Power of performed test: 0.993, n=9 cells from a total of seven different cell lines. Each measurement is combined from at least 3 spots/patches from each cell.

Figure 5.4

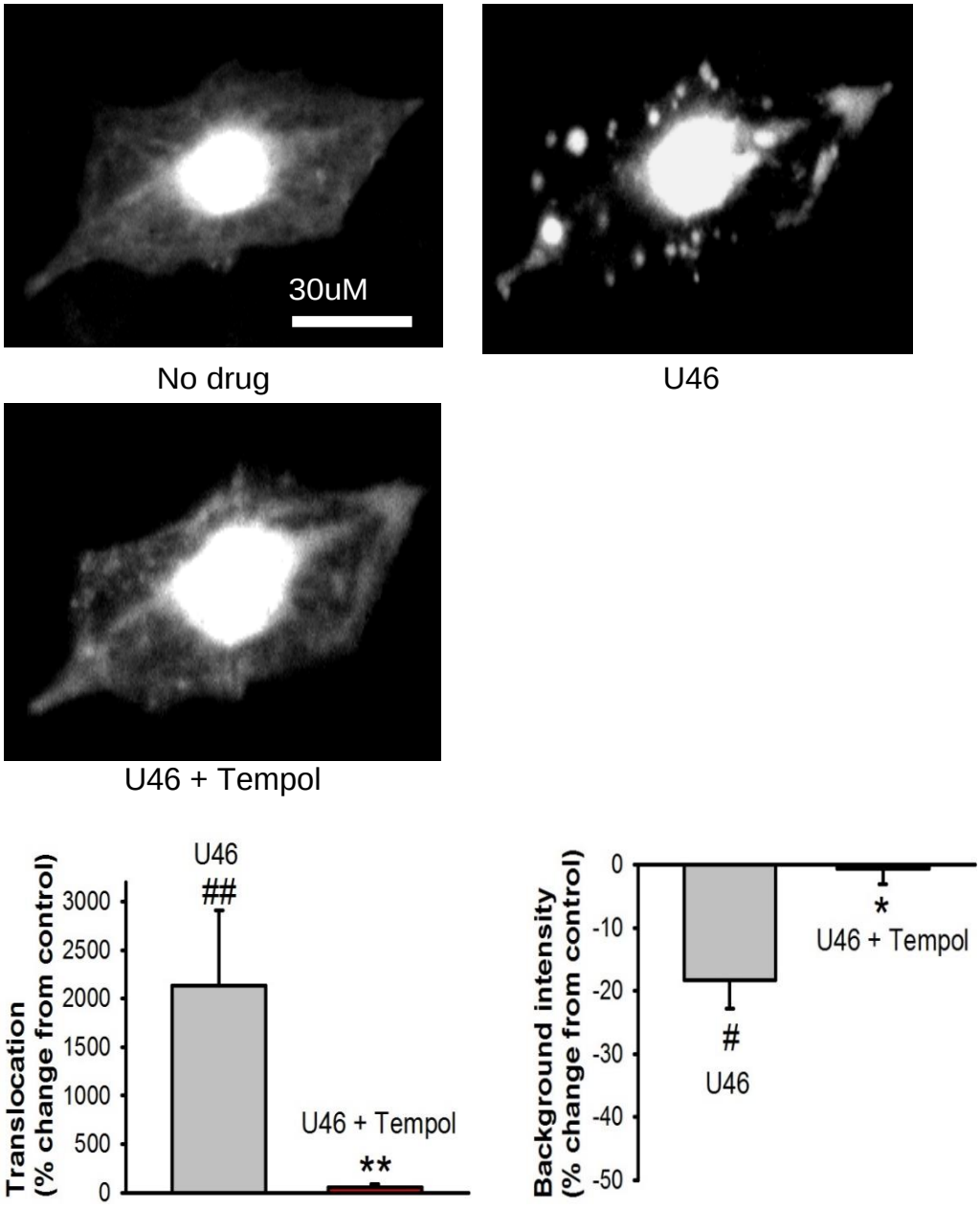

Figure 5.4: Effects of U46619 and tempol on eGFP-tagged RhoA translocation in PASMC. Representative fluorescent images of PASMCs transfected with eGFP-tagged RhoA, unstimulated (top left panel), in the presence of U46619 (top right panel) and in the presence of U46619 plus tempol (middle left panel) (U46619, U46, 100nM, tempol, Temp, 3mM). Background measurements were made from readings inside the cell periphery next to the corresponding spots/patches (top left, right and middle left panel). Quantification of spot/patch fluorescence intensity expressed as % change of control levels during U46619 stimulation and in the presence of U46619 plus tempol (bottom left and right panels) ##P<0.001 vs. baseline, **P<0.001 vs. U46619 alone, #P<0.05 vs. baseline, *P<0.05 vs. U46619 alone, 2-way ANOVA, Factors: U46 alone, U46+ inhibitor, Power of performed test: 0.912, n=9 cells from a total of seven different cell lines. Each measurement is combined from at least 3 spots/patches from each cell.

Figure 5.5

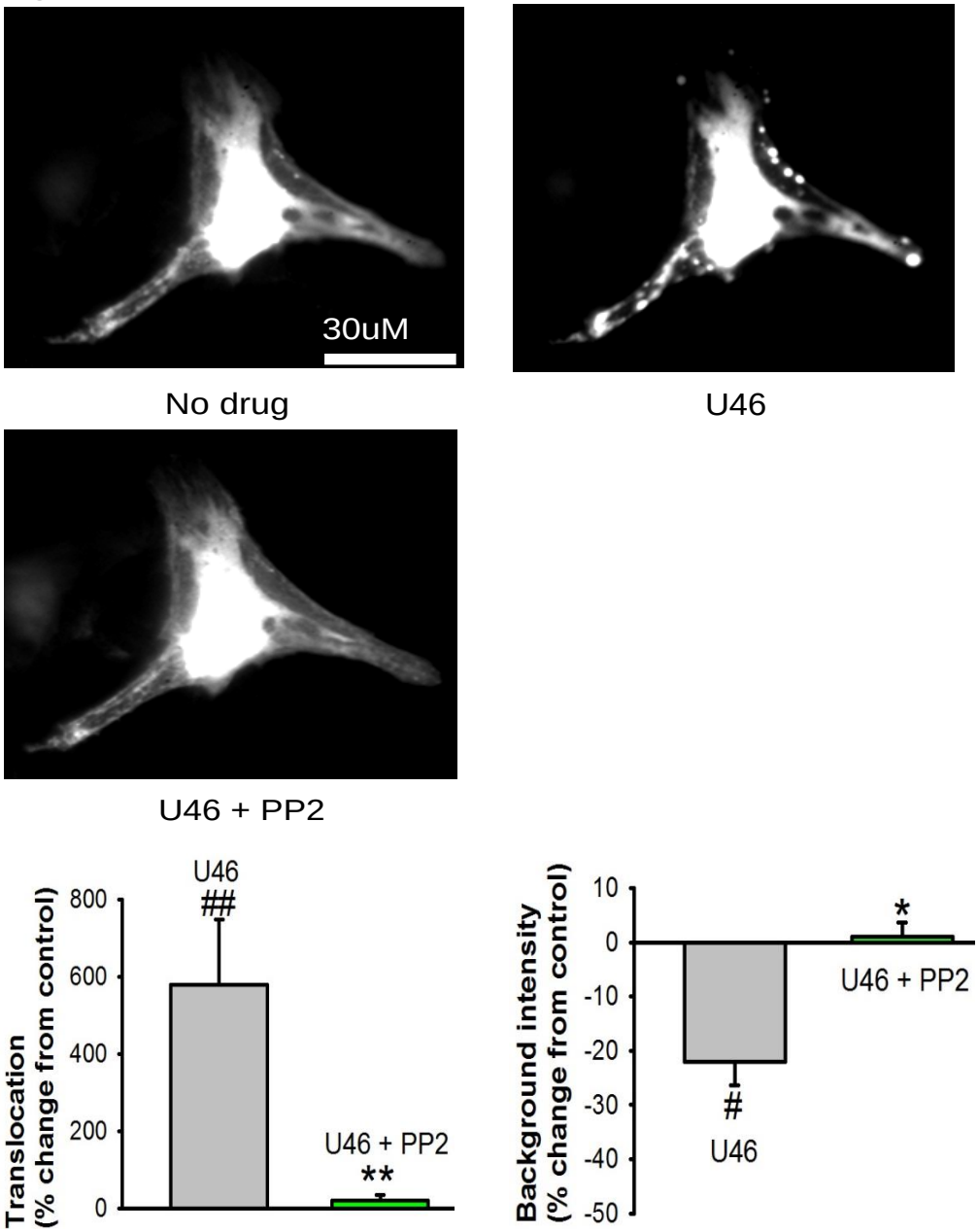

Figure 5.5: Effects of U46619 and PP2 on eGFP-tagged RhoA translocation in PASMC. Representative fluorescent images of PASMCs transfected with eGFP-tagged RhoA, unstimulated (top left panel), in the presence of U46619 (top right panel) and in the presence of U46619 plus PP2 (middle left panel) (E: U46619, U46, 100nM, PP2, 3µM). Background measurements were made from readings inside the cell periphery next to the corresponding spots/patches (top left, right and middle left panel). Quantification of spot/patch fluorescence intensity expressed as % change of control levels during U46619 stimulation and in the presence of U46619 plus PP2 (bottom left and right panels). ##P<0.001 vs. baseline, **P<0.001 vs. U46619 alone, #P<0.05 vs. baseline, *P<0.05 vs. U46619 alone, 2-way ANOVA, Factors: U46 alone, U46+ inhibitor, Power of performed test: 0.977, n=8 cells from a total of seven different cell lines. Each measurement is combined from at least 3 spots/patches from each cell.

Figure 5.6

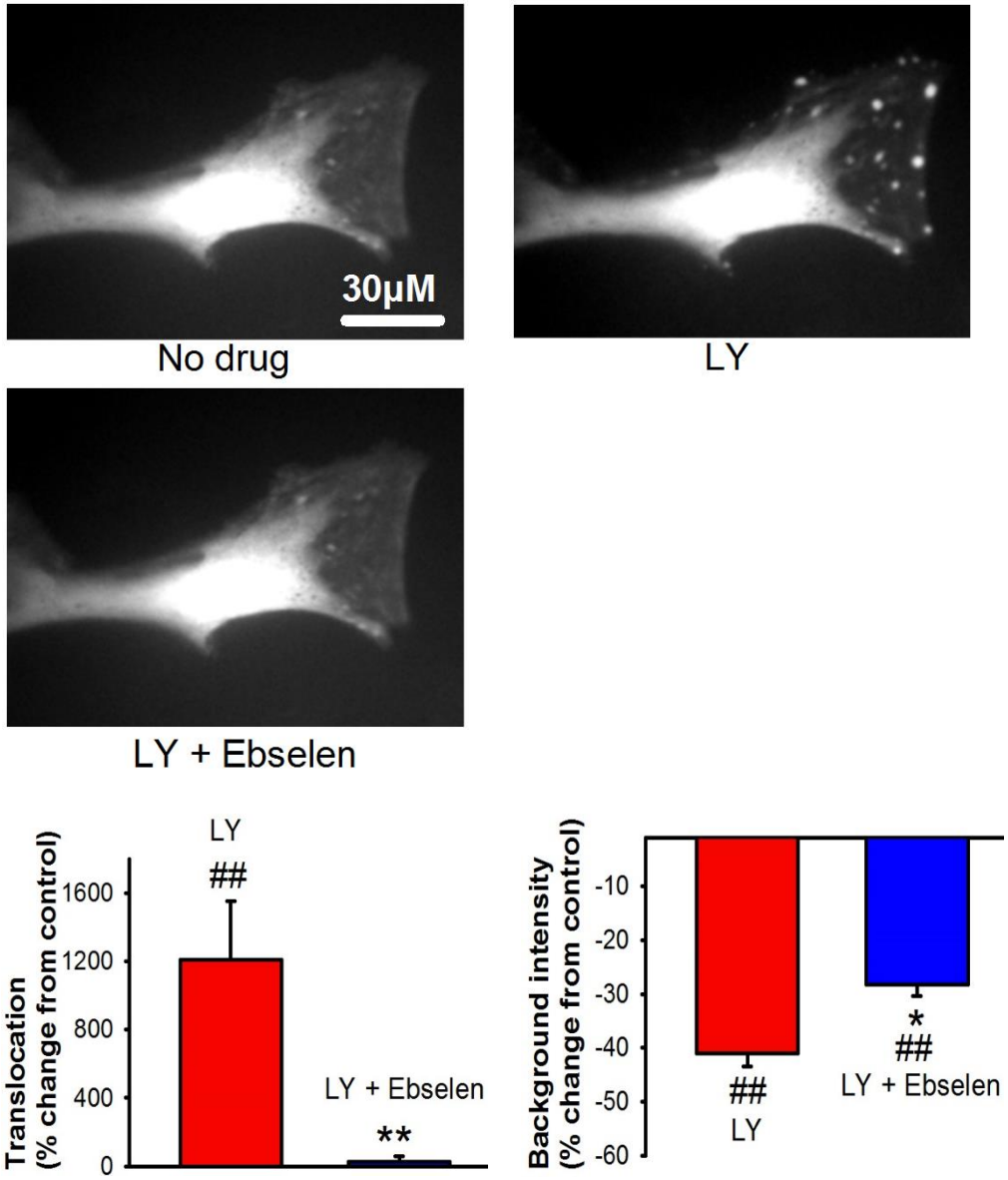

Figure 5.6: Effects of LY83583 and ebselen on eGFP-tagged RhoA translocation in PASMC.

Representative fluorescent images of PASMCs transfected with eGFP-tagged RhoA, unstimulated (top left panel), in the presence of LY83583 (top left panel) and in the presence of LY83583 plus ebselen (middle left panel) (LY8383, LY, 1µM, ebselen, Ebs, 1µM). Background measurements were made from readings inside the cell periphery next to the corresponding spots/patches (top left, right and middle left panels). Quantification of spot/patch fluorescence intensity expressed as % change of control levels during LY83583 stimulation and in the presence of LY83583 plus ebselen (bottom left and right panel) ##P<0.001 vs. baseline, **P<0.001 vs. LY83583 alone, *P<0.05 vs. LY83583 alone, 2-way ANOVA, Factors: LY alone, U46+ inhibitor, Power of performed test: 0.895, n=9 cells from a total of seven different cell lines. Each measurement is combined from at least 3 spots/patches from each cell.

Figure 5.7

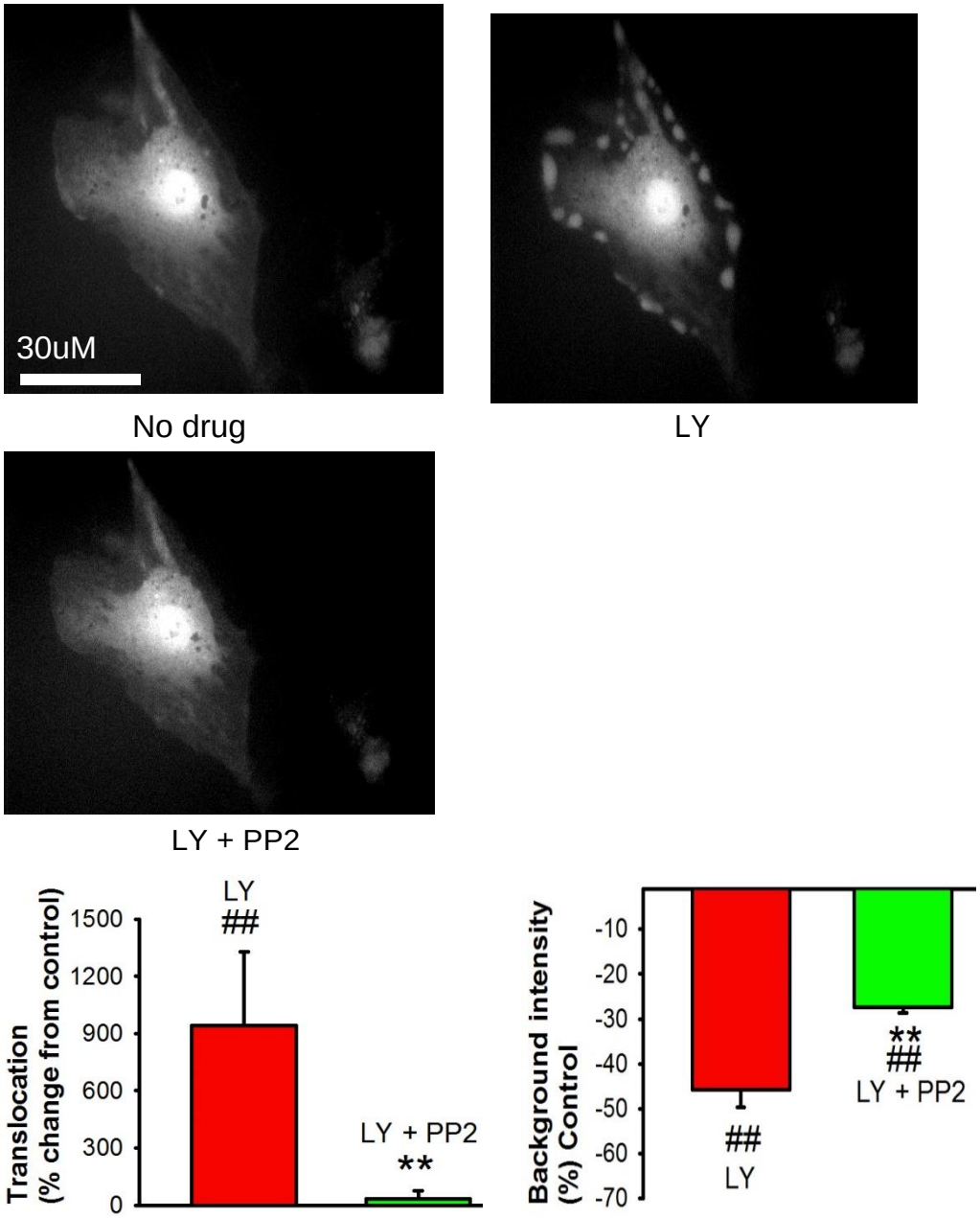

Figure 5.7: Effects of LY83583 and PP2 on eGFP-tagged RhoA translocation in PASMC. Representative fluorescent images of PASMCs transfected with eGFP-tagged RhoA, unstimulated (top left panel), in the presence of LY83585 (top right panel) and in the presence of LY83585 plus PP2 (middle left panel) (LY8383, LY, 1µM, pp2, 3µM). Background measurements were made from readings inside the cell periphery next to the corresponding spots/patches (top left, right and middle left panels). Quantification of spot/patch fluorescence intensity expressed as % change of control levels during LY83583 stimulation and in the presence of LY83585 plus PP2 (bottom left and right panels). ##P<0.001 vs. baseline, **P<0.001 vs. LY83583 alone, 2-way ANOVA, Factors: LY alone, LY+ inhibitor, Power of performed test: 0.592 n=8 cells from a total of seven different cell lines. Each measurement is combined from at least 3 spots/patches from each cell.

5.4.2: eGFP-tagged ARHGEF1 translocates in response to U46619 and LY83583 in a ROS and SrcFK dependent manner in PASMC

Having established that ROS and SrcFK mediate RhoA translocation, I next investigated whether ROS and SrcFK may be mediating RhoA translocation via interaction with one or more RhoGEFs. I therefore examined translocation responses of eGFP-tagged ARHGEF1, a RhoA-specific guanine nucleotide exchange factor, in live PASMC, in response to U46619 and LY83583 as described above for RhoA-GFP.

eGFP-tagged ARHGEF1 responses were similar to those of eGFP-tagged RhoA. Basal eGFP-tagged ARHGEF1 fluorescence was located primarily in the perinuclear region and clearly absent from the nuclei, as opposed to RhoA, which is present in the nuclei. Upon exposure to U46619 or LY83583, bright spots appeared at the cell periphery with a darkening of surrounding background fluorescence (Fig 5.8-5.14). Similarly, the appearance of spots and darkening of background fluorescence was abolished by ebselen, tempol or PP2, confirming a redistribution of eGFP-tagged ARHGEF1 (Fig 5.10- 5.14). Reapplication of either stimulus in control cells, produced a comparable response as the first exposure, confirming that the responses are reproducible (Fig 5.8– 5.9).

5.4.3: U46619 enhanced co-immunoprecipitation between SrcFK and ARHGEF1 in IPA

To further clarify the relationship between SrcFK and ARHGEF1, I also examined protein interactions in IPA by immunoprecipitating c-Src and probing for the co-immunoprecipitated ARHGEF1. U46619 treatment enhanced co-immunoprecipitation between c-Src and ARHGEF1 (Fig 5.15).

Figure 5.8

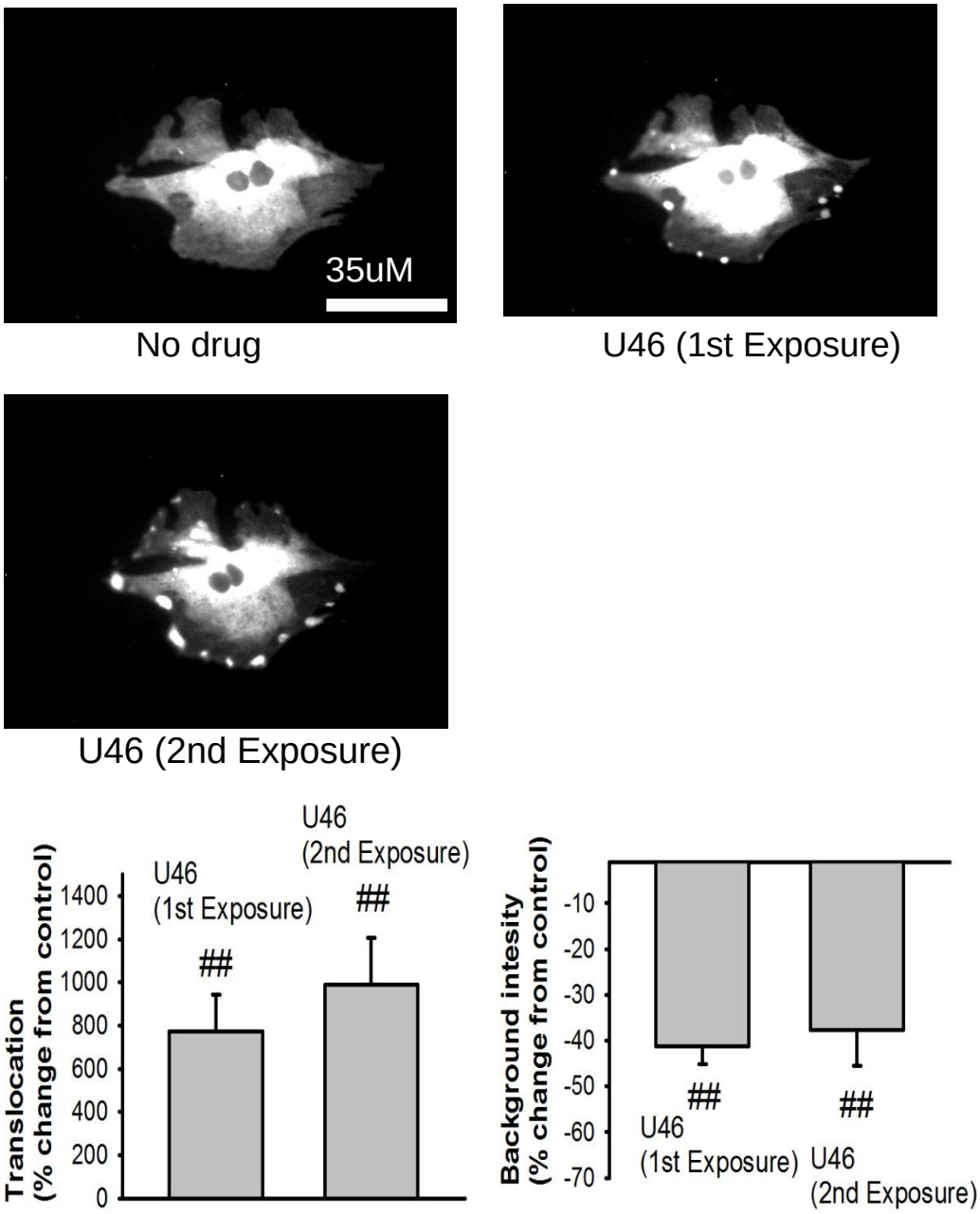

Figure 5.8: Effects of U46619 on eGFP-tagged ARHGEF1 translocation in PASMC.
Representative fluorescent images of PASMCs transfected with eGFP-tagged ARHGEF1, unstimulated (top left panel), in the presence of U46619 (top right and middle left panel) (U46619, U46, 100nM). Background measurements were made from readings inside the cell periphery next to the corresponding spots (top left, right and middle left panels). Quantification of spot/patch fluorescence intensity expressed as % change of control levels during U46619 stimulation (bottom left and right panels) ##P<0.001 vs. baseline, 2-way ANOVA, Factors: U46 alone, U46+ DMSO, Power of performed test: 0.767, n=8 cells from a total of seven different cell lines. Each measurement is combined from at least 3 spots/patches from each cell.

Figure 5.9

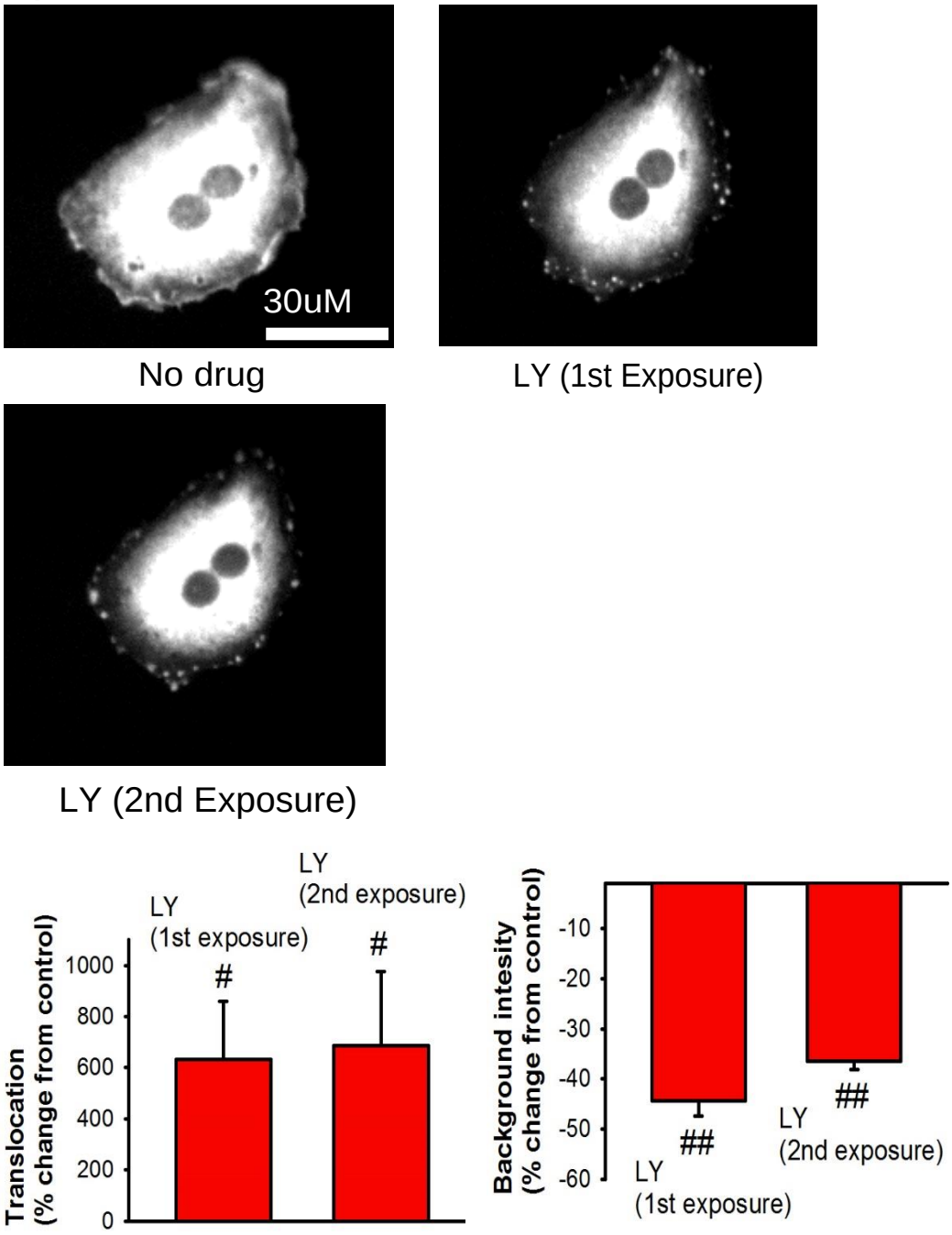

Figure 5.9: Effects of LY83583 on eGFP-tagged ARHGEF1 translocation in PASMC.
Representative fluorescent images of PASMCs transfected with eGFP-tagged ARHGEF1, unstimulated (top left panel), in the presence of LY83583 (top right panel and middle left panel) (LY8383, LY, 1µM). Background measurements were made from readings inside the cell periphery next to the corresponding spots (top left, right and middle left panels). Quantification of spot/patch fluorescence intensity expressed as % change of control levels during LY83583 stimulation ##P<0.001 vs. baseline, #P<0.05 vs. baseline, 2-way ANOVA, Factors: LY alone, LY+ DMSO, Power of performed test: 0.937, n=7 cells from a total of seven different cell lines. Each measurement is combined from at least 3 spots/patches from each cell.

Figure 5.10

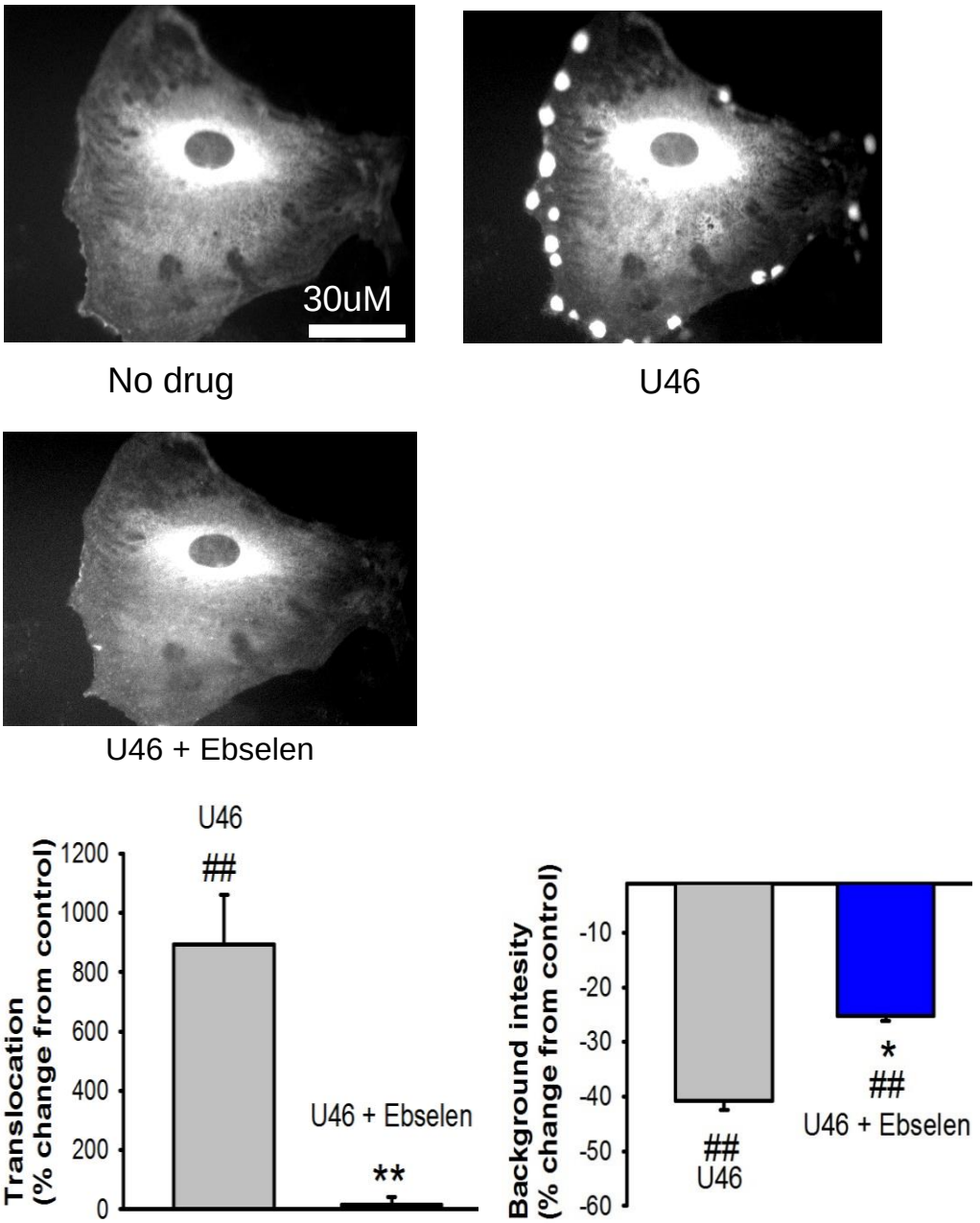

Figure 5.10: Effects of U46619 and ebselen on eGFP-tagged ARHGEF1 translocation in PASMC.

Representative fluorescent images of PASMCs transfected with eGFP-tagged ARHGEF1, unstimulated (top left panel), in the presence of U46619 (top right panel) and in the presence of U46619 plus ebselen (middle left panel) (C: U46619, U46, 100nM, ebselen, Ebs, 1µM). Background measurements were made from readings inside the cell periphery next to the corresponding spots (top left, right and middle left panels). Quantification of spot/patch fluorescence intensity expressed as % change of control levels during U46619 stimulation and in the presence U46619 plus ebselen. ##P<0.001 vs. baseline, **P<0.001 vs. U46619 alone, *P<0.05 vs. U46619 alone. 2-way ANOVA, Factors: U46 alone, U46+ inhibitor, Power of performed test: 0.968, n=9 cells from a total of seven different cell lines. Each measurement is combined from at least 3 spots/patches from each cell.

Figure 5.11

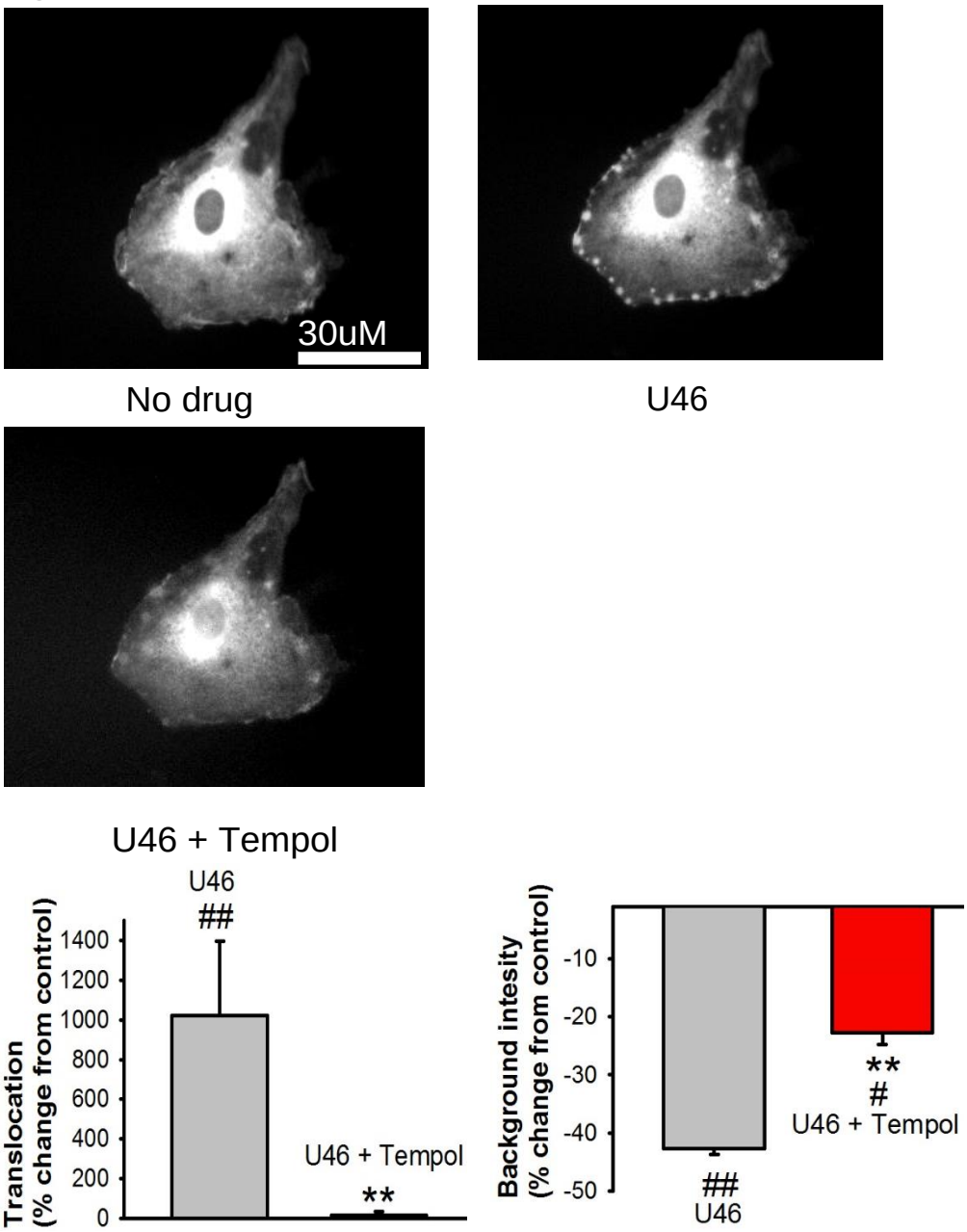

Figure 5.11: Effects of U46619 and tempol on eGFP-tagged ARHGEF1 translocation in PASMC.

Representative fluorescent images of PASMCs transfected with eGFP-tagged ARHGEF1, unstimulated (top left panel), in the presence of U46619 (top right panel) and in the presence of U46619 plus tempol (middle left panel) (D: U46619, U46, 100nM, tempol, Temp, 3mM). Background measurements were made from readings inside the cell periphery next to the corresponding spots (top left, right and middle left panels). Quantification of spot/patch fluorescence intensity expressed as % change of control levels during U46619 stimulation and in the presence U46619 plus tempol ##P<0.001 vs. baseline, **P<0.001 vs. U46619 alone, #P<0.05 vs. U46619 alone, 2-way ANOVA, Factors: U46 alone, U46+ inhibitor, Power of performed test: 0.684, n=8 cells from a total of seven different cell lines. Each measurement is combined from at least 3 spots/patches from each cell.

Figure 5.12

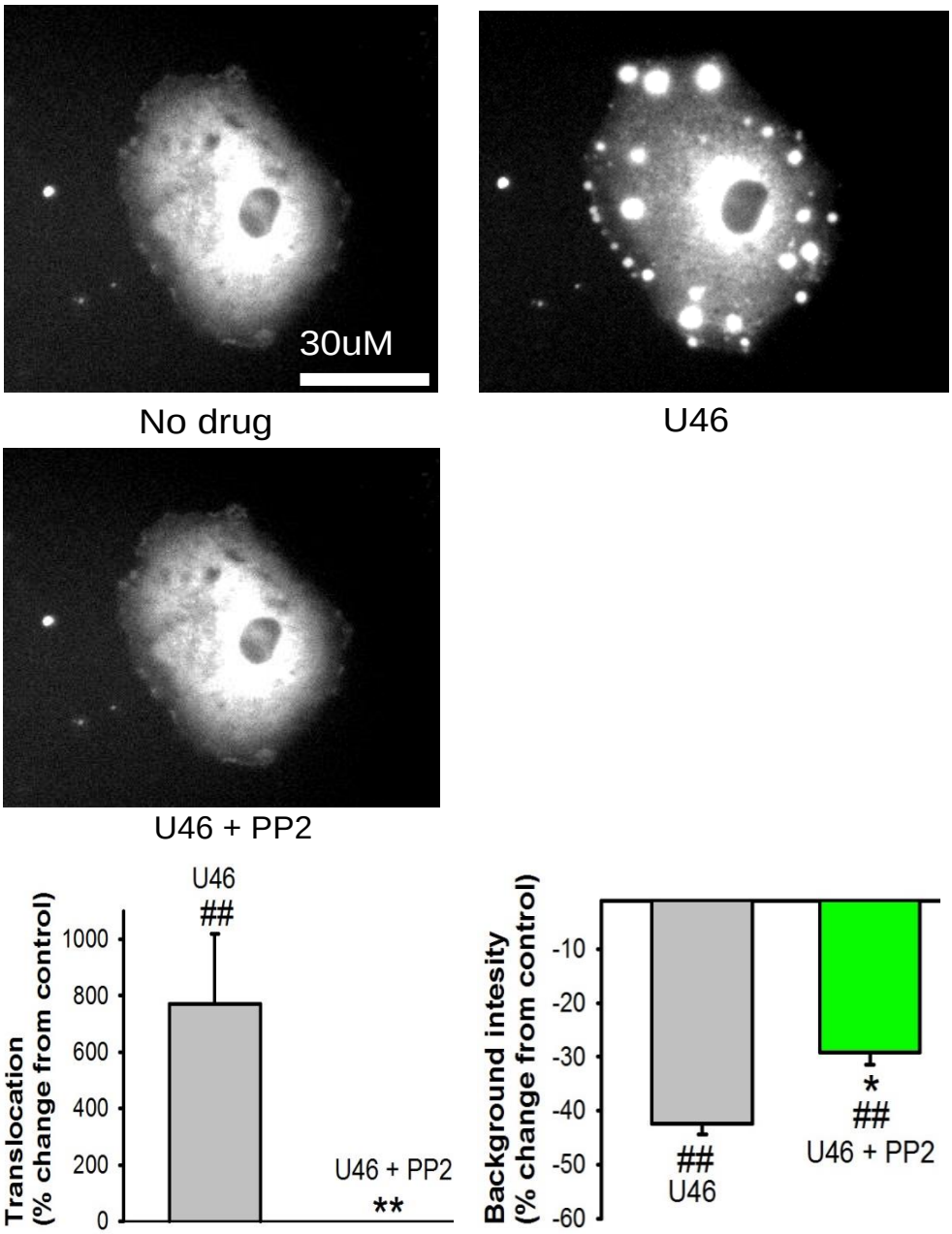

Figure 5.12. Effects of U46619 and PP2 on eGFP-tagged ARHGEF1 translocation in PASMC.

Representative fluorescent images of PASMCs transfected with eGFP-tagged ARHGEF1, unstimulated (top left panel), in the presence of U46619 (top right panel) and in the presence of U46619 plus PP2 (middle left panel) (E: U46619, U46, 100nM, PP2, 3µM). Background measurements were made from readings inside the cell periphery next to the corresponding spots (top left, right and middle left panels). Quantification of spot/patch fluorescence intensity expressed as % change of control levels during U46619 stimulation and in the presence of U46619 plus PP2. ##P<0.001 vs. baseline, **P<0.001 vs. U46619 alone, *P<0.05 vs. U46619 alone, 2-way ANOVA, Factors: U46 alone, U46+ inhibitor, Power of performed test: 0.837, n=9 cells from a total of seven different cell lines. Each measurement is combined from at least 3 spots/patches from each cell.

Figure 5.13

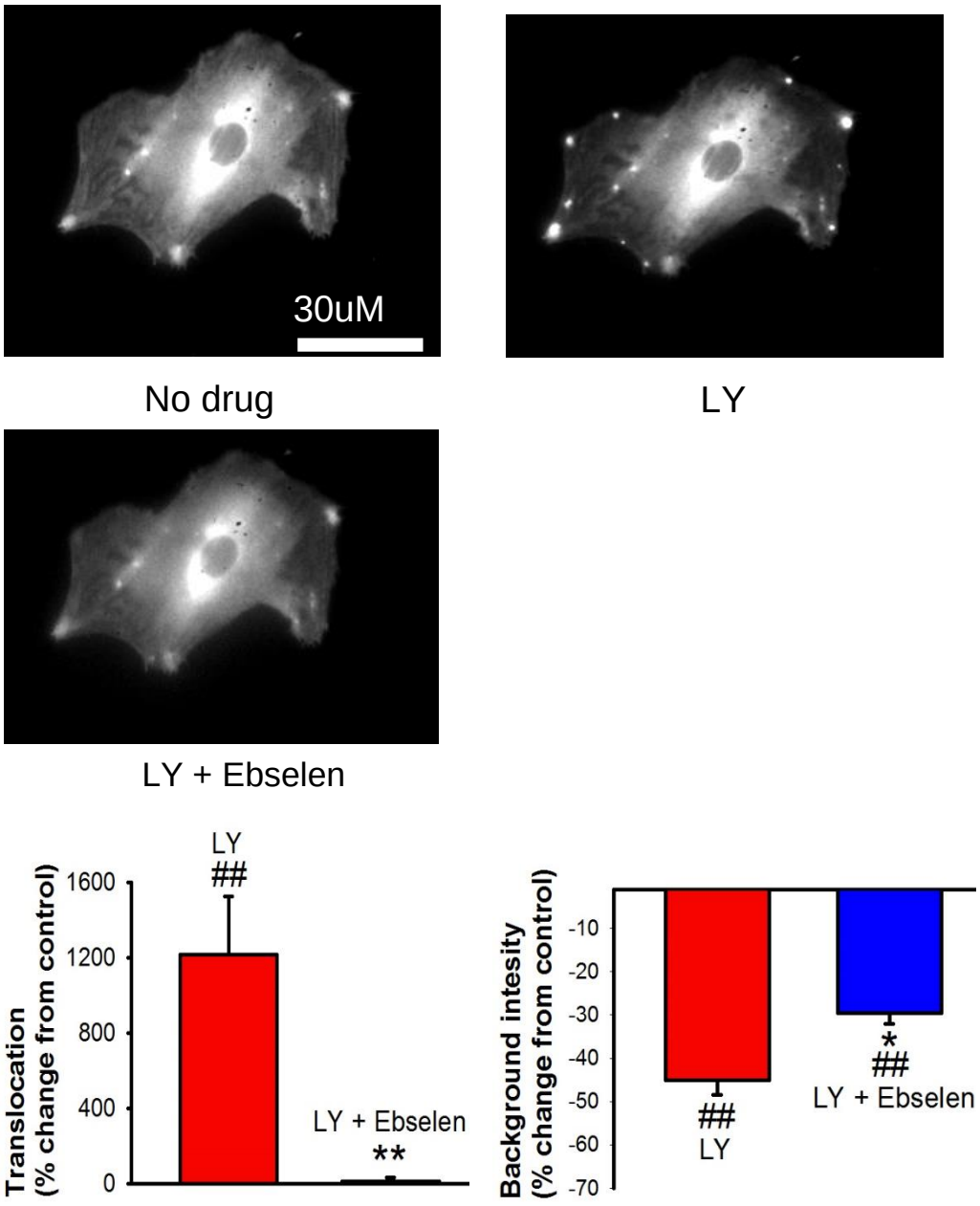

Figure 5.13: Effects of LY83583 and ebselen on eGFP-tagged ARHGEF1 translocation in PASMC.

Representative fluorescent images of PASMCs transfected with eGFP-tagged ARHGEF1, unstimulated (top left panel), in the presence of LY83583 (top right panel) and in the presence of LY83583 plus ebselen (middle left panel) (F: LY83583, LY, 1µM, ebselen, Ebs, 1µM). Background measurements were made from readings inside the cell periphery next to the corresponding spots (top left, right and middle left panel). Quantification of spot/patch fluorescence intensity expressed as % change of control levels during LY83583 stimulation and in the presence LY83583 plus ebselen. ##P<0.001 vs. baseline, **P<0.001 vs. LY83583 alone, *P<0.05 vs. LY83583 alone, 2-way ANOVA, Factors: LY alone, LY+ inhibitor, Power of performed test: 0.963, n=8 cells from a total of seven different cell lines. Each measurement is combined from at least 3 spots/patches from each cell.

Figure 5.14

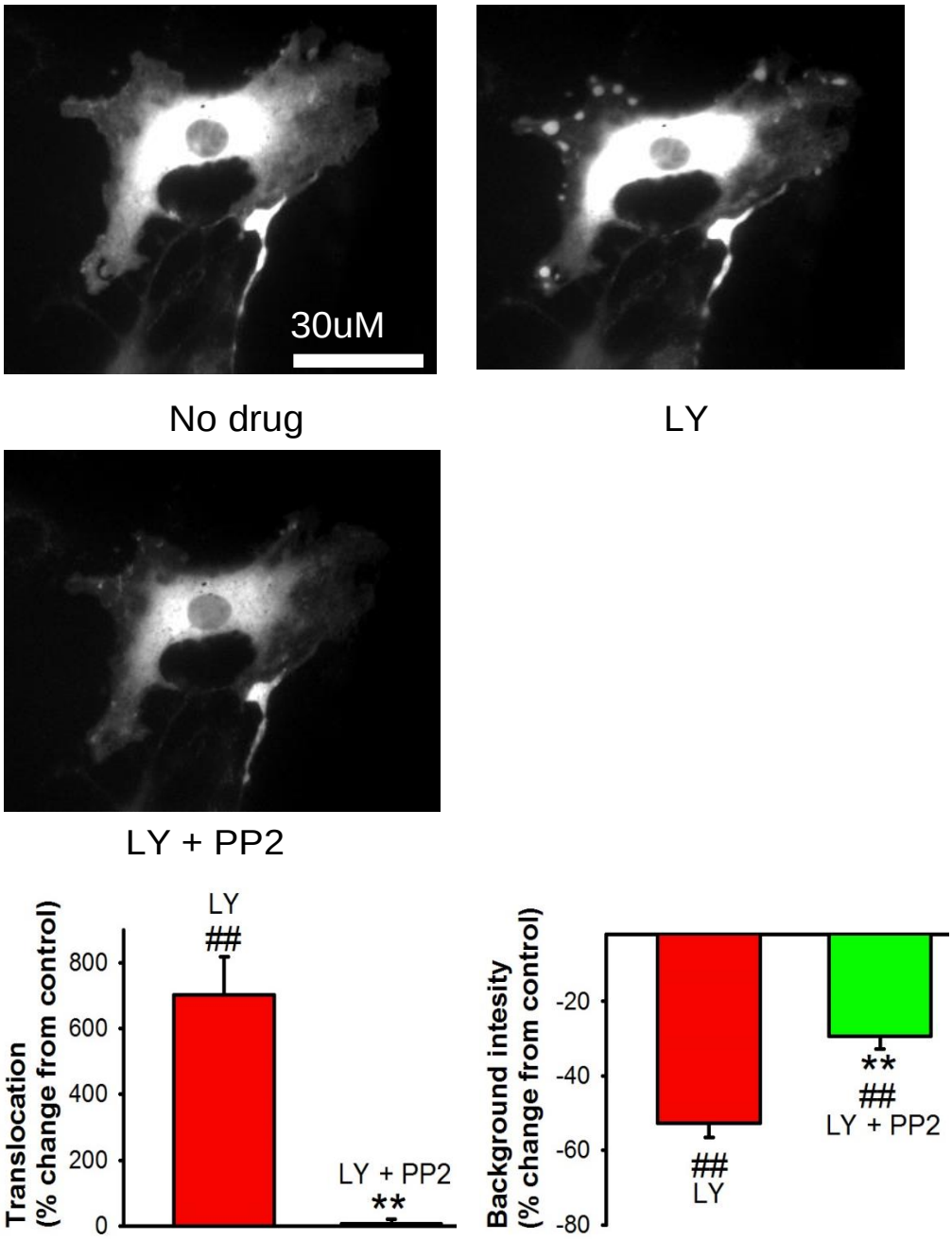

Figure 5.14 Effects of LY83583 and PP2 on eGFP-tagged ARHGEF1 in PASMC.
Representative fluorescent images of PASMCs transfected with eGFP-tagged ARHGEF1, unstimulated (top left panel), in the presence of LY83583 (top right panel) and in the presence of LY83583 plus PP2 (middle left panel) (LY83583, LY, 1µM, PP2, 3µM). Background measurements were made from readings inside the cell periphery next to the corresponding spots (top left, right and middle left panel). Quantification of spot/patch fluorescence intensity expressed as % change of control levels during LY83583 stimulation and in the presence of LY83583 plus PP2. ##P<0.001 vs. baseline, **P<0.001 vs. LY83583 alone, 2-way ANOVA, Factors: LY alone, LY+ inhibitor, Power of performed test: 0.989, n=9 cells from a total of seven different cell lines. Each measurement is combined from at least 3 spots/patches from each cell

Figure 5.15

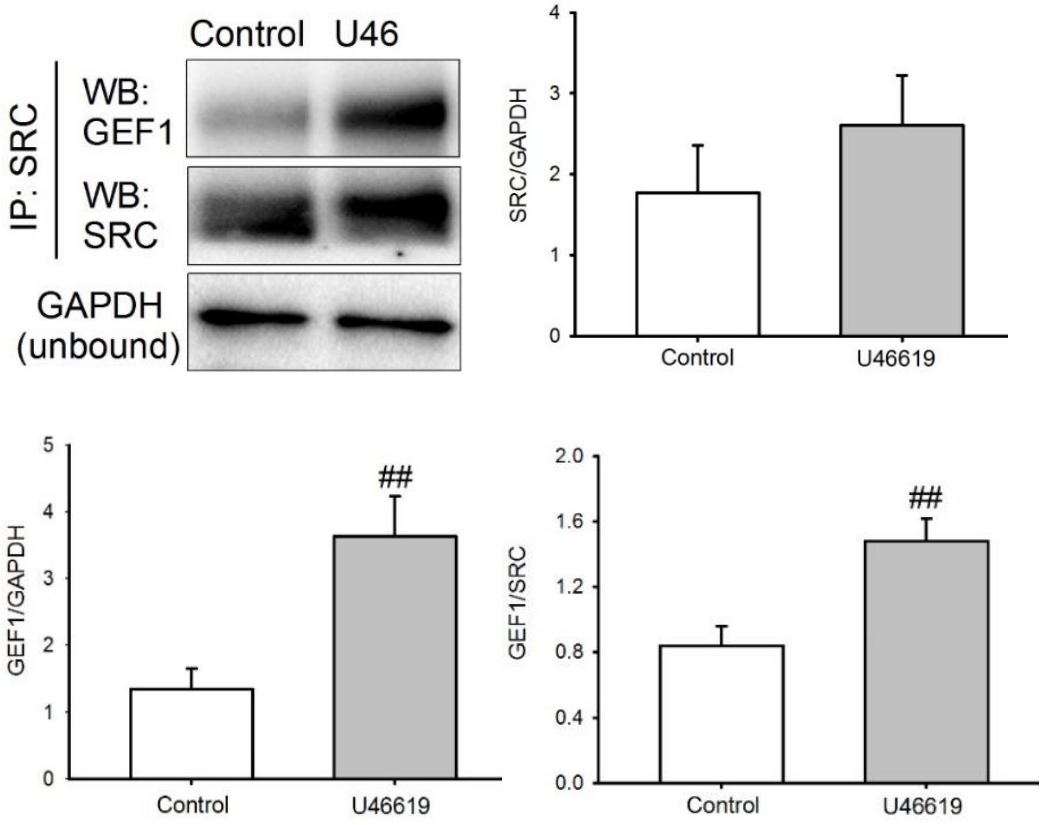

Figure 5.15: U46619 enhances co-immunoprecipitation of c-Src and ARHGEF1.
Representative blots show the effect of U46610 (100nM, 15mins) on ARHGEF1 (WB: GEF1) and c-Src (WB: c-Src) after c-Src immuno-precipitation (IP: c-Src). GAPDH in the u-bound fraction was used as a loading control (WB: GAPDH). Bar charts demonstrate that U46619 increased co-immuno-precipitation of ARHGEF1 with c-Src proportionately to both c-Src IP content and GAPDH loading control, but does not change c-Src IP contents. ##P<0.001 vs. baseline, un-paired t-test, n=4.

5.5 Summary of findings

The purpose of this chapter was to investigate the stated hypotheses of:

"ROS and SrcFK may be mediating RhoA and ARHGEF1 translocation in PASMCs. Furthermore, U46619 will enhance co-immunoprecipitation between c-Src and ARHGEF1 in IPA".

The findings of this chapter are:

- U46619 and LY83583 promotes GFP tagged RhoA translocation in a SrcFK and ROS dependent manner.
- U46619 and LY83583 promotes GFP tagged ARHGEF1 translocation in a SrcFK and ROS dependent manner.
- U46619 promotes CO-IP between SrcFK and ARHGEF1.

The discussion will set out to address how the experimental evidence in the results chapter met the aims and hypotheses.

5.6 Discussion

Results from this chapter describe a new signalling pathway within PASMC's and IPA's, where by, RhoA and ARHGEF1 translocate in response to contractile stimuli (U46 and LY). This translocation appears to be SrcFK and ROS dependent, and may be important in Ca^{2+} sensitization and contraction.

As discussed in the introduction section (section 1.5.2), SrcFK can be activated directly by GPCR via their SH3 domains[256,257] or via direct interactions with Gα subunits such as $G\alpha_s$ and $G\alpha_I$ [258]. $G\alpha_{12}$ has also been shown to activate Src via recruitment of HSP90 [259]. The Gβγ complex has also been shown to act as a key intermediate responsible for the activation of Src [246,261]. Finally, arrestins which inhibit GPCR signalling have also been shown to recruit and bind SrcFK leading to 'second wave' of GPCR signalling [262]. There therefore exists a number of documented pathways whereby GPCR activate SrcFK. This study however provide evidence of a new novel pathway where GPCR induced ROS production may also activate SrcFK which potentially promotes contraction via interactions with ARHGEF1.

Firstly, I demonstrate that translocation of eGFP-tagged RhoA and eGFP-tagged ARHGEF1 is stimulated by U46619 and exogenous ROS. Translocation responses were subsequently shown to be SrcFK and ROS dependent. Secondly and perhaps more importantly, I establish that U46619 enhanced co-immunoprecipitation of ARHGEF1 and c-Src in IPA, suggesting there is a close association between these two proteins. This association, coupled with the translocation data and phosphorylation data presented in chapter 3, may contribute to the activation of RhoA/Rho-kinase. I believe, this is the first study to show that SrcFK potentially interacting with ARHGEF1. This is also supported by phospho-tyrosine data, whereby, LY83583 enhances SrcFK-dependent tyrosine phosphorylation of multiple proteins in IPA, including one at approximately 115 kDa, the expected location of ARHGEF1.

Calcium sensitization occurs in response to constrictor stimuli via activation of RhoA and its principle effector Rho-Kinase [504,516]. GPCR's for various vasoconstrictor agonists such as angiotensin II, lysophosphatidic acid, thrombin, thromboxane (TXA_2), sphingosine-1-phosphoate (SIP) have been shown to be coupled to $G_{12/13}$ [342,517-519]. Activation of $G_{12/13,}$ is known to activate the RhoA/Rho-Kinase pathway and induce RhoA and Rho-Kinase redistribution. RhoA translocates from the cytosol to the plasma membrane and Rho-Kinase translocates from the nucleus to the cytosol [514,520,521]. This coincides with what I see during translocation of eGFP-tagged RhoA. In response to U46619 and LY83583, RhoA translocates to the cell periphery forming spots/patches at specific locations. This is also confirmed by changes in background intensity, which show a redistribution of low level diffuse background fluorescence that surrounds the region where the spots/patches appear, in response to stimuli. Translocation and background fluorescence changes were blocked by ebselen, tempol and PP2, demonstrating that translocation was SrcFK and ROS dependent. A study performed by Knock *et al* [88], demonstrated that LY83583 promotes Rock-2 translocation and increased MYPT-1 and MLC_{20} phosphorylation, which is subsequently inhibited by SOD. Suggesting, that ROS act as upstream mediators of Rho-Kinase.

Rho-Kinase has not been reported to be directly ROS sensitive, however RhoA has been reported to be redox sensitive [311,312]. This activation requires ROS to interact with two cysteine residues in the phosphoryl binding loop of RhoA, thereby bypassing the canonical GEF mediated RhoA activation [312]. This system has been proposed in living cells where oxidation of these cysteine residues promotes guanine nucleotide dissociation, resulting in exchange of GDP to GTP, thus activating RhoA. A more widely studied view of ROS mediated activation of RhoA/Rho-Kinase is via upstream redox sensitive tyrosine kinases[88], particularly by SrcFK.

Previous studies, have demonstrated a role for SrcFK in $PGF_{2\alpha}$ – mediated Ca^{2+} sensitization and contraction. Furthermore, SrcFKs have been implicated as upstream mediators of Rho-

Kinase via increased translocation and enhanced MYPT-1 and MLC_{20} phosphorylation responses[41,82]. Similarly, hypoxia-induced MYPT-1 and MLC_{20} phosphorylation is inhibited by SU6656. Furthermore, translocation of Rho-Kinase from nucleus to the cytosol was prevented by Src siRNA [7].

This conforms to my results as PP2 inhibits U46619 and LY83583 induced RhoA translocation and contraction (chapter 1). PP2 is also shown to inhibit SrcFK autophosphorylation and subsequently MYPT-1 and MLC_{20} phosphorylation in response to U46619. As SrcFK are redox sensitive, as detailed in chapter 1, and the fact that tempol and ebselen inhibit U46619 induced SrcFK autophosphorylation, MYPT-1 and MLC_{20} phosphorylation responses, this is highly suggestive that ROS are acting via SrcFK to activate RhoA/Rho-Kinase.

The direct link between GPCR activation and RhoA/Rho-Kinase has been under investigation by numerous groups. The logical family involved upstream of RhoA/Rho-Kinase activation are RhoGEFs. RhoGEFs reduce the affinity of RhoA for GDP, thus allowing the more abundant GTP to displace it, thereby activating RhoA [306]. RhoGEFs are a large family of proteins with ~70 members in the human genome[522] . Of these 70 members, there are a small family of RGS-containing RhoGEFs which are regulated by $G_{12/13}$ heterotrimeric G-protein [229,230,523]. These are Rho Specific, and some of them such as ARHGEF11 (PDZ), ARHGEF12 (LARG) and ARHGEF1 (p115-RhoGEF) have been shown to be tyrosine phosphorylated [244,320,324,345,524], leading to increased levels of GTP-bound RhoA. This suggests that tyrosine phosphorylation may increase their exchange activity, or stabilize GEFs binding to GPCR, to allow for a longer period of GEF activity.

A number of these RhoA-specific GEFs are expressed in the vasculature[319]. However, there are claims that VSM-RhoGEF is specific to vascular smooth muscle, hence the name [320]. This

particular GEF was shown to be involved ephrin-A1-induced assembly of actin stress fibres in VSMCs and regulate VSMC contractility via the EphA4-Vsm-RhoGEF-RhoA pathway.

A number of RhoGEFs are known to be phosphorylated and activated by three non-receptor tyrosine kinases, focal adhesion kinases (FAK), protein tyrosine kinase-2 (PYK2) and Janus Kinase (JAK2) [299,325,348]. These kinases are not known to be directly ROS sensitive i.e. being oxidised themselves, but are activated by GPCR in a NOX dependent manner and by exogenous ROS[349-351]. This appears to occur through SrcFK mediated phosphorylation [352,353]. This suggests that activation of FAK, PYK2 and JAK2 by ROS, may be indirect via the activation or inhibition of other proteins that are directly ROS sensitive, such as SrcFK. JAK activation also appears to require ROS-dependent activation of PYK2 [354]. To date, there are no studies showing that SrcFK are directly involved in the activation of RhoGEFs. However, SrcFKs have been shown to be directly ROS sensitive [211,213,418] and may act as ROS sensitive activators upstream of these kinases. Furthermore, RhoA has only been shown to be directly phosphorylated by PKG/PKA, which increased GDI interactions and cytosolic re-localisation, therefore inhibiting RhoA activity [525,526]. I am not aware of any studies, which indicate that RhoA is directly phosphorylated by the mentioned kinases.

In my study, I show that translocation of ARHGEF1 occurs in a SrcFK and ROS dependent manner. Furthermore, ARHGEF1 was shown to translocate to the cell periphery in response to U46619 and LY83583. Again, background intensity/fluorescent changes were investigated. Correspondingly, in response to stimulation, I see a clear movement of ARHGEF1 from the cytoplasm, where it is localized when unstimulated, to the cell periphery [336]. This was then blocked in the presence of inhibitors.

Work performed by Bhattacharyya *et al* [308] demonstrated that TP receptor activation, or indeed activation of $G\alpha_{13}$ or $G\alpha_{12}$ by an appropriate GPCR, induced translocation of endogenous

p115RhoGEF (ARHGEF1) from the cytosol to the plasma membrane. Using mutated forms of ARHGEF1, the authors discover that translocation occurs primarily due to the presence of two domains found within the ARHGEF1 structure, the regulator of G protein signalling (RGS) domain which acts as a binding site for $G\alpha_{13}$ or $G\alpha_{12}$ and a pleckstrin homology (PH) domain which is involved in membrane targeting. However, translocation alone may not be enough for GEF activation or indeed activation of RhoA/Rho-kinase signalling [308]. Bhattacharyya *et al* [308] also demonstrate, when using a novel PH domain mutation (leucine residue at position 677 was changed to proline), that PM recruitment is retained, although its signalling function is defective. This indicates a function beyond its role in membrane targeting [527,528]. The authors postulate that further protein interactions may contribute to recruitment of ARHGEF1 and the initiation of Rho activation.

Tyrosine phosphorylation is now believed to be involved in the enhancement of ARHGEF activity and stability, while at the plasma membrane. A study performed by Suzuki *et al* [345] demonstrates, that LARG is phosphorylated by Tec tyrosine kinase. The authors show that non-phosphorylated LARG is stimulated by $G\alpha_{13}$ but not $G\alpha_{12}$. Subsequently, phosphorylation by Tec tyrosine kinase allows $G\alpha_{12}$ to effectively stimulate the RhoGEF activity of LARG. These results suggest a biochemical mechanism of Rho activation through $G\alpha_{12}$, and that the regulation of RhoGEFs by heterotrimeric G proteins $G_{12/13}$ is further modulated by tyrosine phosphorylation.

Kato *et al* [529] provide evidence that the guanine exchange factor DBL, is tyrosine phosphorylated which augments its GEF activity, leading to an accumulation of GTP-bound form of Rho. These findings suggest, that the tyrosine kinase ACK1 may act as a regulator of DBL, which in turn activates Rho family proteins. Also, tyrosine phosphorylation of Vav or Vav-2 is also a requirement for their GEF activity[530]. Finally, the use of several tyrosine kinase inhibitors have been shown to block $G\alpha_{12}$- or $G\alpha_{13}$-mediated Rho activation in cells [531,532].

Taken together, these results suggest that, in response to $G_{12/13}$ activation, ARHGEFs translocate to the membrane due to the RGS and PH/DH domains [308]. However at the membrane, addition interactions are required for full activity and stability such as phosphorylation.

Following on from the initial translocation experiments, co-immunoprecipitation experiments were performed. I show for the first time that SrcFK and ARHGEF1 co-immunoprecipitate with each other in response to U46619 stimulation. This taken together with the translocation data, is highly suggestive that SrcFK interacts with ARHGEF1 in response to U46619, which may be involved in Rho-Kinase activation. CO-IP experiments were not performed in response to LY83583. However, LY83583 did promote translocation, increased SrcFK autophosphorylation and enhanced phospho-tyrosine content at ~ 115kDa (size for ARHGEF1) amongst others, all of which is inhibited by PP2. Taken together with LY83583 induced translocation of Rho-Kinase[88], I think it is fair to predict that LY83583 would have a similar effect to U46619.

Translocation by both U46619 and LY83583 was inhibited by ebselen, tempol and PP2, as were any background intensity/fluorescence changes. In response to U46619, PP2 is shown to inhibit SrcFK autophosphorylation, MYPT-1 and MLC_{20} phosphorylation. Furthermore, ebselen and tempol inhibit SrcFK, MYPT-1 and MLC_{20} phosphorylation. These results indicate that ROS activate SrcFK, which interacts with ARHGEF1 either directly or indirectly, to mediate RhoA/Rho-kinase signalling. Furthermore, as hypoxia is shown to activate SrcFK, this could also activate ARHGEF1. However, as discussed below, this could involve another GEF.

SrcFK can also regulate RhoA/Rho-Kinase signalling via interactions with RhoGDIs. RhoGDIs maintain Rho proteins in the cytoplasm by blocking the binding of RhoA into the cell membrane as well as inhibiting the binding of GTP[303,533,534]. Regulation of RhoGDIs is largely undefined.

However, DerMardirossian *et al* [318] show that that SrcFKs act as a RhoGDI kinases *in vitro* and *in vivo.* Furthermore, phosphorylation of RhoGDI by SrcFK inhibits RhoGDI function. This therefore provides another mechanism whereby SrcFK in response to ROS can regulate RhoA/Rho-kinase signalling.

There are a large number of RhoGEFs (~70) in comparison to 20 Rho proteins, so it has been suggested that different upstream signals use different RhoGEFs to activate Rho proteins, as not all 70 GEFs activate RhoA[522,535]. Accordingly, depending on the upstream signals, different RhoGEFs might be similarly used to activate RhoA in VSMCs. Examples include this study, whereby I demonstrate that U46619 promotes translocation and presumably activation of ARHGEF1 in ROS and SrcFK dependent manner. AngII has also been show to activate ARHGEF1 in a $G_{\alpha q}$ and JAK dependent manner. Furthermore, p63RhoGEF may also be activated in response to $G_{\alpha q}$ stimulation by ET1. This therefore indicates a complex network involving a number of different or receptors and GEFs which can be activated depending on the physiological setting and local factors present.

The data in this chapter demonstrates, a role for SrcFK as a ROS sensitive intermediate which interacts with ARHGEF1 and RhoA, potentially mediating the RhoA/Rho-Kinase pathway. This conclusion was reached due to the fact that inhibition of ROS with antioxidants (ebselen 1μM, tempol 3mM) and SrcFK inhibitor (PP2 1μM) abolished eGFP-tagged RhoA/ARHGEF1 translocation in PASMCs. Furthermore, treatment with U46619 enhanced CO-IP between SrcFK and ARHGEF1.

The following schematic details what I believe to be occurring within this system (Figure 5.16).

Figure 5.16:

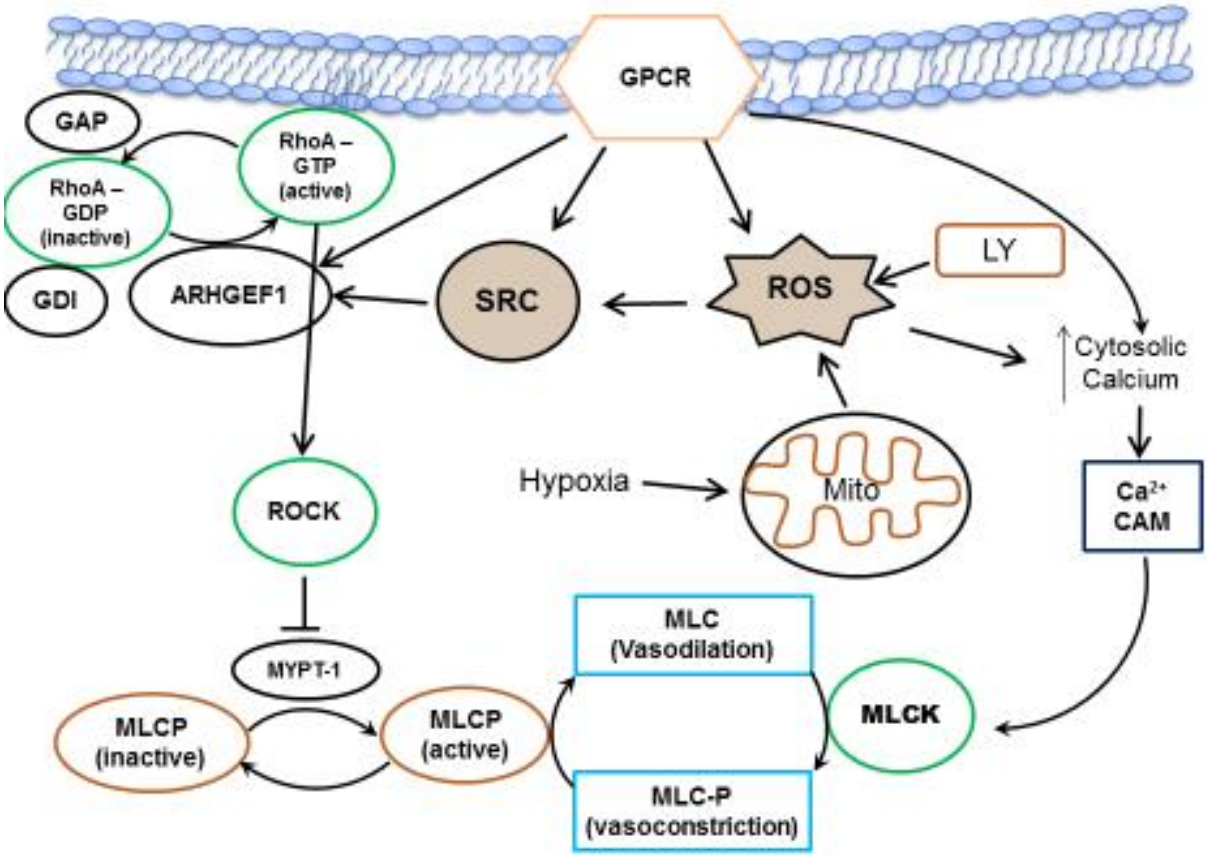

Figure 5.16: Potential upstream regulation of the RhoA/Rho-kinase pathway by ROS and SrcFK.

The data demonstrates that SrcFK act as ROS sensitive intermediates in response to endogenous and exogenous ROS. SrcFK interacts directly or indirectly with ARHGEF, which may activate RhoA/Rho-Kinase signalling.

Chapter 6:

General Discussion

6.1: Summary of Findings

In this study, I demonstrated that U46619 and LY83583 induced ROS production in PASMCs, which is sensitive to antioxidants. Furthermore, U46619 and LY83583 enhance contractile responses in IPA are inhibited by antioxidants and SrcFK inhibition. U46619, hypoxia and LY83583 enhance SrcFK autophosphorylation, ROCK activity and MLC_{20} phosphorylation which are blocked by SrcFK inhibition (U46619 and LY83583), antioxidants (U46619 and LY83583) and mitochondrial inhibitors (hypoxia). U46619 and LY83583 also promote reversible translocation of eGFP-tagged RhoA and eGFP-tagged ARHGEF1 in a SrcFK and ROS dependent. Finally, U46619 enhanced co-immunoprecipitation of ARHGEF1 with SrcFK. Overall, these results suggest that, SrcFK act as ROS sensitive intermediates which enhance contractile responses potentially via interactions with ARHGEF1 and enhanced ROCK activity.

6.2 Wider Ramifications of this work

The signalling pathways involved in smooth muscle contraction are highly diverse and complex, and still not fully understood. Smooth muscle contraction involves crosstalk between a variety of cells and mediators including signalling, structural, contractile and inflammatory molecules. It is only now apparent that reactive oxygen species (ROS) are also important secondary messengers, which can modulate normal smooth muscle function at physiological levels, particularly contractility, however, when produced in excess (oxidative stress), contribute to endothelial dysfunction and cardiovascular diseases.

A few studies, ours amongst them, have suggested that SrcFK and ROS act as upstream mediators which contributes to constriction via activation of the RhoA/Rho-kinase pathway[41,88]. Knock *et al*[7] also demonstrate a role for SrcFKs in hypoxic pulmonary vasoconstriction. However, the role of SrcFKs as a ROS sensitive intermediate activating RhoA/Rho-kinase signalling has so far not been demonstrated. The results generated here are therefore the first

study to demonstrate that SrcFKs act a ROS sensitive mediator's upstream mediator of RhoA/Rho-Kinase.

In addition to contractility, ROS, SrcFK and RhoA/Rho-Kinase are also important regulators of cell migration and proliferation, which are key events in the pathogenesis of cardiovascular diseases such as pulmonary hypertension [267,298,536], atherosclerosis[414] and ischemia-reperfusion injury[205] and represents a signalling axis which could be a therapeutic target.

How ROS and SrcFK or indeed other tyrosine kinases activate RhoA/Rho-kinase signalling is still largely unexplored. I therefore attempted to further clarify the link between SrcFK and Rho-kinase by identifying molecular targets/binding partners for SrcFK. The secondary focus of this research has explored the role of RhoGEFs, in particular the small subfamily of RGS-containing RhoGEFs, which are themselves activated by upstream signals, such as G protein–coupled receptors and tyrosine kinases, [427,537]. This led me to the hypothesis that RGS-containing RhoGEF, ARHGEF1, may be a molecular target/binding partner for SrcFK.

Our observations suggest, ROS and SrcFK are likely to be stimulating Rho-kinase via prior activation of RhoA, which in turn is perhaps associated with altered ARHGEF1 activity downstream of ROS and SrcFK activity. Based on these findings, I suggest that in other contexts, other SrcFK members (Src, Yes, Fyn) might play a similar role in regulating ARHGEF1 and consequently RhoA activity. Finally, I cannot exclude the possibility that ARHGEF1 activation could also lead to activation of the close RhoA relatives RhoB and RhoC, the role of which in vascular tone regulation is unknown.

This study describes a contractile signalling axis involving ROS, SrcFK, ARHGEF1, RhoA and Rho-kinase. In response to GPCR activation and hypoxia, SrcFKs act as ROS sensitive intermediates which may target ARHGEF1 as a potential upstream mediator of RhoA/Rho-kinase in IPA contractile responses. Furthermore, investigations into this signalling axis,

particularly SrcFK and ARHGEF1 interactions, may lead to the discovery of novel therapeutic targets for the treatment of cardiovascular diseases such as pulmonary hypertension.

6.3 Limitations of this work

The primary limitation of this study is not being able to investigate SrcFK and ARHGEF1 interactions further. At present, I show that SrcFK and ARHGEF1 interact in the presence of U46619 in IPA but not in response to LY83583 or in the presence of inhibitors ebselen, tempol or PP2. Therefore, I am unable to say that interactions between SrcFK and ARHGEF1 are SrcFK and ROS dependent or if this interaction is direct or indirect via another kinase. However, there is a precedent for direct interactions, albeit with another NRTK, JAK2[325]. I can hypothesis that LY83583 would enhance SrcFK and ARHGEF1 interactions as LY83583-enhanced U46 contractile responses occurs in a SrcFK-dependent manner, while LY83583 enhanced SrcFK activity and promoted reversible translocation of eGFP-tagged RhoA and ARHGEF1. However, without performing similar experiments to U46619 in the presence of LY83583, this may not be the case (see section 6.4, where I discuss future work).

Furthermore, I would have liked to have performed translocation, CO-IP experiments and measured ROS under hypoxic conditions. Due to the systems currently employed in the laboratory e.g. plate reader for ROS measurement, there is currently no way to keep samples hypoxic for ROS measurements or during visualisation of translocating GFP tagged proteins. However, I was able to show that hypoxia activates SrcFK in an ETC dependent manner, which subsequently activates Rho-Kinase, although the link between SrcFK and Rho-Kinase activation is still unclear. As discussed (in chapter 5), I can hypothesise that SrcFK is indeed signalling via ARHGEF1 in response to hypoxia similar to U46619, but again this may vary as different agonists and contractile stimuli can activate different ARHGEFs. Performing this set of experiments would help elucidate the signalling events involved during hypoxic pulmonary vasoconstriction.

Throughout my investigation, I used overexpression of eGFP tagged proteins as a way of visualising protein movement as a corollary of activation. However, there are a number of potential problems with over-expressing proteins and using GFP as a tag. The first being a change in phenotype and function of the cell. As RhoA is involved in a number of cellular process, overexpression can potentially lead to a fundamental change in how the cell functions. Staining of cells however confirmed that the cells were still VSMCs.

GFP also has the ability to affect the activity of the protein it is attached to either via inhibition of over activation of the protein of interest. The main point of these studies was to visualise protein movement within the cell in response to stimulation (as a corollary of activation) and whether this is affected by prior treatment with inhibitors. Therefore the effect on protein function was of secondary consideration.

Another limitation within this study is that I did not perform experiments in alpha toxin permeabilized IPA in Ca^{2+} clamped conditions. Clamping Ca^{2+} would allow me to control $[Ca^{2+}]_i$ levels at my desired level. I would have therefore been able to investigate the sensitivity of the contractile machinery without any changes in $[Ca^{2+}]_i$. Currently, changes in calcium do need to be taken into consideration. Contractile and phosphorylation studies could therefore be influenced by changes in $[Ca^{2+}]_i$ and not just calcium sensitization. Previous studies from our group, confirmed a role for Src upstream of Rho-Kinase by clamping Ca^{2+} [41] and LY83583 nsitive constriction in alpha-toxin-permeabilized IPA[88], therefore I did not need to perform these experiments myself in Ca^{2+} clamped conditions. However, I could have investigated the interactions between ROS and SrcFK under these conditions by measuring Src autophosphorylation at TYR416, Rho-Kinase via MYPT-1 (Thr-850) and MLC_{20} (ser19) in the presence of antioxidants. Thereby, confirming under these conditions, U46619 enhanced SrcFK activity and subsequently Rho-Kinase activity in a ROS dependent manner.

Ca^{2+} has not been shown to activate or indeed enhance SrcFK activity, however, JAK2[325], PYK2[538] or PKC[539] have been shown to be Ca^{2+} mediated. SrcFK activity could therefore be mediated via an indirect mechanism whereby Ca^{2+} could regulate SrcFK activity via one of these kinases.

Finally, I would have liked to have performed ROS measurements using another probe or in tissue. At present, I have one method showing an increase in ROS production, albeit using multiple PASMC lines. If I was able to demonstrate, using two different methods or using the same method but using a different biological samples e.g. tissue using L-012, or in cells using another method such as Amplex Red, that U46619 and LY83583 enhanced ROS level, this would be much more comprehensive and add more weight behind my claim that ROS are indeed generated by U46619 in my system. There is currently a debate as to whether H_2O_2, superoxide and peroxynitrite are involved in signalling and what pathways they are acting on, as discussed in the introduction and chapter 3. Having a number of methods in different biological samples may allow me to suggest what ROS species are involved e.g. L-012 measures $O_2^{\bullet-}$ and Amplex Red measures H_2O_2. Therefore, if there is an increase in L-012 signal with U46619 which was reduced by SOD, and/or an increase in Amplex Red signal with U46619 in the presence of SOD, I could infer that superoxide is being produced and is probably the main signalling moiety.

6.4 Future Work

I would have liked to perform another technique such as Fluorescence resonance energy transfer (FRET) in IPA to demonstrate protein interactions. This would further enhance my current finding that U46619 enhance SrcFK and ARHGEF1 interactions in IPA. FRET imaging methods have been instrumental in determining the compartmentalization and functional organization of living cells and for tracing the movement of proteins inside cells[540]. This has allowed for an accurate measurement of molecular proximity. FRET relies on the distance-

dependent transfer of energy from a donor molecule to an acceptor molecule [541]. Due to its sensitivity to distance, FRET has been used extensively to investigate molecular interactions and biological phenomena that produce changes in molecular proximity[542-544]. A pair of molecules that interact in such a manner, is often referred to as a donor/acceptor pair. The donor and acceptor molecules must be in close proximity to one another otherwise energy transfer does not occur, suggesting, a close interactions and confirming a close association between proteins.

Although CO-IP and FRET confirm a close interaction between molecules, it does not confirm whether this a direct interaction or whether this interaction via other molecules such as other kinases or adapter proteins. Furthermore, it does not confirm whether this interaction has an effect on activity of the target molecule. Therefore, I can still not categorically say that SrcFK is directly phosphorylating ARHGEF1 in IPA. In order to confirm that ARHGEF1 is being activated by U46619 or LY83583 in IPA, I would have to follow a similar procedure performed by Guilluy *et al*[325], who identify that ARHGEF1 mediates the effects of angiotensin II on vascular tone and blood pressure. This is something that I would have performed if I had more time, money and expertise.

Small GTPases act as molecular switches, their activity is controlled by two different biochemical reactions, GDP/GTP exchange and GTP hydrolysis. To confirm that ARHGEF1 activity is being mediated by U46619 in a ROS and SrcFK dependent manner, an *in vitro* guanine nucleotide exchange assay for RhoA would be used in the presence of U46619 and pharmacological inhibitors, ebselen, tempol and PP2. GDP/GTP ratios can be measured using a number of kits, such as cytoskeleton RhoGEF exchange assay as used by Guilluy *et al*[325]. This kit measures the uptake of the fluorescent nucleotide analog N-methylanthraniloyl-GTP (mant-GTP) into GTPases. The uptake is measured due to different fluorescent properties between free and GTPase-bound mant-GTP. As mant-GTP gets bound to the GTPase, its fluorescence

is increases dramatically. Therefore, the enhancement of mant-GTP fluorescent intensity in the presence of a small GTPase indicates nucleotide uptake (or exchange for already bound nucleotide) by the GTPase. I would therefore expect, that U46619 and LY83583 would enhance the exchange activity which would be blocked by antioxidants and PP2 in IPA.

To determine that SrcFK directly interacts with ARHGEF1, I would like to investigate the phosphorylation status of ARHGEF1. Currently, there are no commercially available phospho-ARHGEF1 antibodies. However, I would expect an increase in ARHGEF1 phosphorylation in response to stimuli which is blocked by inhibitors. This would indicate that phosphorylation of ARHGEF is SrcFK and ROS dependent. The data generated, would also complement the data already obtained (e.g. SrcFK, MYPT-1 and MLC_{20} phosphorylation responses) thus providing a functional role of ARHGEF1 phosphorylation.

To further augment these results, I would have liked to have carried out transient knockdown of Src or ARHGEF1 using small interference (siRNA) in PASMCs. This could be followed by investigating MYPT-1, MLC_{20} and ARHGEF1 phosphorylation along with eGFP-tagged RhoA or eGFP-tagged ARHGEF1 translocation responses. Although pharmacological inhibitors are useful at blocking the effects of a proteins or chemically reactive molecules, siRNA knockdown of a proteins can reduce proteins activity of the specific proteins. This would be more cumbersome and time consuming but offers several advantages including avoiding off-target effects and it is easier to determine the level of protein activity by determining the efficiency of knockdown. I would expect that if siRNA against Src or ARHGEF1 was transfected into PASMCs, then agonist stimulation of MYPT-1, MLC_{20} and ARHGEF1 phosphorylation along with translocation of eGFP-tagged RhoA or eGFP-tagged ARHGEF1 would be inhibited, similar to what was already observed. Furthermore, I would have liked to of used ARHGEF1 knockdown or knockout models in contraction studies to show the importance of ARHGEF1 in contraction.

Finally, to add more depth to my interaction studies, I would have liked to have performed co-localisation studies between SrcFK, ARHGEF1, focal adhesion kinase (FAK) and caveolin. RhoA and ARHGEF1 translocate to the cell periphery however I do not know where they are translocated to i.e. which structure. The primarily structures could be membrane proteins called caveolin or focal adhesions. Caveolin act as scaffold proteins and signalling domains whilst focal adhesions act as sub-cellular structures that mediate the regulatory effects (i.e., signalling events) of a cell in response to ECM adhesion. Therefore, being able to stain for these proteins and investigating where they localise can also give an insight into what other proteins they may interact with.

6.5 Conclusion

In conclusion, this thesis presents novel finding relating to the upstream regulation of the Rho-Kinase pathway in rat Pulmonary arteries. The results presented, represent a valuable mechanism into smooth muscle contractility in Pulmonary arteries.

Many of the studies that have been published has focussed on the role of Rho-Kinase in Ca^{2+} sensitization. However, it is only recently that more attention has been paid to the upstream regulation of Rho-Kinase. In the context of many vascular diseases and oxidative stress, the signalling axis suggested could represent a potential target pathway which should be explored further.

This thesis demonstrates that SrcFK plays an important role as a ROS sensitive mediator acting upstream of Rho-Kinase signalling. I have demonstrated that SrcFK interacts with ARHGEF1. However, SrcFKs interactions with regards to other RhoGEFs and its role in hypoxia mediated Ca^{2+} sensitization remains unclear. My thesis demonstrates crosstalk between agonist induced ROS production, SrcFK and Rho-Kinase activation and therefore shows a new pathway whereby Rho-Kinase is regulated in pulmonary artery.

References

1. Simonneau G, Gatzoulis MA, Adatia I, et al. Updated clinical classification of pulmonary hypertension. *J Am Coll Cardiol*. 2013;62(25 Suppl):D34-41.
2. Stenmark KR, Meyrick B, Galie N, Mooi WJ, McMurtry IF. Animal models of pulmonary arterial hypertension: the hope for etiological discovery and pharmacological cure. *Am J Physiol Lung Cell Mol Physiol*. 2009;297(6):L1013-1032.
3. Chaouat A, Naeije R, Weitzenblum E. Pulmonary hypertension in COPD. *Eur Respir J*. 2008;32(5):1371-1385.
4. Euler USv, Liljestrand G. Observations on the Pulmonary Arterial Blood Pressure in the Cat.
5. Detar R. Mechanism of physiological hypoxia-induced depression of vascular smooth muscle contraction. *Am J Physiol*. 1980;238(6):H761-769.
6. Gupte SA, Wolin MS. Oxidant and redox signaling in vascular oxygen sensing: implications for systemic and pulmonary hypertension. *Antioxid Redox Signal*. 2008;10(6):1137-1152.
7. Knock GA, Snetkov VA, Shaifta Y, Drndarski S, Ward JP, Aaronson PI. Role of src-family kinases in hypoxic vasoconstriction of rat pulmonary artery. *Cardiovasc Res*. 2008;80(3):453-462.
8. Guyton AC, Carrier O, Jr., Walker JR. EVIDENCE FOR TISSUE OXYGEN DEMAND AS THE MAJOR FACTOR CAUSING AUTOREGULATION. *Circ Res*. 1964;15:Suppl:60-69.
9. Michelakis ED, Hampl V, Nsair A, et al. Diversity in mitochondrial function explains differences in vascular oxygen sensing. *Circ Res*. 2002;90(12):1307-1315.
10. Humbert M, Sitbon O, Simonneau G. Treatment of pulmonary arterial hypertension. *N Engl J Med*. 2004;351(14):1425-1436.
11. O'Callaghan DS, Savale L, Montani D, et al. Treatment of pulmonary arterial hypertension with targeted therapies. *Nat Rev Cardiol*. 2011;8(9):526-538.
12. Kitazawa T, Masuo M, Somlyo AP. G protein-mediated inhibition of myosin light-chain phosphatase in vascular smooth muscle. *Proc Natl Acad Sci U S A*. 1991;88(20):9307-9310.
13. Ichikawa K, Ito M, Hartshorne DJ. Phosphorylation of the large subunit of myosin phosphatase and inhibition of phosphatase activity. *J Biol Chem*. 1996;271(9):4733-4740.
14. Stenmark KR, Fagan KA, Frid MG. Hypoxia-induced pulmonary vascular remodeling: cellular and molecular mechanisms. *Circ Res*. 2006;99(7):675-691.

15. Broughton BR, Walker BR, Resta TC. Chronic hypoxia induces Rho kinase-dependent myogenic tone in small pulmonary arteries. *Am J Physiol Lung Cell Mol Physiol*. 2008;294(4):L797-806.

16. Amano M, Nakayama M, Kaibuchi K. Rho-kinase/ROCK: A key regulator of the cytoskeleton and cell polarity. *Cytoskeleton (Hoboken)*. 2010;67(9):545-554.

17. Wray S, Burdyga T. Sarcoplasmic reticulum function in smooth muscle. *Physiol Rev*. 2010;90(1):113-178.

18. Clapham DE. Calcium signaling. *Cell*. 2007;131(6):1047-1058.

19. Mikoshiba K. IP3 receptor/Ca2+ channel: from discovery to new signaling concepts. *J Neurochem*. 2007;102(5):1426-1446.

20. Aires V, Hichami A, Boulay G, Khan NA. Activation of TRPC6 calcium channels by diacylglycerol (DAG)-containing arachidonic acid: a comparative study with DAG-containing docosahexaenoic acid. *Biochimie*. 2007;89(8):926-937.

21. Parekh AB, Putney JW, Jr. Store-operated calcium channels. *Physiol Rev*. 2005;85(2):757-810.

22. McFadzean I, Gibson A. The developing relationship between receptor-operated and store-operated calcium channels in smooth muscle. *Br J Pharmacol*. 2002;135(1):1-13.

23. Endo M. Calcium release from the sarcoplasmic reticulum. *Physiol Rev*. 1977;57(1):71-108.

24. Fabiato A. Calcium-induced release of calcium from the cardiac sarcoplasmic reticulum. *Am J Physiol*. 1983;245(1):C1-14.

25. Collier ML, Ji G, Wang Y, Kotlikoff MI. Calcium-induced calcium release in smooth muscle: loose coupling between the action potential and calcium release. *J Gen Physiol*. 2000;115(5):653-662.

26. Gouaux E, Mackinnon R. Principles of selective ion transport in channels and pumps. *Science*. 2005;310(5753):1461-1465.

27. Amberg GC, Navedo MF. Calcium dynamics in vascular smooth muscle. *Microcirculation*. 2013;20(4):281-289.

28. Periasamy M, Kalyanasundaram A. SERCA pump isoforms: their role in calcium transport and disease. *Muscle Nerve*. 2007;35(4):430-442.

29. Somlyo AP, Somlyo AV. Ca2+ sensitivity of smooth muscle and nonmuscle myosin II: modulated by G proteins, kinases, and myosin phosphatase. *Physiol Rev*. 2003;83(4):1325-1358.

30. Kitazawa T, Kobayashi S, Horiuti K, Somlyo AV, Somlyo AP. Receptor-coupled, permeabilized smooth muscle. Role of the phosphatidylinositol cascade, G-proteins, and modulation of the contractile response to Ca2+. *J Biol Chem*. 1989;264(10):5339-5342.

31. Somlyo AP, Himpens B. Cell calcium and its regulation in smooth muscle. *Faseb j*. 1989;3(11):2266-2276.

32. Trinkle-Mulcahy L, Ichikawa K, Hartshorne DJ, Siegman MJ, Butler TM. Thiophosphorylation of the 130-kDa subunit is associated with a decreased activity of myosin light chain phosphatase in alpha-toxin-permeabilized smooth muscle. *J Biol Chem*. 1995;270(31):18191-18194.

33. Kimura K, Ito M, Amano M, et al. Regulation of myosin phosphatase by Rho and Rho-associated kinase (Rho-kinase). *Science*. 1996;273(5272):245-248.

34. Ito M, Nakano T, Erdodi F, Hartshorne DJ. Myosin phosphatase: structure, regulation and function. *Mol Cell Biochem*. 2004;259(1-2):197-209.

35. Brozovich FV. Myosin light chain phosphatase: it gets around. *Circ Res*. 2002;90(5):500-502.

36. Hirano K, Hirano M, Kanaide H. Regulation of myosin phosphorylation and myofilament Ca2+ sensitivity in vascular smooth muscle. *J Smooth Muscle Res*. 2004;40(6):219-236.

37. Hartshorne DJ, Ito M, Erdodi F. Myosin light chain phosphatase: subunit composition, interactions and regulation. *J Muscle Res Cell Motil*. 1998;19(4):325-341.

38. MacDonald JA, Eto M, Borman MA, Brautigan DL, Haystead TA. Dual Ser and Thr phosphorylation of CPI-17, an inhibitor of myosin phosphatase, by MYPT-associated kinase. *FEBS Lett*. 2001;493(2-3):91-94.

39. Kiss E, Muranyi A, Csortos C, et al. Integrin-linked kinase phosphorylates the myosin phosphatase target subunit at the inhibitory site in platelet cytoskeleton. *Biochem J*. 2002;365(Pt 1):79-87.

40. Velasco G, Armstrong C, Morrice N, Frame S, Cohen P. Phosphorylation of the regulatory subunit of smooth muscle protein phosphatase 1M at Thr850 induces its dissociation from myosin. *FEBS Lett*. 2002;527(1-3):101-104.

41. Knock GA, Shaifta Y, Snetkov VA, et al. Interaction between src family kinases and rho-kinase in agonist-induced Ca2+-sensitization of rat pulmonary artery. *Cardiovasc Res*. 2008;77(3):570-579.

42. Wilson DP, Susnjar M, Kiss E, Sutherland C, Walsh MP. Thromboxane A2-induced contraction of rat caudal arterial smooth muscle involves activation of Ca2+ entry and Ca2+

sensitization: Rho-associated kinase-mediated phosphorylation of MYPT1 at Thr-855, but not Thr-697. *Biochem J*. 2005;389(Pt 3):763-774.

43. Kitazawa T, Eto M, Woodsome TP, Khalequzzaman M. Phosphorylation of the myosin phosphatase targeting subunit and CPI-17 during Ca2+ sensitization in rabbit smooth muscle. *J Physiol*. 2003;546(Pt 3):879-889.

44. Mueed I, Zhang L, MacLeod KM. Role of the PKC/CPI-17 pathway in enhanced contractile responses of mesenteric arteries from diabetic rats to alpha-adrenoceptor stimulation. *Br J Pharmacol*. 2005;146(7):972-982.

45. Zemlickova E, Johannes FJ, Aitken A, Dubois T. Association of CPI-17 with protein kinase C and casein kinase I. *Biochem Biophys Res Commun*. 2004;316(1):39-47.

46. Gong MC, Fujihara H, Somlyo AV, Somlyo AP. Translocation of rhoA associated with Ca2+ sensitization of smooth muscle. *J Biol Chem*. 1997;272(16):10704-10709.

47. Gong MC, Iizuka K, Nixon G, et al. Role of guanine nucleotide-binding proteins--ras-family or trimeric proteins or both--in Ca2+ sensitization of smooth muscle. *Proc Natl Acad Sci U S A*. 1996;93(3):1340-1345.

48. Mita M, Yanagihara H, Hishinuma S, Saito M, Walsh MP. Membrane depolarization-induced contraction of rat caudal arterial smooth muscle involves Rho-associated kinase. *Biochem J*. 2002;364(Pt 2):431-440.

49. Buyukafsar K, Levent A, Ark M. Expression of Rho-kinase and its functional role in the contractile activity of the mouse vas deferens. *Br J Pharmacol*. 2003;140(4):743-749.

50. Asano M, Nomura Y. Comparison of inhibitory effects of Y-27632, a Rho kinase inhibitor, in strips of small and large mesenteric arteries from spontaneously hypertensive and normotensive Wistar-Kyoto rats. *Hypertens Res*. 2003;26(1):97-106.

51. Ghisdal P, Vandenberg G, Morel N. Rho-dependent kinase is involved in agonist-activated calcium entry in rat arteries. *J Physiol*. 2003;551(Pt 3):855-867.

52. Urban NH, Berg KM, Ratz PH. K+ depolarization induces RhoA kinase translocation to caveolae and Ca2+ sensitization of arterial muscle. *Am J Physiol Cell Physiol*. 2003;285(6):C1377-1385.

53. Liu QH, Zheng YM, Korde AS, et al. Membrane depolarization causes a direct activation of G protein-coupled receptors leading to local Ca2+ release in smooth muscle. *Proc Natl Acad Sci U S A*. 2009;106(27):11418-11423.

54. Sakurada S, Takuwa N, Sugimoto N, et al. Ca2+-dependent activation of Rho and Rho kinase in membrane depolarization-induced and receptor stimulation-induced vascular smooth muscle contraction. *Circ Res*. 2003;93(6):548-556.

55. Farnsworth CL, Freshney NW, Rosen LB, Ghosh A, Greenberg ME, Feig LA. Calcium activation of Ras mediated by neuronal exchange factor Ras-GRF. *Nature*. 1995;376(6540):524-527.

56. Janssen LJ, Tazzeo T, Zuo J, Pertens E, Keshavjee S. KCl evokes contraction of airway smooth muscle via activation of RhoA and Rho-kinase. *Am J Physiol Lung Cell Mol Physiol*. 2004;287(4):L852-858.

57. Vetter SW, Leclerc E. Novel aspects of calmodulin target recognition and activation. *Eur J Biochem*. 2003;270(3):404-414.

58. Ito S, Kume H, Yamaki K, et al. Regulation of capacitative and noncapacitative receptor-operated Ca2+ entry by rho-kinase in tracheal smooth muscle. *Am J Respir Cell Mol Biol*. 2002;26(4):491-498.

59. Shabir S, Borisova L, Wray S, Burdyga T. Rho-kinase inhibition and electromechanical coupling in rat and guinea-pig ureter smooth muscle: Ca2+-dependent and -independent mechanisms. *J Physiol*. 2004;560(Pt 3):839-855.

60. Gocek E, Moulas AN, Studzinski GP. Non-receptor protein tyrosine kinases signaling pathways in normal and cancer cells. *Crit Rev Clin Lab Sci*. 2014;51(3):125-137.

61. Di Salvo J, Nelson SR, Kaplan N. Protein tyrosine phosphorylation in smooth muscle: a potential coupling mechanism between receptor activation and intracellular calcium. *Proc Soc Exp Biol Med*. 1997;214(4):285-301.

62. Di Salvo J, Pfitzer G, Semenchuk LA. Protein tyrosine phosphorylation, cellular Ca2+, and Ca2+ sensitivity for contraction of smooth muscle. *Can J Physiol Pharmacol*. 1994;72(11):1434-1439.

63. Touyz RM, Wu XH, He G, et al. Role of c-Src in the regulation of vascular contraction and Ca2+ signaling by angiotensin II in human vascular smooth muscle cells. *J Hypertens*. 2001;19(3):441-449.

64. Marrero MB, Paxton WG, Duff JL, Berk BC, Bernstein KE. Angiotensin II stimulates tyrosine phosphorylation of phospholipase C-gamma 1 in vascular smooth muscle cells. *J Biol Chem*. 1994;269(14):10935-10939.

65. Marrero MB, Schieffer B, Bernstein KE, Ling BN. Angiotensin II-induced tyrosine phosphorylation in mesangial and vascular smooth muscle cells. *Clin Exp Pharmacol Physiol*. 1996;23(1):83-88.

66. Seki T, Yokoshiki H, Sunagawa M, Nakamura M, Sperelakis N. Angiotensin II stimulation of Ca2+-channel current in vascular smooth muscle cells is inhibited by lavendustin-A and LY-294002. *Pflugers Arch*. 1999;437(3):317-323.

67. Wijetunge S, Aalkjaer C, Schachter M, Hughes AD. Tyrosine kinase inhibitors block calcium channel currents in vascular smooth muscle cells. *Biochem Biophys Res Commun*. 1992;189(3):1620-1623.

68. Liu H, Sperelakis N. Tyrosine kinases modulate the activity of single L-type calcium channels in vascular smooth muscle cells from rat portal vein. *Can J Physiol Pharmacol*. 1997;75(9):1063-1068.

69. Xiong Z, Burnette E, Cheung DW. Modulation of Ca(2+)-activated K+ channel activity by tyrosine kinase inhibitors in vascular smooth muscle cell. *Eur J Pharmacol*. 1995;290(2):117-123.

70. Nagaraj C, Tang B, Balint Z, et al. Src tyrosine kinase is crucial for potassium channel function in human pulmonary arteries. *Eur Respir J*. 2013;41(1):85-95.

71. Chopra LC, Hucks D, Twort CH, Ward JP. Effects of protein tyrosine kinase inhibitors on contractility of isolated bronchioles of the rat. *Am J Respir Cell Mol Biol*. 1997;16(4):372-378.

72. Laniyonu AA, Saifeddine M, Yang SG, Hollenberg MD. Tyrosine kinase inhibitors and the contractile action of G-protein-linked vascular agonists. *Can J Physiol Pharmacol*. 1994;72(9):1075-1085.

73. Steusloff A, Paul E, Semenchuk LA, Di Salvo J, Pfitzer G. Modulation of Ca2+ sensitivity in smooth muscle by genistein and protein tyrosine phosphorylation. *Arch Biochem Biophys*. 1995;320(2):236-242.

74. Gordon AR. Contraction of detergent-treated smooth muscle. *Proc Natl Acad Sci U S A*. 1978;75(7):3527-3530.

75. Toma C, Jensen PE, Prieto D, Hughes A, Mulvany MJ, Aalkjaer C. Effects of tyrosine kinase inhibitors on the contractility of rat mesenteric resistance arteries. *Br J Pharmacol*. 1995;114(6):1266-1272.

76. Ohanian J, Ohanian V, Shaw L, Bruce C, Heagerty AM. Involvement of tyrosine phosphorylation in endothelin-1-induced calcium-sensitization in rat small mesenteric arteries. *Br J Pharmacol*. 1997;120(4):653-661.

77. Martinez MC, Randriamboavonjy V, Ohlmann P, et al. Involvement of protein kinase C, tyrosine kinases, and Rho kinase in Ca(2+) handling of human small arteries. *Am J Physiol Heart Circ Physiol*. 2000;279(3):H1228-1238.

78. Sasaki M, Hattori Y, Tomita F, et al. Tyrosine phosphorylation as a convergent pathway of heterotrimeric G protein- and rho protein-mediated Ca2+ sensitization of smooth muscle of rabbit mesenteric artery. *Br J Pharmacol*. 1998;125(8):1651-1660.

79. Asano T, Pedersen SE, Scott CW, Ross EM. Reconstitution of catecholamine-stimulated binding of guanosine 5'-O-(3-thiotriphosphate) to the stimulatory GTP-binding protein of adenylate cyclase. *Biochemistry*. 1984;23(23):5460-5467.

80. Kurose H, Katada T, Haga T, Haga K, Ichiyama A, Ui M. Functional interaction of purified muscarinic receptors with purified inhibitory guanine nucleotide regulatory proteins reconstituted in phospholipid vesicles. *J Biol Chem*. 1986;261(14):6423-6428.

81. Sternweis PC, Robishaw JD. Isolation of two proteins with high affinity for guanine nucleotides from membranes of bovine brain. *J Biol Chem*. 1984;259(22):13806-13813.

82. Nakao F, Kobayashi S, Mogami K, et al. Involvement of Src family protein tyrosine kinases in Ca(2+) sensitization of coronary artery contraction mediated by a sphingosylphosphorylcholine-Rho-kinase pathway. *Circ Res*. 2002;91(10):953-960.

83. Shaifta Y, Irechukwu N, Prieto-Lloret J, et al. Divergent modulation of Rho-kinase and Ca influx pathways by Src family kinases and focal adhesion kinase in airway smooth muscle. *Br J Pharmacol*. 2015.

84. Griendling KK, Minieri CA, Ollerenshaw JD, Alexander RW. Angiotensin II stimulates NADH and NADPH oxidase activity in cultured vascular smooth muscle cells. *Circ Res*. 1994;74(6):1141-1148.

85. Griendling KK, Sorescu D, Lassegue B, Ushio-Fukai M. Modulation of protein kinase activity and gene expression by reactive oxygen species and their role in vascular physiology and pathophysiology. *Arterioscler Thromb Vasc Biol*. 2000;20(10):2175-2183.

86. Liaudet L, Vassalli G, Pacher P. Role of peroxynitrite in the redox regulation of cell signal transduction pathways. *Front Biosci (Landmark Ed)*. 2009;14:4809-4814.

87. Janssen-Heininger YM, Mossman BT, Heintz NH, et al. Redox-based regulation of signal transduction: principles, pitfalls, and promises. *Free Radic Biol Med*. 2008;45(1):1-17.

88. Knock GA, Snetkov VA, Shaifta Y, et al. Superoxide constricts rat pulmonary arteries via Rho-kinase-mediated Ca(2+) sensitization. *Free Radic Biol Med*. 2009;46(5):633-642.

89. Snetkov VA, Smirnov SV, Kua J, Aaronson PI, Ward JP, Knock GA. Superoxide differentially controls pulmonary and systemic vascular tone through multiple signalling pathways. *Cardiovasc Res*. 2011;89(1):214-224.

90. Fridovich I. Superoxide radical: an endogenous toxicant. *Annu Rev Pharmacol Toxicol*. 1983;23:239-257.

91. Nisimoto Y, Diebold BA, Cosentino-Gomes D, Lambeth JD. Nox4: a hydrogen peroxide-generating oxygen sensor. *Biochemistry*. 2014;53(31):5111-5120.

92. Knock GA, Ward JP. Redox regulation of protein kinases as a modulator of vascular function. *Antioxid Redox Signal*. 2011;15(6):1531-1547.

93. Leach RM, Hill HM, Snetkov VA, Robertson TP, Ward JP. Divergent roles of glycolysis and the mitochondrial electron transport chain in hypoxic pulmonary vasoconstriction of the rat: identity of the hypoxic sensor. *J Physiol*. 2001;536(Pt 1):211-224.

94. Waypa GB, Marks JD, Guzy RD, et al. Superoxide generated at mitochondrial complex III triggers acute responses to hypoxia in the pulmonary circulation. *Am J Respir Crit Care Med*. 2013;187(4):424-432.

95. Bedard K, Lardy B, Krause KH. NOX family NADPH oxidases: not just in mammals. *Biochimie*. 2007;89(9):1107-1112.

96. Foreman J, Demidchik V, Bothwell JH, et al. Reactive oxygen species produced by NADPH oxidase regulate plant cell growth. *Nature*. 2003;422(6930):442-446.

97. Nauseef WM. Biological roles for the NOX family NADPH oxidases. *J Biol Chem*. 2008;283(25):16961-16965.

98. Bedard K, Krause KH. The NOX family of ROS-generating NADPH oxidases: physiology and pathophysiology. *Physiol Rev*. 2007;87(1):245-313.

99. Shaifta Y, Snetkov VA, Prieto-Lloret J, et al. Sphingosylphosphorylcholine potentiates vasoreactivity and voltage-gated Ca2+ entry via NOX1 and reactive oxygen species. *Cardiovasc Res*. 2015;106(1):121-130.

100. Dikalov SI, Dikalova AE, Bikineyeva AT, Schmidt HH, Harrison DG, Griendling KK. Distinct roles of Nox1 and Nox4 in basal and angiotensin II-stimulated superoxide and hydrogen peroxide production. *Free Radic Biol Med*. 2008;45(9):1340-1351.

101. Snelgrove R, Williams A, Thorpe C, Hussell T. Manipulation of immunity to and pathology of respiratory infections. *Expert Rev Anti Infect Ther*. 2004;2(3):413-426.

102. Dikalov SI, Nazarewicz RR, Bikineyeva A, et al. Nox2-induced production of mitochondrial superoxide in angiotensin II-mediated endothelial oxidative stress and hypertension. *Antioxid Redox Signal*. 2014;20(2):281-294.

103. Martin JG, Suzuki M, Maghni K, et al. The immunomodulatory actions of prostaglandin E2 on allergic airway responses in the rat. *J Immunol*. 2002;169(7):3963-3969.

104. Briones AM, Tabet F, Callera GE, et al. Differential regulation of Nox1, Nox2 and Nox4 in vascular smooth muscle cells from WKY and SHR. *J Am Soc Hypertens*. 2011;5(3):137-153.

105. Chakraborti S, Roy S, Mandal A, Chowdhury A, Chakraborti T. Role of PKC-zeta in NADPH oxidase-PKCalpha-Gialpha axis dependent inhibition of beta-adrenergic response by

U46619 in pulmonary artery smooth muscle cells. *Arch Biochem Biophys*. 2013;540(1-2):133-144.

106. Banfi B, Malgrange B, Knisz J, Steger K, Dubois-Dauphin M, Krause KH. NOX3, a superoxide-generating NADPH oxidase of the inner ear. *J Biol Chem*. 2004;279(44):46065-46072.

107. Babior BM. NADPH oxidase: an update. *Blood*. 1999;93(5):1464-1476.

108. Noguera A, Batle S, Miralles C, et al. Enhanced neutrophil response in chronic obstructive pulmonary disease. *Thorax*. 2001;56(6):432-437.

109. Fink MP. Ethyl pyruvate: a novel anti-inflammatory agent. *J Intern Med*. 2007;261(4):349-362.

110. Fulton DJ. Nox5 and the regulation of cellular function. *Antioxid Redox Signal*. 2009;11(10):2443-2452.

111. Chen Q, Powell DW, Rane MJ, et al. Akt phosphorylates p47phox and mediates respiratory burst activity in human neutrophils. *J Immunol*. 2003;170(10):5302-5308.

112. Rada B, Leto TL. Characterization of hydrogen peroxide production by Duox in bronchial epithelial cells exposed to Pseudomonas aeruginosa. *FEBS Lett*. 2010;584(5):917-922.

113. Harper RW, Xu C, McManus M, Heidersbach A, Eiserich JP. Duox2 exhibits potent heme peroxidase activity in human respiratory tract epithelium. *FEBS Lett*. 2006;580(22):5150-5154.

114. Yoshizawa-Ogasawara A, Ogikubo S, Satoh M, Narumi S, Hasegawa T. Congenital hypothyroidism caused by a novel mutation of the dual oxidase 2 (DUOX2) gene. *J Pediatr Endocrinol Metab*. 2013;26(1-2):45-52.

115. Brown DI, Griendling KK. Nox proteins in signal transduction. *Free Radic Biol Med*. 2009;47(9):1239-1253.

116. Cruzado MC, Risler NR, Miatello RM, Yao G, Schiffrin EL, Touyz RM. Vascular smooth muscle cell NAD(P)H oxidase activity during the development of hypertension: Effect of angiotensin II and role of insulinlike growth factor-1 receptor transactivation. *Am J Hypertens*. 2005;18(1):81-87.

117. Jernigan NL, Walker BR, Resta TC. Reactive oxygen species mediate RhoA/Rho kinase-induced Ca2+ sensitization in pulmonary vascular smooth muscle following chronic hypoxia. *Am J Physiol Lung Cell Mol Physiol*. 2008;295(3):L515-529.

118. Wedgwood S, Dettman RW, Black SM. ET-1 stimulates pulmonary arterial smooth muscle cell proliferation via induction of reactive oxygen species. *Am J Physiol Lung Cell Mol Physiol*. 2001;281(5):L1058-1067.

119. Patterson C, Ruef J, Madamanchi NR, et al. Stimulation of a vascular smooth muscle cell NAD(P)H oxidase by thrombin. Evidence that p47(phox) may participate in forming this oxidase in vitro and in vivo. *J Biol Chem*. 1999;274(28):19814-19822.

120. Helmcke I, Heumuller S, Tikkanen R, Schroder K, Brandes RP. Identification of structural elements in Nox1 and Nox4 controlling localization and activity. *Antioxid Redox Signal*. 2009;11(6):1279-1287.

121. Banfi B, Tirone F, Durussel I, et al. Mechanism of Ca2+ activation of the NADPH oxidase 5 (NOX5). *J Biol Chem*. 2004;279(18):18583-18591.

122. Ameziane-El-Hassani R, Morand S, Boucher JL, et al. Dual oxidase-2 has an intrinsic Ca2+-dependent H2O2-generating activity. *J Biol Chem*. 2005;280(34):30046-30054.

123. Han CH, Freeman JL, Lee T, Motalebi SA, Lambeth JD. Regulation of the neutrophil respiratory burst oxidase. Identification of an activation domain in p67(phox). *J Biol Chem*. 1998;273(27):16663-16668.

124. el Benna J, Faust LP, Babior BM. The phosphorylation of the respiratory burst oxidase component p47phox during neutrophil activation. Phosphorylation of sites recognized by protein kinase C and by proline-directed kinases. *J Biol Chem*. 1994;269(38):23431-23436.

125. Fontayne A, Dang PM, Gougerot-Pocidalo MA, El-Benna J. Phosphorylation of p47phox sites by PKC alpha, beta II, delta, and zeta: effect on binding to p22phox and on NADPH oxidase activation. *Biochemistry*. 2002;41(24):7743-7750.

126. Chowdhury AK, Watkins T, Parinandi NL, et al. Src-mediated tyrosine phosphorylation of p47phox in hyperoxia-induced activation of NADPH oxidase and generation of reactive oxygen species in lung endothelial cells. *J Biol Chem*. 2005;280(21):20700-20711.

127. Gorzalczany Y, Sigal N, Itan M, Lotan O, Pick E. Targeting of Rac1 to the phagocyte membrane is sufficient for the induction of NADPH oxidase assembly. *J Biol Chem*. 2000;275(51):40073-40081.

128. Serrander L, Cartier L, Bedard K, et al. NOX4 activity is determined by mRNA levels and reveals a unique pattern of ROS generation. *Biochem J*. 2007;406(1):105-114.

129. Bedard K, Jaquet V, Krause KH. NOX5: from basic biology to signaling and disease. *Free Radic Biol Med*. 2012;52(4):725-734.

130. Arakawa N, Katsuyama M, Matsuno K, et al. Novel transcripts of Nox1 are regulated by alternative promoters and expressed under phenotypic modulation of vascular smooth muscle cells. *Biochem J*. 2006;398(2):303-310.

131. Nishiyama A, Yoshizumi M, Hitomi H, et al. The SOD mimetic tempol ameliorates glomerular injury and reduces mitogen-activated protein kinase activity in Dahl salt-sensitive rats. *J Am Soc Nephrol*. 2004;15(2):306-315.

132. Clempus RE, Sorescu D, Dikalova AE, et al. Nox4 is required for maintenance of the differentiated vascular smooth muscle cell phenotype. *Arterioscler Thromb Vasc Biol*. 2007;27(1):42-48.

133. Ellmark SH, Dusting GJ, Fui MN, Guzzo-Pernell N, Drummond GR. The contribution of Nox4 to NADPH oxidase activity in mouse vascular smooth muscle. *Cardiovasc Res*. 2005;65(2):495-504.

134. Cogolludo A, Frazziano G, Cobeno L, et al. Role of reactive oxygen species in Kv channel inhibition and vasoconstriction induced by TP receptor activation in rat pulmonary arteries. *Ann N Y Acad Sci*. 2006;1091:41-51.

135. Chakraborti S, Chowdhury A, Kar P, et al. Role of protein kinase C in NADPH oxidase derived O2*(-)-mediated regulation of KV-LVOCC axis under U46619 induced increase in [Ca2+]i in pulmonary smooth muscle cells. *Arch Biochem Biophys*. 2009;487(2):123-130.

136. Murphy MP. How mitochondria produce reactive oxygen species. *Biochem J*. 2009;417(1):1-13.

137. Kussmaul L, Hirst J. The mechanism of superoxide production by NADH:ubiquinone oxidoreductase (complex I) from bovine heart mitochondria. *Proc Natl Acad Sci U S A*. 2006;103(20):7607-7612.

138. Misra HP, Fridovich I. The univalent reduction of oxygen by reduced flavins and quinones. *J Biol Chem*. 1972;247(1):188-192.

139. Muller FL, Liu Y, Van Remmen H. Complex III releases superoxide to both sides of the inner mitochondrial membrane. *J Biol Chem*. 2004;279(47):49064-49073.

140. Waypa GB, Chandel NS, Schumacker PT. Model for hypoxic pulmonary vasoconstriction involving mitochondrial oxygen sensing. *Circ Res*. 2001;88(12):1259-1266.

141. Waypa GB, Schumacker PT. Hypoxic pulmonary vasoconstriction: redox events in oxygen sensing. *J Appl Physiol (1985)*. 2005;98(1):404-414.

142. Dikalov S, Griendling KK, Harrison DG. Measurement of reactive oxygen species in cardiovascular studies. *Hypertension*. 2007;49(4):717-727.

143. Andrukhiv A, Costa AD, West IC, Garlid KD. Opening mitoKATP increases superoxide generation from complex I of the electron transport chain. *Am J Physiol Heart Circ Physiol*. 2006;291(5):H2067-2074.

144. Doughan AK, Harrison DG, Dikalov SI. Molecular mechanisms of angiotensin II-mediated mitochondrial dysfunction: linking mitochondrial oxidative damage and vascular endothelial dysfunction. *Circ Res*. 2008;102(4):488-496.

145. Korde AS, Yadav VR, Zheng YM, Wang YX. Primary role of mitochondrial Rieske iron-sulfur protein in hypoxic ROS production in pulmonary artery myocytes. *Free Radic Biol Med*. 2011;50(8):945-952.

146. Schumacker PT. Lung cell hypoxia: role of mitochondrial reactive oxygen species signaling in triggering responses. *Proc Am Thorac Soc*. 2011;8(6):477-484.

147. Forstermann U. Oxidative stress in vascular disease: causes, defense mechanisms and potential therapies. *Nat Clin Pract Cardiovasc Med*. 2008;5(6):338-349.

148. Kahles T, Luedike P, Endres M, et al. NADPH oxidase plays a central role in blood-brain barrier damage in experimental stroke. *Stroke*. 2007;38(11):3000-3006.

149. Kondo T, Reaume AG, Huang TT, et al. Reduction of CuZn-superoxide dismutase activity exacerbates neuronal cell injury and edema formation after transient focal cerebral ischemia. *J Neurosci*. 1997;17(11):4180-4189.

150. Alfonso-Prieto M, Biarnes X, Vidossich P, Rovira C. The molecular mechanism of the catalase reaction. *J Am Chem Soc*. 2009;131(33):11751-11761.

151. Bae ON, Lim KM, Han JY, et al. U-shaped dose response in vasomotor tone: a mixed result of heterogenic response of multiple cells to xenobiotics. *Toxicol Sci*. 2008;103(1):181-190.

152. Schafer FQ, Buettner GR. Redox environment of the cell as viewed through the redox state of the glutathione disulfide/glutathione couple. *Free Radic Biol Med*. 2001;30(11):1191-1212.

153. Gilbert HF. Molecular and cellular aspects of thiol-disulfide exchange. *Adv Enzymol Relat Areas Mol Biol*. 1990;63:69-172.

154. Gilbert HF. Thiol/disulfide exchange equilibria and disulfide bond stability. *Methods Enzymol*. 1995;251:8-28.

155. Collet JF, Messens J. Structure, function, and mechanism of thioredoxin proteins. *Antioxid Redox Signal*. 2010;13(8):1205-1216.

156. Holmgren A. Thioredoxin and glutaredoxin systems. *J Biol Chem*. 1989;264(24):13963-13966.

157. Holmgren A. Thioredoxin structure and mechanism: conformational changes on oxidation of the active-site sulfhydryls to a disulfide. *Structure*. 1995;3(3):239-243.

158. Holmgren A, Bjornstedt M. Thioredoxin and thioredoxin reductase. *Methods Enzymol*. 1995;252:199-208.

159. Arner ES, Holmgren A. Physiological functions of thioredoxin and thioredoxin reductase. *Eur J Biochem*. 2000;267(20):6102-6109.

160. Hirota K, Matsui M, Iwata S, Nishiyama A, Mori K, Yodoi J. AP-1 transcriptional activity is regulated by a direct association between thioredoxin and Ref-1. *Proc Natl Acad Sci U S A*. 1997;94(8):3633-3638.

161. Hirota K, Murata M, Sachi Y, et al. Distinct roles of thioredoxin in the cytoplasm and in the nucleus. A two-step mechanism of redox regulation of transcription factor NF-kappaB. *J Biol Chem*. 1999;274(39):27891-27897.

162. Martin H, Dean M. Identification of a thioredoxin-related protein associated with plasma membranes. *Biochem Biophys Res Commun*. 1991;175(1):123-128.

163. Arner ES. Superoxide production by dinitrophenyl-derivatized thioredoxin reductase--a model for the mechanism and correlation to immunostimulation by dinitrohalobenzenes. *Biofactors*. 1999;10(2-3):219-226.

164. Hofmann B, Hecht HJ, Flohe L. Peroxiredoxins. *Biol Chem*. 2002;383(3-4):347-364.

165. Jacobson FS, Morgan RW, Christman MF, Ames BN. An alkyl hydroperoxide reductase from Salmonella typhimurium involved in the defense of DNA against oxidative damage. Purification and properties. *J Biol Chem*. 1989;264(3):1488-1496.

166. Bryk R, Griffin P, Nathan C. Peroxynitrite reductase activity of bacterial peroxiredoxins. *Nature*. 2000;407(6801):211-215.

167. Peshenko IV, Shichi H. Oxidation of active center cysteine of bovine 1-Cys peroxiredoxin to the cysteine sulfenic acid form by peroxide and peroxynitrite. *Free Radic Biol Med*. 2001;31(3):292-303.

168. Chae HZ, Robison K, Poole LB, Church G, Storz G, Rhee SG. Cloning and sequencing of thiol-specific antioxidant from mammalian brain: alkyl hydroperoxide reductase and thiol-specific antioxidant define a large family of antioxidant enzymes. *Proc Natl Acad Sci U S A*. 1994;91(15):7017-7021.

169. Chae HZ, Kim HJ, Kang SW, Rhee SG. Characterization of three isoforms of mammalian peroxiredoxin that reduce peroxides in the presence of thioredoxin. *Diabetes Res Clin Pract*. 1999;45(2-3):101-112.

170. Margis R, Dunand C, Teixeira FK, Margis-Pinheiro M. Glutathione peroxidase family - an evolutionary overview. *Febs j*. 2008;275(15):3959-3970.

171. Forgione MA, Cap A, Liao R, et al. Heterozygous cellular glutathione peroxidase deficiency in the mouse: abnormalities in vascular and cardiac function and structure. *Circulation*. 2002;106(9):1154-1158.

172. Yoshida T, Maulik N, Engelman RM, et al. Glutathione peroxidase knockout mice are susceptible to myocardial ischemia reperfusion injury. *Circulation*. 1997;96(9 Suppl):Ii-216-220.

173. Di Salvo J, Gifford D, Kokkinakis A. ATP- and polyphosphate-mediated stimulation of pp60c-src kinase activity in extracts from vascular smooth muscle. *J Biol Chem*. 1989;264(18):10773-10778.

174. Di Salvo J, Steusloff A, Semenchuk L, Satoh S, Kolquist K, Pfitzer G. Tyrosine kinase inhibitors suppress agonist-induced contraction in smooth muscle. *Biochem Biophys Res Commun*. 1993;190(3):968-974.

175. Hollenberg MD. Tyrosine kinase pathways and the regulation of smooth muscle contractility. *Trends Pharmacol Sci*. 1994;15(4):108-114.

176. Rathore R, Zheng YM, Niu CF, et al. Hypoxia activates NADPH oxidase to increase [ROS]i and [Ca2+]i through the mitochondrial ROS-PKCepsilon signaling axis in pulmonary artery smooth muscle cells. *Free Radic Biol Med*. 2008;45(9):1223-1231.

177. Frank GD, Eguchi S, Yamakawa T, Tanaka S, Inagami T, Motley ED. Involvement of reactive oxygen species in the activation of tyrosine kinase and extracellular signal-regulated kinase by angiotensin II. *Endocrinology*. 2000;141(9):3120-3126.

178. Di Salvo J, Semenchuk LA, Lauer J. Vanadate-induced contraction of smooth muscle and enhanced protein tyrosine phosphorylation. *Arch Biochem Biophys*. 1993;304(2):386-391.

179. Uzun O, Demiryurek AT, Kanzik I. The role of tyrosine kinase in hypoxic constriction of sheep pulmonary artery rings. *Eur J Pharmacol*. 1998;358(1):41-47.

180. Uzun O, Tuncay Demiryurek A. Involvement of tyrosine kinase pathway in acute hypoxic vasoconstriction in sheep isolated pulmonary vein. *Vascul Pharmacol*. 2003;40(3):175-181.

181. Smirnov SV, Aaronson PI. Inhibition of vascular smooth muscle cell K+ currents by tyrosine kinase inhibitors genistein and ST 638. *Circ Res*. 1995;76(2):310-316.

182. Watts SW, Yeum CH, Campbell G, Webb RC. Serotonin stimulates protein tyrosyl phosphorylation and vascular contraction via tyrosine kinase. *J Vasc Res*. 1996;33(4):288-298.

183. Watts SW, Florian JA, Monroe KM. Dissociation of angiotensin II-stimulated activation of mitogen-activated protein kinase kinase from vascular contraction. *J Pharmacol Exp Ther*. 1998;286(3):1431-1438.

184. Ogata R, Kitamura K, Ito Y, Nakano H. Inhibitory effects of genistein on ATP-sensitive K+ channels in rabbit portal vein smooth muscle. *Br J Pharmacol*. 1997;122(7):1395-1404.

185. Bain J, Plater L, Elliott M, et al. The selectivity of protein kinase inhibitors: a further update. *Biochem J*. 2007;408(3):297-315.

186. Hanke JH, Gardner JP, Dow RL, et al. Discovery of a novel, potent, and Src family-selective tyrosine kinase inhibitor. Study of Lck- and FynT-dependent T cell activation. *J Biol Chem*. 1996;271(2):695-701.

187. Liu Y, Bishop A, Witucki L, et al. Structural basis for selective inhibition of Src family kinases by PP1. *Chem Biol*. 1999;6(9):671-678.

188. Schlessinger J. SH2/SH3 signaling proteins. *Curr Opin Genet Dev*. 1994;4(1):25-30.

189. Hubbard SR, Till JH. Protein tyrosine kinase structure and function. *Annu Rev Biochem*. 2000;69:373-398.

190. Arias-Salgado EG, Lizano S, Sarkar S, Brugge JS, Ginsberg MH, Shattil SJ. Src kinase activation by direct interaction with the integrin beta cytoplasmic domain. *Proc Natl Acad Sci U S A*. 2003;100(23):13298-13302.

191. Ward JP, Knock GA, Snetkov VA, Aaronson PI. Protein kinases in vascular smooth muscle tone--role in the pulmonary vasculature and hypoxic pulmonary vasoconstriction. *Pharmacol Ther*. 2004;104(3):207-231.

192. Ardanaz N, Beierwaltes WH, Pagano PJ. Comparison of H2O2-induced vasoconstriction in the abdominal aorta and mesenteric artery of the mouse. *Vascul Pharmacol*. 2007;47(5-6):288-294.

193. Oeckler RA, Arcuino E, Ahmad M, Olson SC, Wolin MS. Cytosolic NADH redox and thiol oxidation regulate pulmonary arterial force through ERK MAP kinase. *Am J Physiol Lung Cell Mol Physiol*. 2005;288(6):L1017-1025.

194. Pourmahram GE, Snetkov VA, Shaifta Y, et al. Constriction of pulmonary artery by peroxide: role of Ca2+ release and PKC. *Free Radic Biol Med*. 2008;45(10):1468-1476.

195. Oeckler RA, Kaminski PM, Wolin MS. Stretch enhances contraction of bovine coronary arteries via an NAD(P)H oxidase-mediated activation of the extracellular signal-regulated kinase mitogen-activated protein kinase cascade. *Circ Res*. 2003;92(1):23-31.

196. Jin N, Rhoades RA. Activation of tyrosine kinases in H2O2-induced contraction in pulmonary artery. *Am J Physiol*. 1997;272(6 Pt 2):H2686-2692.

197. Jin L, Ying Z, Webb RC. Activation of Rho/Rho kinase signaling pathway by reactive oxygen species in rat aorta. *Am J Physiol Heart Circ Physiol*. 2004;287(4):H1495-1500.

198. Lucchesi PA, Belmadani S, Matrougui K. Hydrogen peroxide acts as both vasodilator and vasoconstrictor in the control of perfused mouse mesenteric resistance arteries. *J Hypertens*. 2005;23(3):571-579.

199. Tonks NK. Redox redux: revisiting PTPs and the control of cell signaling. *Cell*. 2005;121(5):667-670.

200. Sakai H, Nishimura A, Watanabe Y, et al. Involvement of Src family kinase activation in angiotensin II-induced hyperresponsiveness of rat bronchial smooth muscle. *Peptides*. 2010;31(12):2216-2221.

201. Boggon TJ, Eck MJ. Structure and regulation of Src family kinases. *Oncogene*. 2004;23(48):7918-7927.

202. Pertel T, Zhu D, Panettieri RA, Yamaguchi N, Emala CW, Hirshman CA. Expression and muscarinic receptor coupling of Lyn kinase in cultured human airway smooth muscle cells. *Am J Physiol Lung Cell Mol Physiol*. 2006;290(3):L492-500.

203. Roskoski R, Jr. Src kinase regulation by phosphorylation and dephosphorylation. *Biochem Biophys Res Commun*. 2005;331(1):1-14.

204. Sato H, Sato M, Kanai H, et al. Mitochondrial reactive oxygen species and c-Src play a critical role in hypoxic response in vascular smooth muscle cells. *Cardiovasc Res*. 2005;67(4):714-722.

205. Li Q, Zhang Y, Marden JJ, Banfi B, Engelhardt JF. Endosomal NADPH oxidase regulates c-Src activation following hypoxia/reoxygenation injury. *Biochem J*. 2008;411(3):531-541.

206. Lee SR, Kwon KS, Kim SR, Rhee SG. Reversible inactivation of protein-tyrosine phosphatase 1B in A431 cells stimulated with epidermal growth factor. *J Biol Chem*. 1998;273(25):15366-15372.

207. Tsai MH, Jiang MJ. Reactive oxygen species are involved in regulating alpha1-adrenoceptor-activated vascular smooth muscle contraction. *J Biomed Sci*. 2010;17:67.

208. Griendling KK, Ushio-Fukai M. Reactive oxygen species as mediators of angiotensin II signaling. *Regul Pept*. 2000;91(1-3):21-27.

209. Rosado JA, Redondo PC, Salido GM, Gomez-Arteta E, Sage SO, Pariente JA. Hydrogen peroxide generation induces pp60src activation in human platelets: evidence for the involvement of this pathway in store-mediated calcium entry. *J Biol Chem*. 2004;279(3):1665-1675.

210. Mehdi MZ, Pandey NR, Pandey SK, Srivastava AK. H2O2-induced phosphorylation of ERK1/2 and PKB requires tyrosine kinase activity of insulin receptor and c-Src. *Antioxid Redox Signal*. 2005;7(7-8):1014-1020.

211. Akhand AA, Pu M, Senga T, et al. Nitric oxide controls src kinase activity through a sulfhydryl group modification-mediated Tyr-527-independent and Tyr-416-linked mechanism. *J Biol Chem*. 1999;274(36):25821-25826.

212. Kemble DJ, Sun G. Direct and specific inactivation of protein tyrosine kinases in the Src and FGFR families by reversible cysteine oxidation. *Proc Natl Acad Sci U S A*. 2009;106(13):5070-5075.

213. Giannoni E, Buricchi F, Raugei G, Ramponi G, Chiarugi P. Intracellular reactive oxygen species activate Src tyrosine kinase during cell adhesion and anchorage-dependent cell growth. *Mol Cell Biol*. 2005;25(15):6391-6403.

214. Minetti M, Mallozzi C, Di Stasi AM. Peroxynitrite activates kinases of the src family and upregulates tyrosine phosphorylation signaling. *Free Radic Biol Med*. 2002;33(6):744-754.

215. Petrone A, Sap J. Emerging issues in receptor protein tyrosine phosphatase function: lifting fog or simply shifting? *J Cell Sci*. 2000;113 (Pt 13):2345-2354.

216. Su J, Muranjan M, Sap J. Receptor protein tyrosine phosphatase alpha activates Src-family kinases and controls integrin-mediated responses in fibroblasts. *Curr Biol*. 1999;9(10):505-511.

217. Chu F, Ward NE, O'Brian CA. Potent inactivation of representative members of each PKC isozyme subfamily and PKD via S-thiolation by the tumor-promotion/progression antagonist glutathione but not by its precursor cysteine. *Carcinogenesis*. 2001;22(8):1221-1229.

218. Jackson EK, Gillespie DG, Zhu C, Ren J, Zacharia LC, Mi Z. Alpha2-adrenoceptors enhance angiotensin II-induced renal vasoconstriction: role for NADPH oxidase and RhoA. *Hypertension*. 2008;51(3):719-726.

219. Seshiah PN, Weber DS, Rocic P, Valppu L, Taniyama Y, Griendling KK. Angiotensin II stimulation of NAD(P)H oxidase activity: upstream mediators. *Circ Res*. 2002;91(5):406-413.

220. Touyz RM, Yao G, Schiffrin EL. c-Src induces phosphorylation and translocation of p47phox: role in superoxide generation by angiotensin II in human vascular smooth muscle cells. *Arterioscler Thromb Vasc Biol*. 2003;23(6):981-987.

221. Fredriksson R, Lagerstrom MC, Lundin LG, Schioth HB. The G-protein-coupled receptors in the human genome form five main families. Phylogenetic analysis, paralogon groups, and fingerprints. *Mol Pharmacol*. 2003;63(6):1256-1272.

222. Ji TH, Grossmann M, Ji I. G protein-coupled receptors. I. Diversity of receptor-ligand interactions. *J Biol Chem*. 1998;273(28):17299-17302.

223. Howard AD, McAllister G, Feighner SD, et al. Orphan G-protein-coupled receptors and natural ligand discovery. *Trends Pharmacol Sci*. 2001;22(3):132-140.

224. Hamm HE. The many faces of G protein signaling. *J Biol Chem*. 1998;273(2):669-672.

225. Lefkowitz RJ. Seven transmembrane receptors: something old, something new. *Acta Physiol (Oxf)*. 2007;190(1):9-19.

226. Wettschureck N, Offermanns S. Mammalian G proteins and their cell type specific functions. *Physiol Rev*. 2005;85(4):1159-1204.

227. Mizuno N, Itoh H. Functions and regulatory mechanisms of Gq-signaling pathways. *Neurosignals*. 2009;17(1):42-54.

228. Simonds WF. G protein regulation of adenylate cyclase. *Trends Pharmacol Sci*. 1999;20(2):66-73.

229. Fukuhara S, Murga C, Zohar M, Igishi T, Gutkind JS. A novel PDZ domain containing guanine nucleotide exchange factor links heterotrimeric G proteins to Rho. *J Biol Chem*. 1999;274(9):5868-5879.

230. Kozasa T, Jiang X, Hart MJ, et al. p115 RhoGEF, a GTPase activating protein for Galpha12 and Galpha13. *Science*. 1998;280(5372):2109-2111.

231. Himpens B, Kitazawa T, Somlyo AP. Agonist-dependent modulation of Ca2+ sensitivity in rabbit pulmonary artery smooth muscle. *Pflugers Arch*. 1990;417(1):21-28.

232. Sit ST, Manser E. Rho GTPases and their role in organizing the actin cytoskeleton. *J Cell Sci*. 2011;124(Pt 5):679-683.

233. Gerthoffer WT. Signal-transduction pathways that regulate visceral smooth muscle function. III. Coupling of muscarinic receptors to signaling kinases and effector proteins in gastrointestinal smooth muscles. *Am J Physiol Gastrointest Liver Physiol*. 2005;288(5):G849-853.

234. Luttrell DK, Luttrell LM. Not so strange bedfellows: G-protein-coupled receptors and Src family kinases. *Oncogene*. 2004;23(48):7969-7978.

235. Janssen LJ, Lu-Chao H, Netherton S. Excitation-contraction coupling in pulmonary vascular smooth muscle involves tyrosine kinase and Rho kinase. *Am J Physiol Lung Cell Mol Physiol*. 2001;280(4):L666-674.

236. Nobe K, Paul RJ. Distinct pathways of Ca(2+) sensitization in porcine coronary artery: effects of Rho-related kinase and protein kinase C inhibition on force and intracellular Ca(2+). *Circ Res*. 2001;88(12):1283-1290.

237. Tosun M, Paul RJ, Rapoport RM. Role of extracellular Ca++ influx via L-type and non-L-type Ca++ channels in thromboxane A2 receptor-mediated contraction in rat aorta. *J Pharmacol Exp Ther*. 1998;284(3):921-928.

238. Dorn GW, 2nd, Becker MW, Davis MG. Dissociation of the contractile and hypertrophic effects of vasoconstrictor prostanoids in vascular smooth muscle. *J Biol Chem*. 1992;267(34):24897-24905.

239. Huang JS, Ramamurthy SK, Lin X, Le Breton GC. Cell signalling through thromboxane A2 receptors. *Cell Signal*. 2004;16(5):521-533.

240. Sparks MA, Makhanova NA, Griffiths RC, Snouwaert JN, Koller BH, Coffman TM. Thromboxane receptors in smooth muscle promote hypertension, vascular remodeling, and sudden death. *Hypertension*. 2013;61(1):166-173.

241. Coleman RA, Sheldrick RL. Prostanoid-induced contraction of human bronchial smooth muscle is mediated by TP-receptors. *Br J Pharmacol*. 1989;96(3):688-692.

242. Kinsella BT. Thromboxane A2 signalling in humans: a 'Tail' of two receptors. *Biochem Soc Trans*. 2001;29(Pt 6):641-654.

243. Breyer RM, Bagdassarian CK, Myers SA, Breyer MD. Prostanoid receptors: subtypes and signaling. *Annu Rev Pharmacol Toxicol*. 2001;41:661-690.

244. Dorsam RT, Kim S, Jin J, Kunapuli SP. Coordinated signaling through both G12/13 and G(i) pathways is sufficient to activate GPIIb/IIIa in human platelets. *J Biol Chem*. 2002;277(49):47588-47595.

245. Siehler S. Regulation of RhoGEF proteins by G12/13-coupled receptors. *Br J Pharmacol*. 2009;158(1):41-49.

246. Luttrell LM, Hawes BE, van Biesen T, Luttrell DK, Lansing TJ, Lefkowitz RJ. Role of c-Src tyrosine kinase in G protein-coupled receptor- and Gbetagamma subunit-mediated activation of mitogen-activated protein kinases. *J Biol Chem*. 1996;271(32):19443-19450.

247. Jeong KJ, Park SY, Seo JH, et al. Lysophosphatidic acid receptor 2 and Gi/Src pathway mediate cell motility through cyclooxygenase 2 expression in CAOV-3 ovarian cancer cells. *Exp Mol Med*. 2008;40(6):607-616.

248. Olianas MC, Dedoni S, Onali P. Antidepressants activate the lysophosphatidic acid receptor LPA(1) to induce insulin-like growth factor-I receptor transactivation, stimulation of

ERK1/2 signaling and cell proliferation in CHO-K1 fibroblasts. *Biochem Pharmacol*. 2015;95(4):311-323.

249. Chen YH, Pouyssegur J, Courtneidge SA, Van Obberghen-Schilling E. Activation of Src family kinase activity by the G protein-coupled thrombin receptor in growth-responsive fibroblasts. *J Biol Chem*. 1994;269(44):27372-27377.

250. Singer CA, Vang S, Gerthoffer WT. Coupling of M(2) muscarinic receptors to Src activation in cultured canine colonic smooth muscle cells. *Am J Physiol Gastrointest Liver Physiol*. 2002;282(1):G61-68.

251. Darmoul D, Gratio V, Devaud H, Peiretti F, Laburthe M. Activation of proteinase-activated receptor 1 promotes human colon cancer cell proliferation through epidermal growth factor receptor transactivation. *Mol Cancer Res*. 2004;2(9):514-522.

252. Caruso R, Pallone F, Fina D, et al. Protease-activated receptor-2 activation in gastric cancer cells promotes epidermal growth factor receptor trans-activation and proliferation. *Am J Pathol*. 2006;169(1):268-278.

253. Simonson MS, Herman WH. Protein kinase C and protein tyrosine kinase activity contribute to mitogenic signaling by endothelin-1. Cross-talk between G protein-coupled receptors and pp60c-src. *J Biol Chem*. 1993;268(13):9347-9357.

254. Ishida M, Marrero MB, Schieffer B, Ishida T, Bernstein KE, Berk BC. Angiotensin II activates pp60c-src in vascular smooth muscle cells. *Circ Res*. 1995;77(6):1053-1059.

255. Walsh M, Foley JF, Kinsella BT. Investigation of the role of the carboxyl-terminal tails of the alpha and beta isoforms of the human thromboxane A(2) receptor (TP) in mediating receptor:effector coupling. *Biochim Biophys Acta*. 2000;1496(2-3):164-182.

256. Cao W, Luttrell LM, Medvedev AV, et al. Direct binding of activated c-Src to the beta 3-adrenergic receptor is required for MAP kinase activation. *J Biol Chem*. 2000;275(49):38131-38134.

257. Liu J, Liao Z, Camden J, et al. Src homology 3 binding sites in the P2Y2 nucleotide receptor interact with Src and regulate activities of Src, proline-rich tyrosine kinase 2, and growth factor receptors. *J Biol Chem*. 2004;279(9):8212-8218.

258. Ma YC, Huang J, Ali S, Lowry W, Huang XY. Src tyrosine kinase is a novel direct effector of G proteins. *Cell*. 2000;102(5):635-646.

259. Sabath E, Negoro H, Beaudry S, et al. Galpha12 regulates protein interactions within the MDCK cell tight junction and inhibits tight-junction assembly. *J Cell Sci*. 2008;121(Pt 6):814-824.

260. Nagao M, Yamauchi J, Kaziro Y, Itoh H. Involvement of protein kinase C and Src family tyrosine kinase in Galphaq/11-induced activation of c-Jun N-terminal kinase and p38 mitogen-activated protein kinase. *J Biol Chem*. 1998;273(36):22892-22898.

261. Shajahan AN, Tiruppathi C, Smrcka AV, Malik AB, Minshall RD. Gbetagamma activation of Src induces caveolae-mediated endocytosis in endothelial cells. *J Biol Chem*. 2004;279(46):48055-48062.

262. Luttrell LM, Ferguson SS, Daaka Y, et al. Beta-arrestin-dependent formation of beta2 adrenergic receptor-Src protein kinase complexes. *Science*. 1999;283(5402):655-661.

263. Zeng Q, Zhou Q, Yao F, O'Rourke ST, Sun C. Endothelin-1 regulates cardiac L-type calcium channels via NAD(P)H oxidase-derived superoxide. *J Pharmacol Exp Ther*. 2008;326(3):732-738.

264. Wang H, Reiser G. The role of the Ca2+-sensitive tyrosine kinase Pyk2 and Src in thrombin signalling in rat astrocytes. *J Neurochem*. 2003;84(6):1349-1357.

265. Leung T, Manser E, Tan L, Lim L. A novel serine/threonine kinase binding the Ras-related RhoA GTPase which translocates the kinase to peripheral membranes. *J Biol Chem*. 1995;270(49):29051-29054.

266. Liu PY, Liao JK. A method for measuring Rho kinase activity in tissues and cells. *Methods Enzymol*. 2008;439:181-189.

267. Connolly MJ, Aaronson PI. Key role of the RhoA/Rho kinase system in pulmonary hypertension. *Pulm Pharmacol Ther*. 2011;24(1):1-14.

268. Nakagawa O, Fujisawa K, Ishizaki T, Saito Y, Nakao K, Narumiya S. ROCK-I and ROCK-II, two isoforms of Rho-associated coiled-coil forming protein serine/threonine kinase in mice. *FEBS Lett*. 1996;392(2):189-193.

269. Leung T, Chen XQ, Manser E, Lim L. The p160 RhoA-binding kinase ROK alpha is a member of a kinase family and is involved in the reorganization of the cytoskeleton. *Mol Cell Biol*. 1996;16(10):5313-5327.

270. Wei L, Roberts W, Wang L, et al. Rho kinases play an obligatory role in vertebrate embryonic organogenesis. *Development*. 2001;128(15):2953-2962.

271. Wibberley A, Chen Z, Hu E, Hieble JP, Westfall TD. Expression and functional role of Rho-kinase in rat urinary bladder smooth muscle. *Br J Pharmacol*. 2003;138(5):757-766.

272. Wang Y, Zheng XR, Riddick N, et al. ROCK isoform regulation of myosin phosphatase and contractility in vascular smooth muscle cells. *Circ Res*. 2009;104(4):531-540.

273. Schofield AV, Bernard O. Rho-associated coiled-coil kinase (ROCK) signaling and disease. *Crit Rev Biochem Mol Biol*. 2013;48(4):301-316.

274. Riento K, Ridley AJ. Rocks: multifunctional kinases in cell behaviour. *Nat Rev Mol Cell Biol*. 2003;4(6):446-456.

275. Alland L, Peseckis SM, Atherton RE, Berthiaume L, Resh MD. Dual myristylation and palmitylation of Src family member p59fyn affects subcellular localization. *J Biol Chem*. 1994;269(24):16701-16705.

276. Webb Y, Hermida-Matsumoto L, Resh MD. Inhibition of protein palmitoylation, raft localization, and T cell signaling by 2-bromopalmitate and polyunsaturated fatty acids. *J Biol Chem*. 2000;275(1):261-270.

277. Hall A, Nobes CD. Rho GTPases: molecular switches that control the organization and dynamics of the actin cytoskeleton. *Philos Trans R Soc Lond B Biol Sci*. 2000;355(1399):965-970.

278. Shimokawa H. Rho-kinase as a novel therapeutic target in treatment of cardiovascular diseases. *J Cardiovasc Pharmacol*. 2002;39(3):319-327.

279. Schaafsma D, Gosens R, Zaagsma J, Halayko AJ, Meurs H. Rho kinase inhibitors: a novel therapeutical intervention in asthma? *Eur J Pharmacol*. 2008;585(2-3):398-406.

280. Matsui T, Amano M, Yamamoto T, et al. Rho-associated kinase, a novel serine/threonine kinase, as a putative target for small GTP binding protein Rho. *Embo j*. 1996;15(9):2208-2216.

281. Feng J, Ito M, Kureishi Y, et al. Rho-associated kinase of chicken gizzard smooth muscle. *J Biol Chem*. 1999;274(6):3744-3752.

282. Maekawa M, Ishizaki T, Boku S, et al. Signaling from Rho to the actin cytoskeleton through protein kinases ROCK and LIM-kinase. *Science*. 1999;285(5429):895-898.

283. Gohla A, Schultz G, Offermanns S. Role for G(12)/G(13) in agonist-induced vascular smooth muscle cell contraction. *Circ Res*. 2000;87(3):221-227.

284. Jackson EK, Andresen BT, Seasholtz TM, Zhu C, Romero GG. Enhanced activation of RhoA by angiotensin II in SHR preglomerular microvascular smooth muscle cells. *J Cardiovasc Pharmacol*. 2005;45(4):283-285.

285. Wikstrom K, Kavanagh DJ, Reid HM, Kinsella BT. Differential regulation of RhoA-mediated signaling by the TPalpha and TPbeta isoforms of the human thromboxane A2 receptor: independent modulation of TPalpha signaling by prostacyclin and nitric oxide. *Cell Signal*. 2008;20(8):1497-1512.

286. Kamiyama M, Utsunomiya K, Taniguchi K, et al. Contribution of Rho A and Rho kinase to platelet-derived growth factor-BB-induced proliferation of vascular smooth muscle cells. *J Atheroscler Thromb*. 2003;10(2):117-123.

287. Romano F, Chiarenza C, Palombi F, et al. Platelet-derived growth factor-BB-induced hypertrophy of peritubular smooth muscle cells is mediated by activation of p38 MAP-kinase and of Rho-kinase. *J Cell Physiol*. 2006;207(1):123-131.

288. Hunter I, Cobban HJ, Vandenabeele P, MacEwan DJ, Nixon GF. Tumor necrosis factor-alpha-induced activation of RhoA in airway smooth muscle cells: role in the Ca2+ sensitization of myosin light chain20 phosphorylation. *Mol Pharmacol*. 2003;63(3):714-721.

289. Ren XD, Kiosses WB, Schwartz MA. Regulation of the small GTP-binding protein Rho by cell adhesion and the cytoskeleton. *Embo j*. 1999;18(3):578-585.

290. Broughton BR, Jernigan NL, Norton CE, Walker BR, Resta TC. Chronic hypoxia augments depolarization-induced Ca2+ sensitization in pulmonary vascular smooth muscle through superoxide-dependent stimulation of RhoA. *Am J Physiol Lung Cell Mol Physiol*. 2010;298(2):L232-242.

291. Bailly K, Ridley AJ, Hall SM, Haworth SG. RhoA activation by hypoxia in pulmonary arterial smooth muscle cells is age and site specific. *Circ Res*. 2004;94(10):1383-1391.

292. Hall A. Rho GTPases and the control of cell behaviour. *Biochem Soc Trans*. 2005;33(Pt 5):891-895.

293. Fukumoto Y, Tawara S, Shimokawa H. Recent progress in the treatment of pulmonary arterial hypertension: expectation for rho-kinase inhibitors. *Tohoku J Exp Med*. 2007;211(4):309-320.

294. Weiss S, Frischknecht K, Greutert H, et al. Different migration of vascular smooth muscle cells from human coronary artery bypass vessels. Role of Rho/ROCK pathway. *J Vasc Res*. 2007;44(2):149-156.

295. Gerthoffer WT, Gunst SJ. Invited review: focal adhesion and small heat shock proteins in the regulation of actin remodeling and contractility in smooth muscle. *J Appl Physiol (1985)*. 2001;91(2):963-972.

296. Zhao L, Sebkhi A, Ali O, et al. Simvastatin and sildenafil combine to attenuate pulmonary hypertension. *Eur Respir J*. 2009;34(4):948-957.

297. Hyvelin JM, Howell K, Nichol A, Costello CM, Preston RJ, McLoughlin P. Inhibition of Rho-kinase attenuates hypoxia-induced angiogenesis in the pulmonary circulation. *Circ Res*. 2005;97(2):185-191.

298. Krymskaya VP, Goncharova EA, Ammit AJ, et al. Src is necessary and sufficient for human airway smooth muscle cell proliferation and migration. *Faseb j*. 2005;19(3):428-430.

299. Lim Y, Lim ST, Tomar A, et al. PyK2 and FAK connections to p190Rho guanine nucleotide exchange factor regulate RhoA activity, focal adhesion formation, and cell motility. *J Cell Biol*. 2008;180(1):187-203.

300. Schoenwaelder SM, Petch LA, Williamson D, Shen R, Feng GS, Burridge K. The protein tyrosine phosphatase Shp-2 regulates RhoA activity. *Curr Biol*. 2000;10(23):1523-1526.

301. Chi AY, Waypa GB, Mungai PT, Schumacker PT. Prolonged hypoxia increases ROS signaling and RhoA activation in pulmonary artery smooth muscle and endothelial cells. *Antioxid Redox Signal*. 2010;12(5):603-610.

302. Gong MC, Gorenne I, Read P, et al. Regulation by GDI of RhoA/Rho-kinase-induced Ca2+ sensitization of smooth muscle myosin II. *Am J Physiol Cell Physiol*. 2001;281(1):C257-269.

303. Gosser YQ, Nomanbhoy TK, Aghazadeh B, et al. C-terminal binding domain of Rho GDP-dissociation inhibitor directs N-terminal inhibitory peptide to GTPases. *Nature*. 1997;387(6635):814-819.

304. Carbone ML, Bregeon J, Devos N, et al. Angiotensin II activates the RhoA exchange factor Arhgef1 in humans. *Hypertension*. 2015;65(6):1273-1278.

305. Loirand G, Pacaud P. Involvement of Rho GTPases and their regulators in the pathogenesis of hypertension. *Small GTPases*. 2014;5(4):1-10.

306. Bos JL, Rehmann H, Wittinghofer A. GEFs and GAPs: critical elements in the control of small G proteins. *Cell*. 2007;129(5):865-877.

307. Patel CA, Rattan S. RhoA prenylation inhibitor produces relaxation of tonic smooth muscle of internal anal sphincter. *J Pharmacol Exp Ther*. 2007;321(2):501-508.

308. Bhattacharyya R, Wedegaertner PB. Characterization of G alpha 13-dependent plasma membrane recruitment of p115RhoGEF. *Biochem J*. 2003;371(Pt 3):709-720.

309. Boulter E, Garcia-Mata R, Guilluy C, et al. Regulation of Rho GTPase crosstalk, degradation and activity by RhoGDI1. *Nat Cell Biol*. 2010;12(5):477-483.

310. Lander HM, Ogiste JS, Pearce SF, Levi R, Novogrodsky A. Nitric oxide-stimulated guanine nucleotide exchange on p21ras. *J Biol Chem*. 1995;270(13):7017-7020.

311. Heo J, Campbell SL. Mechanism of redox-mediated guanine nucleotide exchange on redox-active Rho GTPases. *J Biol Chem*. 2005;280(35):31003-31010.

312. Aghajanian A, Wittchen ES, Campbell SL, Burridge K. Direct activation of RhoA by reactive oxygen species requires a redox-sensitive motif. *PLoS One*. 2009;4(11):e8045.

313. Bregeon J, Loirand G, Pacaud P, Rolli-Derkinderen M. Angiotensin II induces RhoA activation through SHP2-dependent dephosphorylation of the RhoGAP p190A in vascular smooth muscle cells. *Am J Physiol Cell Physiol*. 2009;297(5):C1062-1070.

314. Fukumoto Y, Kaibuchi K, Hori Y, et al. Molecular cloning and characterization of a novel type of regulatory protein (GDI) for the rho proteins, ras p21-like small GTP-binding proteins. *Oncogene*. 1990;5(9):1321-1328.

315. DerMardirossian C, Bokoch GM. GDIs: central regulatory molecules in Rho GTPase activation. *Trends Cell Biol*. 2005;15(7):356-363.

316. Cherfils J, Zeghouf M. Regulation of small GTPases by GEFs, GAPs, and GDIs. *Physiol Rev*. 2013;93(1):269-309.

317. Knezevic N, Roy A, Timblin B, et al. GDI-1 phosphorylation switch at serine 96 induces RhoA activation and increased endothelial permeability. *Mol Cell Biol*. 2007;27(18):6323-6333.

318. DerMardirossian C, Rocklin G, Seo JY, Bokoch GM. Phosphorylation of RhoGDI by Src regulates Rho GTPase binding and cytosol-membrane cycling. *Mol Biol Cell*. 2006;17(11):4760-4768.

319. Cario-Toumaniantz C, Ferland-McCollough D, Chadeuf G, et al. RhoA guanine exchange factor expression profile in arteries: evidence for a Rho kinase-dependent negative feedback in angiotensin II-dependent hypertension. *Am J Physiol Cell Physiol*. 2012;302(9):C1394-1404.

320. Ogita H, Kunimoto S, Kamioka Y, Sawa H, Masuda M, Mochizuki N. EphA4-mediated Rho activation via Vsm-RhoGEF expressed specifically in vascular smooth muscle cells. *Circ Res*. 2003;93(1):23-31.

321. Bear MD, Li M, Liu Y, Giel-Moloney MA, Fanburg BL, Toksoz D. The Lbc Rho guanine nucleotide exchange factor alpha-catulin axis functions in serotonin-induced vascular smooth muscle cell mitogenesis and RhoA/ROCK activation. *J Biol Chem*. 2010;285(43):32919-32926.

322. Bustelo XR. Regulatory and signaling properties of the Vav family. *Mol Cell Biol*. 2000;20(5):1461-1477.

323. Thill R, Campbell WB, Williams CL. Identification and characterization of the unique guanine nucleotide exchange factor, SmgGDS, in vascular smooth muscle cells. *J Cell Biochem*. 2008;104(5):1760-1770.

324. Chikumi H, Fukuhara S, Gutkind JS. Regulation of G protein-linked guanine nucleotide exchange factors for Rho, PDZ-RhoGEF, and LARG by tyrosine phosphorylation: evidence of a role for focal adhesion kinase. *J Biol Chem*. 2002;277(14):12463-12473.

325. Guilluy C, Bregeon J, Toumaniantz G, et al. The Rho exchange factor Arhgef1 mediates the effects of angiotensin II on vascular tone and blood pressure. *Nat Med*. 2010;16(2):183-190.

326. Derewenda U, Oleksy A, Stevenson AS, et al. The crystal structure of RhoA in complex with the DH/PH fragment of PDZRhoGEF, an activator of the Ca(2+) sensitization pathway in smooth muscle. *Structure*. 2004;12(11):1955-1965.

327. Erickson JW, Cerione RA. Structural elements, mechanism, and evolutionary convergence of Rho protein-guanine nucleotide exchange factor complexes. *Biochemistry*. 2004;43(4):837-842.

328. Hilgers RH, Todd J, Jr., Webb RC. Increased PDZ-RhoGEF/RhoA/Rho kinase signaling in small mesenteric arteries of angiotensin II-induced hypertensive rats. *J Hypertens*. 2007;25(8):1687-1697.

329. Jin L, Ying Z, Hilgers RH, et al. Increased RhoA/Rho-kinase signaling mediates spontaneous tone in aorta from angiotensin II-induced hypertensive rats. *J Pharmacol Exp Ther*. 2006;318(1):288-295.

330. Momotani K, Artamonov MV, Utepbergenov D, Derewenda U, Derewenda ZS, Somlyo AV. p63RhoGEF couples Galpha(q/11)-mediated signaling to Ca2+ sensitization of vascular smooth muscle contractility. *Circ Res*. 2011;109(9):993-1002.

331. Momotani K, Somlyo AV. p63RhoGEF: a new switch for G(q)-mediated activation of smooth muscle. *Trends Cardiovasc Med*. 2012;22(5):122-127.

332. Hart MJ, Jiang X, Kozasa T, et al. Direct stimulation of the guanine nucleotide exchange activity of p115 RhoGEF by Galpha13. *Science*. 1998;280(5372):2112-2114.

333. Jackson M, Song W, Liu MY, et al. Modulation of the neuronal glutamate transporter EAAT4 by two interacting proteins. *Nature*. 2001;410(6824):89-93.

334. Fukuhara S, Chikumi H, Gutkind JS. Leukemia-associated Rho guanine nucleotide exchange factor (LARG) links heterotrimeric G proteins of the G(12) family to Rho. *FEBS Lett*. 2000;485(2-3):183-188.

335. Kourlas PJ, Strout MP, Becknell B, et al. Identification of a gene at 11q23 encoding a guanine nucleotide exchange factor: evidence for its fusion with MLL in acute myeloid leukemia. *Proc Natl Acad Sci U S A*. 2000;97(5):2145-2150.

336. Meyer BH, Freuler F, Guerini D, Siehler S. Reversible translocation of p115-RhoGEF by G(12/13)-coupled receptors. *J Cell Biochem*. 2008;104(5):1660-1670.

337. Banerjee J, Wedegaertner PB. Identification of a novel sequence in PDZ-RhoGEF that mediates interaction with the actin cytoskeleton. *Mol Biol Cell*. 2004;15(4):1760-1775.

338. Wong K, Van Keymeulen A, Bourne HR. PDZRhoGEF and myosin II localize RhoA activity to the back of polarizing neutrophil-like cells. *J Cell Biol*. 2007;179(6):1141-1148.

339. Goulimari P, Knieling H, Engel U, Grosse R. LARG and mDia1 link Galpha12/13 to cell polarity and microtubule dynamics. *Mol Biol Cell*. 2008;19(1):30-40.

340. Ying Z, Jin L, Palmer T, Webb RC. Angiotensin II up-regulates the leukemia-associated Rho guanine nucleotide exchange factor (RhoGEF), a regulator of G protein signaling domain-containing RhoGEF, in vascular smooth muscle cells. *Mol Pharmacol*. 2006;69(3):932-940.

341. Nakahata N. Thromboxane A2: physiology/pathophysiology, cellular signal transduction and pharmacology. *Pharmacol Ther*. 2008;118(1):18-35.

342. Riobo NA, Manning DR. Receptors coupled to heterotrimeric G proteins of the G12 family. *Trends Pharmacol Sci*. 2005;26(3):146-154.

343. Booden MA, Siderovski DP, Der CJ. Leukemia-associated Rho guanine nucleotide exchange factor promotes G alpha q-coupled activation of RhoA. *Mol Cell Biol*. 2002;22(12):4053-4061.

344. Medlin MD, Staus DP, Dubash AD, Taylor JM, Mack CP. Sphingosine 1-phosphate receptor 2 signals through leukemia-associated RhoGEF (LARG), to promote smooth muscle cell differentiation. *Arterioscler Thromb Vasc Biol*. 2010;30(9):1779-1786.

345. Suzuki N, Nakamura S, Mano H, Kozasa T. Galpha 12 activates Rho GTPase through tyrosine-phosphorylated leukemia-associated RhoGEF. *Proc Natl Acad Sci U S A*. 2003;100(2):733-738.

346. Sreenivasappa H, Chaki SP, Lim SM, et al. Selective regulation of cytoskeletal tension and cell-matrix adhesion by RhoA and Src. *Integr Biol (Camb)*. 2014;6(8):743-754.

347. Chandra S, Romero MJ, Shatanawi A, Alkilany AM, Caldwell RB, Caldwell RW. Oxidative species increase arginase activity in endothelial cells through the RhoA/Rho kinase pathway. *Br J Pharmacol*. 2012;165(2):506-519.

348. Gadepalli R, Singh NK, Kundumani-Sridharan V, Heckle MR, Rao GN. Novel role of proline-rich nonreceptor tyrosine kinase 2 in vascular wall remodeling after balloon injury. *Arterioscler Thromb Vasc Biol*. 2012;32(11):2652-2661.

349. Frank GD, Mifune M, Inagami T, et al. Distinct mechanisms of receptor and nonreceptor tyrosine kinase activation by reactive oxygen species in vascular smooth muscle cells: role of metalloprotease and protein kinase C-delta. *Mol Cell Biol*. 2003;23(5):1581-1589.

350. Vepa S, Scribner WM, Parinandi NL, English D, Garcia JG, Natarajan V. Hydrogen peroxide stimulates tyrosine phosphorylation of focal adhesion kinase in vascular endothelial cells. *Am J Physiol*. 1999;277(1 Pt 1):L150-158.

351. Daou GB, Srivastava AK. Reactive oxygen species mediate Endothelin-1-induced activation of ERK1/2, PKB, and Pyk2 signaling, as well as protein synthesis, in vascular smooth muscle cells. *Free Radic Biol Med*. 2004;37(2):208-215.

352. Calalb MB, Polte TR, Hanks SK. Tyrosine phosphorylation of focal adhesion kinase at sites in the catalytic domain regulates kinase activity: a role for Src family kinases. *Mol Cell Biol*. 1995;15(2):954-963.

353. Andreev J, Galisteo ML, Kranenburg O, et al. Src and Pyk2 mediate G-protein-coupled receptor activation of epidermal growth factor receptor (EGFR) but are not required for coupling to the mitogen-activated protein (MAP) kinase signaling cascade. *J Biol Chem*. 2001;276(23):20130-20135.

354. Frank GD, Saito S, Motley ED, et al. Requirement of Ca(2+) and PKCdelta for Janus kinase 2 activation by angiotensin II: involvement of PYK2. *Mol Endocrinol*. 2002;16(2):367-377.

355. Abramovitz M, Adam M, Boie Y, et al. The utilization of recombinant prostanoid receptors to determine the affinities and selectivities of prostaglandins and related analogs. *Biochim Biophys Acta*. 2000;1483(2):285-293.

356. Snetkov VA, Knock GA, Baxter L, Thomas GD, Ward JP, Aaronson PI. Mechanisms of the prostaglandin F2alpha-induced rise in [Ca2+]i in rat intrapulmonary arteries. *J Physiol*. 2006;571(Pt 1):147-163.

357. Beasley D, Schwartz JH, Brenner BM. Interleukin 1 induces prolonged L-arginine-dependent cyclic guanosine monophosphate and nitrite production in rat vascular smooth muscle cells. *J Clin Invest*. 1991;87(2):602-608.

358. Wilcox CS, Pearlman A. Chemistry and antihypertensive effects of tempol and other nitroxides. *Pharmacol Rev*. 2008;60(4):418-469.

359. Banday AA, Marwaha A, Tallam LS, Lokhandwala MF. Tempol reduces oxidative stress, improves insulin sensitivity, decreases renal dopamine D1 receptor hyperphosphorylation, and restores D1 receptor-G-protein coupling and function in obese Zucker rats. *Diabetes*. 2005;54(7):2219-2226.

360. Wilcox CS. Effects of tempol and redox-cycling nitroxides in models of oxidative stress. *Pharmacol Ther*. 2010;126(2):119-145.

361. Azad GK, Tomar RS. Ebselen, a promising antioxidant drug: mechanisms of action and targets of biological pathways. *Mol Biol Rep*. 2014;41(8):4865-4879.

362. Sies H. Ebselen, a selenoorganic compound as glutathione peroxidase mimic. *Free Radic Biol Med*. 1993;14(3):313-323.

363. Zhao R, Holmgren A. Ebselen is a dehydroascorbate reductase mimic, facilitating the recycling of ascorbate via mammalian thioredoxin systems. *Antioxid Redox Signal*. 2004;6(1):99-104.

364. Gabryel B, Malecki A. Ebselen attenuates oxidative stress in ischemic astrocytes depleted of glutathione. Comparison with glutathione precursors. *Pharmacol Rep*. 2006;58(3):381-392.

365. Hamacher J, Stammberger U, Weber E, Lucas R, Wendel A. Ebselen improves ischemia-reperfusion injury after rat lung transplantation. *Lung*. 2009;187(2):98-103.

366. Mulvany MJ, Halpern W. Contractile properties of small arterial resistance vessels in spontaneously hypertensive and normotensive rats. *Circ Res*. 1977;41(1):19-26.

367. Mulvany MJ, Halpern W. Mechanical properties of vascular smooth muscle cells in situ. *Nature*. 1976;260(5552):617-619.

368. Mulvany MJ, Hansen OK, Aalkjaer C. Direct evidence that the greater contractility of resistance vessels in spontaneously hypertensive rats is associated with a narrowed lumen, a thickened media, and an increased number of smooth muscle cell layers. *Circ Res*. 1978;43(6):854-864.

369. Mulvany MJ, Nyborg N. An increased calcium sensitivity of mesenteric resistance vessels in young and adult spontaneously hypertensive rats. *Br J Pharmacol*. 1980;71(2):585-596.

370. Robertson TP, Dipp M, Ward JP, Aaronson PI, Evans AM. Inhibition of sustained hypoxic vasoconstriction by Y-27632 in isolated intrapulmonary arteries and perfused lung of the rat. *Br J Pharmacol*. 2000;131(1):5-9.

371. Robertson TP, Hague D, Aaronson PI, Ward JP. Voltage-independent calcium entry in hypoxic pulmonary vasoconstriction of intrapulmonary arteries of the rat. *J Physiol*. 2000;525 Pt 3:669-680.

372. Leach RM, Robertson TP, Twort CH, Ward JP. Hypoxic vasoconstriction in rat pulmonary and mesenteric arteries. *Am J Physiol*. 1994;266(3 Pt 1):L223-231.

373. Seddon AM, Curnow P, Booth PJ. Membrane proteins, lipids and detergents: not just a soap opera. *Biochim Biophys Acta*. 2004;1666(1-2):105-117.

374. Smith PK, Krohn RI, Hermanson GT, et al. Measurement of protein using bicinchoninic acid. *Anal Biochem*. 1985;150(1):76-85.

375. Lowry OH, Rosebrough NJ, Farr AL, Randall RJ. Protein measurement with the Folin phenol reagent. *J Biol Chem*. 1951;193(1):265-275.

376. Bradford MM. A rapid and sensitive method for the quantitation of microgram quantities of protein utilizing the principle of protein-dye binding. *Anal Biochem*. 1976;72:248-254.

377. Towbin H, Staehelin T, Gordon J. Electrophoretic transfer of proteins from polyacrylamide gels to nitrocellulose sheets: procedure and some applications. *Proc Natl Acad Sci U S A*. 1979;76(9):4350-4354.

378. Davis PK, Ho A, Dowdy SF. Biological methods for cell-cycle synchronization of mammalian cells. *Biotechniques*. 2001;30(6):1322-1326, 1328, 1330-1321.

379. el-Mezgueldi M. Calponin. *Int J Biochem Cell Biol*. 1996;28(11):1185-1189.

380. Sjoblom B, Salmazo A, Djinovic-Carugo K. Alpha-actinin structure and regulation. *Cell Mol Life Sci*. 2008;65(17):2688-2701.

381. Daiber A, August M, Baldus S, et al. Measurement of NAD(P)H oxidase-derived superoxide with the luminol analogue L-012. *Free Radic Biol Med*. 2004;36(1):101-111.

382. Sohn HY, Gloe T, Keller M, Schoenafinger K, Pohl U. Sensitive superoxide detection in vascular cells by the new chemiluminescence dye L-012. *J Vasc Res*. 1999;36(6):456-464.

383. Nishinaka Y, Aramaki Y, Yoshida H, Masuya H, Sugawara T, Ichimori Y. A new sensitive chemiluminescence probe, L-012, for measuring the production of superoxide anion by cells. *Biochem Biophys Res Commun*. 1993;193(2):554-559.

384. Zielonka J, Lambeth JD, Kalyanaraman B. On the use of L-012, a luminol-based chemiluminescent probe, for detecting superoxide and identifying inhibitors of NADPH oxidase: a reevaluation. *Free Radic Biol Med*. 2013;65:1310-1314.

385. Daiber A, Oelze M, August M, et al. Detection of superoxide and peroxynitrite in model systems and mitochondria by the luminol analogue L-012. *Free Radic Res*. 2004;38(3):259-269.

386. Kielland A, Blom T, Nandakumar KS, Holmdahl R, Blomhoff R, Carlsen H. In vivo imaging of reactive oxygen and nitrogen species in inflammation using the luminescent probe L-012. *Free Radic Biol Med*. 2009;47(6):760-766.

387. Han W, Li H, Segal BH, Blackwell TS. Bioluminescence imaging of NADPH oxidase activity in different animal models. *J Vis Exp*. 2012(68).

388. Allen RC. Phagocytic leukocyte oxygenation activities and chemiluminescence: a kinetic approach to analysis. *Methods Enzymol*. 1986;133:449-493.

389. Gyllenhammar H. Lucigenin chemiluminescence in the assessment of neutrophil superoxide production. *J Immunol Methods*. 1987;97(2):209-213.

390. Wu R, Millette E, Wu L, de Champlain J. Enhanced superoxide anion formation in vascular tissues from spontaneously hypertensive and desoxycorticosterone acetate-salt hypertensive rats. *J Hypertens*. 2001;19(4):741-748.

391. d'Uscio LV, Baker TA, Mantilla CB, et al. Mechanism of endothelial dysfunction in apolipoprotein E-deficient mice. *Arterioscler Thromb Vasc Biol*. 2001;21(6):1017-1022.

392. Skatchkov MP, Sperling D, Hink U, et al. Validation of lucigenin as a chemiluminescent probe to monitor vascular superoxide as well as basal vascular nitric oxide production. *Biochem Biophys Res Commun*. 1999;254(2):319-324.

393. Ohara Y, Peterson TE, Harrison DG. Hypercholesterolemia increases endothelial superoxide anion production. *J Clin Invest*. 1993;91(6):2546-2551.

394. Storch J, Ferber E. Detergent-amplified chemiluminescence of lucigenin for determination of superoxide anion production by NADPH oxidase and xanthine oxidase. *Anal Biochem*. 1988;169(2):262-267.

395. Hennet T, Richter C, Peterhans E. Tumour necrosis factor-alpha induces superoxide anion generation in mitochondria of L929 cells. *Biochem J*. 1993;289 (Pt 2):587-592.

396. Mohazzab KM, Kaminski PM, Wolin MS. NADH oxidoreductase is a major source of superoxide anion in bovine coronary artery endothelium. *Am J Physiol*. 1994;266(6 Pt 2):H2568-2572.

397. Faulkner K, Fridovich I. Luminol and lucigenin as detectors for O2. *Free Radic Biol Med*. 1993;15(4):447-451.

398. Brestel EP. Co-oxidation of luminol by hypochlorite and hydrogen peroxide implications for neutrophil chemiluminescence. *Biochem Biophys Res Commun*. 1985;126(1):482-488.

399. Oosthuizen MM, Greyling D. Hydroxyl radical generation: the effect of bicarbonate, dioxygen and buffer concentration on pH-dependent chemiluminescence. *Redox Rep*. 2001;6(2):105-116.

400. Selloum L, Djelili H, Sebihi L, Arnhold J. Scavenger effect of flavonols on HOCl-induced luminol chemiluminescence. *Luminescence*. 2004;19(4):199-204.

401. Radi R, Cosgrove TP, Beckman JS, Freeman BA. Peroxynitrite-induced luminol chemiluminescence. *Biochem J*. 1993;290 (Pt 1):51-57.

402. Castro L, Alvarez MN, Radi R. Modulatory role of nitric oxide on superoxide-dependent luminol chemiluminescence. *Arch Biochem Biophys*. 1996;333(1):179-188.

403. Mohanty JG, Jaffe JS, Schulman ES, Raible DG. A highly sensitive fluorescent micro-assay of H2O2 release from activated human leukocytes using a dihydroxyphenoxazine derivative. *J Immunol Methods*. 1997;202(2):133-141.

404. Zhou M, Diwu Z, Panchuk-Voloshina N, Haugland RP. A stable nonfluorescent derivative of resorufin for the fluorometric determination of trace hydrogen peroxide: applications in detecting the activity of phagocyte NADPH oxidase and other oxidases. *Anal Biochem*. 1997;253(2):162-168.

405. Towne V, Will M, Oswald B, Zhao Q. Complexities in horseradish peroxidase-catalyzed oxidation of dihydroxyphenoxazine derivatives: appropriate ranges for pH values and hydrogen peroxide concentrations in quantitative analysis. *Anal Biochem*. 2004;334(2):290-296.

406. Sakai H, Kurihara Y, Hashimoto Y, Chiba Y, Misawa M. Augmented PDBu-mediated contraction of bronchial smooth muscle of mice with antigen-induced airway hyperresponsiveness. *J Smooth Muscle Res*. 2010;46(5):259-266.

407. Ormo M, Cubitt AB, Kallio K, Gross LA, Tsien RY, Remington SJ. Crystal structure of the Aequorea victoria green fluorescent protein. *Science*. 1996;273(5280):1392-1395.

408. Prendergast FG, Mann KG. Chemical and physical properties of aequorin and the green fluorescent protein isolated from Aequorea forskalea. *Biochemistry*. 1978;17(17):3448-3453.

409. Tsien RY. The green fluorescent protein. *Annu Rev Biochem*. 1998;67:509-544.

410. Shigekawa K, Dower WJ. Electroporation of eukaryotes and prokaryotes: a general approach to the introduction of macromolecules into cells. *Biotechniques*. 1988;6(8):742-751.

411. Liu JQ, Zelko IN, Erbynn EM, Sham JS, Folz RJ. Hypoxic pulmonary hypertension: role of superoxide and NADPH oxidase (gp91phox). *Am J Physiol Lung Cell Mol Physiol*. 2006;290(1):L2-10.

412. Waypa GB, Marks JD, Guzy R, et al. Hypoxia triggers subcellular compartmental redox signaling in vascular smooth muscle cells. *Circ Res*. 2010;106(3):526-535.

413. Waypa GB, Guzy R, Mungai PT, et al. Increases in mitochondrial reactive oxygen species trigger hypoxia-induced calcium responses in pulmonary artery smooth muscle cells. *Circ Res*. 2006;99(9):970-978.

414. Park JG, Oh GT. The role of peroxidases in the pathogenesis of atherosclerosis. *BMB Rep*. 2011;44(8):497-505.

415. Kamezaki F, Tasaki H, Yamashita K, et al. Gene transfer of extracellular superoxide dismutase ameliorates pulmonary hypertension in rats. *Am J Respir Crit Care Med*. 2008;177(2):219-226.

416. Lin PJ, Chang CH, Pearson PJ, et al. Thromboxane A2: an endothelium-derived vasoconstrictor in human internal mammary arteries. *Ann Thorac Surg*. 1993;56(1):97-100.

417. Duran MC, Chan HL, Timms JF. Identification of oxidative stress-induced tyrosine phosphorylated proteins by immunoprecipitation and mass spectrometry. *Methods Mol Biol*. 2009;527:33-45, ix.

418. Giannoni E, Taddei ML, Chiarugi P. Src redox regulation: again in the front line. *Free Radic Biol Med*. 2010;49(4):516-527.

419. Kusaka G, Kimura H, Kusaka I, Perkins E, Nanda A, Zhang JH. Contribution of Src tyrosine kinase to cerebral vasospasm after subarachnoid hemorrhage. *J Neurosurg*. 2003;99(2):383-390.

420. Rice DC, Dobrian AD, Schriver SD, Prewitt RL. Src autophosphorylation is an early event in pressure-mediated signaling pathways in isolated resistance arteries. *Hypertension*. 2002;39(2 Pt 2):502-507.

421. Holmes TC, Fadool DA, Ren R, Levitan IB. Association of Src tyrosine kinase with a human potassium channel mediated by SH3 domain. *Science*. 1996;274(5295):2089-2091.

422. Dai S, Hall DD, Hell JW. Supramolecular assemblies and localized regulation of voltage-gated ion channels. *Physiol Rev*. 2009;89(2):411-452.

423. Hasegawa T, Bando A, Tsuchiya K, et al. Enzymatic and nonenzymatic formation of reactive oxygen species from 6-anilino-5,8-quinolinequinone. *Biochim Biophys Acta*. 2004;1670(1):19-27.

424. Murthy KS, Zhou H, Grider JR, Makhlouf GM. Inhibition of sustained smooth muscle contraction by PKA and PKG preferentially mediated by phosphorylation of RhoA. *Am J Physiol Gastrointest Liver Physiol*. 2003;284(6):G1006-1016.

425. Mahavadi S, Nalli A, Al-Shboul O, Murthy KS. Inhibition of MLC20 phosphorylation downstream of Ca2+ and RhoA: A novel mechanism involving phosphorylation of myosin phosphatase interacting protein (M-RIP) by PKG and stimulation of MLC phosphatase activity. *Cell Biochem Biophys*. 2014;68(1):1-8.

426. Thorpe RB, Stockman SL, Williams JM, Lincoln TM, Pearce WJ. Hypoxic depression of PKG-mediated inhibition of serotonergic contraction in ovine carotid arteries. *Am J Physiol Regul Integr Comp Physiol*. 2013;304(9):R734-743.

427. Uehata M, Ishizaki T, Satoh H, et al. Calcium sensitization of smooth muscle mediated by a Rho-associated protein kinase in hypertension. *Nature*. 1997;389(6654):990-994.

428. Lambeth JD. NOX enzymes and the biology of reactive oxygen. *Nat Rev Immunol*. 2004;4(3):181-189.

429. Turrens JF. Mitochondrial formation of reactive oxygen species. *J Physiol*. 2003;552(Pt 2):335-344.

430. Banes-Berceli AK, Ogobi S, Tawfik A, et al. Endothelin-1 activation of JAK2 in vascular smooth muscle cells involves NAD(P)H oxidase-derived reactive oxygen species. *Vascul Pharmacol*. 2005;43(5):310-319.

431. Madamanchi NR, Moon SK, Hakim ZS, et al. Differential activation of mitogenic signaling pathways in aortic smooth muscle cells deficient in superoxide dismutase isoforms. *Arterioscler Thromb Vasc Biol*. 2005;25(5):950-956.

432. El-Awady MS, Ansari HR, Fil D, Tilley SL, Mustafa SJ. NADPH oxidase pathway is involved in aortic contraction induced by A3 adenosine receptor in mice. *J Pharmacol Exp Ther*. 2011;338(2):711-717.

433. Chakraborti S, Roy S, Mandal A, et al. Role of PKCalpha-p(38)MAPK-G(i)alpha axis in NADPH oxidase derived O(2)(.-)-mediated activation of cPLA(2) under U46619 stimulation in pulmonary artery smooth muscle cells. *Arch Biochem Biophys*. 2012;523(2):169-180.

434. Shenker A, Goldsmith P, Unson CG, Spiegel AM. The G protein coupled to the thromboxane A2 receptor in human platelets is a member of the novel Gq family. *J Biol Chem*. 1991;266(14):9309-9313.

435. Neves SR, Ram PT, Iyengar R. G protein pathways. *Science*. 2002;296(5573):1636-1639.

436. Bey EA, Xu B, Bhattacharjee A, et al. Protein kinase C delta is required for p47phox phosphorylation and translocation in activated human monocytes. *J Immunol*. 2004;173(9):5730-5738.

437. Schnackenberg CG, Wilcox CS. The SOD mimetic tempol restores vasodilation in afferent arterioles of experimental diabetes. *Kidney Int*. 2001;59(5):1859-1864.

438. Nakamura Y, Feng Q, Kumagai T, et al. Ebselen, a glutathione peroxidase mimetic seleno-organic compound, as a multifunctional antioxidant. Implication for inflammation-associated carcinogenesis. *J Biol Chem*. 2002;277(4):2687-2694.

439. Tabet F, Schiffrin EL, Callera GE, et al. Redox-sensitive signaling by angiotensin II involves oxidative inactivation and blunted phosphorylation of protein tyrosine phosphatase SHP-2 in vascular smooth muscle cells from SHR. *Circ Res*. 2008;103(2):149-158.

440. Haurani MJ, Cifuentes ME, Shepard AD, Pagano PJ. Nox4 oxidase overexpression specifically decreases endogenous Nox4 mRNA and inhibits angiotensin II-induced adventitial myofibroblast migration. *Hypertension*. 2008;52(1):143-149.

441. Ago T, Kitazono T, Ooboshi H, et al. Nox4 as the major catalytic component of an endothelial NAD(P)H oxidase. *Circulation*. 2004;109(2):227-233.

442. BelAiba RS, Djordjevic T, Petry A, et al. NOX5 variants are functionally active in endothelial cells. *Free Radic Biol Med*. 2007;42(4):446-459.

443. Paravicini TM, Touyz RM. NADPH oxidases, reactive oxygen species, and hypertension: clinical implications and therapeutic possibilities. *Diabetes Care*. 2008;31 Suppl 2:S170-180.

444. Cave AC, Brewer AC, Narayanapanicker A, et al. NADPH oxidases in cardiovascular health and disease. *Antioxid Redox Signal*. 2006;8(5-6):691-728.

445. Brandes RP, Schroder K. Composition and functions of vascular nicotinamide adenine dinucleotide phosphate oxidases. *Trends Cardiovasc Med*. 2008;18(1):15-19.

446. Cai H, Griendling KK, Harrison DG. The vascular NAD(P)H oxidases as therapeutic targets in cardiovascular diseases. *Trends Pharmacol Sci*. 2003;24(9):471-478.

447. Chose O, Sansilvestri-Morel P, Badier-Commander C, et al. Distinct role of nox1, nox2, and p47phox in unstimulated versus angiotensin II-induced NADPH oxidase activity in human venous smooth muscle cells. *J Cardiovasc Pharmacol*. 2008;51(2):131-139.

448. Streeter J, Schickling BM, Jiang S, et al. Phosphorylation of Nox1 regulates association with NoxA1 activation domain. *Circ Res*. 2014;115(11):911-918.

449. Oda Y, Renaux B, Bjorge J, Saifeddine M, Fujita DJ, Hollenberg MD. cSrc is a major cytosolic tyrosine kinase in vascular tissue. *Can J Physiol Pharmacol*. 1999;77(8):606-617.

450. Blake RA, Broome MA, Liu X, et al. SU6656, a selective src family kinase inhibitor, used to probe growth factor signaling. *Mol Cell Biol*. 2000;20(23):9018-9027.

451. Sun G, Ramdas L, Wang W, Vinci J, McMurray J, Budde RJ. Effect of autophosphorylation on the catalytic and regulatory properties of protein tyrosine kinase Src. *Arch Biochem Biophys*. 2002;397(1):11-17.

452. Mills JE, Whitford PC, Shaffer J, Onuchic JN, Adams JA, Jennings PA. A novel disulfide bond in the SH2 Domain of the C-terminal Src kinase controls catalytic activity. *J Mol Biol*. 2007;365(5):1460-1468.

453. Liu C, Tazzeo T, Lippton H, Janssen LJ. Role of tyrosine phosphorylation in U46619-induced vasoconstriction of pulmonary vasculature and its modulation by genistein, daidzein, and equol. *J Cardiovasc Pharmacol*. 2007;50(4):441-448.

454. Abdalla S, Will JA. Potentiation of the hypoxic contraction of guinea-pig isolated pulmonary arteries by two inhibitors of superoxide dismutase. *Gen Pharmacol*. 1995;26(4):785-792.

455. Ungvari Z, Csiszar A, Huang A, Kaminski PM, Wolin MS, Koller A. High pressure induces superoxide production in isolated arteries via protein kinase C-dependent activation of NAD(P)H oxidase. *Circulation*. 2003;108(10):1253-1258.

456. Uzui H, Lee JD, Shimizu H, Tsutani H, Ueda T. The role of protein-tyrosine phosphorylation and gelatinase production in the migration and proliferation of smooth muscle cells. *Atherosclerosis*. 2000;149(1):51-59.

457. Chiarugi P, Pani G, Giannoni E, et al. Reactive oxygen species as essential mediators of cell adhesion: the oxidative inhibition of a FAK tyrosine phosphatase is required for cell adhesion. *J Cell Biol*. 2003;161(5):933-944.

458. Pelaez NJ, Braun TR, Paul RJ, Meiss RA, Packer CS. H(2)O(2) mediates Ca(2+)- and MLC(20) phosphorylation-independent contraction in intact and permeabilized vascular muscle. *Am J Physiol Heart Circ Physiol*. 2000;279(3):H1185-1193.

459. Girouard H, de Champlain J. Acute and chronic effects of free radicals on alpha1-adrenergic-induced vasoconstriction in mesenteric beds of spontaneously hypertensive rats. *J Hypertens*. 2005;23(4):807-814.

460. Shuvaev VV, Christofidou-Solomidou M, Bhora F, et al. Targeted detoxification of selected reactive oxygen species in the vascular endothelium. *J Pharmacol Exp Ther*. 2009;331(2):404-411.

461. Crosswhite P, Sun Z. Nitric oxide, oxidative stress and inflammation in pulmonary arterial hypertension. *J Hypertens*. 2010;28(2):201-212.

462. Gao YJ, Hirota S, Zhang DW, Janssen LJ, Lee RM. Mechanisms of hydrogen-peroxide-induced biphasic response in rat mesenteric artery. *Br J Pharmacol*. 2003;138(6):1085-1092.

463. Torok J. Histamine-induced relaxation in pulmonary artery of normotensive and hypertensive rats: relative contribution of prostanoids, nitric oxide and hyperpolarization. *Physiol Res*. 2000;49(1):107-114.

464. Tsai MH, Jiang MJ. Rho-kinase-mediated regulation of receptor-agonist-stimulated smooth muscle contraction. *Pflugers Arch*. 2006;453(2):223-232.

465. Robertson TP, Aaronson PI, Ward JP. Hypoxic vasoconstriction and intracellular Ca2+ in pulmonary arteries: evidence for PKC-independent Ca2+ sensitization. *Am J Physiol*. 1995;268(1 Pt 2):H301-307.

466. Demiryurek AT, Wadsworth RM, Kane KA, Peacock AJ. The role of endothelium in hypoxic constriction of human pulmonary artery rings. *Am Rev Respir Dis*. 1993;147(2):283-290.

467. Feletou M, Girard V, Canet E. Different involvement of nitric oxide in endothelium-dependent relaxation of porcine pulmonary artery and vein: influence of hypoxia. *J Cardiovasc Pharmacol*. 1995;25(4):665-673.

468. Chandel NS, Maltepe E, Goldwasser E, Mathieu CE, Simon MC, Schumacker PT. Mitochondrial reactive oxygen species trigger hypoxia-induced transcription. *Proc Natl Acad Sci U S A*. 1998;95(20):11715-11720.

469. Queliconi BB, Wojtovich AP, Nadtochiy SM, Kowaltowski AJ, Brookes PS. Redox regulation of the mitochondrial K(ATP) channel in cardioprotection. *Biochim Biophys Acta*. 2011;1813(7):1309-1315.

470. Touyz RM, Briones AM. Reactive oxygen species and vascular biology: implications in human hypertension. *Hypertens Res*. 2011;34(1):5-14.

471. Matoba T, Shimokawa H, Nakashima M, et al. Hydrogen peroxide is an endothelium-derived hyperpolarizing factor in mice. *J Clin Invest*. 2000;106(12):1521-1530.

472. Lee SB, Bae IH, Bae YS, Um HD. Link between mitochondria and NADPH oxidase 1 isozyme for the sustained production of reactive oxygen species and cell death. *J Biol Chem*. 2006;281(47):36228-36235.

473. Hawkins BJ, Madesh M, Kirkpatrick CJ, Fisher AB. Superoxide flux in endothelial cells via the chloride channel-3 mediates intracellular signaling. *Mol Biol Cell*. 2007;18(6):2002-2012.

474. Kimura S, Zhang GX, Nishiyama A, et al. Role of NAD(P)H oxidase- and mitochondria-derived reactive oxygen species in cardioprotection of ischemic reperfusion injury by angiotensin II. *Hypertension*. 2005;45(5):860-866.

475. Ushio-Fukai M, Griendling KK, Becker PL, Hilenski L, Halleran S, Alexander RW. Epidermal growth factor receptor transactivation by angiotensin II requires reactive oxygen species in vascular smooth muscle cells. *Arterioscler Thromb Vasc Biol*. 2001;21(4):489-495.

476. Fukunaga M, Oka M, Ichihashi M, Yamamoto T, Matsuzaki H, Kikkawa U. UV-induced tyrosine phosphorylation of PKC delta and promotion of apoptosis in the HaCaT cell line. *Biochem Biophys Res Commun*. 2001;289(2):573-579.

477. Gopalakrishna R, Gundimeda U, Schiffman JE, McNeill TH. A direct redox regulation of protein kinase C isoenzymes mediates oxidant-induced neuritogenesis in PC12 cells. *J Biol Chem*. 2008;283(21):14430-14444.

478. Konishi H, Tanaka M, Takemura Y, et al. Activation of protein kinase C by tyrosine phosphorylation in response to H2O2. *Proc Natl Acad Sci U S A*. 1997;94(21):11233-11237.

479. Rybin VO, Guo J, Sabri A, Elouardighi H, Schaefer E, Steinberg SF. Stimulus-specific differences in protein kinase C delta localization and activation mechanisms in cardiomyocytes. *J Biol Chem*. 2004;279(18):19350-19361.

480. Seko Y, Tobe K, Takahashi N, Kaburagi Y, Kadowaki T, Yazaki Y. Hypoxia and hypoxia/reoxygenation activate Src family tyrosine kinases and p21ras in cultured rat cardiac myocytes. *Biochem Biophys Res Commun*. 1996;226(2):530-535.

481. Turrens JF, Boveris A. Generation of superoxide anion by the NADH dehydrogenase of bovine heart mitochondria. *Biochem J*. 1980;191(2):421-427.

482. Genova ML, Ventura B, Giuliano G, et al. The site of production of superoxide radical in mitochondrial Complex I is not a bound ubisemiquinone but presumably iron-sulfur cluster N2. *FEBS Lett*. 2001;505(3):364-368.

483. Sabharwal SS, Schumacker PT. Mitochondrial ROS in cancer: initiators, amplifiers or an Achilles' heel? *Nat Rev Cancer*. 2014;14(11):709-721.

484. Zorov DB, Filburn CR, Klotz LO, Zweier JL, Sollott SJ. Reactive oxygen species (ROS)-induced ROS release: a new phenomenon accompanying induction of the mitochondrial permeability transition in cardiac myocytes. *J Exp Med*. 2000;192(7):1001-1014.

485. Wenzel P, Mollnau H, Oelze M, et al. First evidence for a crosstalk between mitochondrial and NADPH oxidase-derived reactive oxygen species in nitroglycerin-triggered vascular dysfunction. *Antioxid Redox Signal*. 2008;10(8):1435-1447.

486. Wang QS, Zheng YM, Dong L, Ho YS, Guo Z, Wang YX. Role of mitochondrial reactive oxygen species in hypoxia-dependent increase in intracellular calcium in pulmonary artery myocytes. *Free Radic Biol Med*. 2007;42(5):642-653.

487. Remington SJ. Fluorescent proteins: maturation, photochemistry and photophysics. *Curr Opin Struct Biol*. 2006;16(6):714-721.

488. Hanson GT, Aggeler R, Oglesbee D, et al. Investigating mitochondrial redox potential with redox-sensitive green fluorescent protein indicators. *J Biol Chem*. 2004;279(13):13044-13053.

489. Waypa GB, Marks JD, Mack MM, Boriboun C, Mungai PT, Schumacker PT. Mitochondrial reactive oxygen species trigger calcium increases during hypoxia in pulmonary arterial myocytes. *Circ Res*. 2002;91(8):719-726.

490. Hodyc D, Snorek M, Brtnicky T, Herget J. Superoxide dismutase mimetic tempol inhibits hypoxic pulmonary vasoconstriction in rats independently of nitric oxide production. *Exp Physiol*. 2007;92(5):945-951.

491. Chakraborti S, Chakraborti T. Down-regulation of protein kinase C attenuates the oxidant hydrogen peroxide-mediated activation of phospholipase A2 in pulmonary vascular smooth muscle cells. *Cell Signal*. 1995;7(1):75-83.

492. Chakraborti S, Michael JR. Role of protein kinase C in oxidant--mediated activation of phospholipase A2 in rabbit pulmonary arterial smooth muscle cells. *Mol Cell Biochem*. 1993;122(1):9-15.

493. Rathore R, Zheng YM, Li XQ, et al. Mitochondrial ROS-PKCepsilon signaling axis is uniquely involved in hypoxic increase in [Ca2+]i in pulmonary artery smooth muscle cells. *Biochem Biophys Res Commun*. 2006;351(3):784-790.

494. Robertson TP, Ward JP, Aaronson PI. Hypoxia induces the release of a pulmonary-selective, Ca(2+)-sensitising, vasoconstrictor from the perfused rat lung. *Cardiovasc Res*. 2001;50(1):145-150.

495. Karamsetty MR, Klinger JR, Hill NS. Evidence for the role of p38 MAP kinase in hypoxia-induced pulmonary vasoconstriction. *Am J Physiol Lung Cell Mol Physiol*. 2002;283(4):L859-866.

496. Tabet F, Schiffrin EL, Touyz RM. Mitogen-activated protein kinase activation by hydrogen peroxide is mediated through tyrosine kinase-dependent, protein kinase C-independent pathways in vascular smooth muscle cells: upregulation in spontaneously hypertensive rats. *J Hypertens*. 2005;23(11):2005-2012.

497. Viedt C, Soto U, Krieger-Brauer HI, et al. Differential activation of mitogen-activated protein kinases in smooth muscle cells by angiotensin II: involvement of p22phox and reactive oxygen species. *Arterioscler Thromb Vasc Biol*. 2000;20(4):940-948.

498. Morrell ED, Tsai BM, Wang M, Crisostomo PR, Meldrum DR. p38 mitogen-activated protein kinase mediates the sustained phase of hypoxic pulmonary vasoconstriction and plays a role in phase I vasodilation. *J Surg Res*. 2006;134(2):335-341.

499. Weir EK, Archer SL. The mechanism of acute hypoxic pulmonary vasoconstriction: the tale of two channels. *Faseb j*. 1995;9(2):183-189.

500. Reeve HL, Weir EK, Nelson DP, Peterson DA, Archer SL. Opposing effects of oxidants and antioxidants on K+ channel activity and tone in rat vascular tissue. *Exp Physiol*. 1995;80(5):825-834.

501. Archer SL, Souil E, Dinh-Xuan AT, et al. Molecular identification of the role of voltage-gated K+ channels, Kv1.5 and Kv2.1, in hypoxic pulmonary vasoconstriction and control of resting membrane potential in rat pulmonary artery myocytes. *J Clin Invest*. 1998;101(11):2319-2330.

502. Archer SL, Huang J, Henry T, Peterson D, Weir EK. A redox-based O2 sensor in rat pulmonary vasculature. *Circ Res*. 1993;73(6):1100-1112.

503. Reeve HL, Michelakis E, Nelson DP, Weir EK, Archer SL. Alterations in a redox oxygen sensing mechanism in chronic hypoxia. *J Appl Physiol (1985)*. 2001;90(6):2249-2256.

504. Corteling RL, Brett SE, Yin H, Zheng XL, Walsh MP, Welsh DG. The functional consequence of RhoA knockdown by RNA interference in rat cerebral arteries. *Am J Physiol Heart Circ Physiol*. 2007;293(1):H440-447.

505. Montani D, Bergot E, Gunther S, et al. Pulmonary arterial hypertension in patients treated by dasatinib. *Circulation*. 2012;125(17):2128-2137.

506. Dumitrescu D, Seck C, ten Freyhaus H, Gerhardt F, Erdmann E, Rosenkranz S. Fully reversible pulmonary arterial hypertension associated with dasatinib treatment for chronic myeloid leukaemia. Eur Respir J. Vol. 38. Switzerland; 2011:218-220.

507. Mattei D, Feola M, Orzan F, Mordini N, Rapezzi D, Gallamini A. Reversible dasatinib-induced pulmonary arterial hypertension and right ventricle failure in a previously allografted CML patient. Bone Marrow Transplant. Vol. 43. England; 2009:967-968.

508. Kantarjian HM, Shah NP, Cortes JE, et al. Dasatinib or imatinib in newly diagnosed chronic-phase chronic myeloid leukemia: 2-year follow-up from a randomized phase 3 trial (DASISION). *Blood*. 2012;119(5):1123-1129.

509. Ghofrani HA, Morrell NW, Hoeper MM, et al. Imatinib in pulmonary arterial hypertension patients with inadequate response to established therapy. *Am J Respir Crit Care Med*. 2010;182(9):1171-1177.

510. Archer SL, Nelson DP, Weir EK. Simultaneous measurement of O2 radicals and pulmonary vascular reactivity in rat lung. *J Appl Physiol (1985)*. 1989;67(5):1903-1911.

511. Nagaoka T, Morio Y, Casanova N, et al. Rho/Rho kinase signaling mediates increased basal pulmonary vascular tone in chronically hypoxic rats. *Am J Physiol Lung Cell Mol Physiol*. 2004;287(4):L665-672.

512. Mori M, Tsushima H. Vanadate activates Rho A translocation in association with contracting effects in ileal longitudinal smooth muscle of guinea pig. *J Pharmacol Sci*. 2004;95(4):443-451.

513. Ying Z, Giachini FR, Tostes RC, Webb RC. Salicylates dilate blood vessels through inhibiting PYK2-mediated RhoA/Rho-kinase activation. *Cardiovasc Res*. 2009;83(1):155-162.
514. Jaffe AB, Hall A. Rho GTPases: biochemistry and biology. *Annu Rev Cell Dev Biol*. 2005;21:247-269.
515. Montezano AC, Callera GE, Yogi A, et al. Aldosterone and angiotensin II synergistically stimulate migration in vascular smooth muscle cells through c-Src-regulated redox-sensitive RhoA pathways. *Arterioscler Thromb Vasc Biol*. 2008;28(8):1511-1518.
516. Amano M, Fukata Y, Kaibuchi K. Regulation and functions of Rho-associated kinase. *Exp Cell Res*. 2000;261(1):44-51.
517. Sauzeau V, Le Jeune H, Cario-Toumaniantz C, et al. P2Y(1), P2Y(2), P2Y(4), and P2Y(6) receptors are coupled to Rho and Rho kinase activation in vascular myocytes. *Am J Physiol Heart Circ Physiol*. 2000;278(6):H1751-1761.
518. Hains MD, Wing MR, Maddileti S, Siderovski DP, Harden TK. Galpha12/13- and rho-dependent activation of phospholipase C-epsilon by lysophosphatidic acid and thrombin receptors. *Mol Pharmacol*. 2006;69(6):2068-2075.
519. Alexander SP, Mathie A, Peters JA. Guide to Receptors and Channels (GRAC), 5th edition. *Br J Pharmacol*. 2011;164 Suppl 1:S1-324.
520. Yonemura S, Hirao-Minakuchi K, Nishimura Y. Rho localization in cells and tissues. *Exp Cell Res*. 2004;295(2):300-314.
521. Michaelson D, Silletti J, Murphy G, D'Eustachio P, Rush M, Philips MR. Differential localization of Rho GTPases in live cells: regulation by hypervariable regions and RhoGDI binding. *J Cell Biol*. 2001;152(1):111-126.
522. Rossman KL, Der CJ, Sondek J. GEF means go: turning on RHO GTPases with guanine nucleotide-exchange factors. *Nat Rev Mol Cell Biol*. 2005;6(2):167-180.
523. Tanabe S, Kreutz B, Suzuki N, Kozasa T. Regulation of RGS-RhoGEFs by Galpha12 and Galpha13 proteins. *Methods Enzymol*. 2004;390:285-294.
524. Kim M, Nozu F, Kusama K, Imawari M. Cholecystokinin stimulates the recruitment of the Src-RhoA-phosphoinositide 3-kinase pathway by Vav-2 downstream of G(alpha13) in pancreatic acini. *Biochem Biophys Res Commun*. 2006;339(1):271-276.
525. Forget MA, Desrosiers RR, Gingras D, Beliveau R. Phosphorylation states of Cdc42 and RhoA regulate their interactions with Rho GDP dissociation inhibitor and their extraction from biological membranes. *Biochem J*. 2002;361(Pt 2):243-254.

526. Lang P, Gesbert F, Delespine-Carmagnat M, Stancou R, Pouchelet M, Bertoglio J. Protein kinase A phosphorylation of RhoA mediates the morphological and functional effects of cyclic AMP in cytotoxic lymphocytes. *Embo j*. 1996;15(3):510-519.

527. Wells CD, Gutowski S, Bollag G, Sternweis PC. Identification of potential mechanisms for regulation of p115 RhoGEF through analysis of endogenous and mutant forms of the exchange factor. *J Biol Chem*. 2001;276(31):28897-28905.

528. Schmidt A, Hall A. Guanine nucleotide exchange factors for Rho GTPases: turning on the switch. *Genes Dev*. 2002;16(13):1587-1609.

529. Kato J, Kaziro Y, Satoh T. Activation of the guanine nucleotide exchange factor Dbl following ACK1-dependent tyrosine phosphorylation. *Biochem Biophys Res Commun*. 2000;268(1):141-147.

530. Crespo P, Schuebel KE, Ostrom AA, Gutkind JS, Bustelo XR. Phosphotyrosine-dependent activation of Rac-1 GDP/GTP exchange by the vav proto-oncogene product. *Nature*. 1997;385(6612):169-172.

531. Katoh H, Aoki J, Yamaguchi Y, Kitano Y, Ichikawa A, Negishi M. Constitutively active Galpha12, Galpha13, and Galphaq induce Rho-dependent neurite retraction through different signaling pathways. *J Biol Chem*. 1998;273(44):28700-28707.

532. Klages B, Brandt U, Simon MI, Schultz G, Offermanns S. Activation of G12/G13 results in shape change and Rho/Rho-kinase-mediated myosin light chain phosphorylation in mouse platelets. *J Cell Biol*. 1999;144(4):745-754.

533. Keep NH, Barnes M, Barsukov I, et al. A modulator of rho family G proteins, rhoGDI, binds these G proteins via an immunoglobulin-like domain and a flexible N-terminal arm. *Structure*. 1997;5(5):623-633.

534. Hoffman GR, Nassar N, Cerione RA. Structure of the Rho family GTP-binding protein Cdc42 in complex with the multifunctional regulator RhoGDI. *Cell*. 2000;100(3):345-356.

535. Garcia-Mata R, Burridge K. Catching a GEF by its tail. *Trends Cell Biol*. 2007;17(1):36-43.

536. Velarde V, de la Cerda PM, Duarte C, et al. Role of reactive oxygen species in bradykinin-induced proliferation of vascular smooth muscle cells. *Biol Res*. 2004;37(3):419-430.

537. Loirand G, Guerin P, Pacaud P. Rho kinases in cardiovascular physiology and pathophysiology. *Circ Res*. 2006;98(3):322-334.

538. Mills RD, Mita M, Nakagawa J, Shoji M, Sutherland C, Walsh MP. A role for the tyrosine kinase Pyk2 in depolarization-induced contraction of vascular smooth muscle. *J Biol Chem*. 2015;290(14):8677-8692.

539. Luo JH, Weinstein IB. Calcium-dependent activation of protein kinase C. The role of the C2 domain in divalent cation selectivity. *J Biol Chem*. 1993;268(31):23580-23584.

540. Hanson MR, Kohler RH. GFP imaging: methodology and application to investigate cellular compartmentation in plants. *J Exp Bot*. 2001;52(356):529-539.

541. Kenworthy AK. Imaging protein-protein interactions using fluorescence resonance energy transfer microscopy. *Methods*. 2001;24(3):289-296.

542. dos Remedios CG, Miki M, Barden JA. Fluorescence resonance energy transfer measurements of distances in actin and myosin. A critical evaluation. *J Muscle Res Cell Motil*. 1987;8(2):97-117.

543. Miyawaki A, Llopis J, Heim R, et al. Fluorescent indicators for Ca2+ based on green fluorescent proteins and calmodulin. *Nature*. 1997;388(6645):882-887.

544. Ting AY, Kain KH, Klemke RL, Tsien RY. Genetically encoded fluorescent reporters of protein tyrosine kinase activities in living cells. *Proc Natl Acad Sci U S A*. 2001;98(26):15003-15008.

Appendix

DATA

Comparison between inhibitor responses to U46619 induced contraction +- L-NAME

Protocols

Cloning of rat RhoA and ARHGEF1 into a C-terminal GFP vector

Procedure for the Pierce Crosslink Magnetic IP/Co-IP Kit

Publications

Shaifta, Y, Irechukwu, N, Prieto-Lloret, J, MacKay, C. E, Marchon, K. A, Ward, J. P, Knock, G. A. Divergent modulation of Rho-kinase and Ca influx pathways by Src family kinases and focal adhesion kinase in airway smooth muscle. Br J Pharmacol. 2015, 172 (22), 5265-5280.

Mackay, C.E, Knock, G. A. Control of vascular smooth muscle function by Src-family kinases and reactive oxygen species in health and disease. Journal of Physiology. 2015, 593 (17), 3815-3828.

Scientific Presentations / Meetings

9th Young investigators meeting on Smooth Muscle in Airway and Vascular Disease, September 2015, London - entitled – "*ROS and Src in Smooth Muscle Function"*.

Physiology, July 2014, London – Tyrosine kinase and Smooth Muscle Function Symposium entitled – "*Tyrosine kinases and smooth muscle function"*.

Scientific Awards

2015 - British Association for Lung Research (BALR) Travel Prize.

Figure A1:

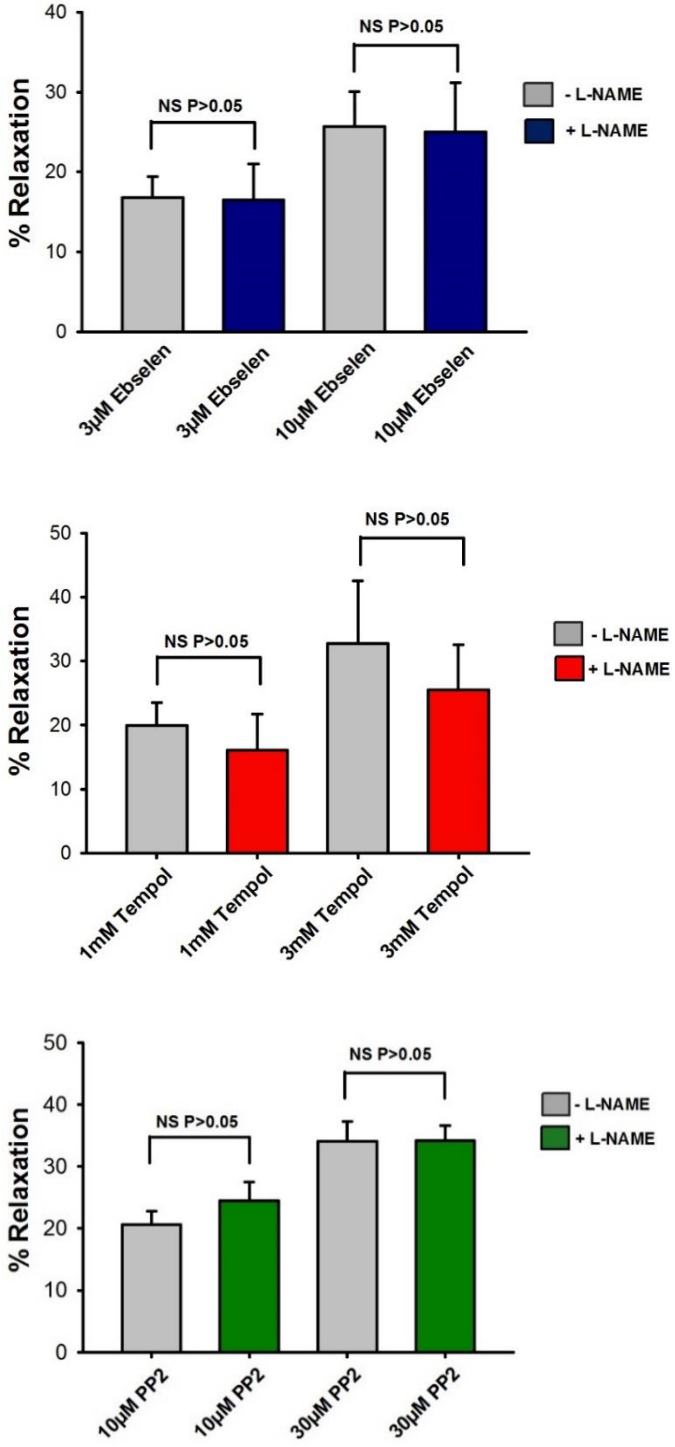

Figure A.1: Comparison between inhibitor responses to U46619 induced contraction +- L-NAME

Bar charts demonstrate that L-NAME has no effect on relaxation responses by (a) ebselen (n=8 vs. n=7(+L-NAME)), (b) tempol (n=8 vs. n=6(+L-NAME)) or (c) PP2 (n=6 vs. n=8 (L-NAME)). Paired t test.

Cloning of rat RhoA and ARHGEF1 into a C-terminal GFP vector

Preperation of Luria Bertani (LB) media and LB agar plates.

Before starting the cloning procedure, bacterial medium and agar plates were prepared. Luria Bertani (LB) media was made up by mixing 10 g tryptone, 5 g yeast extract (Beckton Dickinson, USA), and 10 g NaCl, per litre of ddH_2O. Agar medium was made up by adding 15 g of agar (Beckton Dickinson, USA) per litre of LB medium. Both LB and LB-agar were autoclaved to sterilise the medium. The required antibiotics (filter sterilised) were added at or below 50ºC for LB media. LB-agar was cooled and maintained at 50ºC in a water bath, antibiotic added, and plated onto 10 cm sterile Petri-dishes using sterile techniques.

Cloning of RhoA/GEF1 into pcDNA6.2-C-EmGFP-TOPO® vector

The plasmid vector pcDNA™6.2/C-EmGFP/TOPO® is supplied linearised with single 3'-deoxythymide (T) overhangs for TA cloning. The property of *Taq* polymerase having a non-template-dependant terminal transferase activity that adds a single deoxyadenosine (A) to the 3' ends of PCR products, allows PCR products to ligate efficiently with the vector.

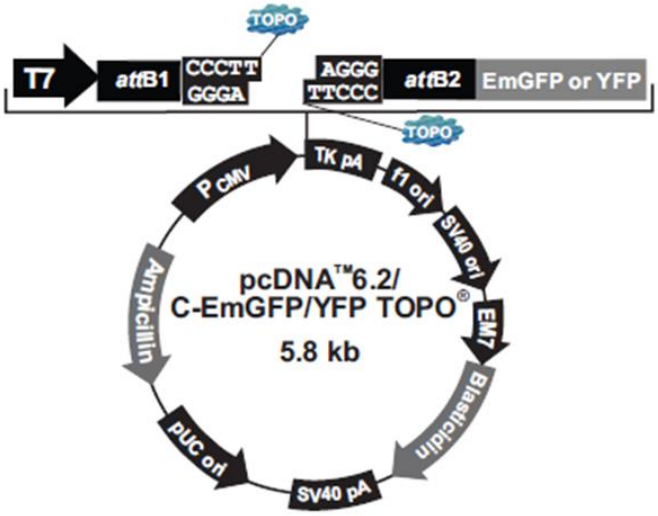

Comments for: | **pcDNA™6.2/ C-EmGFP TOPO® 5814 bp** | **pcDNA™6.2/ C-YFP TOPO® 5814 bp**

CAAT TATA 3´end of CMV promoter Putative transcriptional start

710 CAAATGGGCG GTAGGCGTGT ACGGTGGGAG GTCTATATAA GCAGAGCTCT CTGGCTAACT

T7 promoter/priming site

770 AGAGAACCCA CTGCTTACTG GCTTATCGAA ATTAATACGA CTCACTATAG GGAGACCCAA

att B1

830 GCTGGCTAGT TAAGCTGAGC ATCAACAAGT TTGTACAAAA AAGCAGGCTC CGAATTCGCC

att B2

890 CTT **PCR** AAG GGG GAA TTC GAC CCA GCT TTC TTG TAC AAA GTG GTT
GAA **PRODUCT** TTC CCC CTT AAG CTG GGT CGA AAG AAC ATG TTT CAC CAA
Lys Gly Glu Phe Asp Pro Ala Phe Leu Tyr Lys Val Val

FP 2 Rev priming site

*Hpa*I *Pme*I

932 GAT GCT GTT AAC ATG GTG AGC // --- TGA TAA GTT TAAACGGGGG AGGCTAACTG
CTA CGA CAA TTG **EmGFP or YFP** *** ***
Asp Ala Val Asn --- --- ---// ---

1693 AAACACGGAA GGAGACAA

TOPO® cloning exploits the properties of Topoisomerase I, a 314-amino acid enzyme, from *vaccinia* virus (Shuman, 1994). Topoisomerase I binds to duplex DNA at specific sites and cleaves the phosphodiester backbone after 5'-CCCTT in one strand. It is thought that the energy from the broken phosphodiester backbone is conserved by formation of a covalent bond between the 3'-phosphate of the cleaved strand and a tyrosil residue (Tyr 274) of topoisomerase I. The resulting topoisomerase-DNA complex, containing 5'-single stranded tail, can religate

to an acceptor DNA if the acceptor molecule has a 5'-OH tail complementary to that of the activated donor complex (Shuman, 1994). The plasmid vector pcDNA™6.2/C-EmGFP/TOPO® exploits this reaction to efficiently clone in PCR products.

The oligonucleotide primers for each target, listed in Table 1, were designed in accordance with the manual for GFP Fusion TOPO® TA expression Kit (Invitrogen Life Technologies, UK) and the deposited rat RhoA and GEF1 sequences in the GenBank® database. The Kozak consensus sequence is (G/A)NNATGG, where N is any nucleotide (Kozak, 1987;Kozak, 1990). In designing the reverse primers the termination codons were removed to allow the fusion of the GFP sequence.

Target	Primer Sequence	GenBank® Accession Number
Rat RhoA (rRhoA)	Forward 5'-GTTATGGCTGCCATCAGGAAGAAACTGG-3' Reverse 5'-CAAGATGAGGCACCCCGACT-3'	BC061732
Rat GEF1 (rGEF1)	Forward 5'-GAGATGGGAGAAGTCGCCGGAGGGGC-3' Reverse 5'-TGAAAGGCCTGTCTGAGCAGAGCGC-3'	BC091218

Table 1: PCR primers for C-EmGFP cloning

The RhoA cDNA was obtained by PCR using reverse transcribed RNA from rat PASMC cells and cloned into PCR®2.1-TOPO vector. The GEF1 cDNA was obtained from Source Bioscience (Source BioScience UK Limited).

The PCR reaction was carried out using puReTaq™ Ready-To-Go™ Polymerase Chain Reaction Beads (Amersham Biosciences UK Ltd.). The beads contain the optimised amount of recombinant puReTaq DNA polymerase, nucleotides (dNTPs), buffers, stabilisers and BSA, therefore only template DNA and primer were added and made up to 25 µl with distilled/deionised water (ddH_2O). The concentration of PCR primer mix used in the reactions was 0.6 µM. The PCR cycles were carried out as follows:

95°C	8 mins	
95°C	2 mins	Repeat ×19 to give <u>total cycle number of 20</u>
57°C	2 mins	
72°C	4 mins	
72°C	15 mins	Final extension
4°C	hold	

The PCR samples were run on a 1% agarose gel, 15 µl, with the remaining 10 µl retained for the cloning procedure. GeneRuler™ 1kb DNA Ladder or λ DNA/ EcoRI+HindIII Marker were run alongside the samples to determine the size of the PCR product. To reduce carry-over of template cDNA, the PCR product using lowest concentration of template cDNA was used for

cloning, 50 pg in this case. To 4 µl of PCR product 1 µl of salt solution (1.2 M NaCl, 0.06 M $MgCl_2$) and 1 µl (~10 ng) of pcDNA™6.2/C-EmGFP/TOPO® vector were mixed and incubated for 30 minutes at room temperature. The reaction mix was then chilled on ice before proceeding to One Shot® Chemical Transformation of competent cells (Invitrogen Life Technologies, UK).

To a 50 µl vial of One Shot® TOP10 chemically competent *E .coli* cells 2 µl of TOPO® cloning reaction mix was added, mixed gently and incubated on ice for 30 minutes. The cells were heat shocked for exactly 30 seconds at 42ºC and immediately transferred to ice and then 250 µl of sterile SOC medium (20 g tryptone, 5 g yeast extract, 0.5 g NaCl, 10 mM $MgCl_2$, 10 mM $MgSO_4$, 0.2 mM glucose, per litre of ddH_2O) added. The tubes were tightly capped and shaken horizontally at 225 rpm, 37ºC for 1 hour. The culture (20-200 µl) was then spread onto pre-warmed LB-agar-ampicillin (100 µg/ml) selection plates, inverted and incubated overnight at 37ºC.

Digestion with restriction endonucleases

TOPO® TA cloning allows cloning of the PCR insert in the forward and reverse orientation, due to identical overhangs in the insert and in the vector. The occurrence of both orientations should theoretically be of equal chance. Individual colonies (6-12) were picked and inoculated into 5 ml LB-ampicillin (100 µg/ml) media and cultured overnight at 225 rpm and 37ºC. 1ml of the culture was stored at 4ºC and the remainder purified for plasmid DNA using QIAprep® Miniprep Kit (QIAGEN GmbH, Germany). The bacterial cells were pelleted by spinning at 3000 rpm for 5 minutes and all the media removed. The plasmid DNA was purified from the bacterial cell pellets using the microcentrifuge protocol and re-suspended in 50 µl of ddH_2O.

To identify the clones which have the RhoA/GEF1 PCR insert ligated in the forward orientation, each RhoA/GEF1-CT-GFP clone was assessed for their restriction endonuclease sites. The samples with the correct digestion products were sent for sequencing (Source BioScience UK Limited).

Procedure for the Pierce Crosslink Magnetic IP/Co-IP Kit

A. Binding of Antibody to Protein A/G Magnetic Beads

Note: The following protocol is optimized for coupling 5µg of antibody, but coupling of 2-10µg of antibody can be accomplished by adjusting the protocol for the appropriate amounts.

1. Prepare 2mL of 1X Modified Coupling Buffer for each IP reaction by diluting 0.1mL of 20X Coupling Buffer and 0.1mL of IP Lysis/Wash Buffer with 1.8mL of ultrapure water.

2. Vortex the bottle of Pierce Protein A/G Magnetic Beads to obtain a homogeneous suspension. Add 25µL of beads into a microcentrifuge tube. Place tube on a magnetic stand to collect beads for 1 minute. Remove and discard the storage solution.

3. Add 500µL of 1X Modified Coupling Buffer prepared in Step 1 to the tube. Gently mix and incubate for 1 minute at room temperature on a rotating platform. Collect the beads on a magnetic stand, then remove and discard the supernatant. Repeat this step one time.

4. Dilute antibody 1:20 with 20X Coupling Buffer and 1:20 with IP Lysis/Wash Buffer, so the final concentration of antibody is 5µg per 100µL. For example, to prepare 100µL of antibody solution, dilute antibody stock into 5µL of 20X Coupling Buffer, 5µL of IP Lysis/Wash Buffer and add ultrapure water to bring the final volume to 100µL.

Note: Adjust antibody solution for antibody amounts other than 5µg per IP.

5. Add 100µL of prepared antibody solution to the beads, gently mix and incubate on a rotating platform for 15 minutes at room temperature. Gently vortex the beads every 5-10 minutes during incubation to ensure that the beads stay in suspension.

6. Collect the beads with a magnetic stand. Remove and discard the supernatant

7. Add 100µL of 1X Modified Coupling Buffer and gently vortex or invert the tube to mix. Collect the beads with a magnetic stand, then remove and discard the supernatant.

8. Add 300µL of 1X Modified Coupling Buffer and gently vortex or invert the tube to mix. Collect the beads with a magnetic stand, then remove and discard the supernatant. Repeat this step one time.

B. Crosslinking the Bound Antibody

Note: Conventional IP can be performed by omitting crosslinking; however, if crosslinking is omitted, the antibody will co-elute with the antigen during the elution steps.

Note: The DSS crosslinker is moisture-sensitive. Keep unused DSS in foil pouch. Dissolve DSS in DMSO or DMF immediately before use. DSS is not compatible with amine-containing buffers (e.g., Tris, glycine).

1. Puncture the foil cover of a single tube of DSS with a pipette tip and add 217µL of DMSO or DMF to prepare a 10X solution (25mM). Use the pipette to thoroughly mix the solution (i.e., draw up and expel the solution) until the DSS is dissolved.

2. Dilute the DSS 1:100 in DMSO or DMF (10µL of 10X DSS with 990µL solvent) to make 0.25mM DSS.

3. Add 2.5µL of 20X Coupling Buffer, 4µL of 0.25mM DSS and 43.5µL of ultrapure water to the beads. The total solution volume will be 50µL. The DSS is added at 10X molar excess to the Pierce Protein A/G Magnetic Beads at a working concentration of 20µM.

4. Incubate the crosslinking reaction for 30 minutes at room temperature on a rotator or mixer. Gently vortex the beads every 10-15 minutes during incubation to ensure that the beads stay in suspension.

5. Collect the beads with a magnetic stand. Remove and save the flow-through to verify antibody crosslinking.

6. Add 100µL of Elution Buffer to the beads and gently mix for 5 minutes at room temperature on a rotating platform to remove non-crosslinked antibody and quench the crosslinking reaction. Collect the beads with a magnetic stand, then remove and discard the supernatant.

7. Add 100µL of Elution Buffer to the beads and gently vortex or invert to mix. Collect the beads with a magnetic stand, then remove and discard the supernatant. Repeat one time.

8. Add 200µL of cold IP Lysis/Wash Buffer to the beads and gently vortex or invert to mix. Collect the beads with a magnetic stand, then remove and discard the supernatant. Repeat one time.

9. Proceed to the Manual or Automated Antigen Immunoprecipitation Protocols. If desired, the antibody-crosslinked beads can be stored at 4◦C.

C. Manual Antigen Immunoprecipitation

1. Dilute the lysate solution to 210µL with IP Lysis/Wash Buffer.

2. Add 70µL of diluted lysate solution to the tube containing crosslinked magnetic beads and incubate for 24 hours at 4°C on a rotator or mixer.

3. Collect the beads with a magnetic stand, remove the unbound sample and save for analysis.

4. Add 500µL of IP Lysis/Wash Buffer to the tube and gently mix. Collect the beads and discard the supernatant. Repeat this step one time.

5. Add 500µL of ultrapure water to the tube and gently mix. Collect the beads on a magnetic stand and discard the supernatant.

6. Add 70µL of Elution Buffer to the tube. Incubate for 5 minutes at room temperature on a rotator or mixer. Magnetically separate the beads and save the supernatant containing the target antigen. To neutralize the low pH add 8µL of Neutralization Buffer for each 70µL of eluate. For optimal antigen recovery, repeat this elution one time.

British Journal of Pharmacology

DOI:10.1111/bph.13313
www.brjpharmacol.org

RESEARCH PAPER

Divergent modulation of Rho-kinase and Ca^{2+} influx pathways by Src family kinases and focal adhesion kinase in airway smooth muscle

Yasin Shaifta, Nneka Irechukwu, Jesus Prieto-Lloret, Charles E MacKay, Keisha A Marchon, Jeremy P T Ward and Greg A Knock

Division of Asthma, Allergy and Lung Biology, Faculty of Life Sciences and Medicine, King's College London, London, UK

Correspondence
Dr Greg Knock, 1.20 Henriette Raphael House, Guy's Campus, King's College London, London, SE1 1UL, UK.
E-mail: greg.knock@kcl.ac.uk

Received
12 May 2015
Revised
2 August 2015
Accepted
19 August 2015

BACKGROUND AND PURPOSE

The importance of tyrosine kinases in airway smooth muscle (ASM) contraction is not fully understood. The aim of this study was to investigate the role of Src-family kinases (SrcFK) and focal adhesion kinase (FAK) in GPCR-mediated ASM contraction and associated signalling events.

EXPERIMENTAL APPROACH

Contraction was recorded in intact or α-toxin permeabilized rat bronchioles. Phosphorylation of SrcFK, FAK, myosin light-chain-20 (MLC_{20}) and myosin phosphatase targeting subunit-1 (MYPT-1) was evaluated in cultured human ASM cells (hASMC). $[Ca^{2+}]_i$ was evaluated in Fura-2 loaded hASMC. Responses to carbachol (CCh) and bradykinin (BK) and the contribution of SrcFK and FAK to these responses were determined.

KEY RESULTS

Contractile responses in intact bronchioles were inhibited by antagonists of SrcFK, FAK and Rho-kinase, while after α-toxin permeabilization, they were sensitive to inhibition of SrcFK and Rho-kinase, but not FAK. CCh and BK increased phosphorylation of MYPT-1 and MLC_{20} and auto-phosphorylation of SrcFK and FAK. MYPT-1 phosphorylation was sensitive to inhibition of Rho-kinase and SrcFK, but not FAK. Contraction induced by SR Ca^{2+} depletion and equivalent $[Ca^{2+}]_i$ responses in hASMC were sensitive to inhibition of both SrcFK and FAK, while depolarization-induced contraction was sensitive to FAK inhibition only. SrcFK auto-phosphorylation was partially FAK-dependent, while FAK auto-phosphorylation was SrcFK-independent.

CONCLUSIONS AND IMPLICATIONS

SrcFK mediates Ca^{2+}-sensitization in ASM, while SrcFK and FAK together and individually influence multiple Ca^{2+} influx pathways. Tyrosine phosphorylation is therefore a key upstream signalling event in ASM contraction and may be a viable target for modulating ASM tone in respiratory disease.

Abbreviations

ASM, airway smooth muscle; hASMC, cultured human airway smooth muscle cells; KPSS, PSS with 80 mM equimolar substitution of Na^+ for K^+; MLC_{20}, myosin light-chain 20 KDa subunit; MLCP, myosin light-chain phosphatase; MYPT-1, myosin phosphatase targeting subunit-1; ROCE, receptor-operated Ca^{2+} entry; SOCE, store-operated Ca^{2+} entry; VOCE, voltage-operated Ca^{2+} entry

Tables of Links

TARGETS	
Ion channels[a]	**Enzymes**[b]
Store-operated Ca2+ channels	FAK
Voltage-gated Ca2+ channels	MLCK
	PYK2
	Src family kinases
	Rho-kinase (ROCK)

LIGANDS	
Bradykinin (BK)	GTP
Carbachol (CCh)	Nifedipine
Cyclopiazonic acid (CPA)	Y27632

These Tables list key protein targets and ligands in this article which are hyperlinked to corresponding entries in http://www.guidetopharmacology.org, the common portal for data from the IUPHAR/BPS Guide to PHARMACOLOGY (Pawson *et al.*, 2014) and are permanently archived in the Concise Guide to PHARMACOLOGY 2013/14 ([a,b]Alexander *et al.*, 2013a,b).

Introduction

Airway smooth muscle (ASM) tone is subject to regulation by cholinergic, catecholamine and NANC neurotransmitters as well as local inflammatory mediators. In healthy airways, muscle tone is normally low, providing a low resistance path for airflow. However, contraction may be enhanced in response to chemical irritants or allergens, particularly in lower respiratory tract bronchioles (Gilbert and Auchincloss, 1989; Pinelli *et al.*, 2009). In asthma, airway resistance is increased, partly due to increased basal tone and hypersensitivity to constrictor stimuli in these bronchioles (Doeing and Solway, 2013; Meurs *et al.*, 2008).

Smooth muscle contractile force depends on the degree of myosin light-chain-20 (MLC_{20}) phosphorylation, which is in turn determined by the balance between Ca^{2+}-dependent activation of myosin light-chain kinase (MLCK) and Ca^{2+}-independent inhibition of myosin light-chain phosphatase (MLCP), as well as the formation and recruitment of myofilaments (Gunst *et al.*, 2003; Somlyo and Somlyo, 2003). Increases in $[Ca^{2+}]_i$ result from Ca^{2+} release from the sarcoendoplasmic reticulum (SR) and a combination of Ca^{2+} entry through receptor-operated, store-operated and voltage-operated Ca^{2+} channels (ROCE, SOCE and VOCE, respectively). Inhibition of MLCP occurs via phosphorylation of myosin phosphatase targeting subunit-1 (MYPT-1), primarily by Rho-kinase (Feng *et al.*, 1999), resulting in a further increase in MLC_{20} phosphorylation and contraction without the need for a further increase in $[Ca^{2+}]_i$ (Somlyo and Somlyo, 2003). Although it is likely that bronchoconstrictors act via a combination of the above pathways, the precise mechanisms through which Ca^{2+} influx and Rho-kinase activity are mediated by GPCRs are not fully understood.

Src family kinases (SrcFK) and focal adhesion kinase (FAK) are widely expressed non-receptor tyrosine kinases (TKs) important in many aspects of cellular function, being activated in response to various stimuli including growth factors, GPCRs, reactive oxygen species and adhesion. SrcFK and FAK are often described as being mutually dependent or reciprocally activated, especially when associated with integrin engagement and/or growth factor receptor activation (Owen *et al.*, 1999; Ishigaki *et al.*, 2011). An effect of TKs on ASM tone was first suggested by the relaxant effect of non-selective tyrosine kinase inhibitors on rat isolated bronchioles (Chopra *et al.*, 1997). Subsequently, selective inhibition of SrcFK and FAK was shown to depress GPCR-induced contraction in human, rodent or canine upper airways (Tang and Gunst, 2001; Katsumoto *et al.*, 2013). FAK was linked to elevated $[Ca^{2+}]_i$ in response to various stimuli in trachea, but the relative influence of the kinase on VOCE, ROCE or SOCE or on Rho-kinase was not determined (Tang *et al.*, 1999; Tang and Gunst, 2001). SrcFKs have been identified as upstream mediators of Rho-kinase in vascular smooth muscle (Nakao *et al.*, 2002; Knock *et al.*, 2008), but neither this relationship nor the influence of SrcFK on GPCR $[Ca^{2+}]_i$ responses has yet been examined in ASM. To our knowledge, only one previous study has examined the involvement of SrcFK or FAK specifically in the contraction of intralobar bronchioles, and this was limited to the role of SrcFK in mediating sensitization of rat bronchioles to muscarinic agonists (Sakai *et al.*, 2010).

In this study, we hypothesized that SrcFK and FAK mediate GPCR-induced ASM contraction via multiple signalling pathways and examined their influence on Rho-kinase-dependent MLCP inhibition/Ca^{2+}-sensitization and on SOCE/ROCE and VOCE Ca^{2+} entry pathways, in intra-lobar bronchioles of rat and cultured human ASM cells (hASMC). We found that SrcFK, most likely c-Src itself, modulate Rho-kinase dependent Ca^{2+}-sensitization, but FAK does not, and that the two tyrosine kinases differentially regulate SOCE/ROCE and VOCE. We also suggest the existence of two subpopulations of GPCR-activated SrcFK, one being FAK-dependent and the other FAK-independent.

Methods

Rats and tension measurement by wire myography

All animal care and experimental procedures complied with UK legislation under the Animals (Scientific Procedures) Act 1986 Amendment Regulations (SI 2012/3039) and were

deemed to be as humane as possible. All results involving animals are reported in accordance with the ARRIVE guidelines for reporting experiments involving animals (McGrath *et al.*, 2010). A total of 98 rats were used. Male Wistar rats (~250 g) had free access to food and water and were maintained on a 12:12 h light/dark schedule. The rats were killed by an i.p. injection of sodium pentobarbital and the lungs and trachea were immediately removed. First or second-order intralobar bronchioles (~2 mm length) were dissected free of surrounding parenchyma and mounted on a wire myograph (DMT. dk), bathed in PSS (in mM: 118 NaCl; 24 $NaHCO_3$; 1 $MgSO_4$; 4 KCl; 5.56 glucose; 0.435 NaH_2PO_4; 1.8 $CaCl_2$, pH 7.4), gassed with 95% air, 5% CO_2 at 37°C. Bronchioles were incrementally stretched and alternately exposed to PSS containing 80 mM $[K^+]$ (equimolar substitution for Na^+, KPSS) until the point on the length tension curve at which muscle length was optimum for active tension development was achieved, as described previously (Moir *et al.*, 2003). Viability for contraction experiments was confirmed by a response of at least 3 mN to the last challenge with KPSS. Bronchiole internal diameter after stretch was typically in the range 300–800 μm.

Specific examination of the Rho-kinase dependent Ca^{2+}-sensitization component of contraction was achieved by permeabilizing myograph-mounted bronchioles with α-haemolysin (α-toxin). PSS was first exchanged for relaxing solution (pCa = 10, in mM: 200 PIPES; 100 $Mg(M_s)_2$; 1000 KM_S; 100 K_2EGTA; 5 Na_2ATP; 10 Na_2creatine phosphate, pH 7.1), gassed with air at 26°C. α-toxin (60 μg ml^{-1}) was then applied in relaxing solution with pCa raised to 6.7 for 30 min, permeabilization being confirmed by the development of active tension. pCa was adjusted via proportionate substitution of K_2EGTA for CaEGTA, with 100 CaEGTA, 0 K_2EGTA being equivalent to pCa4.5. Contractile responses to bronchoconstrictors were conducted at pCa 6.5 (~300 nM $[Ca^{2+}]$), which induced a contraction equivalent to 10-20% of that achieved by pCa 4.5. GTP 1 μM and 10 μM cyclopiazonic acid (CPA) were included to support G-protein signalling and to prevent the influence of SR Ca^{2+} release on contraction respectively.

Human tissue and cell culture

Donations of human tissue were obtained following written informed consent and with the approval of the South East London Research Ethics Committee, REC reference number 10/H0804/66. All clinical procedures conformed to the standards set by the latest Declaration of Helsinki. hASMC were obtained from healthy volunteers (n = 11; 7 women, 4 males; age range 22–53 years; life-long absence of respiratory symptoms; lung functions within normal limits) by deep endobronchial biopsy. ASM bundles were bathed in DMEM containing 10% FBS, L-glutamine (2 mM), sodium pyruvate (1 mM), non-essential amino acids and amphotericin B (2 μg ml^{-1}), and subjected to enzymatic digestion in nominally Ca^{2+}-free HEPES buffer containing: 5.56 mM glucose, 2 mg ml^{-1} collagenase Type XI, 1 mg ml^{-1} papaine, 1 mg ml^{-1} trypsin inhibitor and 1 mM DTT, for 30 min at 37°C. Cells were then dispersed into culture flasks containing DMEM (plus supplements) and incubated at 37°C, pH 7.4. Smooth muscle phenotype was confirmed by positive staining with anti-smooth muscle α-actin, anti-desmin and anti-calponin, with Alexa Fluor®488 labelled secondary antibody (Lifetechnologies) and with TRITC-labelled phalloidin to confirm the presence of stress fibres in resting cells (Supporting Information Fig. S1). Cells were used for experiments at passages 4–9, grown to confluence and serum starved for 7 days in DMEM plus supplements, and the addition of 1% BSA, 5 μg ml^{-1} transferrin, 1 μM insulin and 100 μM ascorbate.

siRNA design and transfection

Two siRNAs against human SRC (GenBank accession no. NM_005417) were designed as described previously (Reynolds *et al.*, 2004; Ui-Tei *et al.*, 2004). The 19 nucleotide target sequences (SRC-siRNA1: position 1489–1507 and SRC-siRNA2: position 1684–1702) were synthesized into 64–65 mer oligonucleotides with BamHI/HindIII overhangs (Sigma Aldrich) and cloned into the expression vector pSilencer 3.0-H1, containing pmaxGFP (Ambion Inc.). All clones were purified using an EndoFree Plasmid Maxi Kit (Qiagen Ltd) and sequenced (Geneservice Ltd). hASMC were transfected using the Basic Nucleofector® Kit and nucleofector device (Amaxa Biosystems). After 72 h, the transfection efficiency was >90%, confirmed by fluorescence microscopy.

Protein lysate preparation and western blot

Cultured hASMCs were treated in serum-free DMEM at 37°C. Preliminary studies showed that phosphorylation responses, although sustained for at least 5 min, peaked at ~30 s, so all subsequent acute treatments were for 30 s. Cells were immediately washed twice with ice-cold PBS, followed immediately by application of cell lysis buffer (NEB) containing 1% phosphatase inhibitor cocktails 2 and 3 and 1% protease inhibitor cocktail (all Sigma). Cells were scraped into a tube and agitated before being placed on ice. Rat trachealis muscle was dissected free of adjoining cartilage, and epithelium was removed by scraping. Acute treatments were conducted in PSS/5% CO_2, at 37°C, before the tissue was snap frozen in liquid nitrogen, pulverized and lysed in cell lysis buffer. All lysates were centrifuged at 9.2x g, and the supernatants were stored at −80°C.

Samples were boiled in NuPAGE LDS Sample Buffer (Invitrogen) at 95°C for 5 min before being loaded onto 4–12% NuPAGE Bis-Tris gels (Invitrogen) for SDS-PAGE. Sample protein content was determined using the bicinchoninic acid assay, calibrated against BSA protein standards, to enable loading of ~20 μg of protein per lane. Gels were run at 180 V for 1 h using an Xcell SureLock Mini-Cell (Invitrogen) and MOPS running buffer (Invitrogen). Protein was transferred to a nitrocellulose membrane (Amersham) in 25 mM Tris, 192 mM glycine and 20% methanol, at 35 V for 1 h.

Membranes were blocked with 5% skimmed milk in Tris buffered saline (TBS) for 1 h at room temperature, followed by incubation with specific anti-phospho-protein primary antibody (typically 1:1000 dilution) in TBS with 1% skimmed milk and 0.1% Tween-20 (TBS-T), overnight at 4°C. Following washes in TBS-T, HRP-conjugated secondary antibody (typically 1:5000 dilution) was applied for 1 h at room temperature, followed by a final wash in TBS-T. 'Phospho' proteins were visualized with Super-Signal West

Femto chemi-luminescent Substrate (Thermo scientific). Membranes were then stripped in Restore western blot stripping buffer (Thermo Scientific), re-blocked and re-incubated with corresponding 'total' antibody and appropriate secondary antibodies, as above. 'Total' proteins were visualized with either ECL plus or ECL prime (Amersham, GE healthcare). Images were captured and quantified using the ChemiDoc XRS+ gel-imaging system (Biorad). An estimate of the proportion of target protein that was phosphorylated was calculated as a ratio of 'phospho' over 'total' signal for each protein band from each gel, and the effects of acute treatments on these ratios was expressed as a percentage of control (untreated samples run on the same gel).

$[Ca^{2+}]_i$ measurement

Cultured hASMCs were grown on glass cover-slips until 70% confluent, followed by 7 days of serum starvation. Cells were loaded with 1 μM Fura PE-3/AM in HBSS (containing in mM: 0.49 MgCl, 0.41 $MgSO_4$, 4 KCl, 0.44 KH_2PO_4, 4.2 $NaHCO_3$, 120 NaCl, 0.34 Na_2HPO_4, 20 HEPES and 2 CaCl) at room temperature for 40 min. Coverslips were mounted on an upright microscope and cells perfused with HBSS, containing test reagents as required. Changes in $[Ca^{2+}]_i$ were measured as a ratio of 340 nm over 380 nm emission intensities with a ×20 oil immersion UV objective and a microspectrofluorimeter (CairnResearch Ltd., U.K.). For each coverslip, ratios obtained in zero $[Ca^{2+}]_o$ and the absence of drug were taken as background fluorescence (auto-fluorescence + residual basal $[Ca^{2+}]_i$) and subtracted from all subsequent measurements.

Materials and reagents

Antibodies were obtained from cell signalling (anti-phospho-Src (tyr416); anti-Src; anti-phospho-FAK (Y397); anti-phospho-FAK (Y576/577); anti-FAK; anti-phospho-MLC (S19); anti-MYPT1; anti-MLC), Millipore (anti-phospho-MYPT1 (T696)), Sigma (anti-rabbit IgG; anti-mouse IgG). Kinase inhibitors were obtained from Sigma ((1R, 4r)-4((R)-1-aminoethyl)-*N*-(pyridine-4-yl) cyclohexane carboxamide (Y27632); 6-[4-(3-methanesulfonyl-benzylamino)-5-trifluoromethyl-pyrimidin-2-ylamino]-3,4-dihydro-1H-quinolin-2-one (PF-573228); *N*-[2-[[[2-[(2,3-dihydro-2-oxo-1H-indol-5-yl)amino]-5-(trifluoromethyl)-4-pyrimidinyl] amino]methyl]phenyl]-*N*-methyl-methanesulfonamide hydrate (PF-431396) or Calbiochem: (4-amino-5-(4-chlorophenyl)-7-(dimethylethyl) pyrazolo[3,4-d]pyrimidine (PP2); 4-amino-7-phenylpyrazol[3,4-d]pyrimidine (PP3). Cell culture and western blot materials were obtained from Cell Signalling, Invitrogen, GE Healthcare or Thermo Scientific. Nifedipine, YM58483, and cyclopiazonic acid and α-haemolysin were from Sigma.

Data analysis and statistics

All values are expressed as mean ± SEM. Non-linear regression curve fitting was performed with SigmaPlot 10. Carbachol (CCh) concentration-response curves were fitted using the Hill equation for the calculation of PD_2 (-LogM EC_{50}) and maximum response (Max). Bradykinin concentration responses were biphasic, and were best fitted using a two-site saturation model, for the characterization of a high affinity component (PD2-1 and Max-1) and a low affinity component (PD2-2 and Max-2). Statistical analysis of data was by Student's paired or un-paired *t*-test (two groups of data, single factor), one-way ANOVA (more than two groups of data, single factor) or two-way ANOVA (more than two groups of data, two factors), with Holm–Sidak *post* tests where appropriate, and as indicated in figure or table legends, using SigmaPlot 10. Differences were considered significant if $P < 0.05$.

Results

GPCR-mediated contraction of rat bronchioles is dependent on SrcFK, Rho-kinase and FAK. We examined the contractile responses to CCh and bradykinin (BK) in rat bronchioles, whereby the bronchoconstrictors were applied cumulatively at 5 min intervals. Two concentration-response curves were performed in each bronchiole (0.01–100μM), the first acting as a control and the second after pre-incubation with either the SrcFK inhibitor PP2 (30 μM), the Rho-kinase inhibitor Y27632 (10 μM), the FAK inhibitor PF-573228 (10 μM) or no inhibitor (control). In addition, to account for possible off-target effects of PP2 and PF-573228, key contractile responses were also repeated with PP3 (30 μM), the negative control for PP2 and a dual FAK/PYK2 inhibitor, PF-431396 (10 μM). CCh caused a sustained contraction at each dose (Figure 1A). The maximum response to CCh was significantly reduced by PP2 ($P < 0.01$, paired *t*-test, $n = 8$), Y27632 ($P < 0.01$, paired *t*-test, $n = 6$) and PF-573228 ($P < 0.05$, paired *t*-test, $n = 8$), and the PD_2 was significantly increased by PP2 (−5.55 ± 0.09 vs. control −5.8 ± 0.14, $P < 0.05$, paired *t*-test, $n = 8$), Y27632 (−5.4 ± 0.07 vs. control −5.82 ± 0.07, $P < 0.01$, paired *t*-test, $n = 6$) and PF-573228 (−5.21 ± 0.08 vs. control −5.69 ± 0.07, $P < 0.001$, paired *t*-test, $n = 8$) (Figure 1A–D). PP3 had no significant effect on either PD_2 (−5.6 ± 0.05 vs. control −5.72 ± 0.08, $n = 7$) or maximum contraction (144 ± 5% vs. control 149 ± 3%, $n = 7$). Conversely, PF-431396 had similar effects as those of PF-573228, causing a similar increase in PD_2 (−5.20 ± 0.05 vs. control −5.90 ± 0.07, $P < 0.001$, paired *t*-test, $n = 7$) and a similar reduction in maximum contraction (139 ± 6.3% vs. control 176 ± 9.3%, $P < 0.001$, paired *t*-test, $n = 7$) (Supporting Information Figs. S2A and S3A). In time-matched control responses, repeated in the absence of inhibitor, the maximum contraction of the second response was slightly increased (first repeat: 203 ± 22% vs. second repeat 228 ± 25%, $P < 0.01$, paired *t*-test, n=10), but there was no significant change in PD_2 (first repeat: −5.67 ± 0.11 vs. second repeat −5.63 ± 0.09, $n = 10$).

Bradykinin caused a prominent transient contraction and a smaller sustained component at each dose (Figure 1E). The concentration-dependence of these responses appeared biphasic. Contraction at all concentrations of BK was significantly inhibited by PP2 (Figure 1F), with maximum amplitudes of both high and low affinity components being reduced (Max-1 = 1.66 ± 0.5% vs. control 12.1 ± 4.1%; Max-2 = 6.81 ± 2.0% vs. control 24.4 ± 6.0%, $P < 0.05$, $n = 11$), while PD_2-1 and PD_2-2 were both unchanged (PD_2-1 = −6.7 ± 0.21 vs. control −7.08 ± 0.11; PD_2-2 = −4.85 ± 0.27 vs. control −4.67 ± 0.22, $n = 11$) (see Supporting Information Fig. S4

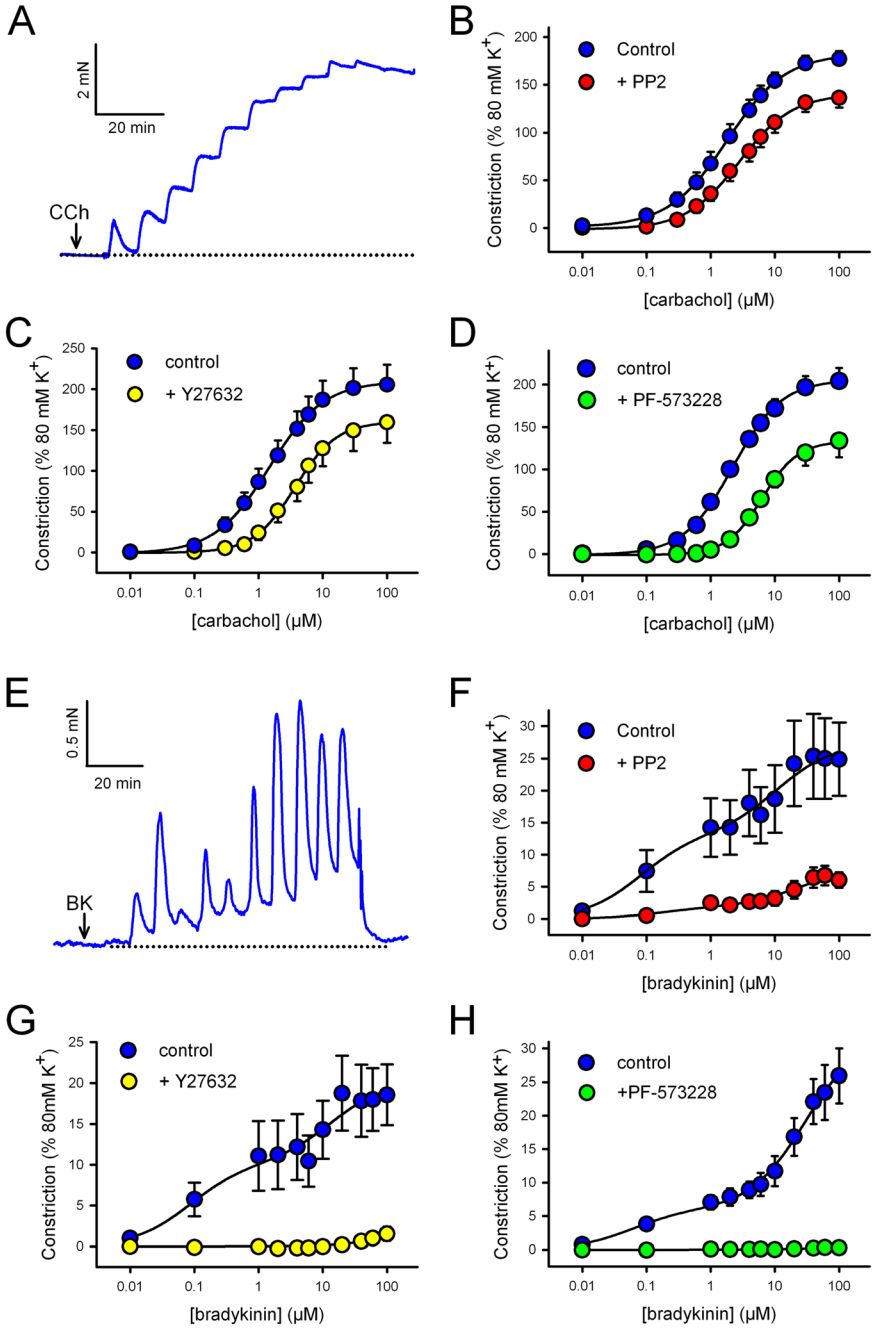

Figure 1

Effects of kinase inhibitors on carbachol and bradykinin-induced contraction in rat bronchioles. Measurement of isometric tension in freshly isolated rat bronchioles. CCh (A–D) or BK (E–H) was applied cumulatively (0.01–100μM) at 5 min intervals. Representative traces show typical cumulative contractile responses to CCh (A) and BK (E). Arrows indicate the points where the first concentration was applied. Two responses were performed in each bronchiole, the second after application of the Src inhibitor PP2 (30 μM, 10 min, B: CCh, $n = 8$ or F: BK, $n = 11$), the Rho-kinase inhibitor Y27632 (10 μM, 10 min, C: CCh, $n = 6$ or **G**: BK, $n = 4$), the FAK inhibitor PF-573228 (10 μM, 10 min, D: CCh, $n = 8$ or H: BK, $n = 5$) or no inhibitor (not shown). Measurements were taken at the end of each 5 min exposure and data fitted by nonlinear regression. Data expressed as a % of that induced by 80 mM KPSS (mean ± SEM); see main text or Supporting Information Fig. S4 for effects on PD_2 and max values.

for all BK dose responses curve fit data). BK-induced responses were nearly abolished by Y27632 (Figure 1G) and abolished by PF-573228 (Figure 1H), rendering curve fitting impossible. In time-matched control responses, repeated in the absence of inhibitor, there were no changes in either Max or PD_2 values for either the high or the low affinity component (not shown).

SrcFKs mediate GPCR-induced Ca^{2+}-sensitization and Rho-kinase activation, but FAK does not. To clarify whether the effects of

kinase inhibitors on bronchoconstrictor-induced contraction is mediated through a Rho-kinase-dependent Ca^{2+}-sensitization pathway, CCh or BK concentration-response curves were repeated in α-toxin-permeabilized rat bronchioles, with $[Ca^{2+}]_i$ fixed at pCa 6.5, in the absence or presence of PP2, Y27632 or PF-573228. After α-toxin-permeabilization, bronchoconstictor concentration-response curves were not repeatable (not shown), so controls and effects of antagonists were compared in separate bronchioles. CCh-induced contraction was almost absent in the presence of Y27632 and was significantly smaller in the presence of PP2 ($P < 0.05$, unpaired *t*-test, $n = 9$), but in the presence of PF-573228 was not different from controls (Figure 2B). The PD_2 was significantly greater after PP2 (−4.64 ± 0.13, vs. control -5.08 ± 0.12, $P < 0.05$, unpaired *t*-test, $n = 9$), but was no different in PF-573228. The underlying pCa 6.5 contraction was unaffected by either PP2 or PF-573228, but was partially inhibited by Y27632 (61 ± 8% block, $P < 0.05$ vs. absence of Y27632, paired *t*-test, $n = 6$). BK also produced a modest (relative to CCh) concentration-dependent contraction in permeabilized bronchioles (Figure 2A and C). The concentration-dependence of these responses again appeared biphasic, but their small amplitude and poor sustainability rendered curve-fitting impossible. Nevertheless, peak responses were significantly smaller or absent in the presence of PP2 or Y27632, respectively, and no different in PF-573228 (Figure 2C).

To confirm that Rho-kinase is being activated by 30 s exposure to BK (1 μM) or CCh (100 μM), and whether this activation relates to subsequent activation of MLCK, we measured phosphorylation of MYPT-1 at T696, a known phosphorylation target of Rho-kinase (Feng *et al.*, 1999), and of MLC_{20} at S19, the main target of MLCK. Furthermore, in order to reveal a possible interaction between Rho-kinase and SrcFK or FAK with relation to MLC_{20} phosphorylation, we examined the effects of inhibitors of Rho-kinase, SrcFK or FAK on both phosphorylation responses in hASMC. Phosphorylation of MLC_{20} and MYPT-1 were both significantly enhanced by BK. This enhancement was significantly reduced by PP2 and abolished by Y27632 at both sites, while PF-573228 significantly reduced the enhancement of MLC_{20}, but not MYPT-1 phosphorylation (Figure 2D and F). CCh also enhanced phosphorylation of both proteins, but to a lesser extent than BK. Basal MLC_{20} phosphorylation was insensitive to all three inhibitors (Figure 2E), while basal MYPT-1 phosphorylation was partially sensitive to Y27632, but insensitive to PP2 or PF-573228 (Figure 2G).

Bronchoconstrictors enhance SrcFK and FAK auto-phosphorylation. In order to confirm that the influence of SrcFK and FAK on contraction and Rho-kinase activity occurs in direct response to bronchoconstrictor stimulation, we also examined the effects of BK or CCh on SrcFK auto-phosphorylation at Y416 and FAK auto-phosphorylation at Y397, as a reflection of respective changes in kinase activity (Calalb *et al.*, 1995; Xu *et al.*, 1999). In hASMC, auto-phosphorylation of both kinases was significantly enhanced by both agents (Figure 3 A–D). As expected, SrcFK phosphorylation was almost abolished by PP2, and FAK phosphorylation was almost abolished by PF-573228, both confirming the selectivity of the phospho-antibodies and validating the choice of kinase inhibitor concentrations used. In rat trachealis muscle, SrcFK and FAK auto-phosphorylation were also enhanced by BK and CCh, as was phosphorylation of MLC_{20} (S19) and MYPT-1 (Y397), (Figure 3E, F). Bronchoconstrictor-induced FAK Y397 phosphorylation was noticeably weaker in rat trachealis than in hASMC.

FAK and SrcFK influence SOCE/ROCE and VOCE. We examined the effects of PP2 and PF-753228 on VOCE-mediated contraction by sub-maximal depolarization with 40 mM KPSS. In control experiments, contraction amplitude induced by two consecutive KPSS exposures was not significantly different, while when PP2 (30 μM) or PF-573228 (10 μM) was applied between the first and second exposures, the contractile response was modestly but significantly reduced by PF-573228, but not by PP2 (Figure 4A and B). To rule out a direct Ca^{2+}-channel antagonist effect of PF-573228, we also examined its effect on contraction induced by maximal depolarization with 80 mM KPSS. This contraction was significantly less sensitive to PF-573228 than the 40 mM KPSS contraction (11.5 ± 2.7% inhibition, $n = 6$, vs. 30.2 ± 6.3% inhibition of 40 mM KPSS, $n = 7$; $P < 0.05$ by unpaired *t*-test). We then examined the effects of PP2 and PF-573228 on SOCE-mediated contraction. SR Ca^{2+} was first depleted with cyclopiazonic acid (CPA, 10 μM) in the absence of extracellular Ca^{2+} and presence of 200 μM EGTA, then 2 mM Ca^{2+} was re-applied. CPA was used here instead of a GPCR agonist because it would have been difficult to separate effects of the agonist on Ca^{2+} entry from those on Rho-kinase-mediated Ca^{2+} sensitization. In control experiments, re-application of 2 mM Ca^{2+} induced a biphasic contraction, which peaked at ~2 min and slowly decayed to ~20% of 80 mM KPSS after 30 min. In the presence of either PP2 or PF-573228, the sustained component was significantly smaller, decaying to <10% of 80 mM KPSS after 30 min (Figure 4C and D). PP3 was without significant effect on this response, ruling out the possibility of a non-specific SOCE blocking effect of PP2 (Supporting Information Fig. S2B), while PF-431396 inhibited the response in a near-identical way to that of PF-573228, supporting a specific role for FAK in this response (Supporting Information Fig. S3B). To see whether these effects of PP2 and PF-573228 were due to an effect of SrcFK or FAK on SOCE itself or on secondary activation of VOCE, the effect of the SOCE blocker YM58483 (10 μM) and the Ca^{2+} channel antagonist nifedipine (2 μM) on the SOCE-mediated contraction was also determined. Apart from a small residual transient contraction, the response was abolished by YM58483, while nifedipine was without effect, apart from a small reduction in the peak response (Figure 4D).

To support contraction data and to further eliminate the possibility that SrcFK and FAK were indirectly influencing SOCE via an action on SR Ca^{2+} release, we also examine the effects of PP2 and PF-753228 on SOCE $[Ca^{2+}]_i$ responses in Fura-2 loaded hASMC, using BK as the initial SR-emptying stimulus. After the recording of an initial baseline in 2 mM Ca^{2+}, and then for 5 min in nominally Ca^{2+}-free buffer, the addition of BK (1 μM) caused a near instantaneous increase in $[Ca^{2+}]_i$. This decayed back to the baseline within ~2 min; a response

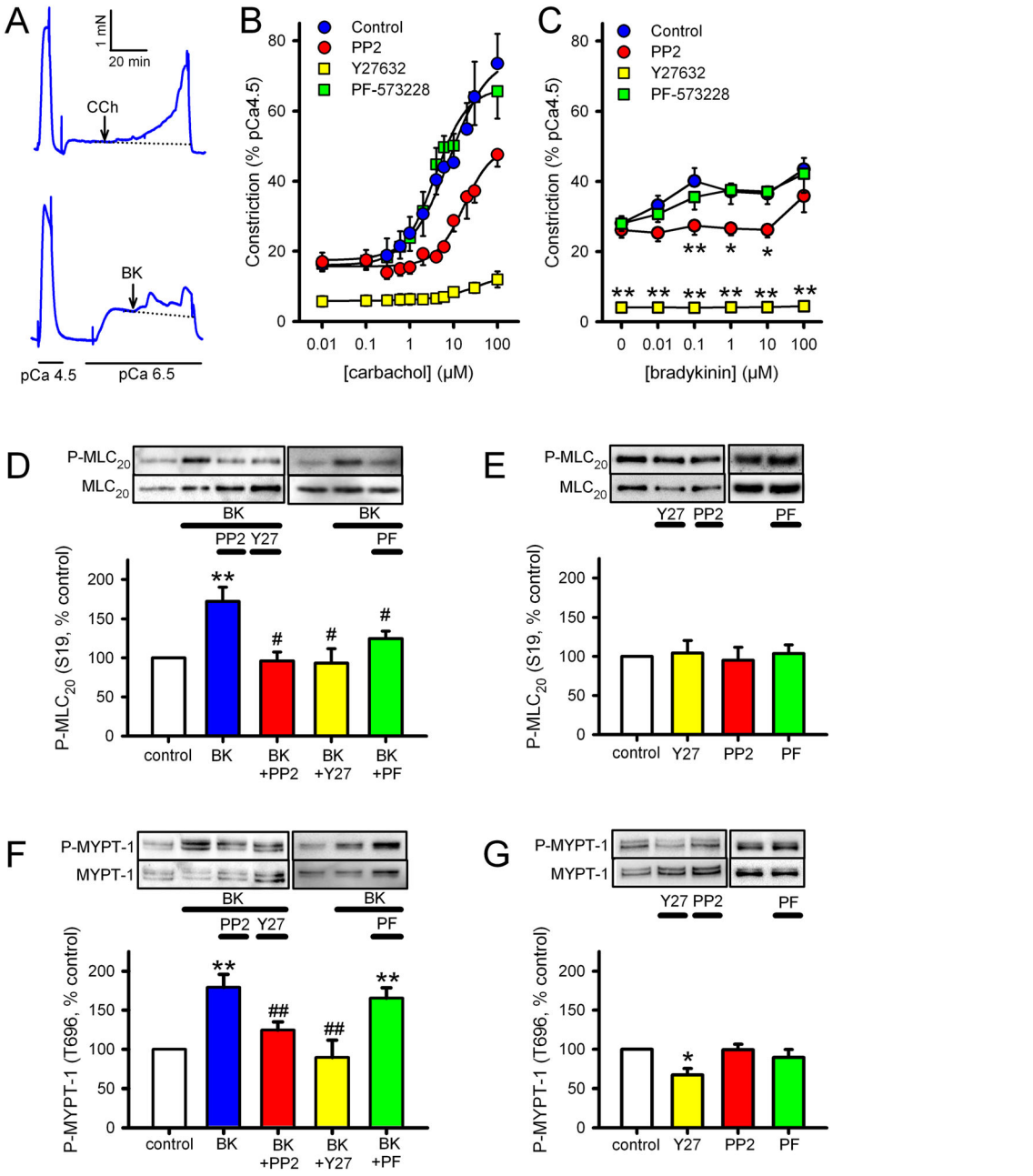

Figure 2

Effects of kinase inhibitors on contraction in α-toxin permeabilized rat bronchioles and MLC_{20}/MYPT-1 phosphorylation in hASMC. (A–C) Measurement of isometric tension in α-toxin permeabilized rat bronchioles. All responses were performed with pCa fixed at 6.5 and in the presence of 10 μM CPA and 1 μM GTP. (A) Representative traces showing CCh (upper panel) or BK (lower panel) being applied cumulatively (0.01–100 μM) at 5 min intervals, with arrows indicating where the first dose was applied. Responses were performed in the absence of inhibitor (control) or after pre-incubation with either the Src inhibitor PP2 (30 μM, 10 min), the Rho-kinase inhibitor Y27632 (10 μM, 10 min) or the FAK inhibitor PF-573228 (10 μM, 10 min). Measurements were taken at the end of each 5 min exposure. Data are expressed as a % of that induced by pCa 4.5 (mean ± SEM). (B) CCh data were fitted by nonlinear regression (control, n = 10; PP2, n = 9; Y27632, n = 4; PF-573228, n = 11); see main text for effects on CCh PD_2. (C) BK data could not be fitted by nonlinear regression so were compared by two-way RM ANOVA (control, n = 6; PP2, n = 6; Y27632, n = 4; PF-573228, n = 6; *$P < 0.05$, **$P < 0.01$ vs. control). (D–G) Measurement of phosphorylation of MLC_{20} at S19 (P-MLC_{20}, D, E) and MYPT-1 at T696 (P-MYPT-1, F, G), in hASMC. Representative blots show effects of treatment on 'phospho' and 'total' immunoreactivity for each protein. Bar charts show the effects of treatments on the degree of phosphorylation (mean ± SEM), expressed as a % of values from untreated (control) samples run on the same gels. (D) Effects of BK (1 μM 30 s) on MLC_{20} phosphorylation in the absence of inhibitor (n = 16) or after pretreatment with either PP2 (30 μM, 10 min, n = 11), Y27632 (10 μM, 10 min, n = 9) or PF-573228 (PF, 10 μM, 10 min, n = 11). (E) Effects of inhibitors on basal MLC_{20} phosphorylation (n = 4–11). (F) Effects of BK (1 μM, 30 s) on MYPT-1 phosphorylation in the absence of inhibitor (n = 13), or after pre-application of PP2 (30 μM, 10 min, n = 13), Y27632 (10 μM, 10 min, n = 13), or PF-573228 (10 μM, 10 min, n = 8). (G) Effects of inhibitors on basal MYPT-1 phosphorylation (n = 4–11). Comparisons were by one-way ANOVA with Holm–Sidak *post* tests: *$P < 0.05$ and **$P < 0.01$ versus control; #$P < 0.5$ and ##$P < 0.01$ versus BK alone.

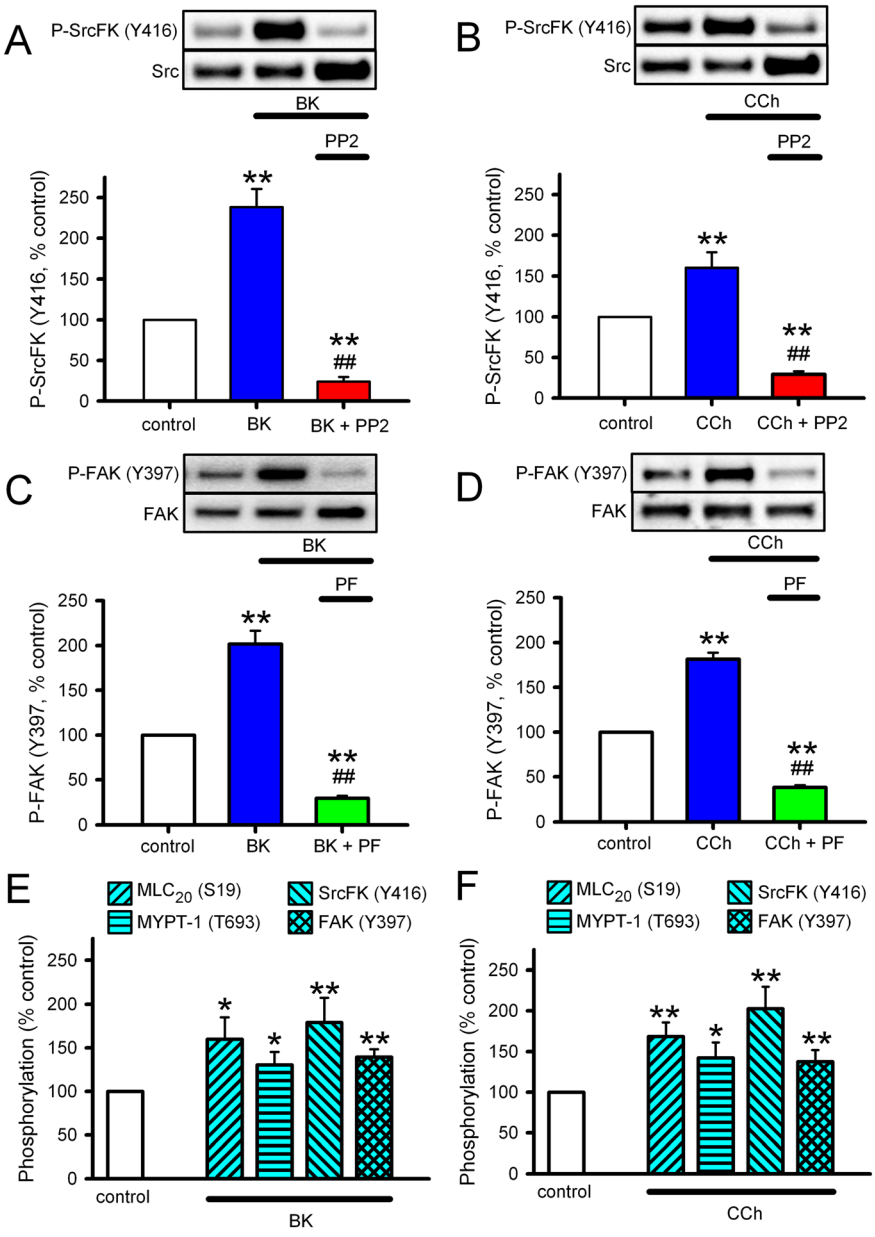

Figure 3

Effects of broncoconstrictors on SrcFK and FAK auto-phosphorylation in hASMC and rat trachealis. (A–D) Measurements of auto-phosphorylation of SrcFK at Y416 (P-SrcFK, A, B) and auto-phosphorylation of FAK at Y397 (P-FAK, C, D) in hASMC. Representative blots show effects of treatments on 'phospho' and 'total' immunoreactivity for each protein. Bar charts show the effects of treatments on the degree of phosphorylation (mean ± SEM), expressed as a % of values from untreated (control) samples run on the same gels. (A) Effect of BK (1 μM, 30 s) in the absence (n = 12) or presence of PP2 (30 μM, 10 min, n = 7) on P-SrcFK (Y416). (B) Effect of CCh (100 μM, 30 s) in the absence (n = 13) or presence of PP2 (n = 8) on P-SrcFK (Y416). (C) Effect of BK in the absence (n = 15) or presence of PF-573228 (PF, 10 μM, 10 min, n = 13) on P-FAK (Y397). (D) Effect of CCh in the absence (n = 16) or presence of PF-573228 (n = 11) on P-FAK (Y397). Comparisons by one-way ANOVA with Holm–Sidak *post* tests: $^{**}P < 0.01$ versus control; $^{\#\#}P < 0.01$ versus BK or CCh alone. (E, F) Measurements of phosphorylation of MLC_{20} (S19), MYPT-1 (T696), SrcFK (Y416) and FAK (Y397) in rat trachealis muscle. (E) Effects of BK (1 μM, 30 s, n = 8). (F) Effects of CCh (100 μM, 30 s, n = 8). Comparisons by unpaired t-test: $^{*}P<0.05$, $^{**}P<0.01$ versus control.

typical of GPCR-induced SR Ca^{2+}-release. 2 mM Ca^{2+} was then re-applied for 20 min, with simultaneous washout of BK. This induced a biphasic rise in $[Ca^{2+}]_i$ with a similar time course to the SOCE contractile responses. In the presence of either PP2 or PF-573228, the sustained component was reduced by ~50%, while the initial transient component and the initial BK-induced SR release were both unaffected (Figure 5).

Interaction between SrcFK and FAK. Because SrcFK and FAK appear to be sharing some but not all of the contraction signalling pathways investigated in this study, and in the

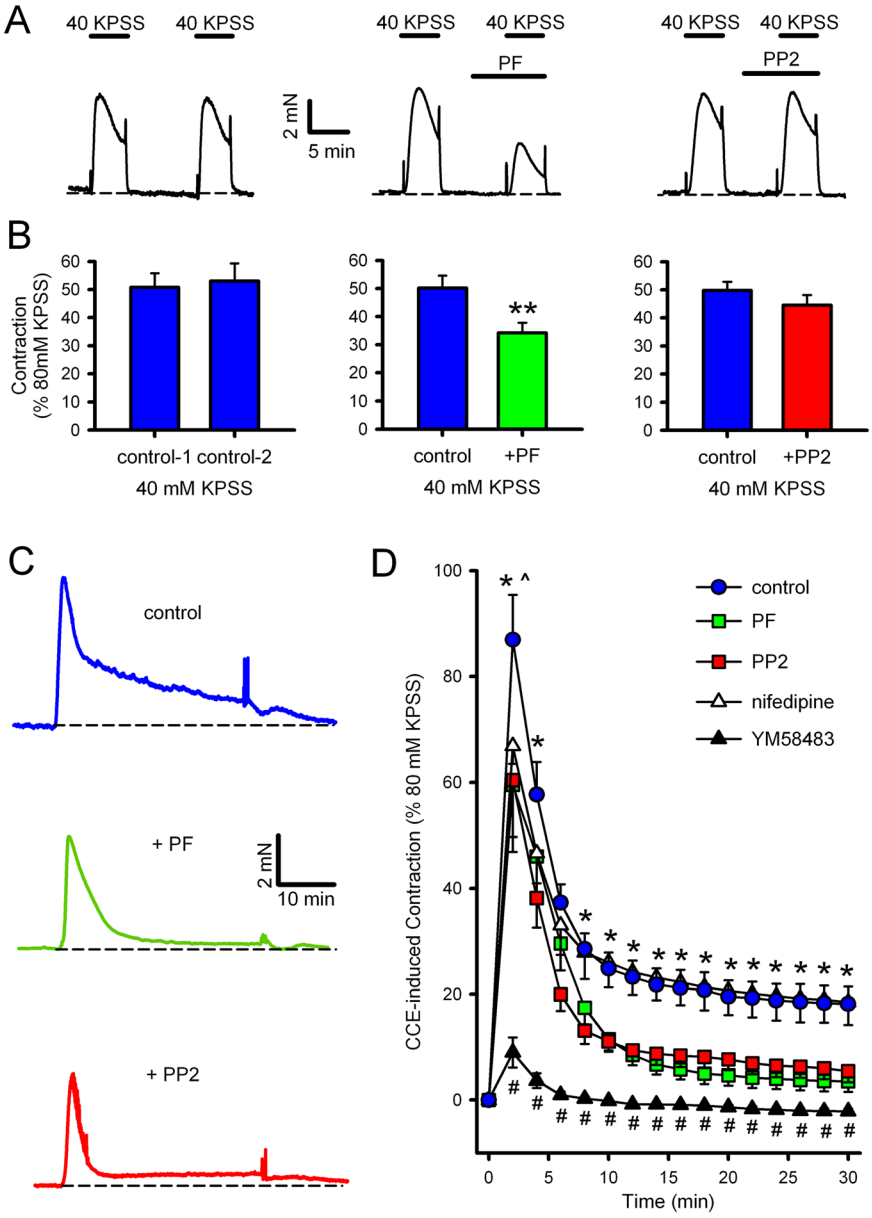

Figure 4

Effects of SrcFK and FAK inhibitors on VOCE- or SOCE-associated contraction in rat bronchioles. (A, B) VOCE-associated contractions induced by 40 mM KPSS. Representative traces (A) and mean measurements of peak amplitude (B, ± SEM), showing effects of two contractions in the absence of inhibitor (left panels, $n = 8$), the effect of PF-573228 on the second contraction (PF, middle panels, 10 μM, 5 min pre-incubation, $n = 7$) or the effect of PP2 on the second contraction (30 μM, right panels, 5 min pre-incubation, $n = 9$). Comparisons by paired *t*-test: $^{**}P < 0.01$ versus control. (C, D) SOCE-associated contraction induced by 10 μM CPA/200 μM EGTA/zero Ca^{2+}, followed by re-application of 2 mM Ca^{2+}. Representative traces (C) and mean measurements of amplitude of contractile responses at 2 min intervals after re-application of Ca^{2+} (D, ± SEM), showing control response ($n = 14$) and effects of pre-incubation with PF-573228 ($n = 9$), PP2 ($n = 9$), nifedipine ($n = 10$) or YM58483 ($n = 5$). Comparisons by two-way ANOVA with Holm–Sidak *post* tests: $^{*}P < 0.05$ for control versus PF-573228 or PP2. $\#P<0.01$ for control versus YM58483. $\wedge P < 0.05$ for control versus nifedipine at 2 min only.

light of previous evidence suggesting cooperation between the two kinases, we investigated the influence of FAK on SrcFK auto-phosphorylation and *vice versa*. Enhancement of SrcFK (Y416) auto-phosphorylation by BK was inhibited by PF-573228 by ~50% (Figure 6A), while basally, this phosphorylation was insensitive to PF-573228 but inhibited by PP2 (Figure 6B). FAK kinase activity is also reportedly influenced by Src-dependent phosphorylation on FAK Y576/577 (Calalb *et al.*, 1995). Phosphorylation at this dual site was enhanced by BK, and this enhancement was nearly abolished by PP2 and partially inhibited by PF-573228 (Figure 6C), while basally, this phosphorylation was inhibited by PP2, but not PF-573228 (Figure 6D). However, BK-induced enhancement of FAK (Y397) auto-phosphorylation was

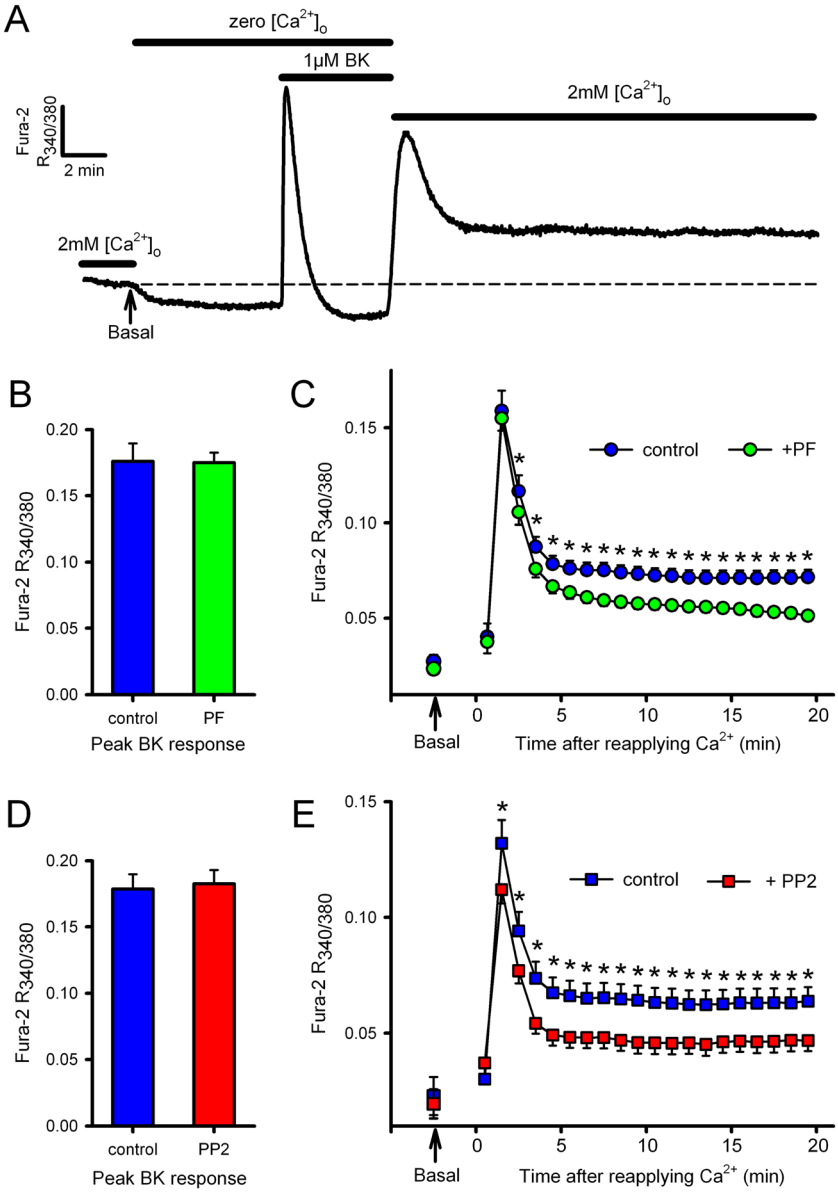

Figure 5

Effects of SrcFK and FAK inhibitors on SOCE/ROCE-associated $[Ca^{2+}]_i$ responses in hASMC. A: Representative control trace of $[Ca^{2+}]_i$ in Fura-2 loaded hASMC, as determined by the ratio of fluorescence at 340 nm/380 nm. Arrow indicates the point at which pre-stimulus basal $[Ca^{2+}]_i$ was recorded in 2 mM $[Ca^{2+}]_o$ (and extrapolated by dashed line). The buffer was then switched to zero $[Ca^{2+}]_o$ until a new baseline was established, and 1 μM BK added for 5 min. Finally, 2 mM $[Ca^{2+}]_o$ was reapplied for 20 min. Responses were performed either in the absence or presence of FAK inhibitor PF-573228 (B, C: PF, 10 μM, added 5 min prior to BK, n = 15 vs. 15 matched controls) or SrcFK inhibitor PP2 (D, E: 30 μM, added 5 min prior to BK, n = 10 vs. eight matched controls). Measurements were made of the peak BK-induced transient (B, D: arbitrary units, mean ± SEM) and of the response to reapplication of 2 mM $[Ca^{2+}]_o$ (C, E: arbitrary units, measured at 1 min intervals, mean ± SEM), compared with the pre-stimulus basal $[Ca^{2+}]_i$ in 2 mM $[Ca^{2+}]_o$ (indicated by arrows). Background fluorescence (in zero $[Ca^{2+}]_o$, prior to the application of BK) was subtracted from all other measurements. Comparisons by un-paired t-test (B, D) or two-way ANOVA with Holm–Sidak post tests (C, E: *$P < 0.05$ vs. matched controls).

unaffected by PP2 (Figure 6E). Basal phosphorylation of FAK (Y397) was also insensitive to PP2, but was inhibited by PF-53228 (Figure 6F).

c-Src is the principle SrcFK mediating bronchoconstrictor-induced phosphorylation responses. Multiple members of the Src-family of kinases are expressed in ASM, including c-Src, Fyn, Yes and Lyn (Sakai *et al.*, 2010). For this reason, and the fact that the phospho-SrcFK antibody cannot distinguish between Src family members, we re-examined the effects of acute BK treatment on MLC_{20} (S19), MYPT-1 (T696), SrcFK (Y416) and FAK (Y576/577) phosphorylation in hASMC after transfection with c-Src siRNA or scrambled siRNA. Specificity of c-Src siRNA was verified by a ~70% reduction in c-Src

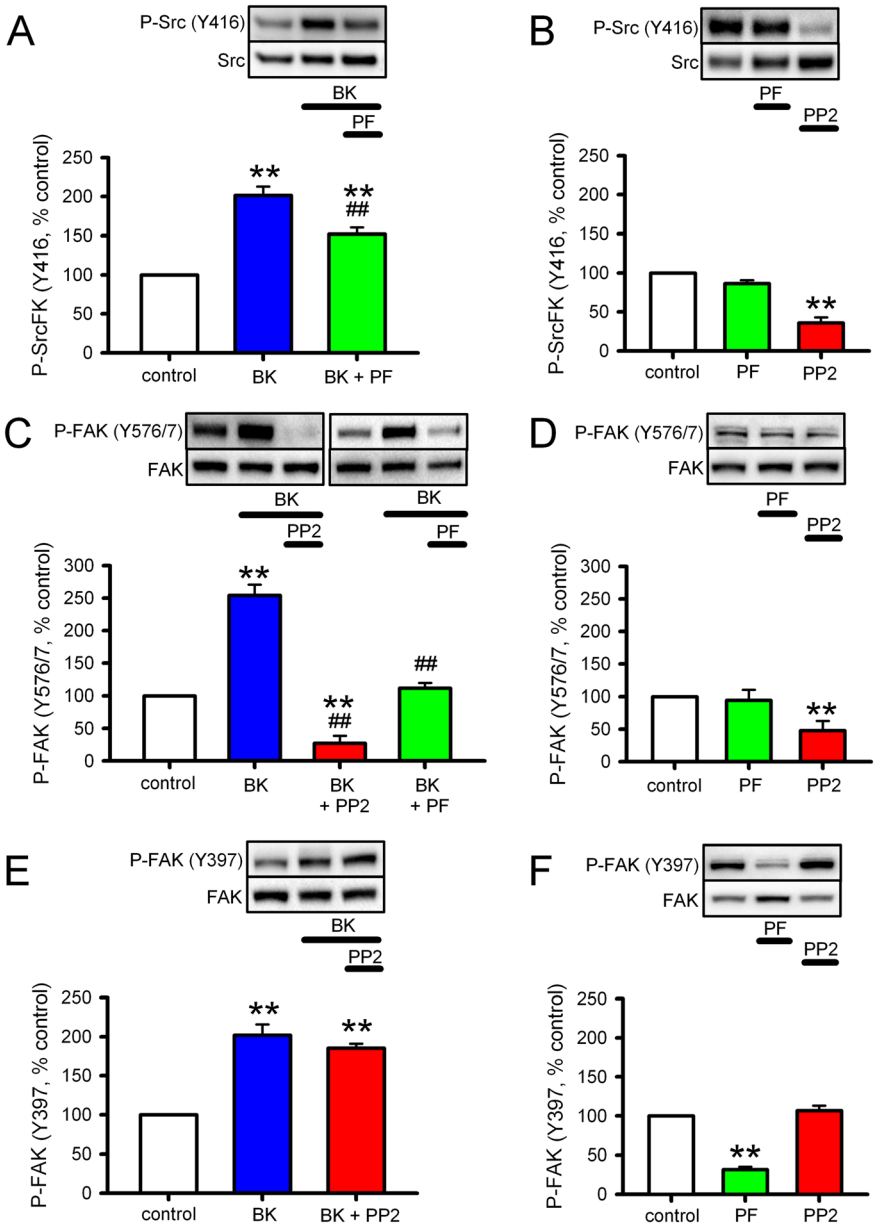

Figure 6

Interaction between SrcFK and FAK in response to BK in hASMCs. Measurements of auto-phosphorylation of SrcFK at Y416 (P-SrcFK, A, B), phosphorylation of FAK at the Y576/577 dual site (C, D), and auto-phosphorylation of FAK at Y397 (P-FAK, E, F) in hASMC. Representative blots show effects of treatments on 'phospho' and 'total' immunoreactivity for each protein. Bar charts show the effects of treatments on the degree of phosphorylation (mean ± SEM), expressed as a % of values from untreated (control) samples run on the same gels. (A) Effects of BK (1μM, 30 s) on P-SrcFK (Y416) in the absence ($n = 14$) or presence of the FAK inhibitor PF-573228 (PF, 10μM 10 min, $n = 7$). (B) Effects of PF ($n = 4$) or the SrcFK inhibitor PP2 (30μM, 10 min, $n = 4$) on basal P-SrcFK (Y416). (C) Effects of BK on P-FAK (Y576/577) in the absence ($n = 11$) or presence of PP2 ($n = 6$) or PF ($n = 7$). (D) Effects of PF ($n = 4$) or PP2 ($n = 5$) on basal P-FAK (Y576/577). (E) Effect of BK on P-FAK (Y397) in the absence ($n = 14$) or presence of PP2 ($n = 4$). (F) Effects of PF ($n = 4$) or PP2 ($n = 4$) on basal P-FAK (Y397). Comparisons by one-way ANOVA with Holm–Sidak *post* tests: $^{**}P < 0.01$ versus control or $^{\#\#}P < 0.01$ versus BK alone.

protein expression, while expressions of MLC_{20}, MYPT-1 and FAK were all unaffected (Figure 7A). The scrambled siRNA had no effect on any of the proteins examined. c-Src siRNA inhibited BK-induced phosphorylation of MLC_{20} by ~80%, while responses of MYPT-1 (T696), SrcFK (Y416) and FAK (Y576/577) to BK were all inhibited by ~60%, compared with matched scrambled siRNA transfected cells (Figure 7 B–D).

Discussion

We examined the role of SrcFK and FAK kinase activity in bronchoconstrictor-induced contraction of rat-isolated bronchioles and in $[Ca^{2+}]_i$ and phosphorylation responses in hASMC. Contraction was induced and MLC_{20} phosphorylation was enhanced by the bronchoconstrictors BK and

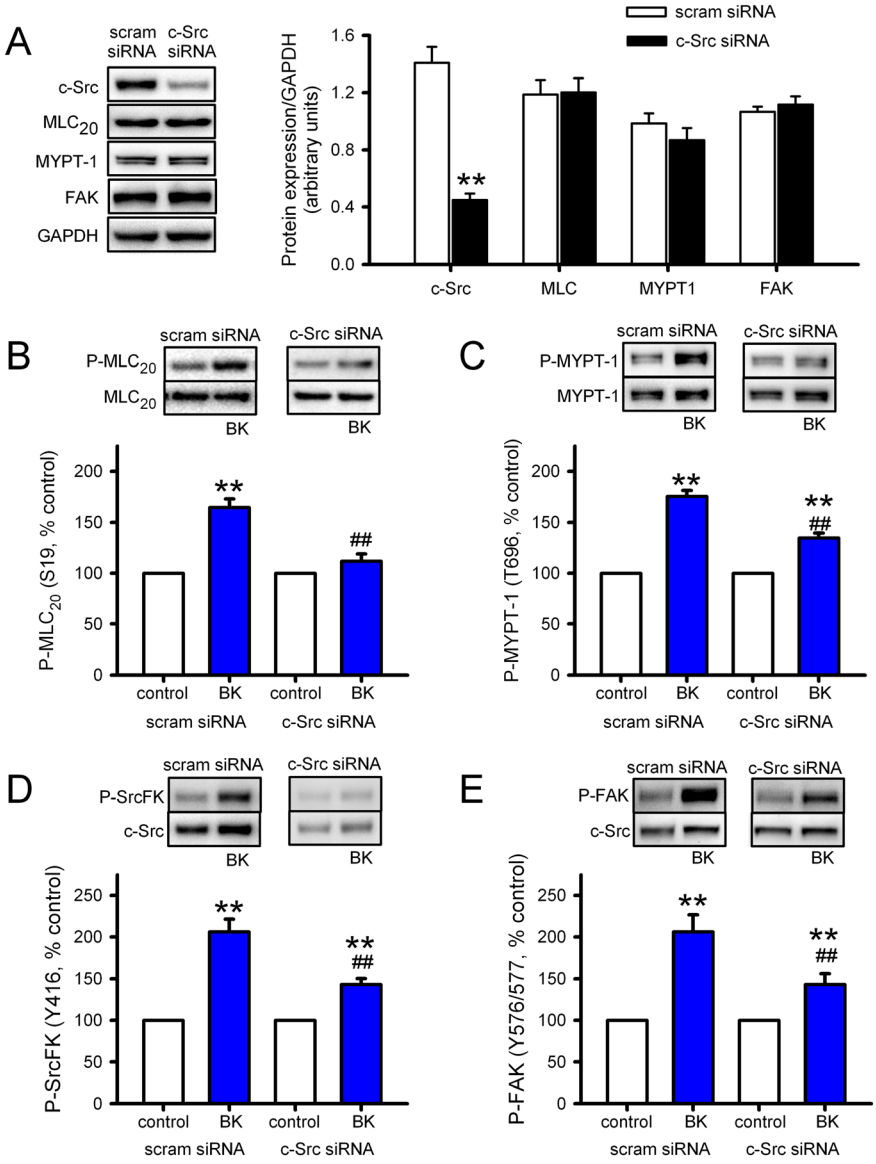

Figure 7

Effects of c-Src siRNA on bronchoconstrictor-induced MLC_{20}, MYPT-1, SrcFK and FAK phosphorylation in hASMCs. Measurement of protein expression and phosphorylation responses to BK (1 μM, 30 s) in hASMCs after transfection with c-Src siRNA or scrambled siRNA (scram). (A) Effect of c-Src siRNA on c-Src protein expression and (lack of) effect on MLC_{20}, MYPT-1 and FAK expression. Data normalized to GAPDH expression in the same samples (arbitrary units, $n = 8–12$). Comparisons by unpaired *t*-test: $^{**}P < 0.01$ versus scram siRNA. (B) Effect of BK on MLC_{20} phosphorylation at S19 (P-MLC_{20}) after transfection with scram siRNA ($n = 16$) or c-Src siRNA ($n = 16$). (C) Effect of BK on MYPT-1 phosphorylation at T696 (P-MYPT-1) after transfection with scram siRNA ($n = 14$) or c-Src siRNA ($n = 14$). (D) Effect of BK on SrcFK phosphorylation at Y416 (P-SrcFK) after transfection with scram siRNA ($n = 16$) or c-Src siRNA ($n = 16$). (E) Effect of BK on FAK phosphorylation at Y576/577 (P-FAK) after transfection with scram siRNA ($n = 10$) or c-Src siRNA ($n = 10$). Comparisons by two-way ANOVA: $^{**}P < 0.01$ versus control; $^{\#\#}P < 0.01$ versus scram siRNA.

CCh, and these responses were sensitive to inhibition of both SrcFK and FAK. Using auto-phosphorylation as an indication of kinase activity, both SrcFK and FAK were activated by both agents in hASMC and rat trachealis, suggesting an important role for these kinases in GPCR-induced ASM contraction in both humans and rodents. PP3, the negative control for PP2, was without effect on contraction, while PF-431396, another inhibitor of FAK, had similar effects as PF-573228, reducing the likelihood of our results being influenced by non-specific effects of PP2 or PF-573228. Amongst the several Src family members, both c-Src and Fyn have been implicated in vascular smooth muscle contraction (Nakao *et al.*, 2002; Knock *et al.*, 2008), and Lyn is activated by muscarinic agonists in ASM (Pertel *et al.*, 2006). Here however, the effects of c-Src siRNA suggest that 60–80% of all the bronchoconstrictor-induced phosphorylation responses investigated herein were specifically mediated by c-Src.

To further characterize the signalling pathways through which SrcFK and FAK mediate ASM contraction, we first focussed on their role in Rho-kinase dependent Ca^{2+}-sensitization, a process whereby inhibition of MLCP results in enhanced MLC_{20} phosphorylation, and hence force generation, without the requirement for an increase in $[Ca^{2+}]_i$ (Somlyo and Somlyo, 2003). Both BK and CCh-induced contraction were highly sensitive to Rho-kinase inhibition with Y27632. Furthermore, a component of the contractile response to both BK and CCh persisted when bronchioles were permeabilized with α-toxin to prevent changes in intracellular Ca^{2+}. We found that these contractile responses were dependent on Rho-kinase and SrcFK, but not FAK. Furthermore, we found that MYPT-1 phosphorylation on T696, an indicator of Rho-kinase-mediated MLCP inhibition (Feng *et al.,* 1999), is also enhanced by BK and CCh and that this enhancement is sensitive to inhibition of Rho-kinase and SrcFK, but not of FAK. This influence of SrcFK on Rho-kinase activity occurred specifically in response to agonist stimulation, because baseline phosphorylation of MYPT-1 and MLC_{20} and baseline pCa6.5 contraction in permeabilized bronchioles were not affected by SrcFK inhibition. Clearly, these results indicate that SrcFK mediates GPCR-induced smooth muscle contraction in part via activation of Rho-kinase. Importantly, this is the first direct demonstration of an interaction between SrcFK and Rho-kinase in ASM and in vessels of a size relevant to the control of airway resistance, consistent with the implied importance of Rho-kinase in airway hyper-responsiveness from studies in whole animal or isolated upper airways (Yoshii *et al.,* 1999; Schaafsma *et al.,* 2006). Interestingly, receptor TK stimulation also induces Rho-kinase-dependent ASM contraction (Gosens *et al.,* 2004), and other responses of ASM to growth factor stimulation are also SrcFK-dependent (Krymskaya *et al.,* 2005). Thus SrcFK may be a point of convergence for the activation of Rho-kinase in response to either GPCR or growth factors.

Rho-kinase is directly activated by the small G-protein RhoA, which is itself activated by guanine nucleotide exchange factors (RhoGEFs). RhoGEFs are known to be activated or modulated by various non-receptor TKs (Chikumi *et al.,* 2002; Ying *et al.,* 2009; Guilluy *et al.,* 2010), in addition to $G_{12/13}$ binding. It is therefore conceivable that SrcFK may be activating RhoA/Rho-kinase via direct phosphorylation of a RhoGEF. Alternatively, they may do so via the prior activation of another kinase, such as FAK, PYK2 or JAK2 (Calalb *et al.,* 1995; Andreev *et al.,* 2001; Singh *et al.,* 2011). Our results are not inconsistent with this hypothesis, but exclude FAK as the intermediary kinase in this instance.

We next focussed on the role of SrcFK and FAK in Ca^{2+} signalling. Gq/PLC-β-coupled GPCRs induce Ca^{2+} entry through three main pathways: DAG-sensitive TRP channel opening (ROCE), IP_3-dependent depletion of SR Ca^{2+} and subsequent STIM1/Orai1/TRP-dependent influx (SOCE), and subsequent depolarization-induced opening of L-type Ca^{2+} channels (VOCE) (Kawasaki *et al.,* 2006; Wang *et al.,* 2008). Several members of the TRPC family of channels, in addition to being modulated by DAG, are subject to modulation by phosphorylation, and tyrosine phosphorylation of TRPC channels is SrcFK-dependent, contributing to either ROCE or SOCE (Kawasaki *et al.,* 2006). Moreover, association of STIM1 with Orai1 in response to SR depletion, and subsequent Ca^{2+} influx, is partially dependent on SrcFK-mediated phosphorylation of STIM1 (Lopez *et al.,* 2012). In accord with these previous studies, we found that CPA-induced SOCE-dependent contraction in rat bronchioles and BK-induced Ca^{2+} influx in hASMC were both similarly sensitive to SrcFK inhibition. Interestingly, we found that these responses were also similarly sensitive to FAK inhibition. This, to our knowledge, is the first indication that FAK may be contributing to GPCR-induced Ca^{2+} responses and contraction in human and rodent ASM, via upstream modulation of SOCE and/or ROCE. Some GPCR agonists, notably angiotensin II, also mediate SR Ca^{2+} release via SrcFK-dependent tyrosine phosphorylation of PLC-γ (Schmitz *et al.,* 1997). However, there is no indication that this is occurring in our study, because we found that neither PP2 nor PF-573228 altered the BK-induced Ca^{2+} transients indicative of SR release.

Our finding that the CPA-induced SOCE contraction was minimally affected by the Ca^{2+} channel antagonist nifedipine suggests that VOCE secondary to SOCE-induced depolarization was not contributing substantially to this response. However, VOCE may also be activated more directly via a number of signalling pathways including stretch-activated phosphatidylcholine-specific PLC-derived DAG (Mauban *et al.,* 2015) or integrin-directed tyrosine phosphorylation. Regarding the latter, engagement of integrin α5β1 induces SrcFK and FAK-dependent phosphorylation of the α1c subunit of the L-type Ca^{2+} channel in vascular smooth muscle, with the likeliest sequence of events being integrin-induced FAK auto-phosphorylation followed by SrcFK recruitment by FAK (Owen *et al.,* 1999; Salazar and Rozengurt, 2001) and subsequent direct phosphorylation of the channel by SrcFK (Wu *et al.,* 2001; Gui *et al.,* 2006). Similarly in ASM, VOCE may also be enhanced via stretch or adhesion-induced FAK activity (Smith *et al.,* 1998; Tang *et al.,* 1999). In bronchioles, we found that contraction induced by depolarization with sub-maximal (40 mM) K^+ was sensitive to PF-573228 but not PP2, which suggests that FAK may be activating VOCE independently of SrcFK. However, contraction induced by maximum depolarization with 80 mM K^+ was considerably less sensitive to PF-573228, ruling out a non-specific effect of PF-573228 on Ca^{2+} channel opening *per se*. We did not systematically examine the effects of stretch on contractile responses, as carried out previously in trachea (Tang *et al.,* 1999), but applied a standard degree of stretch to maximize active tension responses to bronchoconstrictors or KPSS. Similarly, adherent hASMC are assumed to be under a degree of self-induced basal tension (Deguchi *et al.,* 2005). In light of this, it is worth noting that the relatively weak FAK autophosphorylation observed in trachealis samples treated with BK or CCh, compared with similarly treated hASMC, may have been because no stretch was applied to trachealis samples during BK or CCh treatment prior to snap freezing for protein extraction.

In smooth muscle contraction, it has been assumed that the mutual dependence between SrcFK and FAK relates primarily to the recruitment of contractile fibres through actin polymerization and focal attachment formation (Gerthoffer and Gunst, 2001; Tang *et al.,* 1999; Gunst *et al.,* 2003). It is therefore of note that we only see possible evidence of such mutuality with regard to SOCE/ROCE activity, but not in

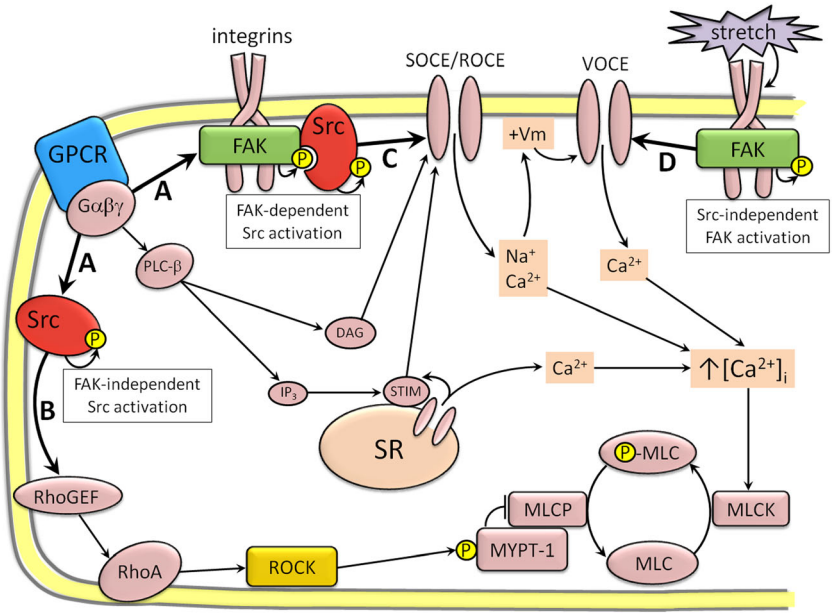

Figure 8

Proposed role for SrcFK and FAK in bronchoconstrictor or depolarization-induced ASM contraction, based on the results of the current study and existing literature. (A) GPCR activate both SrcFK and FAK, presumably via interaction with heterotrimeric G-protein sub-units (e.g. $G\alpha_q$, $G\alpha_{12/13}$ or $G\beta\gamma$) or downstream signalling molecules. Activated SrcFK forms two distinct sub-populations: one FAK-independent and one FAK-dependent. (B) FAK-independent SrcFK induces Rho-kinase to phosphorylate MYPT-1, thus enhancing myosin light-chain phosphorylation (P-MLC) through inhibition of myosin light-chain phosphatase (MLCP). SrcFK are perhaps activating Rho-kinase via the tyrosine phosphorylation of RhoA-associated proteins such as RhoGEFs. (C) A FAK/Src complex may be mediating store-operated and/or receptor-operated Ca^{2+} entry (SOCE/ROCE) via the tyrosine phosphorylation of TRP channels, or associated signalling proteins, such as STIM1, in association with DAG. (D) FAK is also independently enhancing voltage-operated Ca^{2+} entry (VOCE), perhaps via direct phosphorylation of voltage-dependent Ca^{2+} channels, in response to the additional stimulus of stretch or cellular adhesion, via integrin engagement.

relation to Rho-kinase activation (SrcFK only) or VOCE activity (FAK only). The selective sensitivity of basal SrcFK auto-phosphorylation to PP2 and of basal FAK auto-phosphorylation to PF-537228 confirms the specificity of these two antagonists for their intended targets at the concentrations used in this study. Therefore, our finding that BK-induced SrcFK auto-phosphorylation is partially PF-537228-sensitive suggests a partial dependence of GPCR-induced SrcFK activity on FAK. This is probably because SrcFK can be activated via disruption of intramolecular auto-inhibition by association of the SH2 domain with the phosphorylated Y397 of FAK (Xing *et al.*, 1994). Conversely, we show that BK-induced FAK auto-phosphorylation is wholly independent of SrcFK activity. In response to adhesion, in non-muscle cells, FAK auto-phosphorylation is enhanced by SrcFK-mediated phosphorylation on Y576/577 (Calalb *et al.*, 1995; Salazar and Rozengurt, 2001). However, despite the fact that we show that FAK Y576/577 phosphorylation is also induced by BK and almost entirely SrcFK-mediated, this phosphorylation does not correlate with enhanced FAK auto-phosphorylation. A similar discrepancy was observed in fibroblasts where adhesion-induced FAK auto-phosphorylation was SrcFK-dependent but GPCR-induced FAK auto-phosphorylation was not, despite both stimuli inducing SrcFK-dependent Y576/577 phosphorylation (Salazar and Rozengurt, 2001). Taken together, our results imply two things about these interactions in ASM: firstly, that GPCR can induce FAK activation without prior activation of SrcFK, and secondly, that there may be two sub-populations of BK/CCh-activated SrcFK; one FAK-dependent, resulting in modulation of SOCE/ROCE, and the other FAK-independent, resulting in activation of Rho-kinase (as summarized in Figure 8).

In conclusion, our data suggest an important role for SrcFK and FAK in bronchoconstrictor-mediated contraction in ASM, with the two kinases acting together to induce SOCE/ROCE, and independently to mediate Rho-kinase-dependent Ca^{2+} sensitization and VOCE respectively. These findings may inform the search for new drug targets for the treatment of obstructive lung diseases such as asthma, and in particular, support the suggested key role for SrcFK in experimental airway hyper-responsiveness (Sakai *et al.*, 2010; Katsumoto *et al.*, 2013).

Acknowledgements

Thanks to Mrs Kheem Jones and other NHS staff for patient recruitment and provision of bronchoscopy biopsies. This work was supported by the National Institute for Health Research (NIHR) Biomedical Research Centre based at Guy's and St Thomas' NHS Foundation Trust and King's College London. The views expressed are those of the author(s) and not necessarily those of the NHS, NIHR or the Department of Health.

Funding

Wellcome Trust: #087776. British Heart Foundation: FS/12/43/29608.

Author contributions

All other authors reviewed the manuscript critically for important intellectual content. All authors agree to be accountable for all aspects of the work in ensuring that questions related to the accuracy or integrity of any part of the work are appropriately investigated and resolved.

Conflict of interest

Authors declare that they have not any conflict of interest.

References

Alexander SP, Benson HE, Faccenda E, Pawson AJ, Sharman JL, Catterall WA *et al.* (2013a). The concise guide to pharmacology 2013/14: ion channels. Br J Pharmacol 170: 1607–1651.

Alexander SP, Benson HE, Faccenda E, Pawson AJ, Sharman JL, Spedding M *et al.* (2013b). The concise guide to pharmacology 2013/14: enzymes. Br J Pharmacol 170: 1797–1867.

Andreev J, Galisteo ML, Kranenburg O, Logan SK, Chiu ES, Okigaki M *et al.* (2001). Src and Pyk2 mediate G-protein-coupled receptor activation of epidermal growth factor receptor (EGFR) but are not required for coupling to the mitogen-activated protein (MAP) kinase signaling cascade. J Biol Chem 276: 20130–20135.

Calalb MB, Polte TR, Hanks SK (1995). Tyrosine phosphorylation of focal adhesion kinase at sites in the catalytic domain regulates kinase activity: a role for Src family kinases. Mol Cell Biol 15: 954–963.

Chikumi H, Fukuhara S, Gutkind JS (2002). Regulation of G protein-linked guanine nucleotide exchange factors for Rho, PDZ-RhoGEF, and LARG by tyrosine phosphorylation: evidence of a role for focal adhesion kinase. J Biol Chem 277: 12463–12473.

Chopra LC, Hucks D, Twort CH, Ward JP (1997). Effects of protein tyrosine kinase inhibitors on contractility of isolated bronchioles of the rat. Am J Respir Cell Mol Biol 16: 372–378.

Deguchi S, Ohashi T, Sato M (2005). Intracellular stress transmission through actin stress fiber network in adherent vascular cells. Mol Cell Biomech 2: 205–216.

Doeing DC, Solway J (2013). Airway smooth muscle in the pathophysiology and treatment of asthma. J Appl Physiol 114: 834–843.

Feng J, Ito M, Ichikawa K, Isaka N, Nishikawa M, Hartshorne DJ *et al.* (1999). Inhibitory phosphorylation site for Rho-associated kinase on smooth muscle myosin phosphatase. J Biol Chem 274: 37385–37390.

Gerthoffer WT, Gunst SJ (2001). Invited review: focal adhesion and small heat shock proteins in the regulation of actin remodeling and contractility in smooth muscle. J Appl Physiol 91: 963–972.

Gilbert R, Auchincloss JH Jr (1989). Reactive airways dysfunction syndrome presenting as a reversible restrictive defect. Lung 167: 55–61.

Gosens R, Schaafsma D, Grootte Bromhaar MM, Vrugt B, Zaagsma J, Meurs H *et al.* (2004). Growth factor-induced contraction of human bronchial smooth muscle is Rho-kinase-dependent. Eur J Pharmacol 494: 73–76.

Gui P, Wu X, Ling S, Stotz SC, Winkfein RJ, Wilson E *et al.* (2006). Integrin receptor activation triggers converging regulation of Cav1.2 calcium channels by c-Src and protein kinase A pathways. J Biol Chem 281: 14015–14025.

Guilluy C, Bregeon J, Toumaniantz G, Rolli-Derkinderen M, Retailleau K, Loufrani L *et al.* (2010). The Rho exchange factor Arhgef1 mediates the effects of angiotensin II on vascular tone and blood pressure. Nat Med 16: 183–190.

Gunst SJ, Tang DD, Opazo SA (2003). Cytoskeletal remodeling of the airway smooth muscle cell: a mechanism for adaptation to mechanical forces in the lung. Respir Physiol Neurobiol 137: 151–168.

Ishigaki T, Imanaka-Yoshida K, Shimojo N, Matsushima S, Taki W, Yoshida T (2011). Tenascin–C enhances crosstalk signaling of integrin alphavbeta3/PDGFR-beta complex by SRC recruitment promoting PDGF-induced proliferation and migration in smooth muscle cells. J Cell Physiol 226: 2617–2624.

Katsumoto TR, Kudo M, Chen C, Sundaram A, Callahan EC, Zhu JW *et al.* (2013). The phosphatase CD148 promotes airway hyperresponsiveness through Src family kinases. J Clin Invest 123: 2037–2048.

Kawasaki BT, Liao Y, Birnbaumer L (2006). Role of Src in C3 transient receptor potential channel function and evidence for a heterogeneous makeup of receptor- and store-operated Ca^{2+} entry channels. Proc Natl Acad Sci U S A 103: 335–340.

Knock GA, Shaifta Y, Snetkov VA, Vowles B, Drndarski S, Ward JP *et al.* (2008). Interaction between Src family kinases and Rho-kinase in agonist-induced Ca^{2+}-sensitization of rat pulmonary artery. Cardiovasc Res 77: 570–579.

Krymskaya VP, Goncharova EA, Ammit AJ, Lim PN, Goncharov DA, Eszterhas A *et al.* (2005). Src is necessary and sufficient for human airway smooth muscle cell proliferation and migration. FASEB J 19: 428–430.

Lopez E, Jardin I, Berna-Erro A, Bermejo N, Salido GM, Sage SO *et al.* (2012). STIM1 tyrosine-phosphorylation is required for STIM1-Orai1 association in human platelets. Cell Signal 24: 1315–1322.

Mauban JR, Zacharia J, Fairfax S, Wier WG (2015). PC-PLC/sphingomyelin synthase activity plays a central role in the development of myogenic tone in murine resistance arteries. Am J Physiol Heart Circ Physiol 308: H1517–H1524.

McGrath JC, Drummond GB, McLachlan EM, Kilkenny C, Wainwright CL (2010). Guidelines for reporting experiments involving animals: the ARRIVE guidelines. Br J Pharmacol 160: 1573–1576.

Meurs H, Gosens R, Zaagsma J (2008). Airway hyperresponsiveness in asthma: lessons from in vitro model systems and animal models. Eur Respir J 32: 487–502.

Moir LM, Leung SY, Eynott PR, McVicker CG, Ward JP, Chung KF *et al.* (2003). Repeated allergen inhalation induces phenotypic modulation of smooth muscle in bronchioles of sensitized rats. Am J Physiol Lung Cell Mol Physiol 284: L148–L159.

Nakao F, Kobayashi S, Mogami K, Mizukami Y, Shirao S, Miwa S *et al.* (2002). Involvement of Src family protein tyrosine kinases in Ca^{2+} sensitization of coronary artery contraction mediated by a sphingosylphosphorylcholine-Rho-kinase pathway. Circ Res 91: 953–960.

Owen JD, Ruest PJ, Fry DW, Hanks SK (1999). Induced focal adhesion kinase (FAK) expression in FAK-null cells enhances cell spreading and

migration requiring both auto- and activation loop phosphorylation sites and inhibits adhesion-dependent tyrosine phosphorylation of Pyk2. Mol Cell Biol 19: 4806–4818.

Pawson AJ, Sharman JL, Benson HE, Faccenda E, Alexander SP, Buneman OP, Davenport AP, McGrath JC, Peters JA, Southan C, Spedding M, Yu W, Harmar AJ; NC-IUPHAR. (2014) The IUPHAR/BPS Guide to PHARMACOLOGY: an expert-driven knowledgebase of drug targets and their ligands. Nucl. Acids Res. 42 (Database Issue): D1098-106.

Pertel T, Zhu D, Panettieri RA, Yamaguchi N, Emala CW, Hirshman CA (2006). Expression and muscarinic receptor coupling of Lyn kinase in cultured human airway smooth muscle cells. Am J Physiol Lung Cell Mol Physiol 290: L492–L500.

Pinelli V, Marchica CL, Ludwig MS (2009). Allergen-induced asthma in C57Bl/6 mice: hyper-responsiveness, inflammation and remodelling. Respir Physiol Neurobiol 169: 36–43.

Reynolds A, Leake D, Boese Q, Scaringe S, Marshall WS, Khvorova A (2004). Rational siRNA design for RNA interference. Nat Biotechnol 22: 326–330.

Sakai H, Nishimura A, Watanabe Y, Nishizawa Y, Hashimoto Y, Chiba Y *et al*. (2010). Involvement of Src family kinase activation in angiotensin II-induced hyperresponsiveness of rat bronchial smooth muscle. Peptides 31: 2216–2221.

Salazar EP, Rozengurt E (2001). Src family kinases are required for integrin-mediated but not for G protein-coupled receptor stimulation of focal adhesion kinase autophosphorylation at Tyr-397. J Biol Chem 276: 17788–17795.

Schaafsma D, Bos IS, Zuidhof AB, Zaagsma J, Meurs H (2006). Inhalation of the Rho-kinase inhibitor Y-27632 reverses allergen-induced airway hyperresponsiveness after the early and late asthmatic reaction. Respir Res 7(121): 1–7.

Schmitz U, Ishida M, Berk BC (1997). Angiotensin II stimulates tyrosine phosphorylation of phospholipase C-gamma-associated proteins. Characterization of a c-Src-dependent 97-kD protein in vascular smooth muscle cells. Circ Res 81: 550–557.

Singh NK, Wang D, Kundumani-Sridharan V, Van QD, Niu J, Rao GN (2011). 15-Lipoxygenase-1-enhanced Src-Janus kinase 2-signal transducer and activator of transcription 3 stimulation and monocyte chemoattractant protein-1 expression require redox-sensitive activation of epidermal growth factor receptor in vascular wall remodeling. J Biol Chem 286: 22478–22488.

Smith PG, Garcia R, Kogerman L (1998). Mechanical strain increases protein tyrosine phosphorylation in airway smooth muscle cells. Exp Cell Res 239: 353–360.

Somlyo AP, Somlyo AV (2003). Ca^{2+} sensitivity of smooth muscle and nonmuscle myosin II: modulated by G proteins, kinases, and myosin phosphatase. Physiol Rev 83: 1325–1358.

Tang D, Mehta D, Gunst SJ (1999). Mechanosensitive tyrosine phosphorylation of paxillin and focal adhesion kinase in tracheal smooth muscle. Am J Physiol 276: C250–C258.

Tang DD, Gunst SJ (2001). Depletion of focal adhesion kinase by antisense depresses contractile activation of smooth muscle. Am J Physiol Cell Physiol 280: C874–C883.

Ui-Tei K, Naito Y, Takahashi F, Haraguchi T, Ohki-Hamazaki H, Juni A *et al*. (2004). Guidelines for the selection of highly effective siRNA sequences for mammalian and chick RNA interference. Nucleic Acids Res 32: 936–948.

Wang Y, Deng X, Hewavitharana T, Soboloff J, Gill DL (2008). Stim, ORAI and TRPC channels in the control of calcium entry signals in smooth muscle. Clin Exp Pharmacol Physiol 35: 1127–1133.

Wu X, Davis GE, Meininger GA, Wilson E, Davis MJ (2001). Regulation of the L-type calcium channel by alpha 5beta 1 integrin requires signaling between focal adhesion proteins. J Biol Chem 276: 30285–30292.

Xing Z, Chen HC, Nowlen JK, Taylor SJ, Shalloway D, Guan JL (1994). Direct interaction of v-Src with the focal adhesion kinase mediated by the Src SH2 domain. Mol Biol Cell 5: 413–421.

Xu W, Doshi A, Lei M, Eck MJ, Harrison SC (1999). Crystal structures of c-Src reveal features of its autoinhibitory mechanism. Mol Cell 3: 629–638.

Ying Z, Giachini FR, Tostes RC, Webb RC (2009). PYK2/PDZ-RhoGEF links Ca^{2+} signaling to RhoA. Arterioscler Thromb Vasc Biol 29: 1657–1663.

Yoshii A, Iizuka K, Dobashi K, Horie T, Harada T, Nakazawa T *et al*. (1999). Relaxation of contracted rabbit tracheal and human bronchial smooth muscle by Y-27632 through inhibition of Ca2+ sensitization. Am J Respir Cell Mol Biol 20: 1190–1200.

Supporting Information

Additional Supporting Information may be found in the online version of this article at the publisher's web-site:

http://dx.doi.org/10.1111/bph.13313

Figure S1 Identification of hASMC as smooth muscle by positive staining with anti-smooth muscle-actin (panel A), anti-desmin (panel B) and anti-calponin (panel C), visualised with Alexa Fluor®488 labelled secondary antibody (Lifetechnologies) and fluorescent microscopy. Cells were also stained with TRITC-labelled phalloidin to confirm the presence of stress fibres in resting cells (Panel D). In Panel D, nuclei are visualised by staining with Hoechst. Scale bar =20μm.

Figure S2 Effect of PP3 on contractile responses in rat bronchioles.

Figure S3 Effect of PF-431396 on contractile responses in rat bronchioles.

Figure S4 Effects of SrcFK, Rho-kinase and FAK inhibition on bradykinin-induced contractile responses in rat bronchioles.

J Physiol 593.17 (2015) pp 3815–3828

The Journal of Physiology

Control of vascular smooth muscle function by Src-family kinases and reactive oxygen species in health and disease

Charles E. MacKay and Greg A. Knock

Asthma, Allergy and Lung Biology, Faculty of Life Sciences and Medicine, King's College London, London, UK

Abstract Reactive oxygen species (ROS) are now recognised as second messenger molecules that regulate cellular function by reversibly oxidising specific amino acid residues of key target proteins. Amongst these are the Src-family kinases (SrcFKs), a multi-functional group of non-receptor tyrosine kinases highly expressed in vascular smooth muscle (VSM). In this review we examine the evidence supporting a role for ROS-induced SrcFK activity in normal VSM contractile function and in vascular remodelling in cardiovascular disease. VSM contractile responses to G-protein-coupled receptor stimulation, as well as hypoxia in pulmonary artery, are shown to be dependent on both ROS and SrcFK activity. Specific phosphorylation targets are identified amongst those that alter intracellular Ca^{2+} concentration, including transient receptor potential channels, voltage-gated Ca^{2+} channels and various types of K^+ channels, as well as amongst those that regulate actin cytoskeleton dynamics and myosin phosphatase activity, including focal adhesion kinase, protein tyrosine kinase-2, Janus kinase, other focal adhesion-associated proteins, and Rho guanine nucleotide exchange factors. We also examine a growing weight of evidence in favour of a key role for SrcFKs in multiple pro-proliferative and anti-apoptotic signalling pathways relating to oxidative stress and vascular remodelling, with a particular focus on pulmonary hypertension, including growth-factor receptor transactivation and downstream signalling, hypoxia-inducible factors, positive feedback between SrcFK and STAT3 signalling and positive feedback between SrcFK and NADPH oxidase dependent ROS production. We also discuss evidence for and against the potential therapeutic targeting of SrcFKs in the treatment of pulmonary hypertension.

(Received 2 October 2014; accepted after revision 22 October 2014; first published online 10 November 2014)
Corresponding author G. A. Knock: 1.20 Henriette Raphael House, Guy's Campus, King's College London, London SE1 9RT, UK. Email: greg.knock@kcl.ac.uk

Abbreviations BMPRII, bone morphogenetic protein receptor-II; FAK, focal adhesion kinase; GEF, guanine nucleotide exchange factor; GPCR, G-protein-coupled receptor; GRB2, growth factor receptor bound protein-2; MLC_{20}, myosin light-chain-20; MLCK, myosin light-chain kinase; MLCP, myosin light-chain phosphatase; NOX, NADPH oxidase; PAH, pulmonary arterial hypertension; PDGFR, platelet-derived growth factor receptor; PH, (hypoxic) pulmonary hypertension; PLC-β/γ, phospholipase C-β/γ; PTP, protein tyrosine phosphatase; ROCK, Rho-kinase; ROS, reactive oxygen species; SOD, superoxide dismutase; SrcFKs, Src-family kinases; STAT3, signal transducer and activator of transcription-3; TASK channel, two-pore acid-sensitive K^+ channel; VSM, vascular smooth muscle.

Charles MacKay is currently in the second year of his PhD at King's under the supervision of Dr Knock and presented his work to date at the aforementioned symposium. **Greg Knock** is a Lecturer in Physiology at King's College London, appointed in 2010. His research interests are signal transduction in vascular and respiratory smooth muscle, with a focus on protein tyrosine kinases, small G proteins of the RhoA family and reactive oxygen species. He was the organiser of the Physiological Society Research Symposium entitled 'Tyrosine Kinases in Smooth Muscle Function' held in London in July 2014.

This review was presented at the symposium Tyrosine kinases and smooth muscle function, which took place at Physiology 2014, the annual meeting of the Physiological Society, London, UK on 1 July 2014.

DOI: 10.1113/jphysiol.2014.285304

Introduction: SrcFKs as ROS effectors in VSM

The purpose of this review is to highlight the interactions between reactive oxygen species (ROS) and Src-family kinases (SrcFKs), a family of non-receptor tyrosine kinases, in the regulation of vascular smooth muscle (VSM) function. We will examine evidence supporting an important role for this interaction in normal excitation–contraction coupling. We will also provide details of the role of SrcFKs in oxidative stress-related VSM proliferation and migration signalling associated with vascular remodelling, with a focus on pulmonary hypertension, and briefly comment on the potential therapeutic use of SrcFK inhibitors against this group of diseases. Firstly, however, we will set the scene by describing ROS production in VSM, their role as second messengers and mechanism of action on target proteins, and evidence supporting SrcFKs as key proximal ROS effectors in VSM.

Vascular ROS production. ROS are now considered as bona fide second messenger molecules, being produced within cells in response to physiological and pathophysiological stimuli, acting on cellular target proteins to reversibly alter cellular function. There are two main sources of ROS in VSM. Firstly from cytoplasmic oxidoreductase enzymes, most notably NADPH oxidase (NOX), which transfers an electron from cytosolic NADPH to molecular oxygen, generating superoxide ($O_2^{\bullet-}$) (Bedard & Krause, 2007). Secondly, electrons leaking from the mitochondrial electron transport chain form superoxide in the mitochondrial inter-membrane space (Turrens, 2003; Waypa *et al.* 2013). Superoxide readily reacts with nitric oxide (NO•), producing peroxynitrite ($ONOO^-$), or is converted to the more stable hydrogen peroxide (H_2O_2) by superoxide dismutase (SOD) (Bedard & Krause, 2007). H_2O_2 is in turn fully reduced to H_2O by catalase or converted to the highly reactive hydroxyl radical via the Fenton reaction (Fig. 1).

Vascular NOX activity is stimulated by various G-protein-coupled receptor (GPCR) agonists including angiotensin II, endothelin-1, thrombin, ATP and thromboxane (Banes-Berceli *et al.* 2005; Madamanchi *et al.* 2005; El-Awady *et al.* 2011; Chakraborti *et al.* 2012). It is generally agreed that mitochondrial ROS production is enhanced by hypoxia both in the short term and the long term and, acutely, this is considered an important trigger for the normal physiological vasoconstrictor response to regional hypoxia in the pulmonary vascular bed (Waypa *et al.* 2013). GPCR-induced arterial constriction is generally relaxed by antioxidant enzymes, NOX inhibitors, or small molecule antioxidants (El-Awady *et al.* 2011; Connolly *et al.* 2013), while hypoxic pulmonary vasoconstriction is enhanced by inhibitors of endogenous SOD (Abdalla & Will, 1995) and inhibited by antioxidants and inhibitors of mitochondrial electron transport function (Connolly *et al.* 2013; Waypa *et al.* 2013). Conversely, exogenous ROS generally enhance VSM proliferation (Wedgwood *et al.* 2001; Madamanchi *et al.* 2005) and cause constriction, especially in pulmonary artery, although they may relax other vascular beds depending perhaps on the nature of the pre-constricting agent (Knock *et al.* 2009; Snetkov *et al.* 2011).

REDOX regulation of SrcFKs. ROS alter protein function by chemically modifying specific amino acid residues. Cysteine is relatively readily oxidised by superoxide and H_2O_2, and *S*-nitrosylated by peroxynitrite. Peroxynitrite also nitrates serine, threonine and tyrosine residues (Fig. 1). Oxidation of paired cysteine residues within a protein or in adjacent proteins may also result in the formation of disulphide bridges, but is not an absolute requirement for a change in protein function (Janssen-Heininger *et al.* 2008). Cysteine oxidation and nitrosylation, and to a lesser extent nitration, is readily reversible through the action of REDOX buffer systems, most notably glutathione reductase/peroxidase (Janssen-Heininger *et al.* 2008). The susceptibility of individual cysteine residues to oxidation varies between proteins and between residues within the same protein, depending on the ionisation pK_a of the residue in question (Chiarugi *et al.* 2003; Gusan & Anand-Srivastava, 2013).

c-Src is the principle member of a family of closely related tyrosine kinases collectively known as the Src-family kinases (SrcFKs). There are nine in total, of which three (c-Src, Fyn and Yes) are highly expressed in VSM (Nakao *et al.* 2002; Knock *et al.* 2008*a*). Note that in this review we will refer to these kinases collectively as SrcFKs, since Src, Fyn and Yes are difficult to separate pharmacologically, and rarely has genetic manipulation been used to determine their individual contributions to VSM function. SrcFKs feature prominently among the various classes of proteins that possess cysteine residues with a pK_a low enough for them to be oxidised by physiological levels of ROS (Knock & Ward, 2011). Although there may be specific exceptions, cysteine oxidation is generally stimulatory of tyrosine kinase activity and inhibitory of protein tyrosine phosphatase (PTP) activity (Knock & Ward, 2011; Funato & Miki, 2014). Thus, it is no surprise that increased ROS production in response to various vasoactive stimuli is associated with an early increase in total cellular tyrosine phosphorylation (Uzui *et al.* 2000; Chiarugi *et al.* 2003; Knock *et al.* 2008*a*,*b*) and that exogenous ROS enhance tyrosine phosphorylation in vascular preparations, whilst antioxidants do the opposite (Frank *et al.* 2001, 2003). Correspondingly, PTP

inhibitors tend to promote constriction, while tyrosine kinase inhibitors, including those selective for SrcFKs, tend to relax pre-constricted arteries (Jin & Rhoades, 1997; Knock *et al.* 2008*a*, 2009). SrcFKs are normally activated by de-phosphorylation of the auto-inhibitory C-terminal phospho-tyrosine (Tyr-527 in c-Src), and subsequent auto-phosphorylation of the catalytic sub-unit activation loop (Tyr-418 in c-Src) (Xu *et al.* 1999). ROS activate SrcFKs through multiple mechanisms, firstly by oxidising cysteine residues in the SH2 domain, causing inter-molecular disulphide bridge formation and disruption of internal Tyr-527–SH2 domain interaction, secondly by oxidising cysteine residues on the SH2 and kinase domains of the already active kinase, further activating it, and thirdly by inhibiting their inactivation through oxidative inhibition of an Src-specific PTP, and of C-terminal Src-kinase (CSK) (Akhand *et al.* 1999; Giannoni *et al.* 2005; Roskoski, 2005; Mills *et al.* 2007) (Fig. 2).

SrcFKs are activated in smooth muscle by various vaso-constrictor stimuli including GPCR agonists (Nakao *et al.* 2002; Knock *et al.* 2008*a*), stretch (Gui *et al.* 2010; Gonzales *et al.* 2014) and hypoxia (Knock *et al.* 2008*b*), while VSM contraction induced by exogenously applied H_2O_2, or by artificially enhanced superoxide production, is sensitive to SrcFK inhibition (Oeckler *et al.* 2003; Knock *et al.* 2009). Thus, VSM responses to various stimuli may be mediated via an interaction between ROS and SrcFKs. Indeed, as discussed in the following sections, many of the numerous SrcFK phosphorylation targets, including various classes of ion channel, cytoskeletal proteins associated with small G-proteins of the Rho family, growth-factor receptors, other tyrosine kinases, and transcription regulators, are phosphorylated in a ROS-dependent manner.

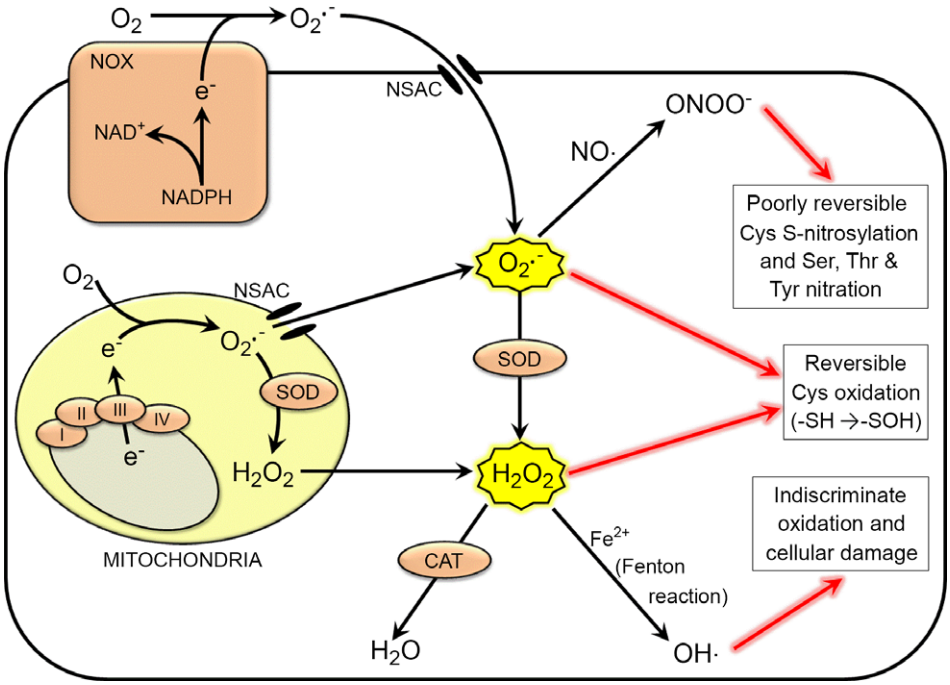

Figure 1. Generation, metabolism and action of ROS in VSM
Superoxide ($O_2^{\bullet-}$) is generated by oxido-reductase enzymes in the plasma membrane, such as NADPH oxidase (NOX). A reducing substrate, in this case NADPH, donates an electron which is transferred to molecular oxygen on the extracellular surface (Bedard & Krause, 2007). Superoxide is generated in a similar manner by the mitochondrial electron transport chain, principally complex III (Waypa *et al.* 2013). Superoxide can re-enter the cell or exit the mitochondria through non-selective anion channels (NSAC), or is converted to H_2O_2 by cytosolic or mitochondrial superoxide dismutase (SOD). Alternatively, superoxide may react with nitric oxide (NO•) to form the similarly reactive peroxynitrite ($ONOO^-$). H_2O_2 is converted to the highly reactive hydroxyl radical (OH•) via the Fe^{2+}-catalysed Fenton reaction or is fully reduced to H_2O by catalase (CAT). Superoxide and H_2O_2 reversibly modify protein function principally via oxidation of the sulfhydryl (R-SH) group of cysteine residues to sulfenic acid (R-SOH). Peroxynitrite *S*-nitrosylates cysteine (R-SH → R-SOH + NO_2^-) and nitrates the hydroxyl groups of serine, threonine and tyrosine residues (R-OH → R-NO_2), and the latter is less readily reversible (Janssen-Heininger *et al.* 2008). OH• is highly reactive, much less discriminating, and therefore potentially damaging to the cell.

SrcFKs and ROS in normal contractile function

The principle function of vascular smooth muscle is to contract or relax in response to circulating or local factors, thus contributing to the control of tissue blood flow and mean arterial blood pressure. Smooth muscle contraction is caused by the ratchet-like movement of the molecular motor myosin along actin fibres. Myosin ATPase activity, which triggers this movement, is initiated by Ca^{2+}/calmodulin-dependent phosphorylation of myosin light-chain-20 (MLC_{20}) by myosin light-chain kinase (MLCK). Polymerisation of actin filaments and their bundling with myosin into contractile fibres is also dynamically regulated, as is the association of these fibres with integrin-rich focal adhesions which permit the transmission of contractile force to the extracellular matrix, as well as acting as platforms for multiple signalling pathways (Ridley & Hall, 1992; Min *et al.* 2012; Sreenivasappa *et al.* 2014). In this section, we describe how ROS and SrcFKs regulate contractile force via changes to the free intracellular Ca^{2+} concentration ($[Ca^{2+}]_i$) to influence MLCK activity, by inhibiting the activity of myosin light-chain phosphatase (MLCP) which de-phosphorylates MLC_{20}, and by regulating actin polymerisation and focal adhesion signalling through the activation of the small monomeric G-protein RhoA and various adaptor proteins associated with integrins.

Regulation of ion channels. Many vasoconstrictors that bind Gq-coupled receptors activate phospholipase C-β (PLC-β) to induce inositol 1,4,5-trisphosphate (IP_3)-dependent Ca^{2+} release from the sarco-endoplasmic reticulum and open diacylglycerol (DAG)-sensitive transient receptor potential (TRP) non-selective cation channels. The resultant depolarisation then triggers influx through voltage-dependent Ca^{2+} channels. Exogenous ROS enhance agonist-induced increases in $[Ca^{2+}]_i$ and contraction in pulmonary artery (Snetkov *et al.* 2011) and these effects may be in part via activation of SrcFKs, since GPCRs stimulate SrcFKs to further activate TRP channels through tyrosine phosphorylation of PLC-γ (Vazquez *et al.* 2004; Gonzales *et al.* 2014), or via direct phosphorylation of canonical TRP family members on the cytosolic N-terminus, which has been shown as an obligatory step in their activation (Kawasaki *et al.* 2006). Alternatively, SrcFKs also directly phosphorylate voltage-gated Ca^{2+} channels, specifically

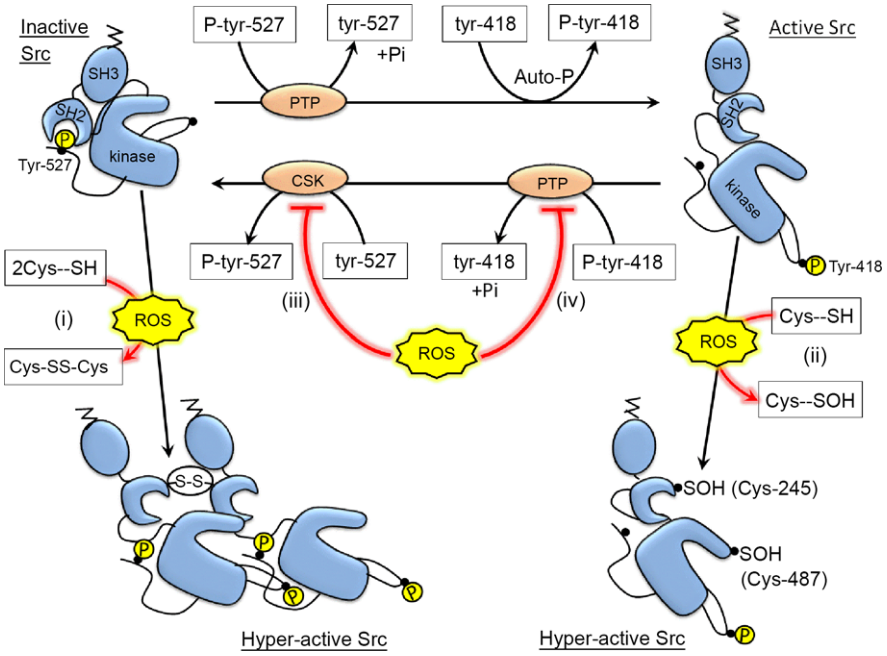

Figure 2. Activation of Src by ROS in VSM
Src activation is normally promoted by de-phosphorylation of the auto-inhibitory Tyr-527, disrupting intra-molecular binding with the SH2 domain. This promotes auto-phosphorylation of Tyr-418 on the activation loop, opening up the kinase domain for substrate binding. Additionally, SrcFKs are both directly and indirectly REDOX sensitive, being activated by: (i) ROS-induced intermolecular disulphide bridge formation which promotes *trans*-phosphorylation of Tyr-418 (Akhand *et al.* 1999), (ii) oxidation of cysteine residues in the SH2 (Cys-245) and kinase (Cys-487) domains, which further activates an already active Src (Giannoni *et al.* 2005), (iii) via oxidative inactivation of the inhibitory c-Src kinase (CSK), which phosphorylates the auto-inhibitory C-terminal Tyr-527 (Mills *et al.* 2007), or (iv) oxidative inactivation of Src-specific PTPs which de-phosphorylate Tyr-418 on the activation loop (Roskoski, 2005). Specific amino acid numbers given refer to the sequence in human c-Src.

the α1C pore-forming subunit of $Ca_V1.2$, which facilitates its binding to $\alpha5\beta1$ integrin, a step which is necessary for its contribution to myogenic contraction (Gui *et al.* 2010) (Fig. 3).

K^+ channels are also phosphorylation targets for SrcFKs and in the systemic circulation there is evidence that this phosphorylation may be stimulatory or inhibitory. In mesenteric artery, serotonin-induced SrcFK activity results in inhibition of K_V current, thus contributing to contraction (Sung *et al.* 2013). There is conflicting evidence over the effects of SrcFK-dependent phosphorylation on large conductance Ca^{2+}-activated potassium (BKCa) channels, with inhibition being reported in rat aorta (Alioua *et al.* 2002) and activation being reported in rat cremaster VSM, which also promotes association of the channel with integrins (Gui *et al.* 2010). The reasons for these discrepancies are unclear, but perhaps relate to differences in vascular bed or experimental conditions. In some vascular beds where K^+ channel activity has a particularly strong influence on vascular tone, a stimulatory effect of SrcFKs on K^+ currents may account at least in part for the occasionally observed relaxing effects of ROS. For example, H_2O_2 enhances large conductance Ca^{2+}-activated K^+ (K_{Ca}) channel activity in coronary VSM, accounting for its endothelium-derived hyperpolarising factor-like activity in that vascular bed (Barlow *et al.* 2000), and mesenteric artery pre-constricted with a GPCR agonist, but not with 30 mM KCl, is relaxed by superoxide and this is associated with reduced $[Ca^{2+}]_i$ and enhanced voltage-gated K^+ (K_V) current (Snetkov *et al.* 2011) (Fig. 3).

As described in the introductory section, pulmonary artery differs from most systemic vascular beds by constricting in response to hypoxia and this constriction is generally considered to occur as a result of increased mitochondrial ROS production (Waypa *et al.* 2013). Coupled with this, SrcFKs are activated by hypoxia (Sato *et al.* 1999, 2005; Knock *et al.* 2008*b*), and SrcFK inhibition

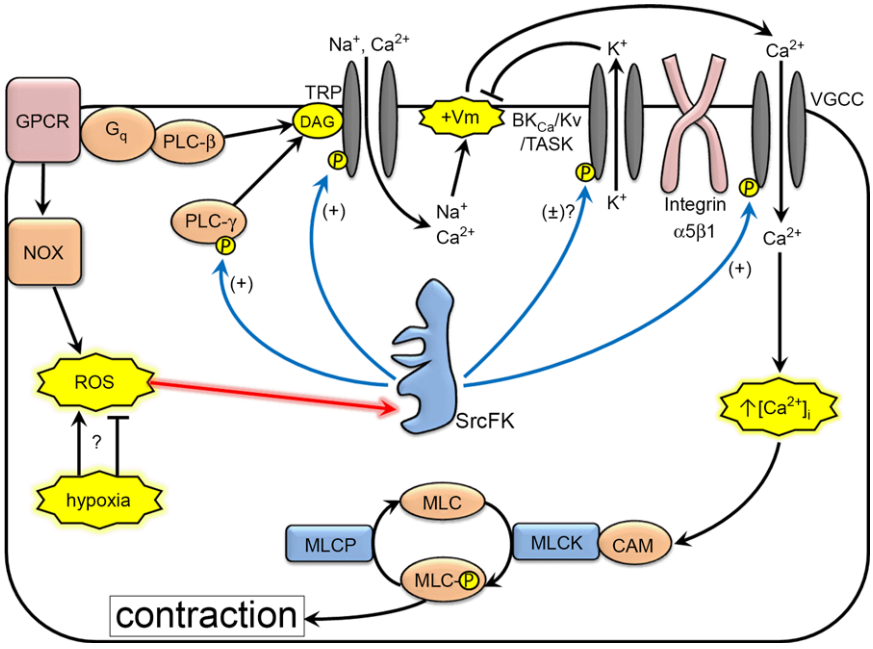

Figure 3. SrcFKs and ROS modulate ion channel activity and contraction in VSM
GPCR stimulation activates Gq and phospholipase C-β (PLC-β) to generate diacylglycerol (DAG), which opens C-type transient receptor potential (TRP) channels. GPCRs also induce ROS-dependent activation of SrcFKs which phosphorylate and activate phospholipase C-γ (PLC-γ) or directly phosphorylate TRP channels on the cytoplasmic N-terminal domain (e.g. Tyr-226 on TRPC3; Kawasaki *et al.* 2006), further enhancing their activity. Resultant cationic influx depolarises the cell ($+V_m$), which in turn opens voltage-gated Ca^{2+} channels (VGCC). SrcFKs also phosphorylate and further activate VGCCs (e.g. Tyr-2122 on the α1C pore-forming subunit of $Ca_V1.2$; Gui *et al.* 2010), promoting their association with integrins (e.g. $\alpha5\beta1$; Gui *et al.* 2010). VGCC opening elevates intracellular $[Ca^{2+}]$ ($[Ca^{2+}]_i$); Ca^{2+} binds calmodulin (CAM), which activates myosin light-chain kinase (MLCK) which in turn phosphorylates myosin light-chain-20 (MLC) to initiate contraction. SrcFKs may also phosphorylate K^+ channels of the Ca^{2+}-activated (BK_{Ca}), voltage-gated (K_V) and two-pore acid-sensitive (TASK) types, thus limiting depolarisation. This phosphorylation may be stimulatory or inhibitory and in pulmonary artery, whether hypoxia enhances (Waypa *et al.* 2013) or inhibits (Wu *et al.* 2007) ROS production, determines whether SrcFKs are activated or inhibited by hypoxia, thus enhancing or limiting cell depolarisation, which is of potential importance in pulmonary hypoxic vasoconstriction (see main text for explanation).

reduces hypoxic constriction in pulmonary artery (Knock *et al.* 2008*b*). A recent study on the two-pore acid-sensitive K^+ channel TASK-1 in pulmonary VSM has shown this channel to be phosphorylated and opened by SrcFKs, and using this model to explain how SrcFKs contribute to hypoxic pulmonary vasoconstriction, SrcFKs are shown to be *inhibited* by hypoxia thus *reducing* TASK-1 current and causing depolarisation (Nagaraj *et al.* 2013). Paradoxically, this latter study is only consistent with the wealth of evidence that SrcFKs are *activated* by ROS if hypoxia *inhibits* mitochondrial ROS production (Wu *et al.* 2007), contradicting the aforementioned work of Waypa *et al.* Perhaps direct evidence for an involvement of SrcFKs in the relationship between ROS and K^+ channels in pulmonary VSM, and the relative importance of K^+ channels to pulmonary vascular tone would help to resolve this apparent discrepancy. Interestingly, ROS do not relax pre-constricted pulmonary artery, despite K^+ current being enhanced by ROS to a degree similar to that in mesenteric VSM (Snetkov *et al.* 2011), perhaps due to a relative dominance of ROS-induced Rho-kinase activity in pulmonary VSM (Knock *et al.* 2009; Snetkov *et al.* 2011), as discussed below.

Regulation of RhoA/ROCK. The monomeric G-protein RhoA and its effector kinase, Rho-kinase (ROCK), are essential regulators of actin polymerisation, focal adhesion assembly and MLCP activity. Many contractile stimuli, including various GPCR agonists, hypoxia and exogenous ROS, activate RhoA/ROCK in VSM, and there is pharmacological evidence that this activity is in part dependent on SrcFKs (Nakao *et al.* 2002; Knock *et al.* 2008*a*,*b*), presumably downstream of RhoA activation. RhoA is activated by exchange of bound GDP for bound GTP and this is promoted by guanine nucleotide exchange factors (GEFs) (Bos *et al.* 2007). Several RhoA-specific GEFs (ARHGEFs) are expressed in VSM (Cario-Toumaniantz *et al.* 2012) and they are activated directly by $G_{12/13}$ and/or by tyrosine phosphorylation, which may be promoted by ROS (Chandra *et al.* 2012). It has been hypothesised that SrcFKs may activate RhoA via GEF phosphorylation (Knock *et al.* 2008*a*; Sreenivasappa *et al.* 2014), but to date this has not been demonstrated directly. Instead, RhoGEFs are known to be phosphorylated and activated by three other non-receptor tyrosine kinases, focal adhesion kinase (FAK), protein tyrosine kinase-2 (PYK2) or Janus kinase (JAK2) (Lim *et al.* 2008; Guilluy *et al.* 2010; Gadepalli *et al.* 2012). Although these three kinases are not known to be directly ROS sensitive, they are activatable by GPCR agonists in the vascular wall in a NOX-dependent manner, as well as by exogenous ROS (Vepa *et al.* 1999; Frank *et al.* 2003; Daou & Srivastava, 2004) and through SrcFK-mediated tyrosine phosphorylation (Calalb *et al.* 1995; Andreev *et al.* 2001; Singh *et al.* 2011). JAK additionally appears to require prior ROS-dependent activation of PYK2 (Frank *et al.* 2002) (Fig. 4).

Active RhoA promotes actin fibre nucleation, polymerisation and bundling into contractile fibres in association with SrcFKs, FAK, paxillin and other adapter proteins at focal attachments as well as chaperone proteins such as mDia (Geneste *et al.* 2002; Lim *et al.* 2008). Also, ROCK phosphorylates and activates LIM-kinase, which in turn phosphorylates and inhibits the actin-severing protein cofilin, thus promoting actin fibre stability (Geneste *et al.* 2002) (Fig. 4). Contractile stimuli induce SrcFKs to phosphorylate several proteins at focal adhesions, including FAK (Tyr-925), paxillin (Tyr-118) and Cas (Tyr-165) (Min *et al.* 2012). MLCP activity is constitutive and does not require active stimulation, but contractile stimuli that raise $[Ca^{2+}]_i$ can further enhance MLC_{20} phosphorylation by actively inhibiting MLCP. The resultant further enhancement of MLC_{20} phosphorylation above that induced by raising $[Ca^{2+}]_i$ is known as 'Ca^{2+} sensitisation'. Rho-kinase phosphorylates myosin phosphatase targeting subunit-1 (MYPT-1) on at least two threonine residues, which result in disassembly of the MLCP holoenzyme (Thr-850), or a reduction in its phosphatase activity (Thr-696), respectively (Ichikawa *et al.* 1996; Velasco *et al.* 2002) (Fig. 4).

SrcFKs and ROS in pulmonary hypertension

Pulmonary hypertension is a spectrum of diseases which includes pulmonary hypertension due to hypoxia and/or respiratory disease (PH) and pulmonary arterial hypertension (PAH) which has various causes, both known and unknown. Both PH and PAH are characterised by remodelling of the pulmonary vasculature and hyper-responsiveness to constrictor stimuli, resulting in increased pulmonary vascular resistance and subsequent right heart failure and death (Simonneau *et al.* 2009). Vascular remodelling includes smooth muscle proliferation and migration which normally contribute to tissue growth and repair, but otherwise are usually suppressed in favour of a contractile phenotype. Occlusive cardiovascular diseases on the other hand, are associated with excessive or dysregulated VSM proliferation and migration. These changes have been strongly linked with excessive and poorly regulated ROS production, with contributions from altered expression of oxidant and antioxidant enzymes, endothelial dysfunction and increased sensitivity to, or increased availability of ROS-stimulating factors, resulting in an abnormal shift in smooth muscle REDOX state in favour of oxidation, commonly described as 'oxidative stress'. Enhanced mitochondrial and/or NOX-derived ROS coupled with reduced expression of antioxidant enzymes have been

implicated in the pathogenesis of both PH and PAH (Liu *et al.* 2006; Crosswhite & Sun, 2010; Reis *et al.* 2013).

SrcFKs, as key ROS targets in VSM, and known mediators of smooth muscle proliferation and migration (Krymskaya *et al.* 2005; Pullamsetti *et al.* 2012), are therefore well placed to contribute to oxidative stress-related vascular remodelling. ROS promote cell migration (Wang *et al.* 2014), acting in part through activation of SrcFKs and FAK at focal adhesions (Timpson *et al.* 2001; Chiarugi *et al.* 2003; Giannoni *et al.* 2005). As discussed in the previous section, and shown in Fig. 4, SrcFKs promote actin contractile fibre formation through tyrosine phosphorylation of multiple protein targets including paxillin, Cas, RhoGEFs and activation of RhoA. This is also important in cell migration, but occurs alongside disassembly of cell–cell junctions (Frame *et al.* 2002) and activation of the monomeric G-proteins cdc42 and Rac-1, which generate cycles of filopodia formation and cell spreading, respectively, at the leading edge of the migrating cell (Nobes & Hall, 1995). In the remaining sections of this review, with a particular focus on pulmonary hypertension, we will examine how ROS and SrcFKs interact to induce VSM proliferation, via transactivation of growth factor receptors, signal transducer and activator of transcription-3 (STAT3) and hypoxic inducible factors, and through positive feedback, further enhance ROS production. Finally, we will discuss evidence for and against targeting SrcFKs as treatments for PH/PAH.

SrFK, ROS and growth factor transactivation. ROS-generating stimuli use multiple signalling pathways to induce VSM growth and proliferation. An early step following activation of SrcFKs is the activation of receptor tyrosine kinases, and here we will focus on two of the most important of these, the epidermal growth factor receptor (EGFR) and the platelet-derived growth factor

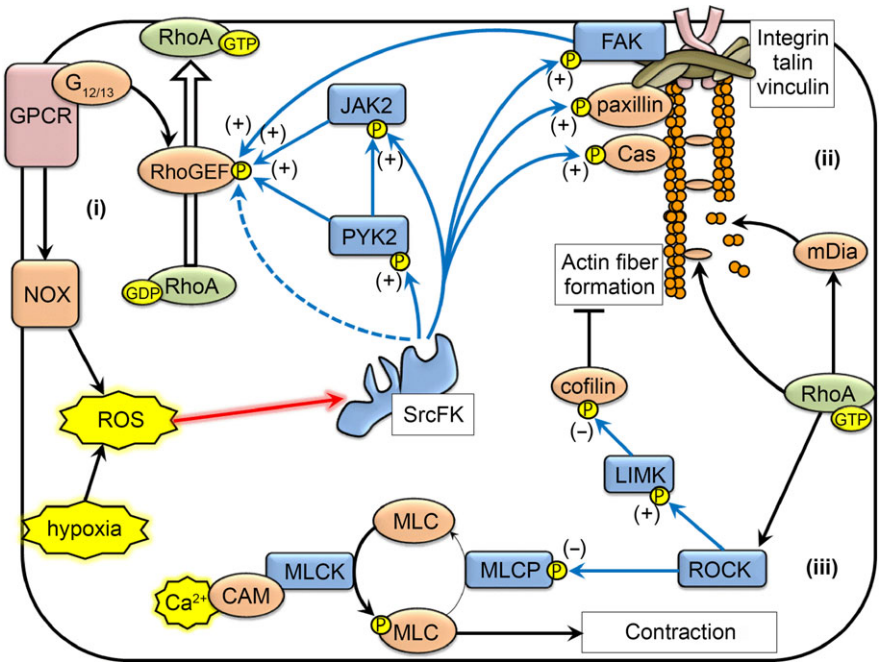

Figure 4. SrcFKs mediate ROS-induced activation of RhoA and Rho-kinase in VSM
(i) GPCRs and hypoxia induce ROS production (via NOX and mitochondrial electron transport chain, respectively, see Fig. 1), which activate SrcFKs. GPCRs also activate $G_{12/13}$. RhoA is activated by exchange of bound GDP for bound GTP and this is promoted by guanine nucleotide exchange factors (RhoGEFs). RhoGEFs may be activated by $G_{12/13}$ and/or by tyrosine phosphorylation. SrcFKs activate other non-receptor tyrosine kinases focal adhesion kinase (FAK), protein tyrosine kinase-2 (PYK2) or Janus kinase (JAK2), all of which may activate RhoGEFs. SrcFKs may also directly activate RhoGEFs but this has not been clearly demonstrated (dotted line). JAK2 activity may also require prior PYK2 activity. (ii) Contraction requires polymerisation and bundling of actin filaments into contractile fibres and their attachment at focal adhesions, which are composed in part of integrins, talin and vinculin, and various adapter proteins including FAK, paxillin and Cas, which are phosphorylated by SrcFKs. RhoA at focal adhesions promotes actin polymerisation and bundling, in part through association with paxillin and activation of the actin chaperone protein mDia. (iii) RhoA also activates Rho-kinase (ROCK) which further promotes actin polymerisation by activating LIM-kinase (LIMK), which in turn prevents cofilin from severing actin filaments. ROCK also phosphorylates the myosin targeting subunit of myosin phosphatase (MLCP) resulting in reduced myosin light-chain de-phosphorylation, thus enhancing net MLC phosphorylation and contraction.

receptor (PDGFR). In response to ROS-generating stimuli, receptor tyrosine kinases are activated in the absence of their natural ligands through a process known as transactivation (Saito & Berk, 2001). After growth factor binding, the receptor forms homodimers and auto-phosphorylates multiple tyrosine residues on its cytoplasmic regions. During transactivation in response to GPCR agonists such as endothelin-1 and angiotensin II, these residues are instead phosphorylated in a ROS-dependent manner by SrcFKs (Heeneman *et al.* 2000; Oeckler *et al.* 2003; Chen *et al.* 2006; Nakashima *et al.* 2006). The resultant phospho-tyrosines then act as docking sites for multiple SH2-domain-containing proteins, which in turn trigger multiple downstream signalling events. Here and in Fig. 5, using PDGFR as an example, we describe four of the most fully characterised of these signalling pathways. Transactivated PDGFR recruits the adapter proteins Shc and growth-factor receptor bound protein-2 (GRB2) (Ward *et al.* 1996; Ravichandran, 2001). SrcFKs subsequently phosphorylated Shc to provide further binding sites for GRB2 (Ravichandran, 2001). GRB2 can then bind and activate the guanine nucleotide exchange factor for Ras, son-of-sevenless (SOS). Activated Ras then initiates the Raf/MEK/ERK mitogen-activated protein (MAP) kinase cascade, promoting cell division. PLC-γ also binds PDGFR in VSM and is activated by ROS-dependent SrcFK-mediated phosphorylation (Saito *et al.* 2002; ten Freyhaus *et al.* 2011), and the subsequent sustained elevation in $[Ca^{2+}]_i$ contributes to sustained ERK activation (Egan *et al.* 2005). Phosphatidyl inositol-3-kinase (PI3K) is also phosphorylated by SrcFKs following binding to the transactivated PDGFR (ten Freyhaus *et al.* 2011; Karoor *et al.* 2013) and this phosphorylation relieves intra-molecular PI3K auto-inhibition (Cuevas *et al.* 2001; Choudhury *et al.* 2006). PI3K then generates phosphatidyl inositol trisphosphate (PIP_3), which through membrane localisation and activation of Akt (protein kinase B) and PDK initiates the Bad and S6 kinase anti-apoptotic and protein synthesis pathways (Eguchi *et al.* 1999). SrcFKs further enhance this signalling by phosphorylating and inhibiting phosphatase and tensin homologue (PTEN), preventing it from de-phosphorylating PIP_3 (Lu *et al.* 2003; Karoor *et al.* 2013).

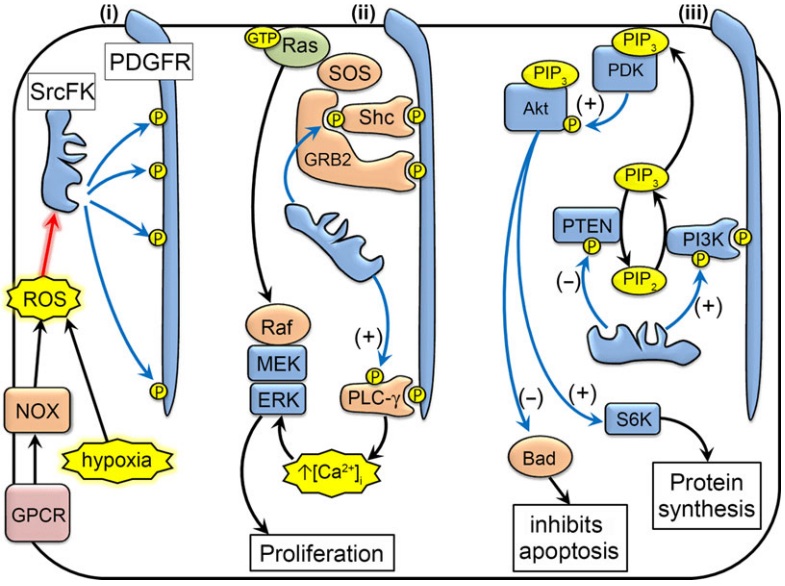

Figure 5. Role of SrcFKs in growth factor receptor transactivation and mitogenic signalling in VSM
(i) GPCR-induced or hypoxia-induced ROS stimulate SrcFKs to phosphorylate platelet-derived growth factor receptor (PDGFR) on multiple tyrosine residues. This occurs in the absence of native PDGF ligand (trans-activation). (ii) PDGFR recruits the adapter proteins Shc and growth factor receptor bound protein-2 (GRB2) on phosphorylated Tyr-557 and Tyr-684, respectively (Ward *et al.* 1996). SrcFKs subsequently phosphorylate Shc to provide further binding sites for GRB2. GRB2 can then bind and activate the guanine nucleotide exchange factor for Ras, son-of-sevenless (SOS). Activated Ras then initiates the Raf/MEK/ERK mitogen-activated protein kinase cascade, promoting cell division. In addition, PLC-γ binds PDGFR at phosphorylated Tyr-1021 (Saito *et al.* 2002) and is then itself phosphorylated and activated by SrcFK. Activated PLC-γ induces a sustained elevation in $[Ca^{2+}]_i$ which contributes to sustained ERK activation. (iii) Phosphatidyl inositol-3-kinase (PI3K) binds PDGFR at phosphorylated Tyr-751 (Karoor *et al.* 2013), following which it is phosphorylated and activated by SrcFKs. PI3K then phosphorylates phosphatidyl inositol bisphosphate (PIP_2) to generate phosphatidyl inositol trisphosphate (PIP_3). SrcFKs also phosphorylate and inhibit phosphatase and tensin homologue (PTEN), preventing de-phosphorylation of PIP_3. PIP_3 promotes the membrane localisation of Akt and PDK, allowing PDK to phosphorylate and activate Akt. Activated Akt initiates the Bad and S6 kinase (S6K) anti-apoptotic and protein synthesis pathways.

Reciprocal relationship between SrcFKs and ROS. Chronic hypoxia triggers a sustained enhancement in mitochondrial ROS production in VSM, resulting in enhanced SrcFK activity (Sato *et al.* 2005). However, as well as being a key downstream effector of ROS, SrcFKs also contribute to the activation of NOX. In response to GPCR stimulation, SrcFKs phosphorylate the $p47^{phox}$ subunit of NOX and trigger the activation of Rac-1, which is required for holoenzyme assembly (Seshiah *et al.* 2002; Chowdhury *et al.* 2005). Coupled with the steady increase in basal mitochondrial ROS production described above, increased expression of NOX, and reduced expression of antioxidant enzymes in PH and PAH (Liu *et al.* 2006; Reis *et al.* 2013), this apparent positive feedback relationship between ROS and SrcFK activity could not only facilitate the prolonged sustained increases in ROS characteristic of oxidative stress in PH/PAH, but may also be required for the long-term changes in VSM phenotype, migration and proliferation induced downstream of SrcFKs (Seshiah *et al.* 2002) characteristic of pulmonary hypertension, acting via growth-factor receptor transactivation, and as discussed below, hypoxia-inducible factor (HIF)-1α/2α and STAT3 activation (Fig. 6).

ROS, SrcFKs and altered gene expression via hypoxia-inducible factor and STAT3. SrcFKs are implicated in several additional signalling pathways considered important in VSM remodelling in PH/PAH. For example, they also contribute to VSM migration and proliferation by increasing the availability of hypoxia-inducible factors (HIF-1α and HIF-2α) (Sato *et al.* 2005). In normoxia, HIF levels are kept low by prolyl hydroxylation and subsequent proteolysis; however, in response to chronic hypoxia, ROS-induced SrcFKs phosphorylate and inhibit prolyl hydroxylase (PLH) and/or von Hippel-Lindau tumour suppressor protein (VHL), thus increasing the availability of HIF (Chan *et al.* 2002; Sato *et al.* 2005; Chou *et al.* 2010). Activated HIF alters the expression of a wide variety of proteins that contribute to the enhanced proliferation,

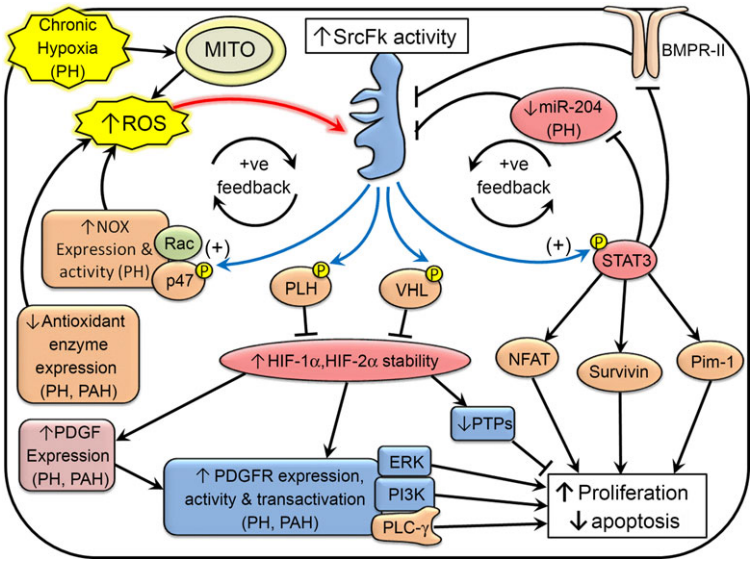

Figure 6. Role of SrcFKs in pulmonary hypertension
(i) Pulmonary hypertension induced by chronic hypoxia (PH) is associated with enhanced mitochondrial ROS production. PH and pulmonary arterial hypertension (PAH) are both also associated with enhanced NOX expression and activity and reduced antioxidant expression and activity, further elevating ROS production. In addition to being activated by ROS, SrcFKs also in turn enhance NOX activity through phosphorylation of the $p47^{phox}$ subunit and activation of Rac-1 which is required for NOX holo-enzyme assembly, therefore generating a positive feedback loop between ROS and SrcFKs. (ii) SrcFKs phosphorylate and inactivate two enzymes, prolyl hydroxylase (PLH) and von Hippel-Lindau tumour suppressor protein (VHL), thus preventing the prolyl hydroxylation and degradation of hypoxia inducible factor-1α or -2α (HIF1α/2α). HIF enhances the expression of platelet-derived growth factor (PDGF) and its receptor (PDGFR) and inhibits the expression of tyrosine phosphatases that oppose the activity of SrcFKs and PDGFR. (iii) SrcFKs phosphorylate and activate the transcription factor, signal transducer and activator of transcription-3 (STAT3). STAT3 inhibits the expression of microRNA-204 (miR-204) and bone morphogenetic protein receptor-II (BMPRII) which inhibit the expression and activity of SrcFKs, respectively. STAT3 therefore indirectly enhances expression and activity of SrcFKs, generating a second positive feedback loop. STAT3 also up-regulates three additional mitogenic signals: nuclear factor of activated T-cells (NFAT), Survivin and Pim-1. This activity, coupled with HIF activation, oxidative stress and direct SrcFK transactivation of PDGFR (Fig. 5), results in greatly enhanced VSM proliferation, migration and inhibition of apoptosis.

migration and hyper-contractility associated with PH, including increases in expression of growth factors and their receptors (Shimoda & Laurie, 2014; Smith & Yuan, 2014) and decreases in expression of protein tyrosine phosphatases that oppose the actions of SrcFKs and PDGFR (ten Freyhaus *et al.* 2011) (Fig. 6).

STATs are activated by tyrosine phosphorylation, which triggers their dimerisation and translocation to the nucleus. This phosphorylation is typically mediated by Janus kinase following cytokine receptor activation. However, in PH, ROS-induced SrcFKs may also phosphorylate and activate STAT3 independently of JAK, perhaps in association with growth-factor receptors. Activated STAT3 subsequently up-regulates the expression of nuclear factor of activated T-cells (NFAT), Pim-1 and Survivin, promoting VSM proliferation and inhibiting apoptosis (Paulin *et al.* 2011). STAT3 also inhibits the expression of the anti-proliferative bone morphogenetic protein receptor-II (BMPRII) and micro-RNA-204 (miR-204) (Paulin *et al.* 2011), and since BMPRII normally inhibits SrcFK auto-phosphorylation (Wong *et al.* 2005), while miR-204 inhibits its expression, STAT3 indirectly stimulates expression and activity of SrcFKs. Furthermore, some forms of familial PAH are also associated with a constitutive deficiency in miR-204 levels and/or mutations in BMPRII that render it unable to inhibit SrcFKs (Wong *et al.* 2005; Courboulin *et al.* 2011). Thus, through STAT3, there is the potential for a second positive feedback loop enhancing the activation of SrcFKs and downstream signalling in both PH and PAH (Fig. 6).

SrcFKs as a therapeutic target in pulmonary hypertension? Considering the evidence in support of a key role for SrcFKs in smooth muscle function, both normal (constriction) and abnormal (oxidative stress, vascular remodelling), one might expect them to be potential therapeutic targets for the treatment of cardiovascular disease in general and pulmonary hypertension in particular. SrcFK-selective inhibitors have been tested against some cancers but so far the focus of the search for effective treatments against pulmonary hypertension has been on a group of mixed specificity inhibitors exemplified by imatinib and related compounds that target PDGFR, c-Kit and c-Abl, originally designed as anti-cancer drugs (Iqbal & Iqbal, 2014). These have been tested against animal models of PAH and PH with promising results (Schermuly *et al.* 2005; Berghausen *et al.* 2013), and a recent clinical trial also suggests that imatinib improves cardiac function in a cohort of patients with PAH (Shah *et al.* 2014). Interestingly, although specific SrcFK inhibitors have yet to be tested in this context, a comparison of two PDGFR antagonists, imatinib and dasatinib, showed dasatinib to be the most potent against hypoxia-induced VSM migration and proliferation and morphological changes associated with PH, and the difference was attributed to the additional inhibition of SrcFKs by dasatinib (Pullamsetti *et al.* 2012). However, the impact of this finding has been muddled somewhat by recent reports that dasatinib, while in use as an anti-cancer drug actually *induces* pulmonary hypertension in human subjects, presumably through vasoconstriction rather than remodelling since it is readily reversible (Godinas *et al.* 2013; Seferian *et al.* 2013). This is consistent with a reported acute enhancement of pulmonary perfusion pressure in isolated mouse lung by both dasatinib and the selective SrcFK inhibitor PP2 (Godinas *et al.* 2013; Nagaraj *et al.* 2013) and consistent with the finding that SrcFKs phosphorylate and activate TASK channels in pulmonary VSM (Nagaraj *et al.* 2013), but not with the weight of evidence showing SrcFK to be both pro-contractile and pro-proliferative in its actions. Nevertheless, whether these unwanted effects of dasatinib in the clinical setting are indeed mediated through SrcFKs or are independent of tyrosine kinase inhibition remains to be confirmed, considering that no reports of *selective* SrcFK inhibitors inducing PH in humans have been made.

Conclusions

In summary, there is clear evidence placing SrcFKs as key ROS effectors in VSM, acting both as mediators of normal smooth muscle contractile responses, via modulation of ion channel and RhoA/Rho-kinase activity, and as mediators of uncontrolled VSM proliferation and migration in response to oxidative stress, acting upon multiple downstream signalling pathways including growth-factor receptor transactivation, STAT3 and hypoxia-inducible factors. More specifically, there is also considerable evidence implicating SrcFKs in the pathogenesis of pulmonary hypertension, but more research is required to attribute the experimental and clinical effects of mixed-specificity kinase inhibitors to specific tyrosine kinases such as SrcFKs.

References

Abdalla S & Will JA (1995). Potentiation of the hypoxic contraction of guinea-pig isolated pulmonary arteries by two inhibitors of superoxide dismutase. *Gen Pharmacol* **26**, 785–792.

Akhand AA, Pu M, Senga T, Kato M, Suzuki H, Miyata T, Hamaguchi M & Nakashima I (1999). Nitric oxide controls Src kinase activity through a sulfhydryl group modification-mediated Tyr-527-independent and Tyr-416-linked mechanism. *J Biol Chem* **274**, 25821–25826.

Alioua A, Mahajan A, Nishimaru K, Zarei MM, Stefani E & Toro L (2002). Coupling of c-Src to large conductance voltage- and Ca^{2+}-activated K^+ channels as a new mechanism of agonist-induced vasoconstriction. *Proc Natl Acad Sci USA* **99**, 14560–14565.

Andreev J, Galisteo ML, Kranenburg O, Logan SK, Chiu ES, Okigaki M, Cary LA, Moolenaar WH & Schlessinger J (2001). Src and Pyk2 mediate G-protein-coupled receptor activation of epidermal growth factor receptor (EGFR) but are not required for coupling to the mitogen-activated protein (MAP) kinase signaling cascade. *J Biol Chem* **276**, 20130–20135.

Banes-Berceli AK, Ogobi S, Tawfik A, Patel B, Shirley A, Pollock DM, Fulton D & Marrero MB (2005). Endothelin-1 activation of JAK2 in vascular smooth muscle cells involves NAD(P)H oxidase-derived reactive oxygen species. *Vascul Pharmacol* **43**, 310–319.

Barlow RS, El-Mowafy AM & White RE (2000). H_2O_2 opens BK_{Ca} channels via the PLA_2-arachidonic acid signaling cascade in coronary artery smooth muscle. *Am J Physiol Heart Circ Physiol* **279**, H475–H483.

Bedard K & Krause KH (2007). The NOX family of ROS-generating NADPH oxidases: physiology and pathophysiology. *Physiol Rev* **87**, 245–313.

Berghausen E, ten Freyhaus H & Rosenkranz S (2013). Targeting of platelet-derived growth factor signaling in pulmonary arterial hypertension. *Handb Exp Pharmacol* **218**, 381–408.

Bos JL, Rehmann H & Wittinghofer A (2007). GEFs and GAPs: critical elements in the control of small G proteins. *Cell* **129**, 865–877.

Calalb MB, Polte TR & Hanks SK (1995). Tyrosine phosphorylation of focal adhesion kinase at sites in the catalytic domain regulates kinase activity: a role for Src family kinases. *Mol Cell Biol* **15**, 954–963.

Cario-Toumaniantz C, Ferland-McCollough D, Chadeuf G, Toumaniantz G, Rodriguez M, Galizzi JP, Lockhart B, Bril A, Scalbert E, Loirand G & Pacaud P (2012). RhoA guanine exchange factor expression profile in arteries: evidence for a Rho kinase-dependent negative feedback in angiotensin II-dependent hypertension. *Am J Physiol Cell Physiol* **302**, C1394–C1404.

Chakraborti S, Roy S, Mandal A, Dey K, Chowdhury A, Shaikh S & Chakraborti T (2012). Role of PKCα–p^{38}MAPK–$G_i\alpha$axis in NADPH oxidase derived $O_2^{\bullet -}$-mediated activation of $cPLA_2$ under U46619 stimulation in pulmonary artery smooth muscle cells. *Arch Biochem Biophys* **523**, 169–180.

Chan DA, Sutphin PD, Denko NC & Giaccia AJ (2002). Role of prolyl hydroxylation in oncogenically stabilized hypoxia-inducible factor-1α. *J Biol Chem* **277**, 40112–40117.

Chandra S, Romero MJ, Shatanawi A, Alkilany AM, Caldwell RB & Caldwell RW (2012). Oxidative species increase arginase activity in endothelial cells through the RhoA/Rho kinase pathway. *Br J Pharmacol* **165**, 506–519.

Chen CH, Cheng TH, Lin H, Shih NL, Chen YL, Chen YS, Cheng CF, Lian WS, Meng TC, Chiu WT & Chen JJ (2006). Reactive oxygen species generation is involved in epidermal growth factor receptor transactivation through the transient oxidization of Src homology 2-containing tyrosine phosphatase in endothelin-1 signaling pathway in rat cardiac fibroblasts. *Mol Pharmacol* **69**, 1347–1355.

Chiarugi P, Pani G, Giannoni E, Taddei L, Colavitti R, Raugei G, Symons M, Borrello S, Galeotti T & Ramponi G (2003). Reactive oxygen species as essential mediators of cell adhesion: the oxidative inhibition of a FAK tyrosine phosphatase is required for cell adhesion. *J Cell Biol* **161**, 933–944.

Chou MT, Anthony J, Bjorge JD & Fujita DJ (2010). The von Hippel-Lindau tumor suppressor protein is destabilized by Src: Implications for tumor angiogenesis and progression. *Genes Cancer* **1**, 225–238.

Choudhury GG, Mahimainathan L, Das F, Venkatesan B & Ghosh-Choudhury N (2006). c-Src couples PI 3 kinase/Akt and MAPK signaling to PDGF-induced DNA synthesis in mesangial cells. *Cell Signal* **18**, 1854–1864.

Chowdhury AK, Watkins T, Parinandi NL, Saatian B, Kleinberg ME, Usatyuk PV & Natarajan V (2005). Src-mediated tyrosine phosphorylation of $p47^{phox}$ in hyperoxia-induced activation of NADPH oxidase and generation of reactive oxygen species in lung endothelial cells. *J Biol Chem* **280**, 20700–20711.

Connolly MJ, Prieto-Lloret J, Becker S, Ward JP & Aaronson PI (2013). Hypoxic pulmonary vasoconstriction in the absence of pretone: essential role for intracellular Ca^{2+} release. *J Physiol* **591**, 4473–4498.

Courboulin A, Paulin R, Giguere NJ, Saksouk N, Perreault T, Meloche J, Paquet ER, Biardel S, Provencher S, Cote J, Simard MJ & Bonnet S (2011). Role for miR-204 in human pulmonary arterial hypertension. *J Exp Med* **208**, 535–548.

Crosswhite P & Sun Z (2010). Nitric oxide, oxidative stress and inflammation in pulmonary arterial hypertension. *J Hypertens* **28**, 201–212.

Cuevas BD, Lu Y, Mao M, Zhang J, LaPushin R, Siminovitch K & Mills GB (2001). Tyrosine phosphorylation of p85 relieves its inhibitory activity on phosphatidylinositol 3-kinase. *J Biol Chem* **276**, 27455–27461.

Daou GB & Srivastava AK (2004). Reactive oxygen species mediate endothelin-1-induced activation of ERK1/2, PKB, and Pyk2 signaling, as well as protein synthesis, in vascular smooth muscle cells. *Free Radic Biol Med* **37**, 208–215.

Egan CG, Wainwright CL, Wadsworth RM & Nixon GF (2005). PDGF-induced signaling in proliferating and differentiated vascular smooth muscle: effects of altered intracellular Ca^{2+} regulation. *Cardiovasc Res* **67**, 308–316.

Eguchi S, Iwasaki H, Ueno H, Frank GD, Motley ED, Eguchi K, Marumo F, Hirata Y & Inagami T (1999). Intracellular signaling of angiotensin II-induced p70 S6 kinase phosphorylation at Ser^{411} in vascular smooth muscle cells. Possible requirement of epidermal growth factor receptor, Ras, extracellular signal-regulated kinase, and Akt. *J Biol Chem* **274**, 36843–36851.

El-Awady MS, Ansari HR, Fil D, Tilley SL & Mustafa SJ (2011). NADPH oxidase pathway is involved in aortic contraction induced by A_3 adenosine receptor in mice. *J Pharmacol Exp Ther* **338**, 711–717.

Frame MC, Fincham VJ, Carragher NO & Wyke JA (2002). v-Src's hold over actin and cell adhesions. *Nat Rev Mol Cell Biol* **3**, 233–245.

Frank GD, Eguchi S, Inagami T & Motley ED (2001). *N*-Acetylcysteine inhibits angiotensin II-mediated activation

of extracellular signal-regulated kinase and epidermal growth factor receptor. *Biochem Biophys Res Commun* **280**, 1116–1119.

Frank GD, Mifune M, Inagami T, Ohba M, Sasaki T, Higashiyama S, Dempsey PJ & Eguchi S (2003). Distinct mechanisms of receptor and nonreceptor tyrosine kinase activation by reactive oxygen species in vascular smooth muscle cells: role of metalloprotease and protein kinase C-δ. *Mol Cell Biol* **23**, 1581–1589.

Frank GD, Saito S, Motley ED, Sasaki T, Ohba M, Kuroki T, Inagami T & Eguchi S (2002). Requirement of Ca^{2+} and PKC$\delta$for Janus kinase 2 activation by angiotensin II: involvement of PYK2. *Mol Endocrinol* **16**, 367–377.

Funato Y & Miki H (2014). Reversible oxidation of PRL family protein-tyrosine phosphatases. *Methods* **65**, 184–189.

Gadepalli R, Singh NK, Kundumani-Sridharan V, Heckle MR & Rao GN (2012). Novel role of proline-rich nonreceptor tyrosine kinase 2 in vascular wall remodeling after balloon injury. *Arterioscler Thromb Vasc Biol* **32**, 2652–2661.

Geneste O, Copeland JW & Treisman R (2002). LIM kinase and Diaphanous cooperate to regulate serum response factor and actin dynamics. *J Cell Biol* **157**, 831–838.

Giannoni E, Buricchi F, Raugei G, Ramponi G & Chiarugi P (2005). Intracellular reactive oxygen species activate Src tyrosine kinase during cell adhesion and anchorage-dependent cell growth. *Mol Cell Biol* **25**, 6391–6403.

Godinas L, Guignabert C, Seferian A, Perros F, Bergot E, Sibille Y, Humbert M & Montani D (2013). Tyrosine kinase inhibitors in pulmonary arterial hypertension: a double-edge sword? *Semin Respir Crit Care Med* **34**, 714–724.

Gonzales AL, Yang Y, Sullivan MN, Sanders L, Dabertrand F, Hill-Eubanks DC, Nelson MT & Earley S (2014). A PLCγ1-dependent, force-sensitive signaling network in the myogenic constriction of cerebral arteries. *Sci Signal* **7**, ra49.

Gui P, Chao JT, Wu X, Yang Y, Davis GE & Davis MJ (2010). Coordinated regulation of vascular Ca^{2+} and K^+ channels by integrin signaling. *Adv Exp Med Biol* **674**, 69–79.

Guilluy C, Bregeon J, Toumaniantz G, Rolli-Derkinderen M, Retailleau K, Loufrani L, Henrion D, Scalbert E, Bril A, Torres RM, Offermanns S, Pacaud P & Loirand G (2010). The Rho exchange factor Arhgef1 mediates the effects of angiotensin II on vascular tone and blood pressure. *Nat Med* **16**, 183–190.

Gusan S & Anand-Srivastava MB (2013). cAMP attenuates the enhanced expression of G_i proteins and hyperproliferation of vascular smooth muscle cells from SHR: role of ROS and ROS-mediated signaling. *Am J Physiol Cell Physiol* **304**, C1198–C1209.

Heeneman S, Haendeler J, Saito Y, Ishida M & Berk BC (2000). Angiotensin II induces transactivation of two different populations of the platelet-derived growth factor βreceptor. Key role for the p66 adaptor protein Shc. *J Biol Chem* **275**, 15926–15932.

Ichikawa K, Ito M & Hartshorne DJ (1996). Phosphorylation of the large subunit of myosin phosphatase and inhibition of phosphatase activity. *J Biol Chem* **271**, 4733–4740.

Iqbal N & Iqbal N (2014). Imatinib: a breakthrough of targeted therapy in cancer. *Chemother Res Pract* **2014**, 357027.

Janssen-Heininger YM, Mossman BT, Heintz NH, Forman HJ, Kalyanaraman B, Finkel T, Stamler JS, Rhee SG & van der Vliet A (2008). Redox-based regulation of signal transduction: principles, pitfalls, and promises. *Free Radic Biol Med* **45**, 1–17.

Jin N & Rhoades RA (1997). Activation of tyrosine kinases in H_2O_2-induced contraction in pulmonary artery. *Am J Physiol Heart Circ Physiol* **272**, H2686–H2692.

Karoor V, Oka M, Walchak SJ, Hersh LB, Miller YE & Dempsey EC (2013). Neprilysin regulates pulmonary artery smooth muscle cell phenotype through a platelet-derived growth factor receptor-dependent mechanism. *Hypertension* **61**, 921–930.

Kawasaki BT, Liao Y & Birnbaumer L (2006). Role of Src in C3 transient receptor potential channel function and evidence for a heterogeneous makeup of receptor- and store-operated Ca^{2+} entry channels. *Proc Natl Acad Sci USA* **103**, 335–340.

Knock GA, Shaifta Y, Snetkov VA, Vowles B, Drndarski S, Ward JP & Aaronson PI (2008a). Interaction between src family kinases and rho-kinase in agonist-induced Ca^{2+}-sensitization of rat pulmonary artery. *Cardiovasc Res* **77**, 570–579.

Knock GA, Snetkov VA, Shaifta Y, Connolly M, Drndarski S, Noah A, Pourmahram GE, Becker S, Aaronson PI & Ward JP (2009). Superoxide constricts rat pulmonary arteries via Rho-kinase-mediated Ca^{2+} sensitization. *Free Radic Biol Med* **46**, 633–642.

Knock GA, Snetkov VA, Shaifta Y, Drndarski S, Ward JP & Aaronson PI (2008b). Role of src-family kinases in hypoxic vasoconstriction of rat pulmonary artery. *Cardiovasc Res* **80**, 453–462.

Knock GA & Ward JP (2011). Redox regulation of protein kinases as a modulator of vascular function. *Antioxid Redox Signal* **15**, 1531–1547.

Krymskaya VP, Goncharova EA, Ammit AJ, Lim PN, Goncharov DA, Eszterhas A & Panettieri RA Jr (2005). Src is necessary and sufficient for human airway smooth muscle cell proliferation and migration. *FASEB J* **19**, 428–430.

Lim Y Jr, Lim ST, Tomar A, Gardel M, Bernard-Trifilo JA, Chen XL, Uryu SA, Canete-Soler R, Zhai J, Lin H, Schlaepfer WW, Nalbant P, Bokoch G, Ilic D, Waterman-Storer C & Schlaepfer DD (2008). PyK2 and FAK connections to p190Rho guanine nucleotide exchange factor regulate RhoA activity, focal adhesion formation, and cell motility. *J Cell Biol* **180**, 187–203.

Liu JQ, Zelko IN, Erbynn EM, Sham JS & Folz RJ (2006). Hypoxic pulmonary hypertension: role of superoxide and NADPH oxidase ($gp91^{phox}$). *Am J Physiol Lung Cell Mol Physiol* **290**, L2–L10.

Lu Y, Yu Q, Liu JH, Zhang J, Wang H, Koul D, McMurray JS, Fang X, Yung WK, Siminovitch KA & Mills GB (2003). Src family protein-tyrosine kinases alter the function of PTEN to regulate phosphatidylinositol 3-kinase/AKT cascades. *J Biol Chem* **278**, 40057–40066.

Madamanchi NR, Moon SK, Hakim ZS, Clark S, Mehrizi A, Patterson C & Runge MS (2005). Differential activation of

mitogenic signaling pathways in aortic smooth muscle cells deficient in superoxide dismutase isoforms. *Arterioscler Thromb Vasc Biol* **25**, 950–956.

Mills JE, Whitford PC, Shaffer J, Onuchic JN, Adams JA & Jennings PA (2007). A novel disulfide bond in the SH2 domain of the C-terminal Src kinase controls catalytic activity. *J Mol Biol* **365**, 1460–1468.

Min J, Reznichenko M, Poythress RH, Gallant CM, Vetterkind S, Li Y & Morgan KG (2012). Src modulates contractile vascular smooth muscle function via regulation of focal adhesions. *J Cell Physiol* **227**, 3585–3592.

Nagaraj C, Tang B, Balint Z, Wygrecka M, Hrzenjak A, Kwapiszewska G, Stacher E, Lindenmann J, Weir EK, Olschewski H & Olschewski A (2013). Src tyrosine kinase is crucial for potassium channel function in human pulmonary arteries. *Eur Respir J* **41**, 85–95.

Nakao F, Kobayashi S, Mogami K, Mizukami Y, Shirao S, Miwa S, Todoroki-Ikeda N, Ito M & Matsuzaki M (2002). Involvement of Src family protein tyrosine kinases in Ca^{2+} sensitization of coronary artery contraction mediated by a sphingosylphosphorylcholine-Rho-kinase pathway. *Circ Res* **91**, 953–960.

Nakashima H, Suzuki H, Ohtsu H, Chao JY, Utsunomiya H, Frank GD & Eguchi S (2006). Angiotensin II regulates vascular and endothelial dysfunction: recent topics of angiotensin II type-1 receptor signaling in the vasculature. *Curr Vasc Pharmacol* **4**, 67–78.

Nobes CD & Hall A (1995). Rho, rac, and cdc42 GTPases regulate the assembly of multimolecular focal complexes associated with actin stress fibers, lamellipodia, and filopodia. *Cell* **81**, 53–62.

Oeckler RA, Kaminski PM & Wolin MS (2003). Stretch enhances contraction of bovine coronary arteries via an NAD(P)H oxidase-mediated activation of the extracellular signal-regulated kinase mitogen-activated protein kinase cascade. *Circ Res* **92**, 23–31.

Paulin R, Meloche J, Jacob MH, Bisserier M, Courboulin A & Bonnet S (2011). Dehydroepiandrosterone inhibits the Src/STAT3 constitutive activation in pulmonary arterial hypertension. *Am J Physiol Heart Circ Physiol* **301**, H1798–H1809.

Pullamsetti SS, Berghausen EM, Dabral S, Tretyn A, Butrous E, Savai R, Butrous G, Dahal BK, Brandes RP, Ghofrani HA, Weissmann N, Grimminger F, Seeger W, Rosenkranz S & Schermuly RT (2012). Role of Src tyrosine kinases in experimental pulmonary hypertension. *Arterioscler Thromb Vasc Biol* **32**, 1354–1365.

Ravichandran KS (2001). Signaling via Shc family adapter proteins. *Oncogene* **20**, 6322–6330.

Reis GS, Augusto VS, Silveira AP, Jordao AA Jr, Baddini -Martinez J, Poli NO, Rodrigues AJ & Evora PR (2013). Oxidative-stress biomarkers in patients with pulmonary hypertension. *Pulm Circ* **3**, 856–861.

Ridley AJ & Hall A (1992). The small GTP-binding protein rho regulates the assembly of focal adhesions and actin stress fibers in response to growth factors. *Cell* **70**, 389–399.

Roskoski R Jr (2005). Src kinase regulation by phosphorylation and dephosphorylation. *Biochem Biophys Res Commun* **331**, 1–14.

Saito S, Frank GD, Mifune M, Ohba M, Utsunomiya H, Motley ED, Inagami T & Eguchi S (2002). Ligand-independent *trans*-activation of the platelet-derived growth factor receptor by reactive oxygen species requires protein kinase C-$\delta$and c-Src. *J Biol Chem* **277**, 44695–44700.

Saito Y & Berk BC (2001). Transactivation: a novel signaling pathway from angiotensin II to tyrosine kinase receptors. *J Mol Cell Cardiol* **33**, 3–7.

Sato H, Sato M, Kanai H, Uchiyama T, Iso T, Ohyama Y, Sakamoto H, Tamura J, Nagai R & Kurabayashi M (2005). Mitochondrial reactive oxygen species and c-Src play a critical role in hypoxic response in vascular smooth muscle cells. *Cardiovasc Res* **67**, 714–722.

Schermuly RT, Dony E, Ghofrani HA, Pullamsetti S, Savai R, Roth M, Sydykov A, Lai YJ, Weissmann N, Seeger W & Grimminger F (2005). Reversal of experimental pulmonary hypertension by PDGF inhibition. *J Clin Invest* **115**, 2811–2821.

Seferian A, Chaumais MC, Savale L, Günther S, Tubert-Bitter P, Humbert M & Montani D (2013). Drugs induced pulmonary arterial hypertension. *Presse Med* **42**, e303–e310.

Seko Y, Takahashi N, Sabe H, Tobe K, Kadowaki T & Nagai R (1999). Hypoxia induces activation and subcellular translocation of focal adhesion kinase ($p125^{FAK}$) in cultured rat cardiac myocytes. *Biochem Biophys Res Commun* **262**, 290–296.

Seshiah PN, Weber DS, Rocic P, Valppu L, Taniyama Y & Griendling KK (2002). Angiotensin II stimulation of NAD(P)H oxidase activity: upstream mediators. *Circ Res* **91**, 406–413.

Shah AM, Campbell P, Rocha GQ, Peacock A, Barst RJ, Quinn D & Solomon SD (2014). Effect of imatinib as add-on therapy on echocardiographic measures of right ventricular function in patients with significant pulmonary arterial hypertension. *Eur Heart J* (in press; DOI: http://dx.doi.org /10.1093/eurheartj/ehu035).

Shimoda LA & Laurie SS (2014). HIF and pulmonary vascular responses to hypoxia. *J Appl Physiol (1985)* **116**, 867–874.

Simonneau G, Robbins IM, Beghetti M, Channick RN, Delcroix M, Denton CP, Elliott CG, Gaine SP, Gladwin MT, Jing ZC, Krowka MJ, Langleben D, Nakanishi N & Souza R (2009). Updated clinical classification of pulmonary hypertension. *J Am Coll Cardiol* **54**, S43–S54.

Singh NK, Wang D, Kundumani-Sridharan V, Van QD, Niu J & Rao GN (2011). 15-Lipoxygenase-1-enhanced Src-Janus kinase 2-signal transducer and activator of transcription 3 stimulation and monocyte chemoattractant protein-1 expression require redox-sensitive activation of epidermal growth factor receptor in vascular wall remodeling. *J Biol Chem* **286**, 22478–22488.

Smith KA & Yuan JX (2014). Hypoxia-inducible factor-1αin pulmonary arterial smooth muscle cells and hypoxia-induced pulmonary hypertension. *Am J Respir Crit Care Med* **189**, 245–246.

Snetkov VA, Smirnov SV, Kua J, Aaronson PI, Ward JP & Knock GA (2011). Superoxide differentially controls pulmonary and systemic vascular tone through multiple signalling pathways. *Cardiovasc Res* **89**, 214–224.

Sreenivasappa H, Chaki SP, Lim SM, Trzeciakowski JP, Davidson MW, Rivera GM & Trache A (2014). Selective regulation of cytoskeletal tension and cell-matrix adhesion by RhoA and Src. *Integr Biol (Camb)* **6**, 743–754.

Sung DJ, Noh HJ, Kim JG, Park SW, Kim B, Cho H & Bae YM (2013). Serotonin contracts the rat mesenteric artery by inhibiting 4-aminopyridine-sensitive Kv channels via the 5-HT_{2A} receptor and Src tyrosine kinase. *Exp Mol Med* **45**, e67.

ten Freyhaus H, Dagnell M, Leuchs M, Vantler M, Berghausen EM, Caglayan E, Weissmann N, Dahal BK, Schermuly RT, Ostman A, Kappert K & Rosenkranz S (2011). Hypoxia enhances platelet-derived growth factor signaling in the pulmonary vasculature by down-regulation of protein tyrosine phosphatases. *Am J Respir Crit Care Med* **183**, 1092–1102.

Timpson P, Jones GE, Frame MC & Brunton VG (2001). Coordination of cell polarization and migration by the Rho family GTPases requires Src tyrosine kinase activity. *Curr Biol* **11**, 1836–1846.

Turrens JF (2003). Mitochondrial formation of reactive oxygen species. *J Physiol* **552**, 335–344.

Uzui H, Lee JD, Shimizu H, Tsutani H & Ueda T (2000). The role of protein-tyrosine phosphorylation and gelatinase production in the migration and proliferation of smooth muscle cells. *Atherosclerosis* **149**, 51–59.

Vazquez G, Wedel BJ, Kawasaki BT, Bird GS & Putney JW Jr (2004). Obligatory role of Src kinase in the signaling mechanism for TRPC3 cation channels. *J Biol Chem* **279**, 40521–40528.

Velasco G, Armstrong C, Morrice N, Frame S & Cohen P (2002). Phosphorylation of the regulatory subunit of smooth muscle protein phosphatase 1 M at Thr850 induces its dissociation from myosin. *FEBS Lett* **527**, 101–104.

Vepa S, Scribner WM, Parinandi NL, English D, Garcia JG & Natarajan V (1999). Hydrogen peroxide stimulates tyrosine phosphorylation of focal adhesion kinase in vascular endothelial cells. *Am J Physiol Lung Cell Mol Physiol* **277**, L150–L158.

Wang Y, Ji L, Jiang R, Zheng L & Liu D (2014). Oxidized high-density lipoprotein induces the proliferation and migration of vascular smooth muscle cells by promoting the production of ROS. *J Atheroscler Thromb* **21**, 204–216.

Ward CW, Gough KH, Rashke M, Wan SS, Tribbick G & Wang J (1996). Systematic mapping of potential binding sites for Shc and Grb2 SH2 domains on insulin receptor substrate-1 and the receptors for insulin, epidermal growth factor, platelet-derived growth factor, and fibroblast growth factor. *J Biol Chem* **271**, 5603–5609.

Waypa GB, Marks JD, Guzy RD, Mungai PT, Schriewer JM, Dokic D, Ball MK & Schumacker PT (2013). Superoxide generated at mitochondrial complex III triggers acute responses to hypoxia in the pulmonary circulation. *Am J Respir Crit Care Med* **187**, 424–432.

Wedgwood S, Dettman RW & Black SM (2001). ET-1 stimulates pulmonary arterial smooth muscle cell proliferation via induction of reactive oxygen species. *Am J Physiol Lung Cell Mol Physiol* **281**, L1058–L1067.

Wong WK, Knowles JA & Morse JH (2005). Bone morphogenetic protein receptor type II C-terminus interacts with c-Src: implication for a role in pulmonary arterial hypertension. *Am J Respir Cell Mol Biol* **33**, 438–446.

Wu W, Platoshyn O, Firth AL & Yuan JX (2007). Hypoxia divergently regulates production of reactive oxygen species in human pulmonary and coronary artery smooth muscle cells. *Am J Physiol Lung Cell Mol Physiol* **293**, L952–L959.

Xu W, Doshi A, Lei M, Eck MJ & Harrison SC (1999). Crystal structures of c-Src reveal features of its autoinhibitory mechanism. *Mol Cell* **3**, 629–638.

Additional information

Competing interests

None declared.

Funding

C. Mackay is funded by British Heart Foundation studentship (FS/12/43/29608).